THE ULTRA-HIGH LIME WITH ALUMINUM PROCESS FOR REMOVING CHLORIDE FROM RECIRCULATING COOLING WATER

A Dissertation

by

AHMED IBRAHEEM ALI ABDEL-WAHAB

Submitted to the Office of Graduate Studies of
Texas A&M University
in partial fulfillment of the requirements for the degree of

DOCTOR OF PHILOSOPHY

May 2003

Major Subject: Civil Engineering

THE ULTRA-HIGH LIME WITH ALUMINUM PROCESS FOR REMOVING CHLORIDE FROM RECIRCULATING COOLING WATER

A Dissertation

by

AHMED IBRAHEEM ALI ABDEL-WAHAB

Submitted to Texas A&M University
in partial fulfillment of the requirements
for the degree of

DOCTOR OF PHILOSOPHY

Approved as to style and content by:

Bill Batchelor (Chair of Committee)	
Robin L. Autenrieth (Member)	Bruce E. Herbert (Member)
Anthony T. Cahill (Member)	Paul Roschke (Head of Department)

May 2003

Major Subject: Civil Engineering

ABSTRACT

The Ultra-High Lime with Aluminum Process for Removing Chloride from Recirculating Cooling Water.

(May 2003)

Ahmed Ibraheem Ali Abdel-Wahab, B.S., Al-Minia University;

M.S., Al-Minia University, Egypt

Chair of Advisory Committee: Dr. Bill Batchelor

Chloride is a deleterious ionic species in cooling water systems because it is important in promoting corrosion. Chloride can be removed from cooling water by precipitation as calcium chloroaluminate using the ultra-high lime with aluminum process (UHLA). This research program was conducted to study equilibrium characteristics and kinetics of chloride removal by UHLA process, to study interactions between chloride and sulfate or silica, and to develop a model for multicomponent removal by UHLA.

Kinetics of chloride removal with UHLA was investigated. Chloride removal was found to be fast and therefore, removal kinetics should not be a limitation to applying the UHLA process. Equilibrium characteristics of chloride removal with UHLA were characterized. Good chloride removal was obtained at reasonable ranges of lime and aluminum doses. However, the stoichiometry of chloride removal with UHLA deviated from the theoretical stoichiometry of calcium chloroaluminate precipitation. Equilibrium modeling of experimental data and XRD analysis of precipitated solids

indicated that this deviation was due to the formation of other solid phases such as tricalcium hydroxyaluminate and tetracalcium hydroxyaluminate. The effect of pH on chloride removal was characterized. The optimum pH for maximum chloride removal was pH 12 ± 0.2. Results of equilibrium experiments at different temperatures indicated that final chloride concentrations slightly increased when water temperature increased at temperatures below 40^{o}C. However, at temperatures above 40^{o}C, chloride concentration substantially increased with increasing water temperature.

An equilibrium model was developed to describe the chemical behavior of chloride removal from recycled cooling water using UHLA. Formation of a solid solution of calcium chloroaluminate, tricalcium hydroxyaluminate, and tetracalcium hydroxyaluminate was found to be the best mechanism to describe the chemical behavior of chloride removal with UHLA.

Results of experiments that studied interactions between chloride and sulfate indicated that sulfate is preferentially removed over chloride. Final chloride concentration increased with increasing initial sulfate concentration. Silica was found to have only a small effect on chloride removal. The equilibrium model was modified in order to include sulfate and silica reactions along with chloride in the UHLA process and it was able to accurately predict the chemical behavior of simultaneous removal of chloride, sulfate, and silica with UHLA.

To my wife and my children with love

ACKNOWLEDGMENTS

First, I would like to express my sincere appreciation and thanks to my advisor and chair of my committee, Professor Bill Batchelor, for his guidance and support during my studies at Texas A&M University. His creativity, insight into environmental engineering, and keeping me focused on the whole picture helped me in my research. His energy and love of what he is doing inspires me. I feel lucky that I had a chance to work under his supervision. I am very grateful for his supervision both on the technical and the personal levels during my Ph.D. study. I learned from him much more than I ever thought I would.

I would like to thank and acknowledge my committee members, Dr. Robin Autenrieth, Dr. Bruce Herbert, and Dr. Anthony Cahill for their advice and comments on my research program and dissertation. I enjoyed and learned much from the interesting technical discussions that I had with them.

This research has been funded in part with funds from the State of Texas as part of the program of the Texas Hazardous Waste Research Center. The contents do not necessarily reflect the views and policies of the sponsor nor does mention of trade names or commercial products constitute endorsement or recommendations for use. I also acknowledge the Egyptian Government for providing me with financial support during my Ph.D. study.

I would like to express my thanks to my colleagues Dr. Inseong Hwang, Dr. Jon Schwantes, Dr. Woojin Lee, and Sae Bom Ko for sharing their ideas and knowledge with me.

I am grateful to my mother for being a constant source of love and support throughout my life and to my father for being my most profound mentor. I am indebted to my wife, Hoda, for her companionship over the past decade and for being a mother and a father at the same time for our children while I was busy working in my Ph.D. Without her great deal of love, support, encouragement, and never-ending patience, I would not have been able to complete this work. Finally, I am grateful to my daughters, Maha, Rehab, Eithar, and Rawan for tolerating lost evenings, weekends, and vacations as “Dad is making a contribution to treating water and preventing pollution”.

TABLE OF CONTENTS

CHAPTER Page

CHAPTER Page

LIST OF FIGURES

Page

Page

LIST OF TABLES

CHAPTER I

INTRODUCTION

The current trend in industrial wastewater management focuses on pollution prevention both by source reduction/clean technologies and by closed water systems, in which water recycling plays a major role. Cooling water discharges are major environmental problems, constituting from 60 to 90% by volume of industrial discharges (Matson and Harris, 1979). Heat, toxic chemicals, and organic and inorganic materials are contained in these discharges. Furthermore, cooling water contributes the highest single water demand in industry, which accounted for 49% of all water withdrawals in 1990 (U.S. Dept. of the Interior, 1996).

The need for pollution control, water conservation, and reduced costs are sufficient incentives to overcome the limitations to increased recycle of cooling water. The major limitations to increased cooling water recycle are associated with water quality problems. The underlying cause of these problems is the continuous evaporation of water in the cooling tower that concentrates nonvolatile compounds that enter the system in the makeup water. These higher concentrations cause increased corrosion, biological growth, and scale formation on heat transfer surfaces. Such fouling can substantially decrease the heat transfer efficiency of the system and shorten the equipment life. To prevent scaling and corrosion on the metal heat transfer surfaces, various chemicals are added to the cooling water. After eliminating chromate as an anti-

---

This dissertation follows the format and style of the *Water Environment Research.*

corrosion agent for environmental safety, zinc (Sekine et al., 1992) and other compounds such as nitrites (Moccari, 1999) and molybdate (Boffardi, 1984, and Mustafa and Shahinoor, 1996) are now used to inhibit corrosion. Polyphosphates and phosphonates inhibit both corrosion and scale formation (Bohnsack et al., 1986, and Patel and Nicol, 1996). These chemical additives are discharged in the blowdown, although they can be toxic to aquatic life. Zinc ions are hazardous to the environment and can precipitate in the form of insoluble zinc salts (Boffardi, 1984, and Gunasekaran et al., 1997). Use of heavy metals for corrosion control came under criticism and eventually was restricted by law (Bohnsack et al., 1986). Phosphates and phosphonates also have limitations. Phosphonates are susceptible both to degradation by oxidizing biocides and to precipitation with calcium (Geiger, 1996). Due to their environmental effects, restrictions on phosphorus discharges are under continued review by state environmental agencies and limits have been imposed to prevent overloading receiving water. Nontoxic chemicals have been found generally to be ineffective in corrosion control (Breske, 1976, and Kumar and Fairfax, 1976).

An attractive alternative for promoting pollution prevention through extensive recycling, while avoiding the problems of corrosion and scale inhibitors, is to remove chemicals that promote corrosion and scale formation from the cooling water. These chemicals are calcium, magnesium, phosphate, silica, sulfate, and chloride. The technologies that are under most active consideration for removing these materials are: high lime softening, reverse osmosis, ion exchange, and electrodialysis (Matson and Harris 1979). With the exception of the high lime softening process, these technologies

are very expensive and have many operating problems. The unit price of water treatment with reverse osmosis is about three times the price of lime softening (You et al. 1999).

The conventional lime soda process is used in cooling water systems to minimize or eliminate scale formation by removing calcium and magnesium hardness and by reducing alkalinity. A portion of the silica present can also be removed by sorption onto magnesium hydroxide solids or precipitation as magnesium silicate (Matson and Harris, 1979, and Nurdogan et al, 1998). The amount of silica removed depends on the concentration of magnesium in the feed water. More efficient and consistent silica removal can be obtained with conventional high lime softening if supplemental magnesium compounds are added, but this can significantly increase treatment costs. Lime softening is also ineffective in removing sulfate and chloride.

Ultra-High Lime (UHL) treatment is an attractive modification of lime softening that can remove all of the major scalants (Ca^{2+}, Mg^{2+}, CO_3^{2-}, PO_4^{3-}, and SiO_2), regardless of feed water quality (Batchelor et al., 1991, and Batchelor and McDevitt, 1984). The essential element of the ultra-high lime process is the addition of higher doses of lime to maintain an area of high pH and high calcium concentration. This results in removal of silica as a calcium silicate precipitate (Batchelor and McDevitt, 1984). A number of significant advantages can be claimed for the ultra-high lime process. Its most important advantage is that it is capable of removing all major scale-forming chemicals regardless of the chemical composition of the water to be treated (Batchelor and McDevitt, 1984). Furthermore, heavy metals are removed by precipitation as hydroxide solids under conditions of high pH found in the UHL process (Charentanyarak, 1999). The ultra-high

lime process is attractive economically because its primary treatment chemical is lime, which is less expensive than many other treatment chemicals. If the lime is recycled, the advantage is even greater.

The Ultra-High Lime with Aluminum process (UHLA) is an innovative modification of UHL in which aluminum is added to promote removal of sulfate as calcium sulfoaluminate ($Ca_6Al_2(SO_4)_3(OH)_{12}$). The UHLA process has demonstrated the ability to achieve high sulfate removal efficiency (Batchelor et al., 1985, Schaezler, 1978, and Nebgen et al., 1973). By expanding the process to also remove chloride, the UHLA process will be able to fill the need for a low cost tool for improved industrial water management. The conditions found in the UHLA are suitable for removing chloride by precipitation as calcium chloroaluminate ($Ca_4Al_2Cl_2(OH)_{12}$) in order to reduce corrosion and to prolong equipment life.

Despite the attractiveness of UHLA technology, there is limited data to support its use for chloride removal. Research on formation of chloroaluminates in Portland cement demonstrates the feasibility of the fundamental approach for chloride removal by the UHLA process. However, insufficient data is available to characterize the equilibrium and kinetics of the formation of calcium chloroaluminate under conditions found in recycled industrial water systems. Therefore, the goal of this research is to characterize the equilibrium conditions and kinetics of calcium chloroaluminate precipitation and to evaluate chloride removal from recycled cooling water using UHLA process affected by chemical doses, water quality, pH, initial chloride concentration, and

temperature; and to develop an equilibrium model for chloride removal by UHLA. This goal was achieved by accomplishing the following objectives:

1. Study the kinetics of calcium chloroaluminate precipitation.
2. Develop basic information on chloride precipitation.
3. Study the interactions among components in UHLA process.
4. Develop a model for UHLA process.

Four tasks were conducted to achieve the four research objectives. The first task studied the kinetics of calcium chloroaluminate precipitation and obtained the reaction time for equilibrium experiments. The second task focused on developing basic information on chloride precipitation through the determination of the stoichiometric coefficients and the solubility products of precipitated solids as affected by lime dose, aluminum dose, initial chloride concentration, pH, and temperature. The third task studied the interactions between chloride and sulfate or silica. The effect of the presence of sulfate or silica on chloride precipitation was investigated. Similarly, the effect of the presence of chloride on sulfate or silica precipitation was investigated. The forth task focused on developing an equilibrium model for chloride removal using ultra-high lime with aluminum process in order to predict chemical behavior in treated cooling water using information on chemical doses and feed water quality.

This dissertation is organized into five chapters. Chapter II describes cooling water process and problems of recycled cooling water as well as the technologies that are used for recycled cooling water treatment. It also reviews the feasibility of ultra-high lime as an innovative technology for cooling water treatment. Additionally, it includes

information about calcium chloroaluminate formation and characteristics that have been reported by previous researchers. Chapter III explains in detail the experimental and analytical procedures developed and used in this research as well as the procedures used to develop the equilibrium model. Chapter IV presents the results of experiments and the analysis of these results. It also contains results of the equilibrium modeling and model evaluations. Finally, Chapter V summarizes results obtained in this research and their relevance to recycled industrial water treatment and future research needs in this area.

CHAPTER II

BACKGROUND

2.1 Open Recirculating Cooling Water

Cooling systems are used in many locations in industry for dissipating residual heat from processes. Most cooling water systems use water as the coolant because this medium permits relatively compact cooling systems, it is available almost everywhere, and its cost is low compared to other fluids that could be used. The most common cooling water system consists of a cooling tower, conveyance system, and heat exchangers as shown in Figure 2.1 (Aronson et al., 1982). The cooling tower in the cooling water system dissipates waste process heat into the atmosphere through the evaporation of water to the atmosphere. As water is evaporated, fresh water, called makeup water, is used to replace water that is evaporated in the cooling tower. While evaporation is occurring within the cooling tower, ions normally dissolved in the makeup water are being concentrated within the cooling water. Concentration of nonvolatile compounds causes increased corrosion, biological growth, and scale formation within the cooling water system if allowed to increase. To prevent scaling and corrosion and to maintain the ion concentrations at an acceptable level, a purge stream from the cooling tower, called blowdown, must be removed. However, discharge of cooling water blowdown is a major environmental problem. The environmental impact related to the discharge of cooling water consists of (Kolk, 1996, and Matson and Harris, 1979):

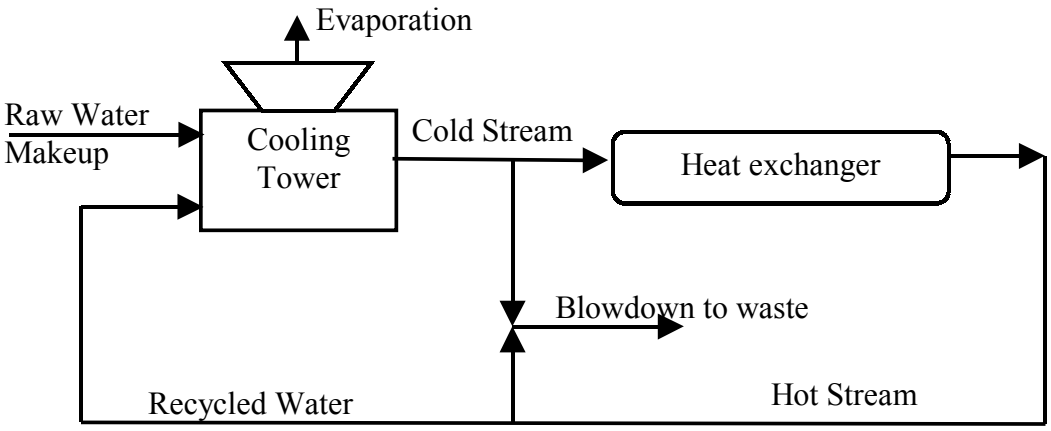

Figure 2.1 Schematic diagram of open recirculating cooling water system (Aronson et al., 1982).

1. Emission of heat: both temperature level and soluble oxygen levels are affected, resulting in disturbance of the natural surface water ecology.
2. The discharge of conditioning chemicals used to prevent biological and physical fouling of the cooling system (e.g. biocides, dispersing agents, and anti corrosives, or their degradation products).
3. The contamination of surface water by process chemicals leaking into the cooling water. Data available from water quality authorities reveal that leakage of chemicals from shell and tube heat exchangers into cooling water systems could add up to several hundreds of tons per year (oil, aromatics, organochlorine).

The need for pollution control, water conservation, and reduced costs are sufficient incentives to eliminate or minimize cooling tower blowdown from open recirculating cooling water systems. The elimination or minimization of cooling tower blowdown requires an increase in the cooling water's cycles of concentration. The cooling water cycles of concentration is a measure of the cooling water's salt content produced by the evaporation of water in the cooling tower. The salt content is maintained at a constant concentration by the "blowing down" of a portion of the cooling water to wastewater treatment. The cycles of concentration (COC) can be obtained by conducting a material balance on such a conservative component, which results in (Batchelor et al., 1991),

$$COC = \frac{Q_M}{(Q_B + Q_D)} \tag{2-1}$$

where: Q_M = cooling tower makeup water flow rate (L^3T^{-1})

Q_B = cooling tower blowdown water flow rate (L^3T^{-1})

Q_D = cooling tower drift water flow rate (L^3T^{-1})

An increase in the cooling water's cycle of concentration increases the probability of scaling and corrosion caused by increasing total dissolved solids (TDS), pH, and conductivity (Jones, 1991, and Matson and Harris, 1979).

2.2 Limitations to Cooling Water Recycle

The major limitations to increased cooling water recycle are associated with water quality problems. The underlying cause of these problems is the continuous evaporation in the cooling tower. This results in the concentration of nonvolatile constituents that enter the cooling water system in the makeup water. The problem manifests itself as scaling, corrosion, or biofouling in the cooling system.

2.2.1 Scale Formation

Scale formation can result from two phenomena (Aronson et al., 1982). The first is a precipitation and sedimentation phenomenon in which a sparingly soluble salt, such as calcium carbonate, precipitates from water. This precipitate then settles in pipelines or on heat exchange surfaces where it frequently solidifies into a relatively soft, amorphous scale. The second and more significant mechanism for scale formation is the "in situ" crystallization of sparingly soluble salts as the result of elevated temperatures and/or low flow velocity. This scale is a dense crystalline nature, which is difficult to remove. These precipitates form directly on heat transfer surfaces and produce a higher resistance to heat transfer. Furthermore, deposits of these solids on heat transfer surfaces shorten the

useful service life of process equipment (Aronson et al., 1982). The most common solids that form direct deposits on heat transfer surfaces are calcium carbonate, calcium sulfate, and calcium phosphate (Mathie, 1998). Most scale results from the breakdown of calcium bicarbonate as water is heated. Several factors determine the rate that calcium combines to form deposits. The rate of calcium bicarbonate breakdown to form calcium carbonate increases with increasing pH and temperature. However, calcium sulfate becomes less soluble with decreasing pH and increasing temperature. Calcium phosphate, like calcium carbonate, becomes less soluble at higher pH and temperature. Typical scales that occur in cooling water system include,

1. Calcium carbonate scaling results primarily from localized heating of water containing calcium bicarbonate. Limits to prevent calcium carbonate scaling are:
    a) pH and alkalinity adjustment and frequently coupled with the judicious use of scale inhibiting chemicals (Aronson et al., 1982).
    b) Calcium hardness should be less than 300 mg/L $CaCO_3$ to ensure that calcium precipitation does not occur, using normal concentration of treatment chemicals (Balaban, 1991).
2. Calcium sulfate scaling usually forms as gypsum, which includes two waters of hydration at temperatures below 42^{o}C, whereas above 42^{o}C, the predominant precipitant is anhydrite. To prevent $CaSO_4$ scale, calcium concentration should be less than 300 mg/l (Kunz et al., 1977).
3. Silica scaling results from many possible complex silica compounds such as pure quartz scales, calcium silicate, magnesium silicate, and aluminum silicate. This scale

formation can be avoided by:

a) Silica concentration should be less than 150 mg/l SiO_2 (Kunz et al., 1977, and Aronson et al., 1982).

b) Maintain (Mg * SiO_2) product to below 8540 mg/l (Jones, 1991).

4. Phosphate scaling results from a reaction between calcium salts and orthophosphate, which may result from polyphosphate inhibitors, present in recycled water. Phosphate scaling can be prevented by maintaining orthophosphate at < 5.0 mg/l (as PO_4) (Aronson et al., 1982).

2.2.2 Corrosion

The potential causes of condenser tube corrosion that can influence system design and operation are (Aronson et al., 1982),

1. Low alkalinity waters have little pH buffering capacity. Consequently, this type of water can become quite aggressive when pH in the cooling water drops due to absorption of acidic gases as it cascades through the cooling tower. Acidic gasses, such as sulfur dioxide, are most frequently encountered in highly industrialized areas.

2. Some contaminants, such as hydrogen sulfide and ammonia, can produce corrosive waters even when the total hardness and alkalinity is relatively high.

3. Water that contains a high concentration of total dissolved solids has a high conductivity, which provides a considerable potential for galvanic attack. Chloride and sulfate are the most aggressive ions that promote corrosion and limit the function

of inhibitors as will be discussed in detail later.

Guidelines to control corrosion are:

a) The pH should be kept within the control range for the corrosion inhibitor program in use. Generally, the pH value should be kept above 6 (Kunz et al., 1977).
b) Calcium hardness should be at least 20 to 50 mg/l $CaCO_3$ to enable formation of protective film (Kunz et al., 1977).
c) Chloride concentration should be kept below 200 mg/l (Jones, 1991).
d) Total dissolved solids (TDS) concentration should be kept below 2,000 mg/l (Sussman, 1975).
e) Conductivity should be kept below 4,000 micromhos/cm (Kunz, 1977).

2.2.3 Microbiological Fouling

Growths of algae, fungi, and bacteria can result in significant fouling in recycled cooling water systems. Since the various organisms flourish under a variety of conditions (e.g., presence or absence of sunlight, presence or absence of food supply, etc.), it is virtually impossible to control biological fouling without an adequate chemical treatment program (Aronson et al., 1982). Chlorination systems are normally quite effective, but must be carefully controlled and monitored due to effluent quality control guidelines. Other proprietary biocide additives are available, which can often be adapted to discharge limitations.

Due to the fact that bromine breaks down rapidly to environmentally benign

byproducts, bromine can be used instead of chlorine as a biocide (Jones, 1991). An alternative strategy to biofouling control uses the simultaneous addition of sodium bromide and chlorine to the water used for power plant condenser cooling. The function of sodium bromide is to convert hypochlorous acid into hypobromous acid (Fisher et al., 1999). Ozone also is one of the most powerful compounds that can be used for biofouling control (Ruisinger, 1996).

2.2.4 Effect of Chloride on Cooling Water Systems

Metal-chlorides are generally very soluble in water, so they almost always accumulate in solution (Mathie, 1998). Chloride is important in promoting corrosion because of the ability of chloride to promote pitting by penetration or local destruction of otherwise protective iron oxide films (Schroeder, 1986, and Foley, 1970). It has been reported that chloride is the most deleterious individual ionic species normally occurring in natural waters (Schroeder, 1986). Furthermore, increased chloride and sulfate concentrations enhance the corrosive effect of oxygen and carbon dioxide (NACE, 1976). Recycling of lime-treated blowdown returns soluble salts such as sulfate and chloride not removed in the softener to the cooling tower system. Since continued recycling necessarily raises their concentration, higher corrosion and scaling tendency are a possible consequence (Mathie, 1998). It is difficult, however, to quantify the relation of corrosivity to chloride concentration in water. The threshold concentration of chloride above which pitting of iron is possible is reported to be about 10 mg/L (Foley, 1970). Chloride is about 3 times as active as sulfate in pitting metals. It reacts with the metals in solution and causes them to stay soluble, thus preventing the formation of

protective metallic oxide films (Singley et al., 1985). The Larson Index of corrosion (LIC) is a corrosion indicator that is used to measure the aggressive nature of specific ions and is defined as (Larson and Sullo, 1967),

$$\text{LIC} = \frac{\text{Cl} + \text{SO}_4}{\text{ALK}} \qquad (2\text{-}2)$$

Where: LIC = Larson Index, Cl = chloride concentration, SO_4 = sulfate concentration, and ALK = total alkalinity. All three are expressed in mg/L of equivalent $CaCO_3$.

When this ratio of reactive anions to alkalinity is greater than 0.5, the possibility of corrosive action exists (Singley et al., 1985).

High chloride concentration limits the cycles of concentration and requires increasing the amount of corrosion inhibitor or changing to more effective inhibitors (Schroeder, 1986). Therefore, extent of cooling water recycle in many cases is controlled by chloride concentration in the recycled water.

2.2.5 Corrosion Inhibitors and Effect of Chloride on their Function in Cooling Water

The approach to corrosion inhibitors in the cooling water system has been based on chromate. This approach has generally been considered the most effective, but for environmental safety it was dropped from use. The use of other inorganic inhibitors such as zinc, molybdate, nitrites, and inorganic phosphates in cooling water systems has been investigated (Sekine et al., 1992). Zinc ions are hazardous to the environment and can precipitate in the form of insoluble zinc salts (Boffardi, 1984, and Gunasekaran et al., 1997). Particularly heavy metals for corrosion control came under criticism and

eventually were restricted by law (Bohnsack et al., 1986).

Moccari (1999) reported that nitrites are extensively used as corrosion inhibitors in closed recirculating water systems. He stated that the level of inhibition depends on the chloride (Cl^-) and sulfate (SO_4^{2-}) species in the solution. To effectively inhibit corrosion, the concentration of nitrite should equal the chloride concentration and exceed the sulfate concentration by 250 to 500 mg/l (Boffardi, 1984).

Sodium molybdate (Na_2MoO_4) was tested as a corrosion inhibitor. It was found that the presence of aggressive ions such as chloride and sulfate reduce the efficiency of Na_2MoO_4 and higher concentrations are necessary for corrosion inhibition (Boffardi, 1984, and Mustafa and Shahinoor, 1996).

Gluconates and Gluconic acids are known to be effective inhibitors for iron and mild steel in cooling water. It has been reported that the inhibition power of Gluconates and Gluconic acids increases with the addition of borate ions, because of their combined synergistic effect. Moreover, boro-gluconate is harmless to the environment (Singh et al., 1994). However, gluconate-borate is effective only in chloride-free solutions. Gluconate-borate mixtures can be extended to water containing up to 100 mg/l chloride by the addition of nitrite (Singh et al., 1994). Singh et al. (1994) reported that formation of soluble metal complexes with iron is one of the major problems with compounds containing gluconate and hence their effectiveness decays within a few hours after immersion.

The generic types of inhibitors that are currently used for both scale and

corrosion control are polyphosphates and organic phosphonates (Bohnsack et al., 1986, and Patel and Nicol, 1996). Polyphosphates have generally been replaced by phosphonates due to their poor thermal and hydrolytic stability. They are also incompatible with oxidizing biocides (Patel and Nicol, 1996). The most common phosphonates used today as corrosion inhibitors are hydroxy-ethylene-diphosphonic acid (HEPT) and phosphono-butane-tricarboxylic acid (PBTC). Other phosphonates include hydroxy-phospho-acetic acid (HPA), amino-trimethylene-phosphonate (AMP), phosphono-carboxylic acid (POCA), and complex amino-phosphonates (CAP) are also used. Phosphonates work under alkaline conditions in cooling water. Although phosphonates are the cornerstone of alkaline technology and have served industry well, they have limitations. Phosphonates are susceptible to both degradation by oxidizing biocides and precipitation with calcium (Geiger, 1996). Restrictions on phosphorus discharge are under continued review by state environmental agencies and limits have been imposed to prevent overloading receiving water. For example, phosphorus effluent discharge is restricted to less than 3 mg/l PO_4 in the Lake Michigan Basin (Geiger, 1996). Furthermore, both AMP and HEDP, the most common phosphonate corrosion inhibitors, are sensitive to overall water quality (Boffardi, 1984). The protection afforded to alloys decreases with increasing chloride and sulfate concentrations. They also show some sensitivity to temperature. Although the more alkaline solutions reduced corrosion, they increased the driving force for inorganic scale formation (Boffardi, 1984). Additionally, Gunasekaran et al. (1997) reported that, with very few exceptions, most of the phosphonic acids as such are not good corrosion inhibitors and their corrosion

inhibition properties are increased by the addition of metallic ions. Predominantly zinc ions are used for elevating the corrosion inhibiting properties of phosphonic acids. However, Geiger (1996) indicated that when zinc is included, the inhibitor must also be capable of preventing zinc phosphate precipitation.

2.3 Lime Softening of Cooling Water

Lime softening is a process in which lime and soda ash are added to precipitate scale-forming materials such as calcium and magnesium and reduce the water alkalinity. A portion of silica can be removed. The amount of silica removed depends on the magnesium concentration in the water (Nurdogan et al., 1998; Matson and Harris, 1979; Wohlberg and Buchloz, 1974; and Mujeriego, 1976). The softening process will not affect species such as sodium, potassium, chloride, and sulfate. In recirculating cooling water systems the concentrations of these ions will be controlled by drift losses and blowdown (Micheletti and Owen, 1979). Lime softening can be applied in various configurations. It can be applied to treat makeup water, blowdown water, or the mixture of both. However, the most common application of lime softening in cooling water treatment is called sidestream softening and it is applied to cooling tower blowdown. This allows the cooling water to be concentrated in the cooling tower and thereby reduce cooling tower blowdown (Lancaster and Sanderson, 1993, and Matson and Harris, 1979). There are two types of sidestream softening processes that are used to treat cooling water. They are lime softening process and caustic softening process. In both softening processes, calcium carbonate ($CaCO_3$) and magnesium hydroxide ($Mg(OH)_2$) are precipitated at a pH value of approximately 11. Silica (SiO_2) is also removed by

adsorption onto magnesium hydroxide (Matson and Harris, 1979 , and Nurdogan et al., 1998). It was reported that the adsorption isotherm of silica onto magnesium hydroxide follows a Freundlich isotherm and can be expressed as (Matson and Harris, 1979),

$$q = 0.018\ C^{0.309} \qquad (T = 50\ ^{o}C) \qquad (2\text{-}3)$$

Where: q = silica removed (mg/l) per mg magnesium in the precipitated or solid form,

C = residual concentration of the adsorbed species

If the magnesium concentration is not high enough to remove the desired amount of silica, magnesium addition may be required.

The theory of operation for the lime softening process can be described as follows (Jones, 1991):

1. Lime ($Ca(OH)_2$) is added to the cooling water being treated to provide the softener's hydroxide ion (OH^-) demand. The hydroxide ion is required to increase pH of the cooling water to about 11, convert carbon dioxide (H_2CO_3) and bicarbonate (HCO_3^-) to carbonate ions (CO_3^{2-}) convert magnesium ions (Mg^{2+}) and ion pairs to magnesium hydroxide ($Mg(OH)_2$) and convert orthosilicic acid ($Si(OH)_4$) to trihydrogen silicate ion ($H_3SiO_4^-$).
2. Soda ash (Na_2CO_3) is added to supply the softener's demand of carbonate ion that is required to precipitate excess calcium as calcium carbonate ($CaCO_3$). Because calcium in the form of lime is added to the system to satisfy the softener's hydroxide demand, soda ash is often necessary to precipitate some or all of this calcium.

3. Acid is added to supply the softener's hydrogen ion demand, which is required to decrease the pH of the cooling water to its original value after removing the scalants, convert carbonate ions and carbonate ion pairs to carbon dioxide, convert magnesium hydroxide to magnesium ions and ion pairs, and convert trihydrogen silicate ion to orthosilicic acid, $Si(OH)_4$. Sulfuric acid (H_2SO_4) was usually used to supply hydrogen ion demand. The trend now is to eliminate using sulfuric acid in order to avoid an increase in sulfate ions in the system due to the problems associated with sulfate such as scale and corrosion. Carbon dioxide (CO_2) can be used instead.

The basic theory of the caustic softening process is as follow (Jones et al., 1991):

1. Caustic soda (NaOH) is added to the cooling water being treated to provide the softener's hydroxide ion demand.
2. Lime is added to supply the softener with calcium ion that is required to precipitate excess carbonate as $CaCO_3$ if needed.
3. Soda ash is added to supply the softener with carbonate ion that is required to precipitate excess calcium as $CaCO_3$.

Because calcium in the form of lime is not added to the system to satisfy the softener's hydroxide demand, soda ash is not often necessary, but it may be needed sometimes. If lime is required because of calcium ion demand, then soda ash addition is not necessary. Similarly, if soda ash is required because of a carbonate ion demand, then lime addition is not necessary.

Recirculating cooling waters usually contain corrosion or scale inhibitors, which interfere with the normal lime softening reactions. For example, scale and corrosion inhibitors such as dispersants, zinc, and trivalent chromium are removed by the softening process (Micheletti and Owen, 1979). In systems that use zinc-based corrosion inhibitors, this metal is precipitated along with the hardness and must be replaced (Goldstein and Griffin, 1975). It was reported that the softening process removes scale inhibitors such as polyphosphates to varying degrees depending on the type of compound and mode of system operation (Reed, 1977). On the other hand, scale inhibitor chemicals that act as crystal growth inhibitors such as polyphosphates can be expected to decrease the performance of a sidestream softener (Micheletti and Owen, 1979). The cost of replacing the inhibitor that is removed by softening must be compared to other costs such as the cost of replacing chemicals lost with blowdown and the cost of makeup water, both of which will increase without sidestream treatment (Frazer, 1975).

2.4 Ultra-High Lime Softening (UHL)

Lime softening is an attractive method to remove the scale-forming materials such as calcium, magnesium, and phosphate (Fair et al., 1968, and Clark et al., 1977). However, it is not effective in removing silica and it is limited to waters that are not high in chlorides or dissolved solids concentrations (Matson and Harris, 1979). The conventional lime softening process can be modified to the ultra-high lime process with good results (Batchelor et al., 1991, and Batchelor and McDevitt, 1984). A two-stage configuration for the ultra-high lime process is shown in Figure 2.2 (Batchelor et al., 1991). High pH and calcium concentration are maintained in the first stage, which result

in removal of silica by precipitation as a calcium silicate solid with solubility product of $10^{-7.9}$ (Batchelor and McDevitt 1984). Excess lime is added to the first stage to achieve high calcium concentration and high pH (pH11-pH12). Silica, magnesium, and phosphate are removed in this stage as solid precipitates. In the second stage, inorganic carbon is added as carbon dioxide or soda ash to remove calcium by precipitation as calcium carbonate. The pH of the effluent from the second stage is adjusted to the value desired for the cooling water system. This process could be applied to remove scale-forming chemicals from the makeup to a cooling water system, to a sidestream of the recycled cooling water, or to both. Depending on the composition of the water to be treated, this configuration might be modified to operate more economically by having a fraction of the flow bypass the first stage.

A configuration of the ultra-high lime process that is particularly attractive for application to recycled cooling water systems is shown in Figure 2.3 (Batchelor et al., 1991). In this configuration, a sidestream of the recycled cooling water is treated by the ultra-high lime process and the make-up stream is treated by lime softening.

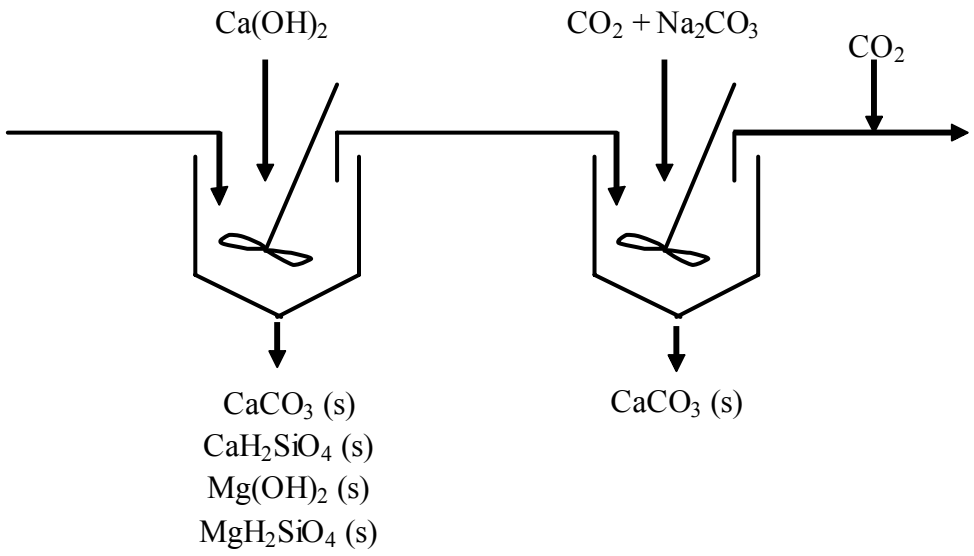

Figure 2.2 Two-stage configuration of ultra-high lime process (Batchelor et al., 1991).

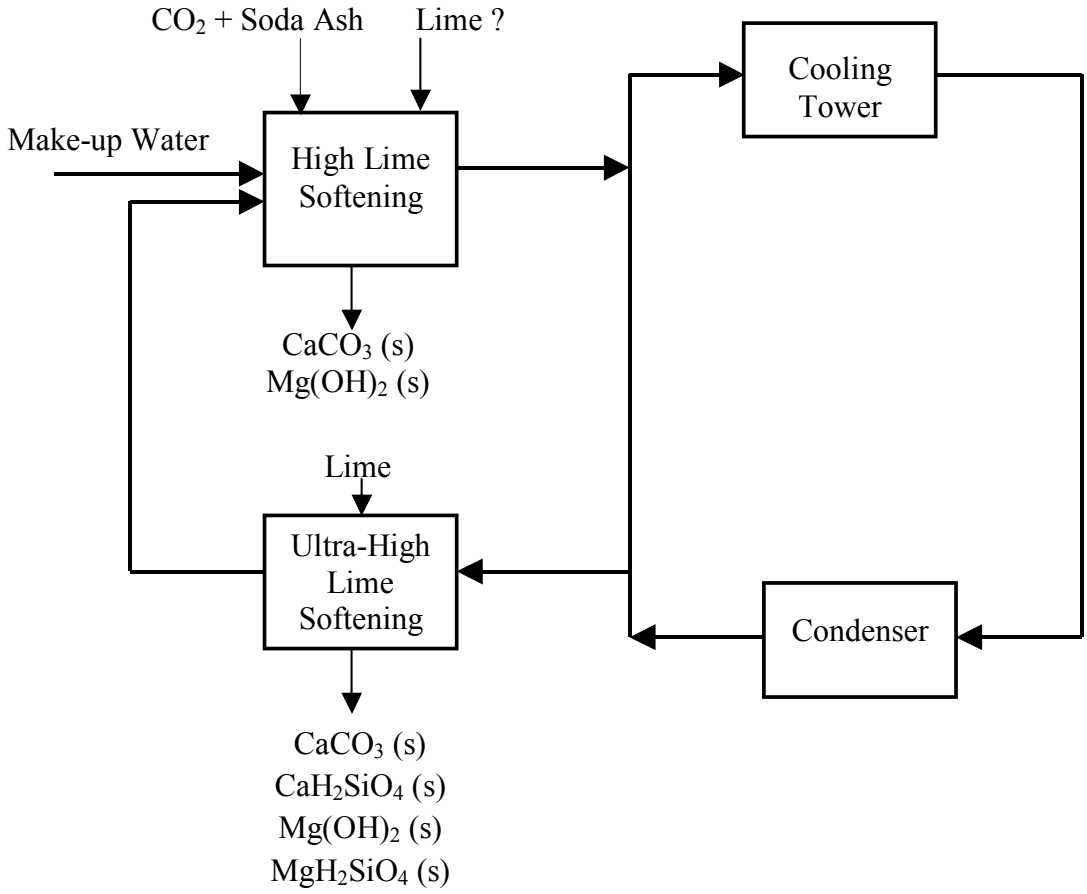

Figure 2.3 Combined configuration for ultra-high lime process (Batchelor et al., 1991).

2.5 Ultra-High Lime with Aluminum Process (UHLA)

Lime softening is an attractive method to remove the scale-forming materials. However it is not effective in removing silica, chloride, or sulfate. Ultra-high lime softening process (UHL) is an alternative to the lime softening process that can remove silica, but it is not effective in removing sulfate and chloride. Reverse osmosis, ion exchange, and electrodialysis can be used to remove chloride and sulfate (Masson and Deans, 1996; Rapp and Pfromm, 1998; and Ericsson and Hallmans, 1996). However, lime softening is the cheapest of all treatment alternatives for recycled cooling water (You et al, 1999). Furthermore, the use of other technologies is limited in many cases by operating problems such as fouling of membranes that lead to the need for frequent cleaning. They produce brine, which is also a problem to dispose (Westbrook, 1977). Furthermore, they are sensitive to water quality and water temperature (Balaban, 1991). Additionally, pretreatment is needed in most cases (Hoek et al., 2000).

The UHLA process is an innovative technology with excellent potential for improving industrial water use efficiency and achieving zero discharge. The high pH and calcium concentration found in the first stage in the two-stage configuration shown in Figure 2.2 allows for removal of sulfate by precipitation as calcium sulfoaluminate ($Ca_6Al_2(SO_4)_3(OH)_{12}$). Furthermore, the conditions found in the first stage of UHLA are suitable for removing chloride by precipitation as calcium chloroaluminate ($Ca_4Al_2Cl_2(OH)_{12}$). Capital costs for UHLA should be the same as for conventional lime softening, because the same equipment and techniques would be used. Operating costs of UHLA are expected to be slightly higher than those of conventional lime softening

due to the need to add aluminum. One way in which the UHLA process can be made more economically attractive is by reducing the cost of reagents. This could be accomplished by using waste alum sludge from water treatment plants as the source of some or all of the aluminum needed. This sludge contains approximately 39% aluminum by weight (Chu 1999). Every day about 10,000 tons of alum sludge are generated from water treatment plants and disposed (Dharmappa et al. 1997). Development of the UHLA process does not require development of new equipment. In fact, existing lime softening plants that have been used for many years may be able to convert to UHLA with minor modifications.

2.6 Sulfate Removal in the UHLA Process

Sulfate removal is required to facilitate recycle of cooling water. An important source of information about the behavior of sulfate at high pH is the chemistry of hydrated Portland cement and concrete. Sulfate is known to precipitate in cement porewaters in the form of a calcium sulfoaluminate called ettringite ($Ca_6(SO_4)_3Al_2(OH)_{12}$) (Clark and Brown, 2000; Perkins and Palmer, 1999; Myneni et al., 1998; and Lea, 1956). Ettringite is produced when gypsum (or gypsum saturated solutions) react with a phase such as tricalcium aluminate, calcium aluminate sulfate, or another source of calcium and aluminate ions. Ettringite was found to be stable in low silica and low carbon dioxide activity environments (Grutzeck and Roy 1985). Ettringite is stable above a pH of 10.7 and dissolved congruently with a log K_{sp} of –111.6 (± 0.8) (Myneni et al. 1998). Jones (1944) studied the stable and metastable mineral phases of

the $Ca(OH)_2 - Al_2(SO_4)_3 - H_2O$ system and the effects of alkali on the stability of these mineral phases in the alkaline pH range. He concluded that solid solutions of ettringite and monosulfoaluminate ($Ca_4Al_2(SO_4)(OH)_{12}.6H_2O$) formed in these systems and that they coexisted with portlandite, gypsum, and gibbsite. However, ettringite was found to be the most stable phase in the presence of highly alkaline and sulfate-rich solutions (Jones, 1944, and Damidot and Glasser, 1993).

UHLA treatment is capable of removing sulfate by precipitation of calcium sulfoaluminate ($Ca_6(SO_4)_3Al_2(OH)_{12}$) or calcium sulfoferrate ($Ca_6(SO_4)_3Fe_2(OH)_{12}$) (Batchelor et al., 1985; Nebgen et al., 1973; and Schaezler, 1978). The high pH and calcium concentration found in the first stage of the two-stage configuration shown in Figure 2.2 allows for removal of sulfate by precipitation as calcium sulfoaluminate. It was reported that when sufficient calcium was available, the molar ratio of sulfate removed to aluminum removed was 1.5, in agreement with theoretical stoichiometry (Batchelor et al. 1985). The kinetics of sulfate removal by precipitation of calcium sulfoaluminate was found to be rapid enough for practical application. Furthermore, aluminum and iron have been found to promote silica removal by precipitation and adsorption mechanisms (Lidsay and Ryznar 1939, and Bell et al. 1968).

2.7 Chloride Removal in the UHLA Process

The UHLA process has demonstrated the ability to achieve high sulfate removal efficiency. By expanding the process to also remove chloride, the UHLA process will be able to fill the need for a low-cost tool for improved industrial water management. The

conditions found in the first stage of ultra-high lime process allow for removal of chloride by precipitation as calcium chloroaluminate ($Ca_4Cl_2Al_2(OH)_{12}$). Limited knowledge exists on the formation of calcium chloroaluminate in aqueous solution. Most of the previous research has focused on its chemistry in concrete and hydrated Portland cement due to the effect of chloride on the corrosion of reinforcing steel in concrete (Worthington et al., 1988; Fu et al., 1996; Mehta, 1991; Janotka et al., 1992; Page et al., 1986; Hussain et al. 1995; and Rasheeduzzafar et al. 1992).

2.7.1 Calcium Chloroaluminate in Cement Chemistry

Calcium chloroaluminate is a layered double hydroxide (LDH) with chemical formula $Ca_4Al_2Cl_2(OH)_{12}$ that is also known as Friedel's salt (Rapin et al., 2002). This compound was mentioned for the first time in 1897 by Friedel, who studied the reactivity of lime with aluminum chloride (Friedel, 1897). Calcium chloroaluminate belongs to a family of solids known in cement chemistry as aluminoferrite mono (AFm) phases. Therefore calcium chloroaluminate is sometimes called chloro-AFm.

Aluminoferrite mono (AFm) family of solids belongs to a big family of layered materials called layered double hydroxides (LDHs). This class of compounds contains two kinds of metallic cations in the main layers and interlayer domains containing anionic species and water molecules (Renaudin et al., 1999b, and De Roy et al., 1992). This wide family of LDHs compounds is also referred to as anionic clays, by comparison with the more usual cationic clays whose interlamellar domains contain cationic species (Rives, 2001). LDHs contain divalent cation (M^{2+}) hydroxide sheets in which a fraction

of the M^{2+} sites have been substituted with trivalent cations (M^{3+}). The isomorphous substitution of the divalent cations with the trivalent cations develops permanent positive charge on the hydroxide layers that is counterbalanced by the interlayer anions (Crepaldi et al., 2000, and Goswamee et al., 1998). Figure 2.4 show a schematic diagram of an LDH's structure (You et al., 2002). The general chemical composition of LDHs can be represented as (Olanrewaju et al., 2000, Rives, 2001, and Ulibarri and Hermosin, 2001):

$$M^{2+}_x M^{3+}_y (OH)_{2x+3y-nz} (A^{n-})_z .mH_2O \qquad (2\text{-}4)$$

Where M^{2+} = divalent cations (Ca^{2+}, Mg^{2+}, Zn^{2+}, Co^{2+}, Ni^{2+}, Cu^{2+}, Mn^{2+}, but also the monovalent cation Li^{+}),

M^{3+} = trivalent cations (Al^{3+}, Cr^{3+}, Fe^{3+}, Co^{3+}, Mn^{3+}),

A^{n-} = interlayer anions with charge (n-) (almost freely selected, organic and inorganic anions), and

x, y, and z = The stoichiometric ratios of M^{2+}, M^{3+}, and A^{n-}

LDHs are of great academic, industrial, and environmental interest owing to their various potential applications. One of the remarkable features of LDHs is that the interlayer anions are exchangeable, and in addition, can be exchanged with various organic and inorganic charged compounds (Drits and Bookin, 2001). Because of the high anion-exchange capacity, LDHs can be used as adsorbents for anionic pollutants in aqueous media (Ulibarri and Hermosin, 2001). In addition, LDHs are resistant to high temperature treatments. Therefore, they are used as ion exchangers in some high temperature applications. It was reported that LDHs were used in the treatment of

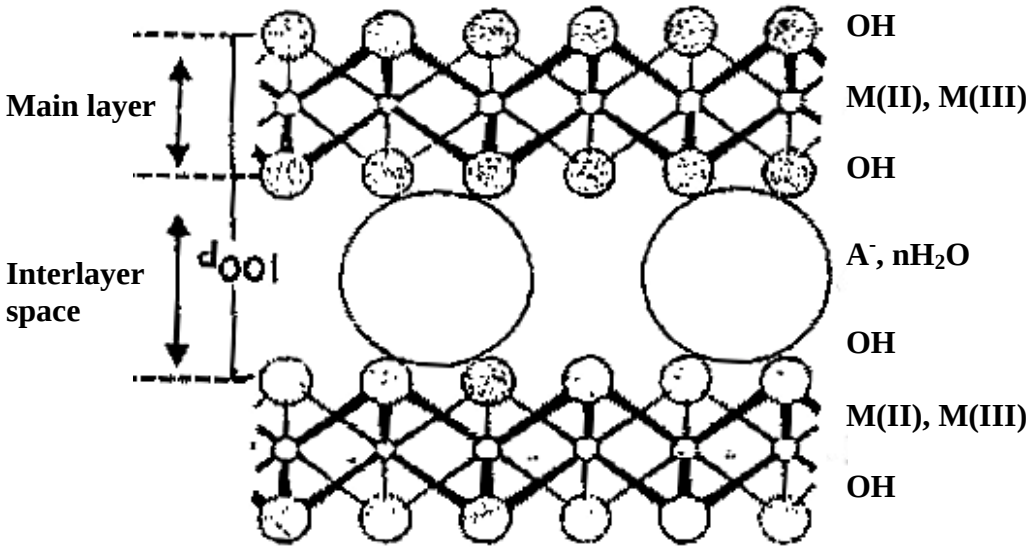

Figure 2.4 Schematic diagram of LDHs structure (You et al., 2002).

cooling water of nuclear reactors (Ulibarri and Hermosin, 2001).

AFm and Aluminoferrite tri (AFt) phases are calcium derivatives of LDHs in which octahedral sheets of $Ca(OH)_2$ are substituted with Al^{3+} or Fe^{3+} and the charge is neutralized by interlayer anions such as CO_3^{2-}, SO_4^{2-}, OH^-, NO_3^-, Cl^-, Br^-, I^-, etc (Rapin et al., 2002, Glasser et al, 1999, Birnin-Youri and Glasser, 1998; Rapin et al., 1999a; Rapin et al., 1999b; Francois et al., 1998; Renaudin et al., 1999a; Renaudin et al., 1999c; and Renaudin et al., 2000). Examples of the AFm phase are: calcium monosulfoaluminate ($Ca_4Al_2SO_4(OH)_{12}$) (Glasser et al., 1999), calcium chloroaluminate ($Ca_4Al_2Cl_2(OH)_{12}$) (Birnin-Youri, 1993), nitrated AFm phase ($Ca_4Al_2(NO_3)_2(OH)_{12}$) (Renaudin et al.,2000) while ettringite ($Ca_6Al_2(SO_4)_3(OH)_{12}$) is a well known example of AFt phases (Clark and Brown, 2000; Perkins and Palmer, 1999; and Myneni et al., 1998).

Calcium chloroaluminate is composed of positively charged main layers of composition $[Ca_2Al\ (OH)_6]^+$ and negatively charged interlayers of composition [Cl^-, $2H_2O$]. The chloride anions are surrounded by 10 hydrogen atoms, of which six belong to hydroxyl groups and four of water molecules (Rapin et al., 2002; Renauldin et al., 1999b; Glasser et al., 1999; and Birnin-Yauri and Glasser, 1998).

Inter-ionic exchange between two or more solids of AFm phases via the aqueous phase with which they are in contact is possible, because the interlayer anions in an AFm phase are loosely held by electrostatic forces. This exchange attains an equilibrium, thereby producing solid solutions of varying compositions (Birnin-Yauri, 1993; Glasser

et al., 1999; Birnin-Yauri and Glasser, 1998; Stronach, 1996; and Pöllmann, 1986). For example, in solutions containing OH^- and Cl^-, the interlayer Cl^- of calcium chloroaluminate can be replaced by OH^- from the aqueous phase to form hydroxyaluminate ($Ca_4Al_2(OH)_{14}$). When there is only partial replacement of the chloride, a solid solution is formed containing a mixture of chloroaluminate ($Ca_4Al_2Cl_2(OH)_{12}$) and hydroxyaluminate ($Ca_4Al_2(OH)_{14}$), which has been reported by several researchers (Birnin-Yauri and Glasser, 1998; Stronach, 1996; Pöllmann, 1986; and Turriziani, 1960). However, there is uncertainty about the composition of the solid solution. Glasser et al. (1999) reported that during preparation of calcium chloroaluminate, tetracalcium hydroxyaluminate ($Ca_4Al_2(OH)_{14}$) solid solutions occurred in several discrete hydration states as well as a partial breakdown to the more stable solids such as tricalcium hydroxyaluminate ($Ca_3Al_2(OH)_{12}$) and gibbsite ($Al(OH)_3$). Such behavior results in complicated X-ray diffraction (XRD) patterns with poor quality and leaves investigators the difficult task of assessing Cl^- substitution with OH^- in the solid phase (Glasser et al., 1999). Birnin-Yauri (1993) concluded from his results that solid solution between calcium hydroxyaluminate and calcium chloroaluminate was essentially complete and the XRD powder patterns changed with changes in the Cl/OH ratio of the solid.

Calcium chloroaluminate precipitation was reported to be fast. It has been reported that a crystalline precipitate of calcium chloroaluminate was formed immediately upon the addition of calcium chloride to a solution of Al_2O_3 and CaO (Wells, 1928). Different conclusions about the mechanism of calcium chloroaluminate

formation in porewaters of hydrated cement were drawn. According to Ben-Yair (1974), the formation of calcium chloroaluminate is due to a direct chemical reaction between tricalcium aluminate $(CaO)_3.Al_2O_3$, (C_3A), and $CaCl_2$ salt. According to Yonezawa et al. (1988), the formation of calcium chloroaluminate salt involves an ion exchange between the OH^- ions present in the interlayers of the C_3A hydrates and the free chloride ions. According to Lambert et al (1985), the removal of free chloride ions from the aqueous phase to form calcium chloroaluminate salt would necessitate either the removal of an equivalent quantity of cations from the aqueous phase or the entry of other anions to aqueous phase to maintain the ionic charge neutrality in the pore solution. The OH^- ions from the $Ca(OH)_2$ crystals are the main source of anions to balance the charge. In another study, it was reported that in the presence of NaCl, calcium chloroaluminate salt forms by two mechanisms: an adsorption mechanism and an anion exchange mechanism (Suryavanshi et al., 1996).

The solubility product of calcium chloroaluminate in porewaters of hydrated Portland cement was found to be low (Birnin-Yauri and Glasser, 1998, and Abate and Scheetz, 1993). Birnin-Yauri and Glasser (1998) studied the system at 20 ± 2^oC by mixing Friedel's salt with water at solid/liquid ratio of 1:10 and agitated the mixture for 28 days. The average value of log (K_{sp}) obtained by Birnin-Yauri and Glasser was -27.10. This value agreed with the value of -27.09 that was reported by Naken and Mosebach (1936) who studied the system $CaO-Al_2O_3-CaCl_2-H_2O$ at 30^oC. However, the later observed the presence of tri-calcium aluminate as an impurity along with the Friedel's salt and their results were based on the crystallization rather than dissolution.

2.8 Flow Streams and Parameters of Ultra-High Lime with Aluminum Process in A Cooling Water System

A schematic diagram of flow streams and parameters of UHLA in a cooling water system is shown in Figure 2.5. The dissolved ion concentrations in the makeup water, blowdown, and drift are C_M, C_B, and C_D, respectively. Because the sources of blowdown and drift are from the recirculating cooling water, it is assumed that the dissolved ion concentrations in the blowdown and drift (C_B and C_D) are identical to that in the cooling tower basin (C_T). Dissolved ions remain with the cooling water during evaporation. Therefore, the ion concentration, C_E, in the water vapor plume is zero.

A water balance of the cooling water around the whole system in Fig 2.5 assuming the water density are the same for all the flow streams in the system gives,

$$Q_M = Q_E + Q_D + Q_B \qquad (2\text{-}5)$$

Where: Q_M = cooling tower makeup water flow rate (L^3T^{-1})

Q_E = cooling tower evaporation water flow rate (L^3T^{-1})

Q_B = cooling tower blowdown water flow rate (L^3T^{-1})

Q_D = cooling tower drift water flow rate (L^3T^{-1})

A material balance of a non-volatile compound around the cooling tower can be made assuming that the concentration of the ion in the blowdown, C_B, and the drift, C_D, are the same as that in the cooling tower basin (C_T). The system boundary for this balance is shown by dotted line in Fig. 2.5.

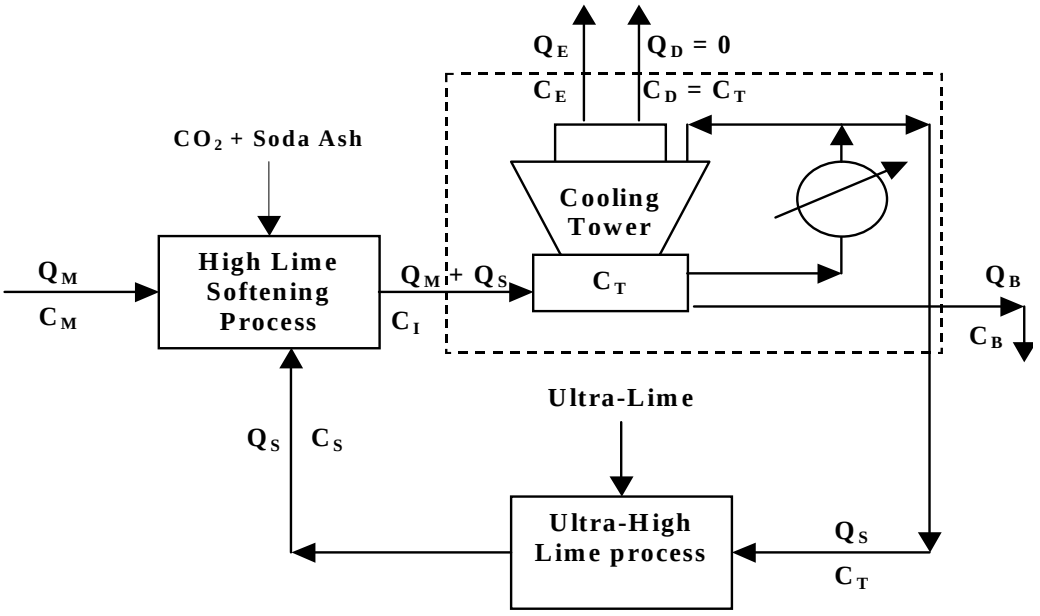

Figure 2.5 Schematic of flow streams and parameters in UHLA process.

$$(Q_M + Q_S)\, C_I = Q_D\, C_T + Q_B\, C_T + Q_S\, C_T = C_T\, (Q_D + Q_B + Q_S) \qquad (2\text{-}6)$$

where C_I = ion concentration from the treatment system to the cooling tower (ML^{-})

C_T = ion concentration exiting the cooling tower (ML^{-3})

Q_S = sidestream softener flow rate (L^3T^{-1})

Dividing both sides of Equation 2-6 by (Q_M * C_I) gives,

$$1 + \left(\frac{Q_S}{Q_M}\right) = \left(\frac{Q_D + Q_B}{Q_M} + \frac{Q_S}{Q_M}\right)\left(\frac{C_T}{C_I}\right) \qquad (2\text{-}7)$$

Substituting Equation 2-1 into 2-7 and rearranging, gives,

$$\frac{Q_S}{Q_M} = \left(\frac{C_I * COC - C_T}{(C_T - C_I) * COC}\right) \qquad (2\text{-}8)$$

Knowing the desired ion concentration in the cooling water (C_T) and the expected ion concentration in the treatment system effluent (C_I), the sidestream softener to makeup water flow rate ratio, (Q_M / Q_S) can be calculated for each cycle of concentration.

Q_E can be estimated using the following relationship, which is based on the assumption that all of the heat lost from the water in the cooling tower is due to evaporation (Jones, 1991).

$$Q_E = Q_C * \frac{C_p}{\Delta H} * \Delta T \;=\; Q_C * 0.001 * \Delta T \qquad (2\text{-}9)$$

Where: Q_C = cooling tower circulating water flow rate (gpm)

C_p = heat capacity of water ≅ 1 (BTU/lb)/^{o}F,

ΔH = latent heat of evaporation of water ≅ 1000 BTU/lb, and

ΔT = temperature difference across the heat source (e.g., condenser) (^{o}F).

The drift flow rate can be calculated as:

$$Q_D = \frac{\text{Drift Factor}}{100} * Q_C \qquad (2\text{-}10)$$

Where: Drift Factor (D_F) = design cooling tower drift flow rate as a percent of the cooling tower circulation flow rate (%). Its value depends on the operating conditions and design of cooling tower.

Drift flow rate is normally very low, minimized by drift eliminators installed in the air outlet at top of the cooling tower. Obtainable cooling tower drift factor of 0.003 % of the cooling tower circulation flow rate is normal (Jones, 1991).

2.9 Chemical Equilibrium Modeling

Chemical behavior in UHLA process is complicated and cannot be fully understood from only inspecting experimental data such as concentrations. This is due to the possibility of occurrence of mechanisms that are difficult to describe using only experimental results, such as solid-solutions formation and interactions among components in the system. Equilibrium models provide a powerful tool for predicting chemical behavior in such engineered systems, if the reactions are fast enough so that the assumption of equilibrium or metastable equilibrium is valid. They also help in developing understanding of the chemical behavior of a system and in interpreting experimental results. Furthermore, they can be used to predict effluent concentrations or

doses of chemicals by combining material balance equations with chemical equilibrium equations.

2.9.1 Solubility of the Solids

The solubilities of solid phases are determined experimentally by measuring the concentrations of relevant ions in a saturated solution of the solid phase. In most cases the concentrations of important species cannot be measured directly, but may be calculated from the total component concentration using well-known equilibrium constants and equilibrium models. For example, in calculating the solubility product of aluminum hydroxide solid using Al^{3+} and OH^- species, it is difficult to quantify the concentration of Al^{3+} experimentally but the total aluminum concentration can be measured easily in the laboratory. Then an equilibrium model can be used to predict the speciation among known soluble aluminum species. From the data obtained on the concentration of specific ionic species, a solubility product (K_{sp}) can be calculated. In general for the reaction,

$$A_m B_n (s) \quad = \quad mA^{+n}(aq) + nB^{-m}(aq) \qquad (2\text{-}11)$$

The solubility product (K_{sp}) is,

$$K_{sp} = \{A^{+n}(aq)\}^m \ \{B^{-m}(aq)\}^n \qquad (2\text{-}12)$$

Where {} indicate the activity of the species within the braces

This results if the activity of the pure solid phase is set equal to unity (Stumm and Morgan, 1996).

2.9.2 Activity and Ionic Strength

The ions in the solution have powerful interactions with each other due to their electrostatic charges. This results in deviations from ideality even in dilute solutions. Non-ideality can be accounted for by considering the activity of species as opposed to concentration. Activity and concentration are related by the equation (Stumm and Morgan, 1996):

$$\{C\} = \gamma [C] \qquad (2\text{-}13)$$

where: [C] is the aqueous concentration of the ion in the solution, γ is the activity coefficient.

The activity coefficient can be estimated from the ionic strength. The ionic strength of a solution describes the intensity of the electric field created by ions in the solution and is defined as follows. (Stumm and Morgan, 1996)

$$I = 0.5 \sum_{1}^{n} [C_i] Z_i^2 \qquad (2\text{-}14)$$

Where: I = ionic strength (mole/L)

$[C_i]$ = Concentration of the i^{th} ion (mole/L)

Z_i = charge (valence) of the i^{th} ion (dimensionless), and

n = total number of types of ions in the solution (dimensionless)

Various empirical expressions have been derived to calculate activity coefficients for each ion in solution as a function of the ionic strength and the charge of the ion (Morel and Hering, 1993, and Stumm and Morgan, 1996). The theoretical expressions

based on the Debye-Hückel limiting law together with more empirical expressions are given in Table 2.1.

Table 2.1 Individual ion activity coefficients (Stumm and Morgan, 1996).

Method	Equation	Applicability (ionic strength (M)
Debye- Hückel	$\log\gamma = -Az^2\sqrt{I}$	$< 10^{-2.3}$
Extended Debye-Hückel	$\log\gamma = -Az^2\frac{\sqrt{I}}{1+Ba\sqrt{I}}$	$< 10^{-1}$
Güntelberg	$\log\gamma = -Az^2\frac{\sqrt{I}}{1+\sqrt{I}}$	$< 10^{-1}$ useful in solutions of several electrolytes
Davies	$\log\gamma = -Az^2\left(\frac{\sqrt{I}}{1+\sqrt{I}} - bI\right)$	< 0.5

Where: I= ionic strength, γ_i = activity coefficient for the i^{th} ion, $A = 1.82*10^6\ (\varepsilon T)^{-3/2}$ (where ε = electric constant), A = 0.5 for water at 25 ^oC, Z = charge of ion, $B=50.3(\varepsilon T)^{-1/2}$, $B \approx 0.33$ in water at 25 ^oC , a = adjustable parameter (angstroms) corresponding to the size of the ion, b = constant, $b \approx 0.2$-0.3.

When the objective is to study the chemistry of concentrated solutions above the values of ionic strength indicated in Table 2.1, an approach more sophisticated than the semi-empirical formula becomes necessary. The activity coefficients must account for specific

as well as nonspecific ion interactions and exhibit a large increase at high ionic strengths. The most commonly used solution to this problem is the Bronsted specific ion interaction model and its extensions (Pitzer, 1991). The general formula for this model consists of a virial expansion of the form,

$$\mathrm{Ln}(\gamma_i) = \mathrm{Ln}(\gamma_{DH}) + \sum_i B_{ij}[S_j] + \sum_j \sum_k C_{ijk}[S_j][S_k] + \ . \ . \ . \ . \ . \qquad (2\text{-}15)$$

The first term is simply the Debye-Hückel activity coefficient. The second virial coefficients (B_{ij}) account for specific interactions among pairs of ions, the third virial coefficients (C_{ijk}) for specific interactions among three ions, and so on. [S_j] represent the molar concentration of a particular ion S_j (Pitzer, 1991). Up to ionic strength of about 4 M, good agreement with experimental data can be obtained using an expansion that stops with the second virial coefficients. The higher-order terms become important only in the most concentrated systems (Morel and Hering, 1993).

2.9.3 Modeling Programs

A wide range of computer-based techniques has been employed to predict chemical behavior in both natural and engineered systems. Most of the equilibrium modeling programs were developed from the ion-association model for seawater of Garrels and Thompson (1962) (Stronach, 1996).

EQUIL was the first of these programs that introduced Newton's method to titration calculations in analytical chemistry (Bos and Meershoek, 1972). The second family of equilibrium models used successive approximation programs for natural water equilibria. The Garrels-Thompson method was the first of this type, with the calculations

being done by hand rather than by computer (Garrels and Thompson, 1962). Other first generation programs of this type are WATEQ (Truesdell and Jones, 1974), SOLMNEQ (Kharaka and Barnes, 1973), and EQ3 (Wolery, 1992). WATEQ was revised and translated into the programming language FORTRAN by Plummer et al (1976) and renamed WATEQF. Newton-Raphson programs for experimental and natural waters were the third group of programs. MINEQL (Westall et al., 1976) and MINTEQA2 (Allison et al., 1991) were among these programs that make use of Gaussian elimination to solve the simultaneous matrix of equations. The final type of programs were those that simulated the reaction pathway. PATHI is an example of this type of program which takes the general approach of describing a partial equilibrium reaction path in terms of ordinary differential equations that are linear and can be solved by matrix algebra (Helgeson et al., 1970).

Parkhurst et al., (1980) wrote the program PHREEQE, which was coded in the FORTRAN language. PHREEQE could calculate pH, redox potential, and mass transfer as a function of reaction progress and it can determine the composition of solutions in equilibrium with multiple phases. PHREEQC version 1 (Parkhurst, 1995) was a completely new program written in the C programming language that implemented all the capabilities of PHREEQE and added many capabilities including ion exchange equilibria, surface-complexation equilibria, fixed-pressure gas phase equilibria, and advective transport.

PHREEQC version 2 (Parkhurst, 1999) is a modification of PHREEQC version 1 that retains all the capabilities of version 1 and adds several new features, including

kinetically controlled reactions, solid solution equilibria, fixed-volume gas-phase equilibria, and isotope mole balance in inverse modeling. A powerful inverse modeling capability allows identification of reactions that account for observed water compositions along a flow-line or in the time course of an experiment. An extensible chemical database allows application of the reaction, transport, and inverse-modeling capabilities to almost any chemical reaction that is recognized to influence rain-, soil-, ground-, and surface water quality.

The input to PHREEQC is free format and is based on chemical symbolism. Balanced equations, written in chemical symbols, are used to define aqueous species, exchange species, surface-complexation species, solid solutions, and pure phases, which eliminates all use of index numbers to identify elements or species. A graphical user interface with charting options is available for version 2. The free-format structure of the data, the use of order-independent keyword data blocks, and the relatively simple syntax facilitate the generation of input data sets with a standard editor. The C programming language allows dynamic allocation of computer memory, so there are very few limitations on array sizes, string lengths, or numbers of entities, such as solutions, phases, sets of phases, exchangers, solid solutions, or surfaces that can be defined to the program. PHREEQC uses the extended Debye- Hückel equation or Davies equation to account for the non-ideality of aqueous solutions.

2.9.4 INVRS K

In order to develop a model that is capable of predicting chemical behavior accurately in the UHLA process, the values of unknown equilibrium coefficients have to be determined. Information about formation of solid phases that are possibly formed in UHLA process is available only in research that is related to cement chemistry. Solubility products of such compounds have not been investigated in systems similar to those found in water and wastewater treatment systems. The usual means of estimating equilibrium constants is to calculate them directly from the measured experimental data. The solubility products of many solids are easily measured experimentally. In systems such as UHLA process in which the precipitated solids have to be identified and their solubility products have to be determined, it is not possible to determine the solubility products directly from the experimental data. Furthermore, because the solid-solution formations in such systems occurred in several discrete hydration states, this behavior results in complicated X-ray diffraction (XRD) patterns with poor quality and it becomes difficult to identify precipitated solids in such systems based on XRD diffraction (Glasser et al., 1999).

The total concentration of a component in the solution is non-linearly related to each of its species or to solid phases containing this element. Nonlinear regression, like linear least squares regression, determines the values of the parameters that minimize the sum of the squares of the errors. However, an equation having nonlinear dependence on its parameters requires that the answer be converged upon in an iterative fashion.

INVRS K (Schwantes, 2002) integrates a Gauss-Newton nonlinear regression routine (Chapra and Canale, 1998) with the chemical equilibrium modeling power of PHREEQC (Parkhurst, 1999) to enable inverse calculations of unknown or poorly defined equilibrium constants. Given at least the number of sets of experimental data for solutions of differing chemical character that have sufficiently approached chemical equilibrium with respect to the particular master species of interest, INVRS K will usually converge on the actual values of unknown equilibrium constants. The iterative process by which INVRS K converges is based on a Gauss-Newton non-linear regression routine. Initial information is input by the user and usually includes the chemical and physical description of each data set and initial guesses for unknown constants. INVRS K then writes an input file that can be read by PHREEQC and that defines the number of simulations to be conducted as the number of unknown constants to be calculated plus one. It also transfers information to be used by PHREEQC to generate a series of selected output files during each run. The first in the series of simulations and selected output files produced corresponds to hypothetical equilibrium state reached by PHREEQC for the initial guesses of the unknown constants. Each subsequent simulation makes a small change in the equilibrium constant of a single unknown and recalculates equilibrium. The results of these simulations provide the necessary information for calculating the partial derivative of the master species in each of the batch systems with respect to each of the unknown constants.

Once PHREEQC finishes running, INVRS K proceeds by reading the data (total master species concentrations in solution) from each of the selected output files. Error

analysis determines whether the initial guesses for the equilibrium constants predict chemical behavior within acceptable limits. The sum of the squares of the residuals of calculated batch systems is used to quantify goodness of fit and if it is not acceptable, the change in each equilibrium constant is calculated based on Gauss-Newton non-linear regression. These changes are included in a new input file that is used to initiate the next iterative cycle. A flow diagram is provided in Figure 2.6 to better illustrate the flow of INVRS K.

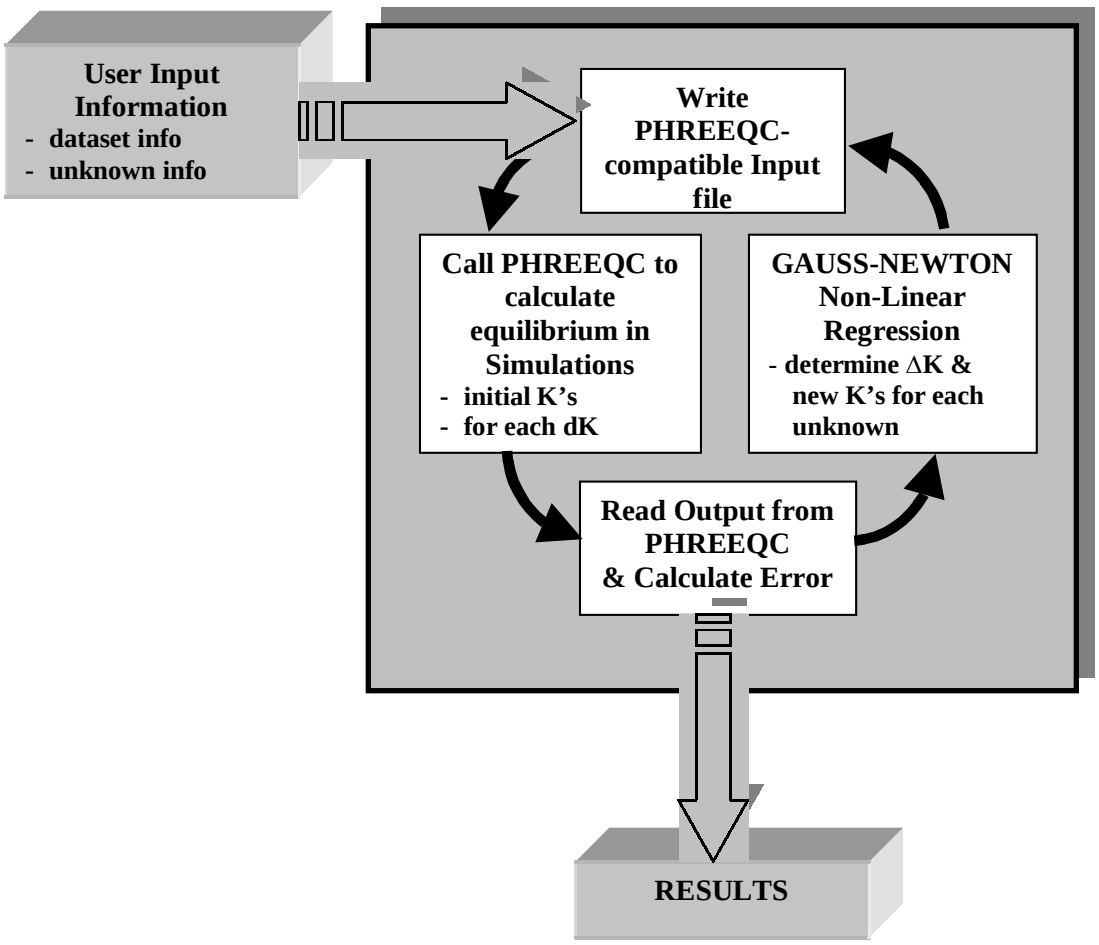

Figure 2.6 Flow diagram of the INVRS K (Schwantes, 2002).

CHAPTER III

MATERIALS AND METHODS

3.1 Experimental Plan

A four-part experimental plan was conducted to meet the four objectives for this research. First, experiments were conducted to study the kinetics of calcium chloroaluminate precipitation and to obtain the reaction time for equilibrium experiments. Additionally, a set of preliminary equilibrium experiments to develop the best experimental and analytical procedures was conducted. Second, equilibrium experiments were conducted to evaluate the characteristics of chloride precipitation as affected by lime dose, aluminum dose, initial chloride concentration, pH, and temperature. Third, the effect of the presence of sulfate or silica on chloride precipitation was investigated by conducting similar equilibrium experiments at three different concentrations of chloride in the presence of various concentrations of sulfate or silica. Finally, equilibrium model development was performed using two computer programs, PHREEQC and INVRS K. The model was developed concurrently with the completion of the first three tasks.

3.2 Chemicals and Reagents

The chemicals used in this research were: calcium hydroxide (USP, Fisher), sodium aluminate (VWR), sodium chloride (ACS 99.7%, Fisher), calcium chloride dihydrate (USP, Fisher), sodium sulfate (USP, Fisher), sodium silicate nanohydrate (ACS, Fisher), sodium carbonate (ACS 100%, Fisher), sodium bicarbonate (ACS, 100%,

Fisher), potassium chloride (USP, Fisher), strontium chloride (ACS, Fisher), nitric acid (trace metal grade, 70%, Fisher), acetic acid (trace metal grade, 99.7%, Fisher), sulfuric acid (trace metal grade 95%, Fisher), sodium hydroxide (1.0 M, 0.2 M, Fisher), ethylenediamine-tetraacetic acid (EDTA) (0.25 M, Fisher), ascorbic acid (99.7%, Fisher), eriochrome cyanine R (Sigma), methyl orange (ACS, Fisher), sodium acetate (99.5%, Fisher), Ionic Strength Adjustment Buffer (sodium nitrate, 5M, Fisher), ammonium molybdate (ACS, Fisher), oxalic acid (99%, EM), ascarite II (Thomas Scientific).

All solutions were prepared with decarbonated deionized water (DI water, hereafter) purified with a Barnstead Nanopure system to greater than 18 MΩ and degassed by purging with nitrogen gas. All lab ware was cleaned according to the following protocol: (1) soak 24 hours in 2 % laboratory detergent (VWR), (2) soak 24 hours in 10% nitric acid, (3) wash and rinse at least five times with deionized water; and dry before use. The stock solutions of sodium chloride, sodium sulfate, and sodium silicate were prepared daily by dissolving appropriate amounts of the chemical reagents in the DI water. All primary standard solutions (aluminum, calcium, chloride, sulfate, and silicon) were reagent grade chemicals (Fisher). Secondary standard solutions used in samples calibration curves were freshly prepared daily from the primary stock solutions by dilution with DI water.

3.3 Experimental Procedures

High-density polyethylene (HDPE) sealed plastic bottles (250 mL) were used as completely mixed batch reactors for kinetic and equilibrium experiments. To avoid CO_2 transfer from atmosphere into solution, the reactors were put in a closed container with a CO_2 absorbent (Ascrite II, Fisher) during the reaction time. After the addition of chemical reagents, the reactors were rapidly closed, tightly sealed, and mixed by shaking at room temperature (23 – 25^{o}C). However, experiments that were conducted to study effect of temperature were mixed at the desired temperatures using a controlled temperature shaker. Reaction time for all equilibrium experiments was set at two days based on the results of kinetic experiments that showed that chloride removal is fast, being essentially complete at the first sampling time of one hour. At the end of the reaction time, the reactors were removed from the shaker and pH of the solutions was measured before filtration. Then samples were taken from the reactors with a plastic syringe and filtered with 0.45 μm Whatman® membrane filters (VWR). After filtration, samples were acidified to below pH 2 and stored in the refrigerator until analysis.

Experiments that studied the effect of lime dose, effect of aluminum dose, effect of initial chloride concentration, effect of sulfate, and effect of silica were similar in their experimental procedures. However, experiments that studied effect of pH and effect of temperature were slightly different.

3.3.1 Kinetics of Chloride Removal

An experiment was conducted in order to study the kinetics of chloride removal and to obtain the time required to reach equilibrium or at least metastable equilibrium. This experiment was conducted by adding 40 mM lime and 20 mM sodium aluminate to a 30 mM solution of sodium chloride in sealed plastic bottles. The reactors were shaken at 250 rpm at room temperature. Samples were taken, filtered, and analyzed for chloride after reaction times of 1, 2, 4, 8, 12 hours, 1, 2, 5, and 10 days.

3.3.2 Effect of Lime Dose, Sodium Aluminate Dose, and Initial Chloride Concentration on Chloride Precipitation

A set of equilibrium experiments (48) was conducted at room temperature 23 - 25 °C to evaluate the effects of lime dose (0, 10, 30, 60, 90, 120, 150, and 200 mM) and sodium aluminate dose (0, 10, 20, 30, 40, 50, 60, 80, 100 mM) on chloride removal and to study the characteristics of calcium chloroaluminate precipitation. All combinations of these doses were investigated except at the aluminum dose of 60 mM the only lime doses investigated were 90, 120, 150, and 200 mM and at the aluminum doses of 80 mM and 100 mM the only lime dose investigated was 200 mM. Chloride concentration was fixed at 30 mM, which is an average concentration found in recycled cooling water systems (Matson and Harris 1979). The experiments were initiated by adding dry lime and dry sodium aluminate chemicals to a 200 mL of 30 mM NaCl solution in the reactor. NaCl solutions were prepared daily by dissolving the dry solid in DI water. After chemical additions, the reactors were capped rapidly and sealed in order to avoid CO_2

transfer from the atmosphere. Then the reactors were placed in closed plastic container with CO_2 absorbent (Ascrite II) and the container was sealed and placed on the shaker and mixed for two days at 250 rpm. At the end of the experiments, the reactors were released from the shaker and pH values of the solutions were measured in the reactors before filtration. An appropriate aliquot (10-20 mL) was taken from the reactor with a plastic syringe and filtered immediately into a plastic tube using 0.45 μm membrane filters. Then an aliquot of the sample was taken with an auto-pipette and was immediately diluted, acidified, and stored in the refrigerator until analysis. Samples were analyzed for total calcium (TOT(Ca)), total aluminum (TOT(Al)), and total chloride (TOT(Cl)).

Similar experiments were conducted to study the effect of initial chloride concentration (10, 50, and 100 mM) on chloride removal. Ratios of lime doses and aluminum doses to initial chloride concentration were kept constant at 400% and 160%, respectively. Those ratios were chosen based on results of previous experiments that studied the effect of lime dose and aluminum dose on chloride removal, which indicated that those are the optimum ratios for maximum chloride removal efficiency.

3.3.3 Effect of pH on Chloride Precipitation

A set of equilibrium experiments (27) was conducted in order to evaluate the effect of pH on chloride precipitation. A range of pH values (10.80 – 13.05) was investigated. Each pH was investigated at each one of three initial chloride concentrations (10, 50, and 100 mM). Calcium chloride ($CaCl_2$) was used as both a

source of chloride and a partial source of calcium in order to minimize the additions of lime required to supply the desired calcium doses. Lime and aluminum doses were set at 200% and 100% of the initial chloride concentration, respectively. Three solutions of acetic acid with concentrations of 0.1 M, 1.0 M, and 10.0 M were prepared and used to lower pH to the desired values. Similarly, three solutions of NaOH with concentrations of 0.1M, 1.0 M, and 10.0 M were used to raise pH to the desired values.

First, a set of experiments was conducted to obtain the amount of acetic acid required to lower the pH to the minimum desired value. These experiments were conducted by titrating solutions containing the desired concentrations of $CaCl_2$, $Ca(OH)_2$, and $NaAlO_2$ with acetic acid until the desired pH was obtained. During the titration, the solutions were mixed and nitrogen gas was passed over their surfaces. The concentration of acetic acid and pH obtained at each experimental condition are listed in Table 3.1.

Table 3.1 Experimental conditions for effect of pH experiments.

Initial $CaCl_2$ (mM)	$Ca(OH)_2$ dose (mM)	$NaAlO_2$ dose (mM)	Acetic acid (mM)	pH
5	15	10	43	10.80
25	75	50	183	10.82
50	150	100	330	10.87

Second, effect of pH experiments were conducted by adding the desired doses of lime and sodium aluminate chemicals to a 180 mL volume of a solution contains the desired concentrations of $CaCl_2$ and acetic acid (final volume, 200 mL, based). Then the reactors were closed tightly, sealed and mixed on the shaker for about one hour to equilibrate the solution with the acetic acid and to allow dissolution of the added solids (lime and sodium aluminate). Then the reactors were removed from the shaker and pH was adjusted to the desired pH value using NaOH while mixing using magnetic stirrer and flowing nitrogen gas on top of the solution. Then the volume of added NaOH was calculated and a certain volume of DI water equal [200 – (180 + volume of added NaOH solution) mL] was added to make up 200 mL final solution volume. Then the reactors were closed tightly, sealed, placed on a closed container with CO_2 absorbent, and mixed for two days. After that the reactors were released from the shaker and final pH values were measured before filtration then samples were taken, filtered, acidified, stored in the refrigerator, and analyzed for TOT(Ca), TOT(Al), and TOT(Cl).

3.3.4 Effect of Sulfate and Silica on Chloride Removal

A series of experiments (72) was conducted to evaluate interactions among the processes removing chloride, sulfate, and silica. Initial concentrations of each component were chosen to cover a range of possible applications of the UHLA process, such as cooling water treatment, membrane pretreatment, and brine treatment. Table 3.2 describes the experimental conditions for these experiments.

These experiments were conducted by first preparing stock solutions of NaCl and Na_2SO_4 (or Na_2SiO_3). A volume of the stock solution was added to the reactor along with sufficient DI water to make a total volume of 200 mL. Then, doses of lime and sodium aluminate were added to the solution as dry solids. The rest of experimental procedures were similar to previous experiments that studied the effect of lime dose and sodium aluminate dose on chloride precipitation. Samples were analyzed for pH, TOT(Cl), TOT(Ca), TOT(Al), and total sulfate (TOT(SO_4)) or total silica (TOT(Si)).

Table 3.2 Experimental conditions for experiments evaluating the effects of sulfate and silica.

Effect of sulfate				
NaCl mM	Na_2SO_4 mM	$Ca(OH)_2$ (% of (initial [Cl] + initial [SO_4]))	$NaAlO_2$ mM	No. of expts.
0.0, 10, 50, 100	10 , 50, 100	100%, 200%, 300%	0.5 lime dose	36
Effect of silica				
NaCl mM	Na_2SiO_3 mM	$Ca(OH)_2$ (% of (initial [Cl] + initial [SiO_3]))	$NaAlO_2$ mM	No. of expts.
0.0, 10, 50, 100	0, 1.5, 3.0	100%, 200%, 300%	0.5 lime dose	36

3.3.5 Aluminum – Chloride – Hydroxide Complexation

In order to test the hypothesis that Al-Cl-OH complexes are formed in equilibrium experiments at high aluminum concentration and high pH values, a set of experiments was conducted to evaluate the effect of aluminum concentration on the activity of free chloride ($\{Cl^-\}$) at high pH. Three experiments were conducted at three initial concentrations of $NaAlO_2$ (10, 20, 30 mM), while the initial chloride concentration was fixed at 10 mM. The pH was adjusted with NaOH to maintain a value of 12.70, which is the value at which high chloride concentration was observed at high aluminum doses in other experiments. Another reason of adjusting pH for this set of experiments was to minimize the variation in pH values among these experiments in order to minimize any effect that might result from pH change. Table 3.3 shows the experimental conditions for these experiments. The experiments were conducted by adding dry sodium aluminate solids to a solution that contained sufficient NaCl to achieve a concentration of 10 mM NaCl when the final volume of 200 mL was achieved. Then, volumes of 1.0 M NaOH were added so that that the total "free" hydroxide ion calculated from additions of $NaAlO_2$ + NaOH would be the same for all experiments. The same reactors and total sample volumes that were used in other experiments were used here. The reactors were closed, tightly sealed, and mixed for two days on the shaker. Then, the reactors were released from the shaker and pH was measured. After that, 2 mL of 5.0 M sodium nitrate (Ionic Strength Adjustment Buffer, Fisher) was added per 100 mL of solution (Orion, 2001). Then the activity of free chloride was measured in the reactor.

Table 3.3 Experimental conditions for Al-Cl-OH complexation experiments.

Initial NaCl (mM)	$NaAlO_2$ dose (mM)	NaOH (mM)	Final measured pH
10	10	50	12.77
10	20	40	12.73
10	30	30	12.67

3.3.6 Solubility of Aluminum Hydroxide Solid

A set of experiments (9) was conducted to evaluate the ion activity product (IAP) of the aluminum hydroxide solid that was formed. The experiments were conducted with a 50 mM initial concentration of $NaAlO_2$ and with a range of pH values (6.79 - 12.5) using the same reactors that were used in experiments that were previously described. The experiments were conducted by adding a sufficient amount of dry $NaAlO_2$ solid to achieve a concentration of 50 mM in the final solution volume of 200 mL. The pH of the solution was adjusted to values using HCl or NaOH, while mixing. Then the reactors were closed, sealed, and mixed for two days. After that, the pH of the solution was measured and samples were taken, filtered, and analyzed for TOT(Al). Then activities of Al^{3+} and OH^- were calculated with PHREEQC using the measured pH and measured total aluminum concentrations. Then the ion activity product (IAP) was calculated for each experimental condition.

3.4 Analytical Procedures

All analytical procedures were made following the Standard Methods for The Examination of Water and Wastewater (APHA, AWWA, WEF, 1995) and according to the instrumental instructions.

3.4.1 Chloride, Sulfate, and Nitrate

Cl^-, SO_4^{2-}, and NO_3^- were analyzed by a computerized Dionex DX-500 IC/HPLC equipped with a self-regenerating suppressor, a CD-20 conductivity detector, IonPac® AS9A-HC column (250 mm x 4 mm I.D., Dionex), and autosampler. The eluent was 10.0 mM Na_2CO_3 and the flow rate was 1.0 mL/min. Samples were automatically injected into the column through a 10 μL sample loop. Analyte concentration was quantified by comparing peak area to a standard calibration curve using an external standard method. Standards for calibration of 2, 5, 10, 20, 50, and 100 mg/L were prepared by dilution from 1000 ppm Fisher analyte standard solution. Samples were analyzed after dilution in duplicates and the results agreed well within 5%.

3.4.2 Calcium

Calcium was analyzed by flame atomic absorption spectroscopy (AAS), which utilizes a flame to provide a means of atomizing elements in an environment free of any surrounding chemicals. The AAS used was Perkin Elmer 460 and was employed in the analysis of calcium using air/acetylene flame with air flow rate of 21.5 L/min and acetylene flow rate of 3.5 L/min at wavelength of 422.7 nm and slit width of 0.7 nm. Calcium standards of 0.5, 1.0, 2.0, 3.0, and 5.0 mg/L were prepared for calibration

purpose by dilution from a 1000 ppm Fisher atomic absorption calcium standard. Ionization interference was minimized by the addition of 0.1% potassium (as potassium chloride) while aluminum interference was minimized by the addition of 0.5 % strontium (as strontium chloride). Method detection limit was 0.1 mg/L and the linear range was 0.0 – 5.0 mg/L. Samples were analyzed after dilution in duplicate and the results agreed well within 5%.

3.4.3 Aluminum

Total aluminum was determined by spectroscopic analysis using a computerized Agilent 8452 Diode-Array Spectrophotometer. Aluminum was measured using Eriochrome Cyanine R Method at wavelength of 535 nm (APHA, AWWA, WEF, 1995). The method detection limit was 10 μg/L and the linear range was from 0.0 to 200 μg/L. The concentration of aluminum was quantified by comparing absorbance to a standard calibration curve. Standards for calibration of 10, 50, 100, 150, 200, and 250 μg/L were prepared from 1000 ppm Fisher aluminum standard solution. Standards and samples preparation were prepared after dilution and analyzed following the procedures described for the method (APHA, AWWA, WEF, 1995). Samples were analyzed in duplicate and the results agreed well within 5%.

3.4.4 Silica

Silica was determined by spectroscopic analysis using the same spectrophotometer used in aluminum analysis. Molybdosilicate Method was used for quantification of silica at wavelength of 410 nm (APHA, AWWA, WEF, 1995). The

method detection limit was 0.1 mg/l (as Si) and the linear range was from 0.0 to 20 mg/L. The concentration of silicon was quantified by comparing absorbance to a standard calibration curve. Standards for calibration of 1, 5, 10, and 20 mg/L were prepared from 1000 ppm Fisher silicon standard solution. Samples were analyzed in duplicate and the results agreed well within 5%.

3.4.5 pH

pH was measured using a pH meter (Orion 420A) with an Orion Ross Sure-Flow combination electrode standardized with pH 10 (VWR) and pH 13.0 buffers. pH 13 buffer was prepared in our lab by mixing 25% of 0.2 M KCl with 66% of 0.2 M NaOH and 9% of DI water (Lide, 1991, and Dean, 1985).

In experiments that studied the effect of temperature on chloride removal, the pH of a sample was measured at the desired temperature by transferring the reactor from the temperature-controlled shaker quickly to a water bath that had the same temperature. The pH electrode was calibrated at the same temperature of the experiment by placing the calibration buffers in the same water bath for enough time to make sure that the buffers have the same temperature as the target samples before they were used in the calibration purpose. Then the electrode was calibrated and the pH of a sample was measured while the reactor and the buffer solutions are placed in the water bath. The pH values of the buffers that were used for the electrode calibration at the corresponding reaction temperature for pH 10 buffer (VWR) and for pH 13 buffer (Dean, 1985) are shown in Table 3.4.

Table 3.4 pH values of buffer solutions at the reaction temperatures.

Type of buffer	Temperature (^{o}C)				
	20	25	30	40	50
pH 10 buffer	10.05	10.00	9.95	9.87	9.81
pH 13 buffer	13.16	13.00	12.84	12.51	12.18

3.4.6 Activity of Free Chloride

The activity of free chloride $\{Cl^{-}\}$ was measured by an Orion Chloride Combination Electrode Model 96-17B connected with Orion pH meter Model 420A. Chloride activity of a sample was quantified without dilution by comparing electrode potential to a standard calibration curve. A three-point calibration of the electrode was conducted using standard chloride solutions (10, 100, 1000 ppm) at room temperature. A 10-ppm and a 100-ppm standard were prepared by dilution from the 1000-ppm chloride standard (Orion). In order to avoid the effect of ionic strength on the measurements, an amount of Ionic Strength Adjustment Buffer was added to the standard solutions and to the samples so that the resulting concentration of the buffer was 100 mM.

3.4.7 Identification of the Precipitated Solids

XRD spectroscopy was used to identify the solid phases formed in precipitation experiments. The solids were allowed to precipitate using the same procedures used in

equilibrium experiments. Eight solid samples were prepared, each one at different combinations or initial concentrations of chemical compounds used to form the solids (Cl, Ca, Al, SO_4, and SiO_2). The experimental conditions that were used in the equilibrium experiments to form the solids are listed in Table 3.5. The precipitated solids were collected by centrifugation. Then the separated solids were dried at room temperature in a CO_2-free atmosphere. The solids were scanned between 0^o and 80^o 2θ with a scan speed of 2^o /min by a Rigaku automated diffractometer using Cu Kα radiation.

Table 3.5 Experimental conditions used in preparing solids for XRD analysis.

Experiment No.	Experimental conditions				
	NaCl (mM)	Na_2SO_4 (mM)	Na_2SiO_3 (mM)	$Ca(OH)_2$ (mM)	$NaAlO_2$ (mM)
XRD10	10	0.0	0.0	20	10
XRD30	30	0.0	0.0	60	30
XRD50	50	0.0	0.0	100	50
XRD100	100	0.0	0.0	200	100
XRDCa	30	0.0	0.0	120	30
XRDAl	30	0.0	0.0	60	60
$XRDSO_4$	30	30	0.0	200	100
XRDSi	30	0.0	3.0	60	30

3.5 Equilibrium Model Development

A fundamental model of the chemical processes in UHLA was developed in order to predict final chloride concentration and chemical behavior in treated cooling water using information on the chemical doses and initial chloride concentration in the feed water. Precipitation was assumed to be the mechanism that controls the solubility of the species in the system. The model was based on the geochemical modeling software, PHREEQC (Parkhurst, 1999), and INVRS K (Schwantes, 2002). INVRS K integrates the modeling power of PHREEQC with a Gauss-Newton nonlinear regression routine to calculate values of unknown or poorly defined chemical equilibrium and kinetic constants. Initial conditions of 36 experimental data sets (solutions) representing various lime doses and aluminum doses were used in the simulations. Four parameters from each dataset, or a total of 144 measured values, were used as dependent variables during the regression. These parameters include the final soluble concentrations of chloride, aluminum, calcium, and corresponding solution final pH. Total initial concentrations for each data set and solids for which equilibrium constants were to be calculated, were defined in the PHREEQC input file. The remaining aqueous species and solids used by the model are defined in the database file. The initial input file, as well as a file containing dependent variable information, is introduced into INVRS K by the user. INVRS K then rewrites the user-defined input file to include additional simulations and the production of output files required by the regression routine. Subsequently, INVRS K calls PHREEQC to run the re-defined input file. PHREEQC used known thermodynamic data and initial guesses of unknown equilibrium constants specified in

the model to generate solution parameters within each of the simulations specified in the input file. Output generated by PHREEQC is then read and used by INVRS K to calculate the residuals of these parameters with respect to the experimental results. If the values of these residuals are within the specified tolerances, the acceptable values for each of the unknown constants are displayed. Otherwise, a Gauss-Newton non-linear regression routine is used to estimate the change in the unknown constants that will more accurately predict the experimental results. New values for each of the unknowns are then calculated. Another iteration of the regression process starts when INVRS K writes a new input file that incorporates the updated values of the unknown constants and once again calls PHREEQC. The original database that is used by PHREEQC was modified. Solids that are not expected to form in the system were excluded from the database Thermodynamic data for new solid phases were included in the input file. Input files for PHREEQC are shown in Appendix B.

Different hypotheses describing the chemical behavior of chloride removal by UHLA process were generated and tested. The process of hypotheses generation was based on available information in the literature and preliminary analysis of experimental results. A list of possible solid phases that are believed able to precipitate in the system and their solubility products is listed in Table 3.6. The solubility product of $Ca_4Al_2Cl_2(OH)_{12}$ was reported by two different researchers to have the value of $10^{-27.10}$ (Birnin-Yauri and Glasser, 1998, and Nacken and Mosebach, 1936) and it has been fixed in this study at that value throughout the model development. However, the solubility

products for $Ca_3Al_2(OH)_{12}$ and $Ca_4Al_2(OH)_{14}$ have not been studied previously in systems similar to recycled cooling water.

Different combinations of the solid phases $Ca_4Al_2Cl_2(OH)_{12}$, $Ca_3Al_2(OH)_{12}$, and $Ca_4Al_2(OH)_{14}$ were allowed to form with $Ca(OH)_2$ and $Al(OH)_3$ throughout the model development. The assumption that pure solids precipitated independently and the assumption that solid solutions were formed were tested with each of the combinations of different solid phases. Unknown solubility products were calculated each time with INVRS K. The model was tested and modified concurrently with the completion of the research objectives as will be described in more detail in Chapter IV.

Table 3.6 Solid phases that could be formed in Cl – OH system.

Solid phase	Log Ksp	Reference
$Ca_4Al_2Cl_2(OH)_{12}$	-27.10	(Birnin-Yauri and Glasser, 1998; Nacken and Mosebach, 1936)
$Ca_3Al_2(OH)_{12}$	unknown	-
$Ca_4Al_2(OH)_{14}$	unknown	-
$Ca(OH)_2$	-22.81	(Stumm & Morgan, 1996)
$Al(OH)_3$ (Gibbsite)	-33.50	

CHAPTER IV

RESULTS AND DISCUSSIONS

4.1 Kinetics of Chloride Removal with UHLA

An experiment to study the kinetics of chloride removal with UHLA was conducted by adding 40 mM lime and 20 mM sodium aluminate to a 30 mM solution of sodium chloride. Samples were taken at various times and analyzed for chloride. Results are shown in Figure 4.1 and demonstrate that chloride removal is fast, being essentially complete at the first sampling time of one hour. This indicates that kinetics should not be a limitation to applying the UHLA process.

4.2 Evaluate Equilibrium Characteristics of Chloride Removal with UHLA

Forty-eight batch equilibrium experiments were conducted in order to evaluate chloride removal with UHLA. Solutions with 30 mM NaCl were used with a range of doses of lime (0 – 200 mM) and sodium aluminate (0 – 100 mM). Figure 4.2 shows the effect of lime dose and sodium aluminate dose on final chloride concentration. Good chloride removal was observed at reasonable ranges of aluminum dose and lime dose. Chloride concentration decreased with increasing doses of both lime and sodium aluminate. This indicates that precipitation of chloride with calcium and aluminum to form Ca-Al-Cl-OH precipitate is the proper mechanism that can describe chloride

---

Part of the data reported in this chapter is reprinted with permission from Abdel-Wahab, A.; Batchelor, B. (2002) Chloride Removal from Recycled Cooling Water Using Ultra-High Lime with Aluminum Process. *Water Environ. Res.*, **74,** 256.

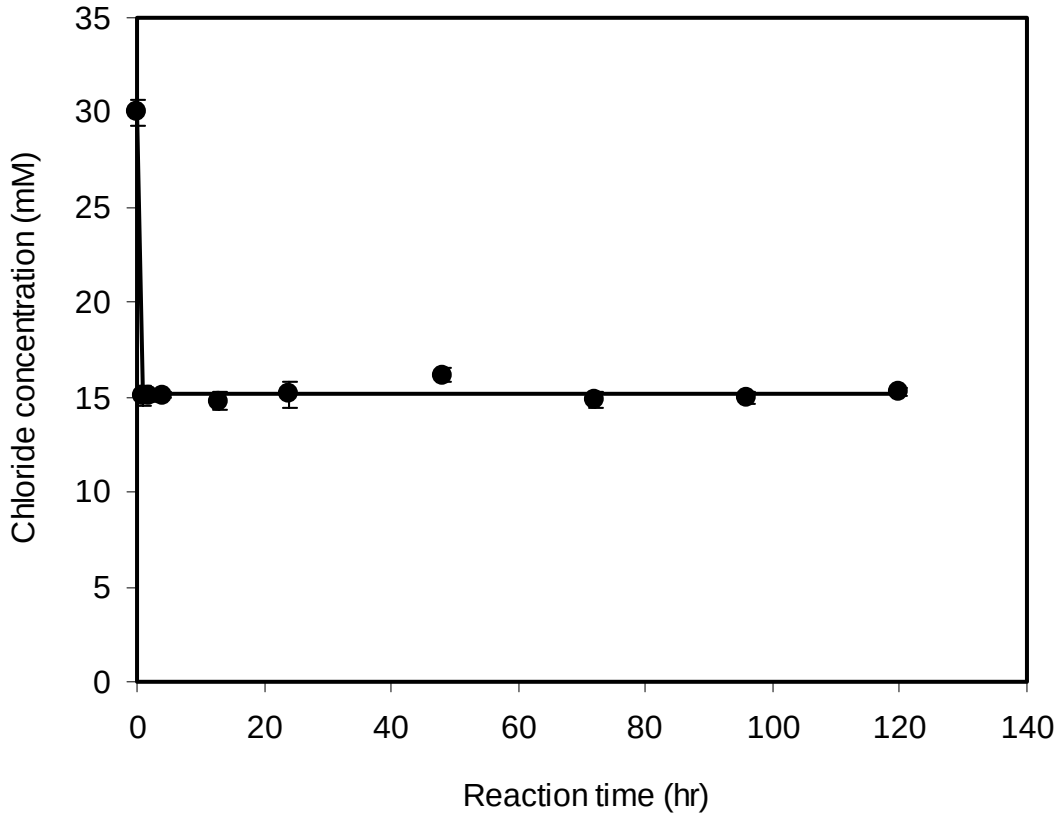

Figure 4.1 Kinetics of chloride removal with UHLA. Lime dose = 40 mM, sodium aluminate dose = 20 mM.

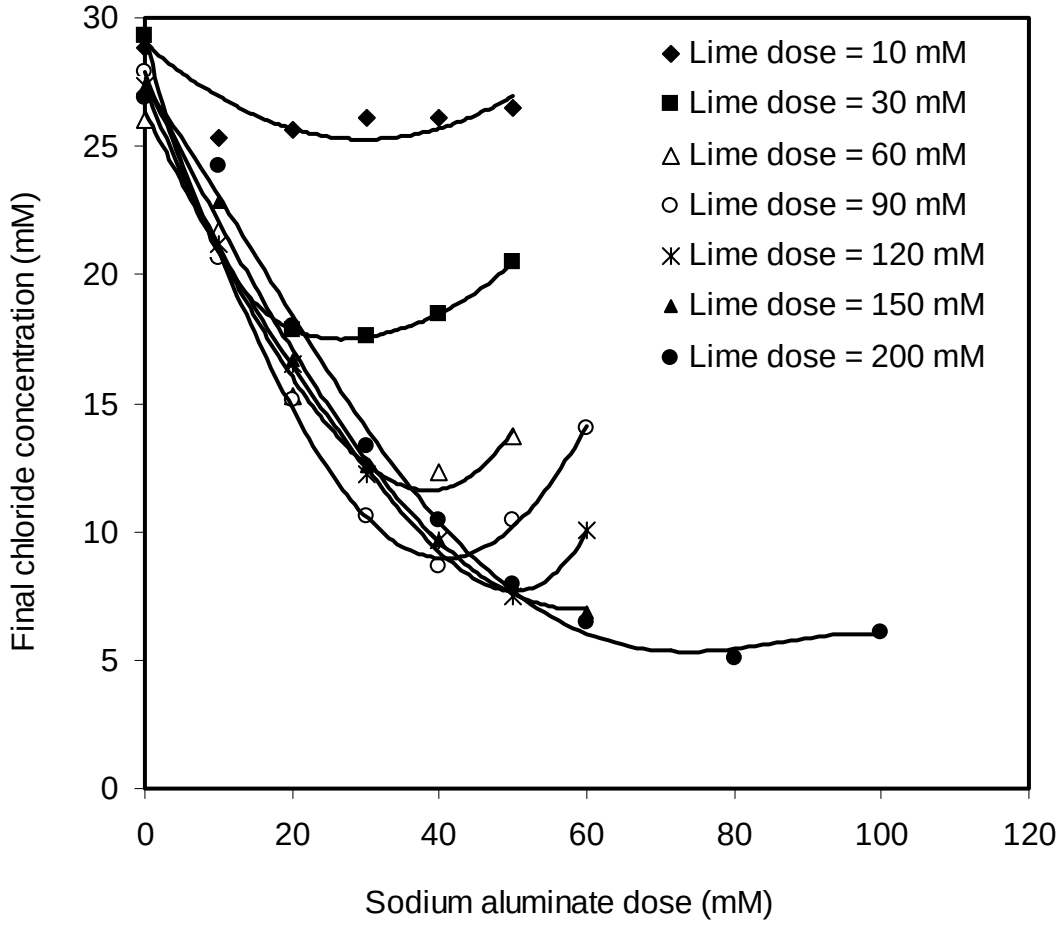

Figure 4.2 Effect of lime dose and aluminum dose on chloride removal.

removal with UHLA. The hypothesis was made that chloride removal was primarily controlled by calcium chloroaluminate ($Ca_4Al_2Cl_2(OH)_{12}$) precipitation assuming the following reaction,

$$4Ca^{2+} + 2Al(OH)_4^- + 2Cl^- + 4(OH)^- = Ca_4Al_2Cl_2(OH)_{12}(s) \qquad (4\text{-}1)$$

However, deviations from the stoichiometry shown in Equation 4-1 occurred in the equilibrium experiments. If $Ca_4Al_2Cl_2(OH)_{12}$ is the only important solid that precipitates, then the ratio of aluminum removed to chloride removed ($\Delta Al/\Delta Cl$) should equal 1.0 and the ratio of calcium removed to chloride removed ($\Delta Ca/\Delta Cl$) should equal 2.0. Figures 4.3 and 4.4 show the effect of sodium aluminate dose on $\Delta Al/\Delta Cl$ and $\Delta Ca/\Delta Cl$, respectively. The observed stoichiometry shows that those ratios are usually higher than the theoretical stoichiometry. This deviation of the observed stoichiometry from that expected can be explained by the hypothesis that another solid phase was formed. Calcium hydroxyaluminate ($Ca_4Al_2(OH)_{14}$) could be formed by replacing two Cl^- ions in $Ca_4Al_2Cl_2(OH)_{12}$ with two OH^- ions to form $Ca_4Al_2(OH)_{14}$ and its formation could explain the observed stoichiometry. This hypothesis agrees with the results of other researchers that have been obtained in systems with Portland cement, but with a similar environment of high pH and presence of calcium and aluminum (Birnin-Yauri and Glasser, 1998, Glasser et al., 1999). Based on this hypothesis, the ratio of calcium removed to aluminum removed ($\Delta Ca/\Delta Al$) should equal 2. This occurs when there is a sufficient dose of aluminum to react with all the calcium in solution (Figure 4.5). When the ratio of aluminum dose to lime dose is ≥ 0.5 all the data fall around the theoretical

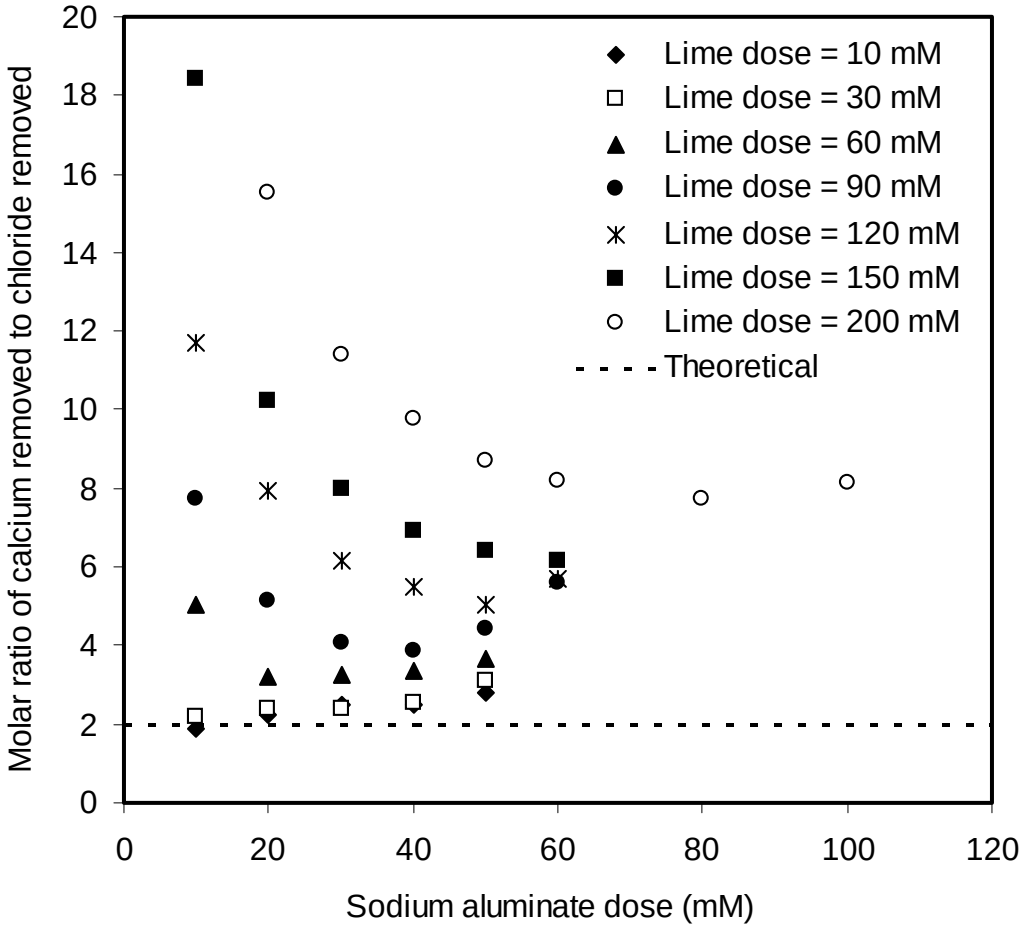

Figure 4.3 Effect of aluminum dose and lime dose on the molar ratio of calcium removed to chloride removed.

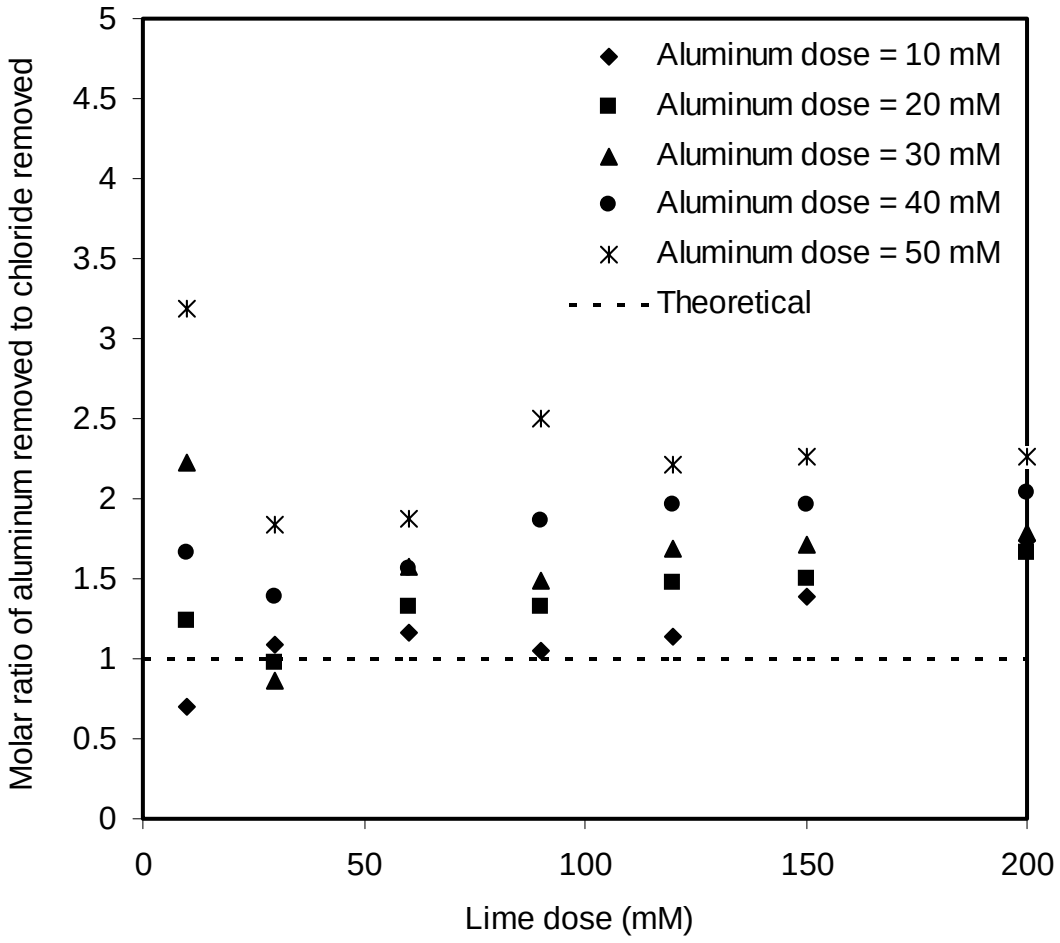

Figure 4.4 Effect of aluminum dose and lime dose on the molar ratio of aluminum removed to chloride removed.

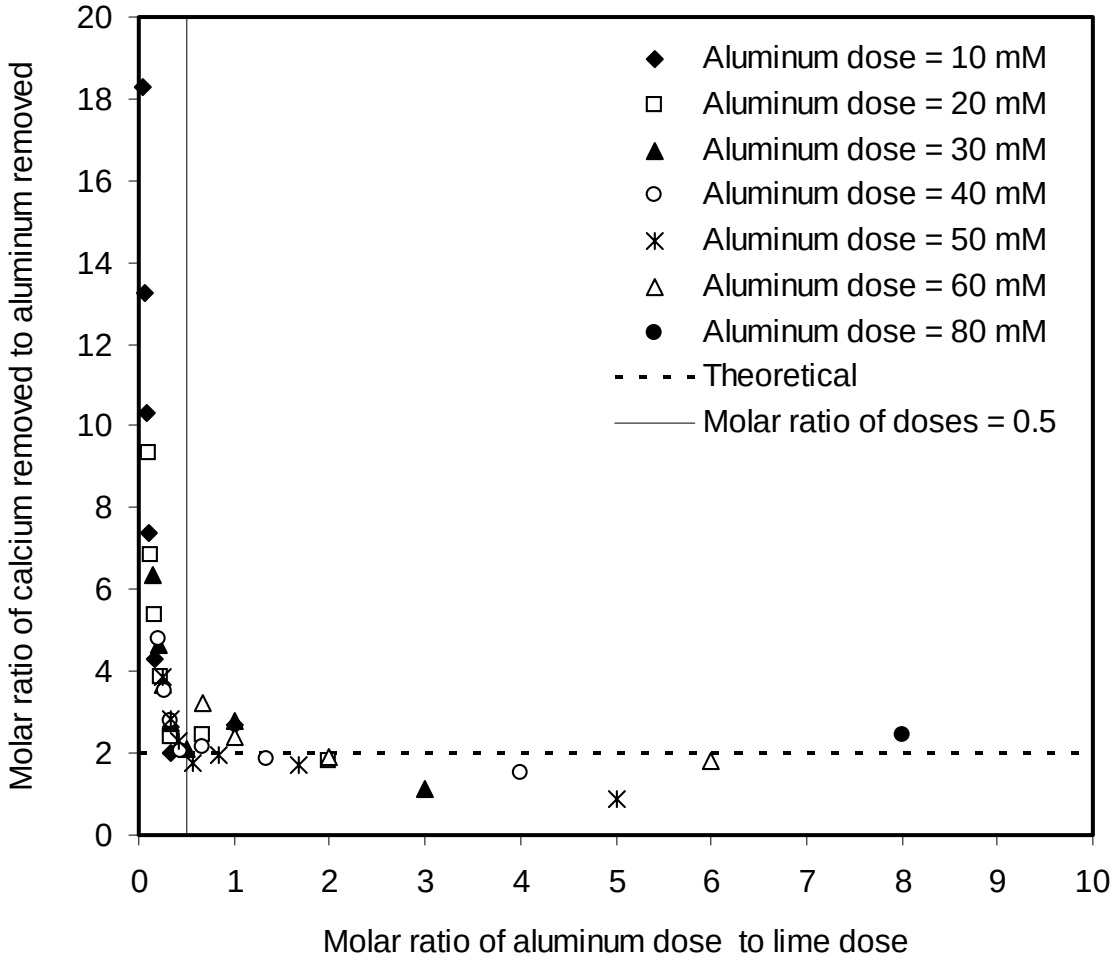

Figure 4.5 Effect of ratio of aluminum dose to lime dose on the molar ratio of calcium removed to aluminum removed.

stoichiometric ratio. However, when the aluminum dose is lower than the stoichiometric amount, the ratio of calcium removed to aluminum removed was higher than the theoretical stoichiometry. This was presumed to be due to the failure of some of the lime to dissolve.

Higher aluminum doses resulted in higher concentrations of aluminum. This occurs when there is not enough calcium to react with all the aluminum in solution to form Ca-Al-containing solid(s). Figure 4.6 shows the relationship of calcium concentration to aluminum concentration and demonstrates that high aluminum concentrations are possible when the concentration of calcium is low.

The optimal ratio of lime dose to aluminum dose to achieve maximum chloride removal was found to be about 2.5 (Figure 4.7). Higher aluminum doses also resulted in some increase in chloride concentration (Figure 4.2). The increase in chloride concentration at higher aluminum doses was initially hypothesized to be the result of the formation of soluble aluminum-chloride-hydroxide complexes. Higher concentrations of aluminum could form complexes with the chloride ion resulting in higher total chloride concentrations (Cl^- and complexes) in solution. A set of equilibrium experiments was conducted to test this hypothesis. The activity of free chloride $\{Cl^-\}$ was measured in solutions containing aluminum and chloride and high pH. Results of these experiments showed evidence that there were no chloride complexes being formed in the system. No change in chloride activity was observed over a range of aluminum concentrations (Table 4.1).

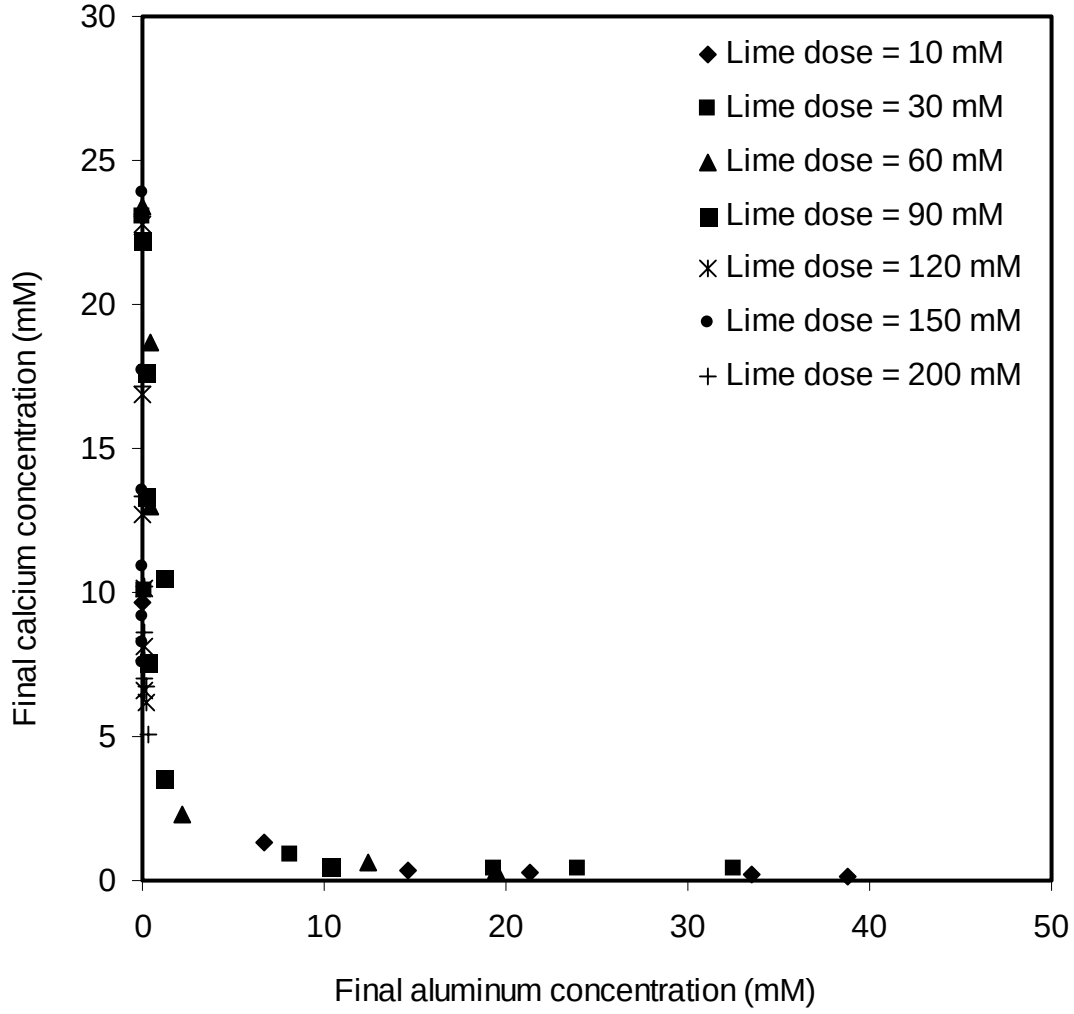

Figure 4.6 Relationship between soluble calcium concentrations and soluble aluminum concentrations.

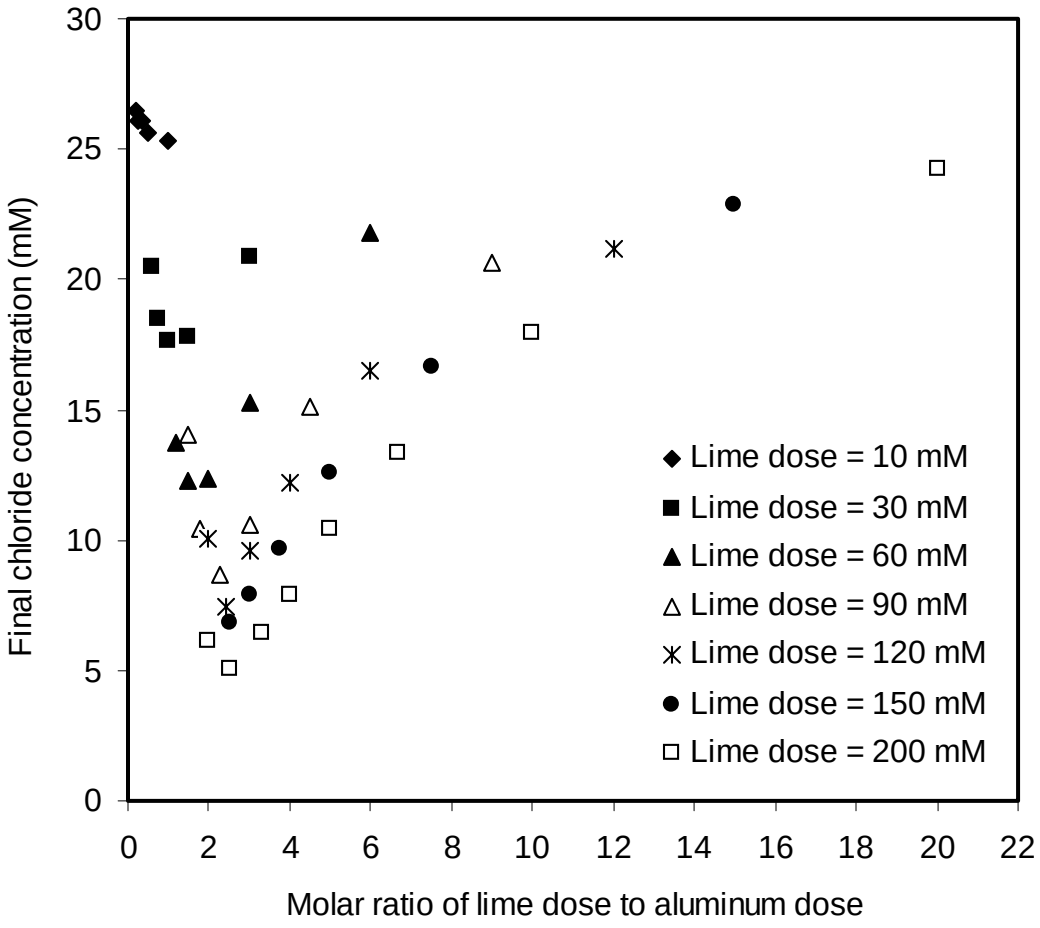

Figure 4.7 Effect of ratio of lime dose to aluminum dose on chloride removal.

Table 4.1 Effect of aluminum concentration on chloride activity.

Aluminum concentration (mM)	10	20	30
Measured chloride activity (mM)	9.98 ± 0.03	10.07 ± 0.11	10.21 ± 0.16
Solution pH	12.77	12.73	12.67

4.3 An Equilibrium Model for Chloride Removal with UHLA

4.3.1 Chemical Behavior of Chloride Removal with UHLA

In an effort to further understand the behavior of chloride in the UHLA process and the mechanisms of chloride removal, a fundamental chemical equilibrium model of the chemical processes was developed. Experimental data obtained from studying the effects of lime dose and aluminum dose on chloride removal were used in the model development as described in detail in Chapter III.

Different hypothesis were developed and tested. The standard error in the model-predicted concentrations for the dependent variables was compared for each hypothesis. Error analysis indicated that the experimental results of chloride removal with UHLA could be best described by assuming the formation of an ideal solid solution of calcium chloroaluminate ($Ca_4Al_2Cl_2(OH)_{12}$), tricalcium hydroxyaluminate ($Ca_3Al_2(OH)_{12}$), and tetracalcium hydroxyaluminate ($Ca_4Al_2(OH)_{14}$). When calcium or aluminum concentrations are above the stoichiometric amount needed to form the solid solution,

the model allows formation of solids such as $Ca(OH)_2$ or gibbsite ($Al(OH)_3$). The solubility products of tricalcium hydroxyaluminate and tetracalcium hydroxyaluminate were determined with INVRS K to be $10^{-19.72}$ and $10^{-25.02}$ respectively, assuming the following reactions,

$$Ca_3Al_2(OH)_{12} = 3Ca^{+2} + 2Al(OH)_4^- + 4OH^- \qquad \text{Log } K_{sp} = -19.72 \qquad (4\text{-}2)$$

$$Ca_4Al_2(OH)_{14} = 4Ca^{+2} + 2Al(OH)_4^- + 6OH^- \qquad \text{Log } K_{sp} = -25.02 \qquad (4\text{-}3)$$

The results of INVRS K simulations for calculating Log K values are shown in Appendix C-1.

Table 4.2 shows the error analysis for predicted concentrations of chloride, aluminum, and calcium as well as pH values. The average values of absolute error are low for all the constituents. Also, the results of linear regression of the residuals with ratio of lime dose to aluminum dose show that the values of all the coefficients of determination (r^2) and slopes are low. This shows that there is not a consistent bias in the predictions of the model. These results indicate that the model can adequately predict chemical behavior that results in chloride removal with UHLA. The values of predicted concentrations of chloride, calcium, and aluminum as well as pH values compared to measured values are shown in Appendix C-2.

Figure 4.8 shows comparison between measured and model-predicted concentrations of chloride and indicates that the model adequately predicted the measured concentrations of chloride. The predicted and measured concentrations of chloride followed the same trend of decreasing to a minimum and then increasing as the

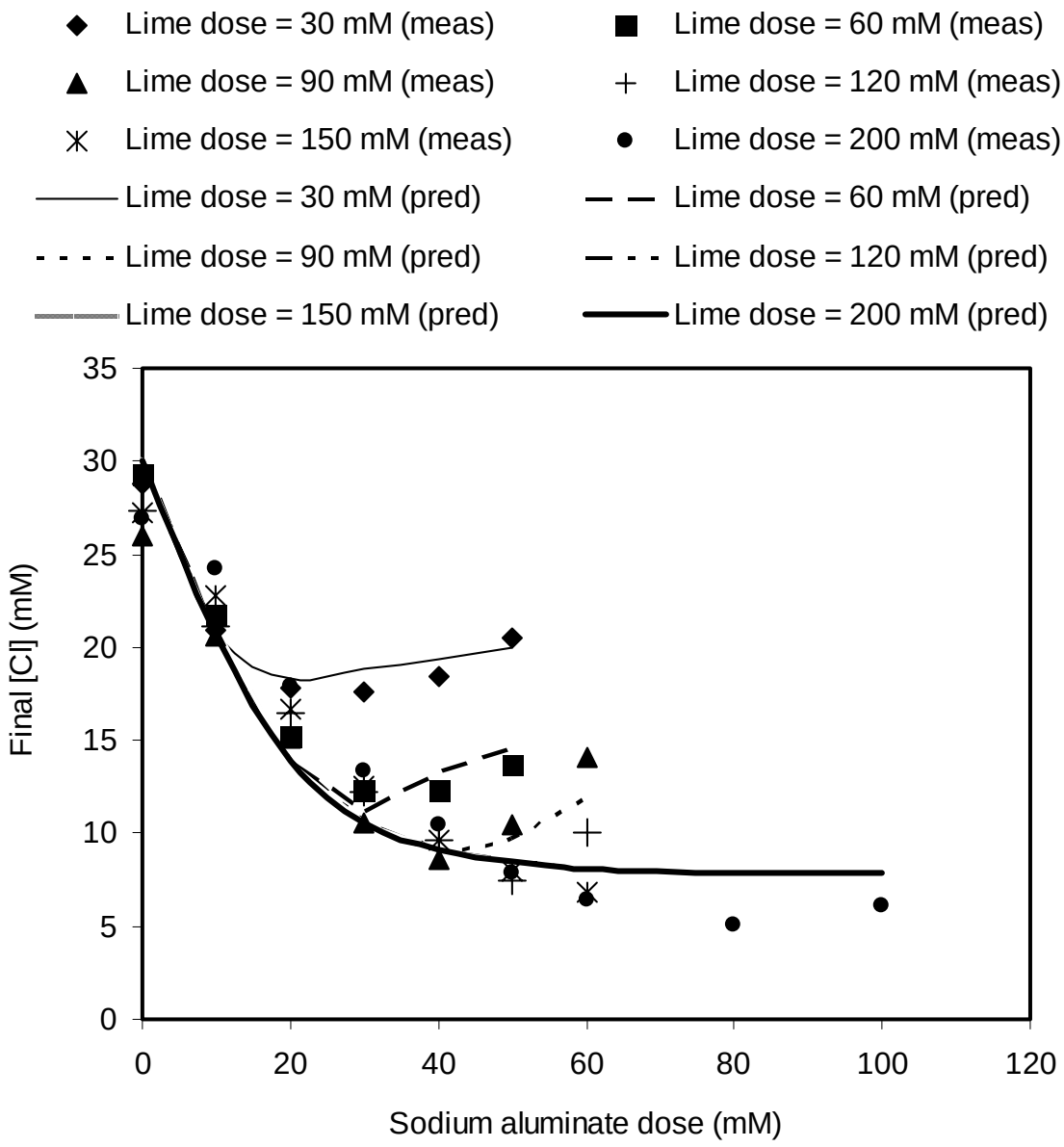

Figure 4.8 Comparison between model-predicted and measured chloride concentration. "Meas" refers to measured concentrations and "pred" refers to predicted concentrations.

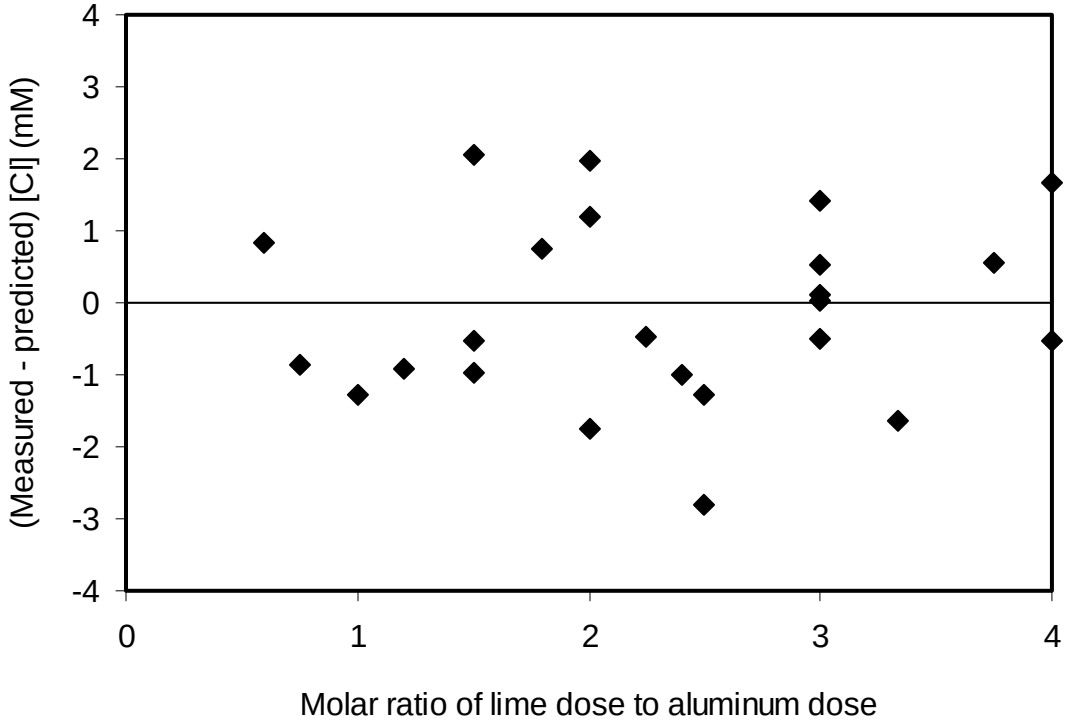

Figure 4.9 Error distribution of predicted chloride concentrations.

aluminum dose increased. The residuals are distributed randomly around 0.0 over a range of calcium doses and aluminum doses (Figure 4.9).

Table 4.2 Error analysis for model predicted concentrations in Cl – OH system.

Constituent	Concentration range (mM)	Average absolute error (mM)	Standard deviation of error (mM)	r^2	Slope	Number of points
Chloride	5.05 – 20.90	1.38	0.89	0.25	0.24	36
Aluminum	0.0 – 32.52	1.02	1.83	0.14	-0.17	36
Calcium	0.34 – 18.70	1.37	0.71	0.25	0.15	36
pH	12.35 – 12.84	0.062	0.044	0.001	-0.0004	36

Comparison between model-predicted concentrations and measured concentrations for aluminum are shown in Figure 4.10 and are listed in Appendix C-2. The predicted concentrations followed the same trend of measured concentrations. Model predictions showed that soluble aluminum concentrations were controlled by gibbsite ($Al(OH)_3$) when $Ca(OH)_2$ doses were less than the stoichiometric amount required to precipitate all the aluminum as chloroaluminate and hydroxyaluminate solids (molar ratio of calcium to aluminum = 1.5). Error analysis showed, however, that the model underestimated measured aluminum concentrations under these conditions (Figure 4.11). This indicates that gibbsite is probably not one of the solid phases present in the system, which was assumed by the model. A hypothesis was made that the

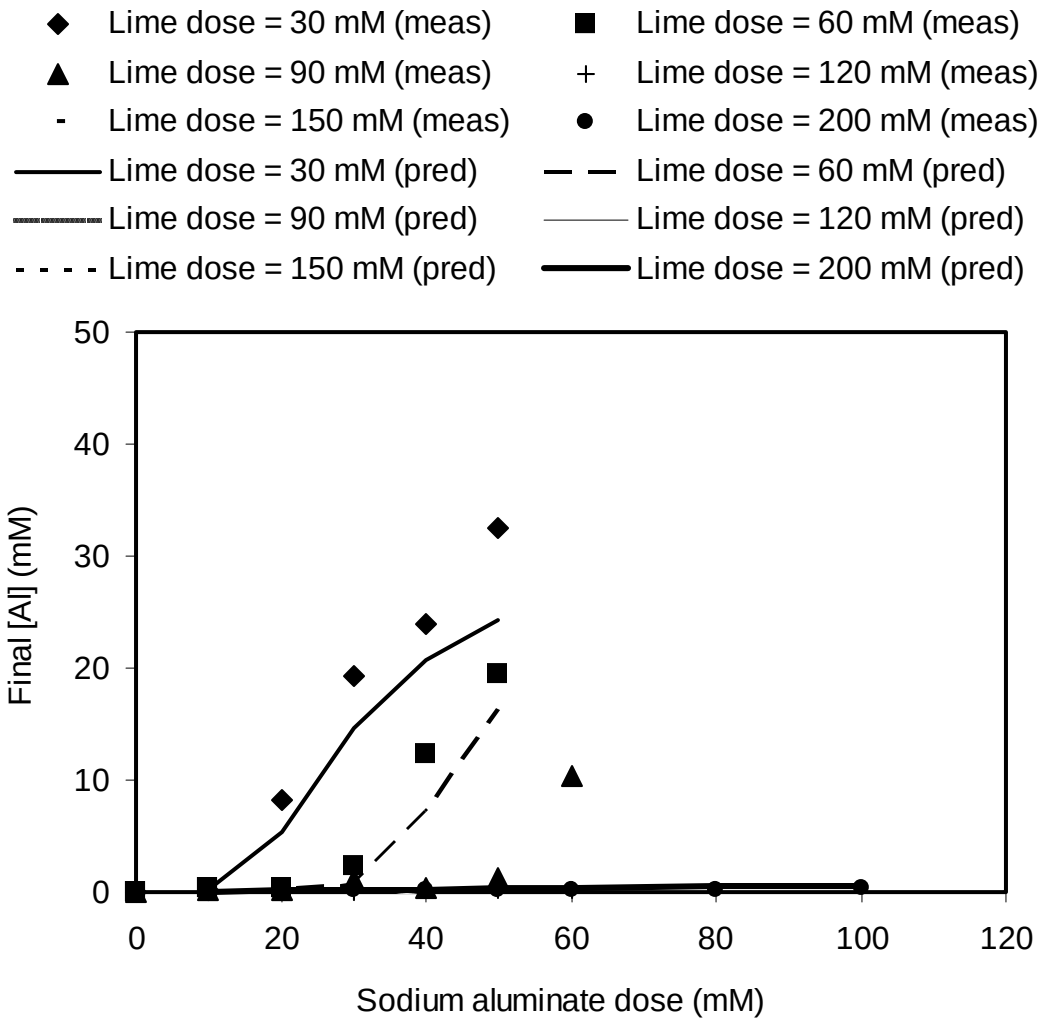

Figure 4.10 Comparison between predicted and measured aluminum concentration with preliminary model.

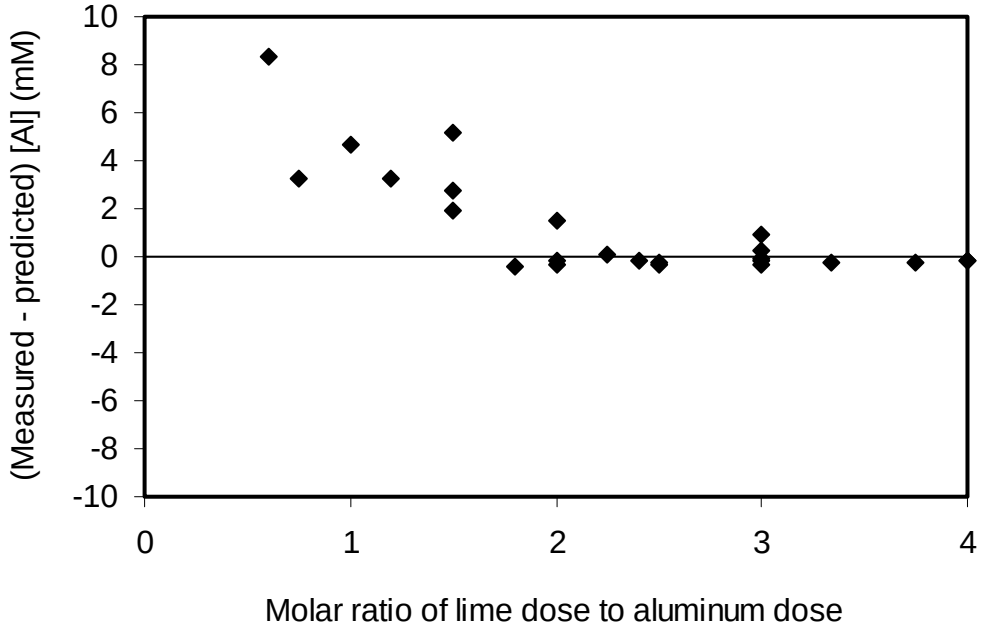

Figure 4.11 Error distribution of predicted aluminum concentrations with preliminary model.

precipitated solid could be a poorly crystallized aluminum hydroxide solid phase that has a solubility product that falls in the range between amorphous $Al(OH)_3$ and gibbsite ($10^{-31.2}$ – $10^{33.5}$) (Stumm and Morgan, 1996). Figure 4.12 shows a comparison between measured aluminum concentrations and concentrations calculated from equilibrium models that assumed the presence of either amorphous $Al(OH)_3$ or gibbsite. PHREEQC was used to do the calculations over a range of pH values. The results indicate that aluminum concentrations are controlled by a solid phase with solubility that is intermediate between that for amorphous $Al(OH)_3$ and gibbsite. In order to test this hypothesis, aluminum solubility was studied independently by conducting a set of completely mixed batch experiments over a range of pH and at the same conditions and reaction time that were used in equilibrium experiments for chloride precipitation. The values of the ion activity product (IAP) for the precipitated $Al(OH)_3$ solid were calculated from measured pH and aluminum concentrations with PHREEQC. An average value of the IAP of $10^{-33.33 \pm 0.09}$ was obtained. The solubility product of gibbsite was replaced with the calculated average value of the IAP. After that, the model predicted measured aluminum concentrations accurately as shown in Figure 4.13. The new model predicted aluminum concentrations with lower values for the average absolute error, slope, and the r^2 (0.77, 0.10, and – 0.11 respectively) than the corresponding values (1.02, 0.14, - 0.17) for the old model. This indicates that the new model predicted final aluminum concentration more accurately than the preliminary model. Comparison between model-predicted and measured calcium concentrations showed that the model predicted calcium concentrations accurately (Figure 4.14). Both

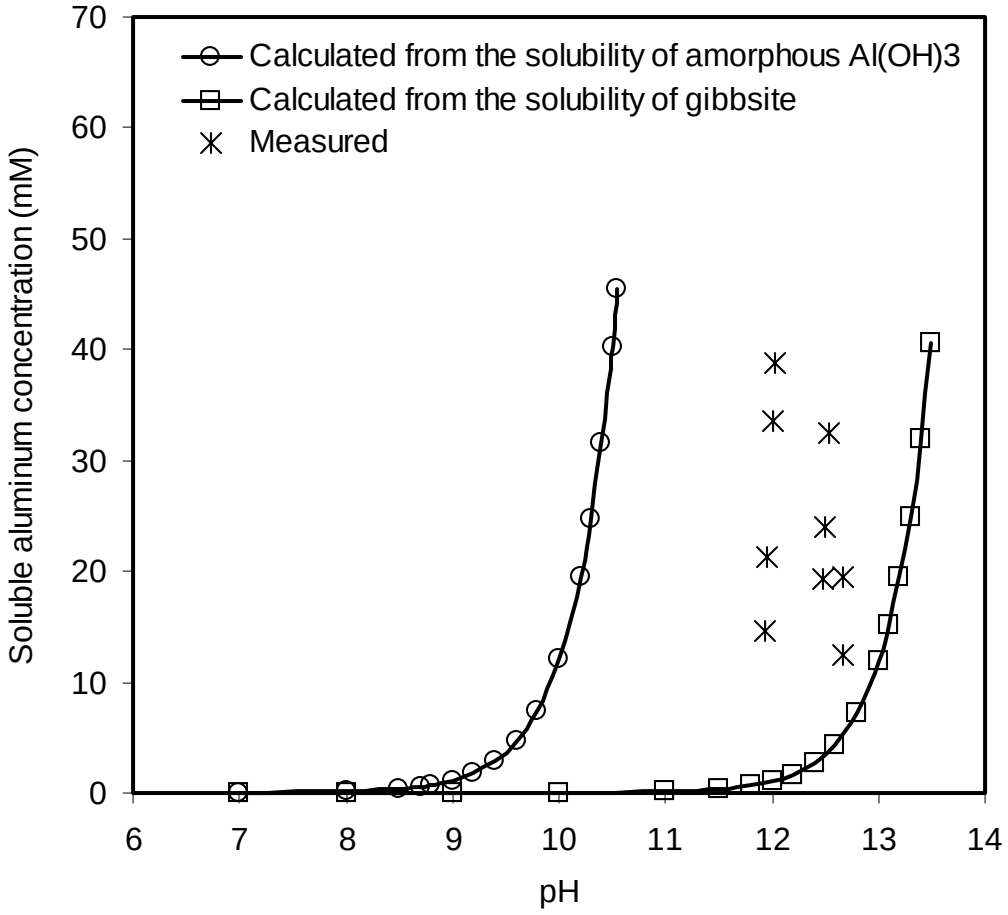

Figure 4.12 Comparison among measured aluminum concentrations and calculated from the precipitation of aluminum hydroxide solids.

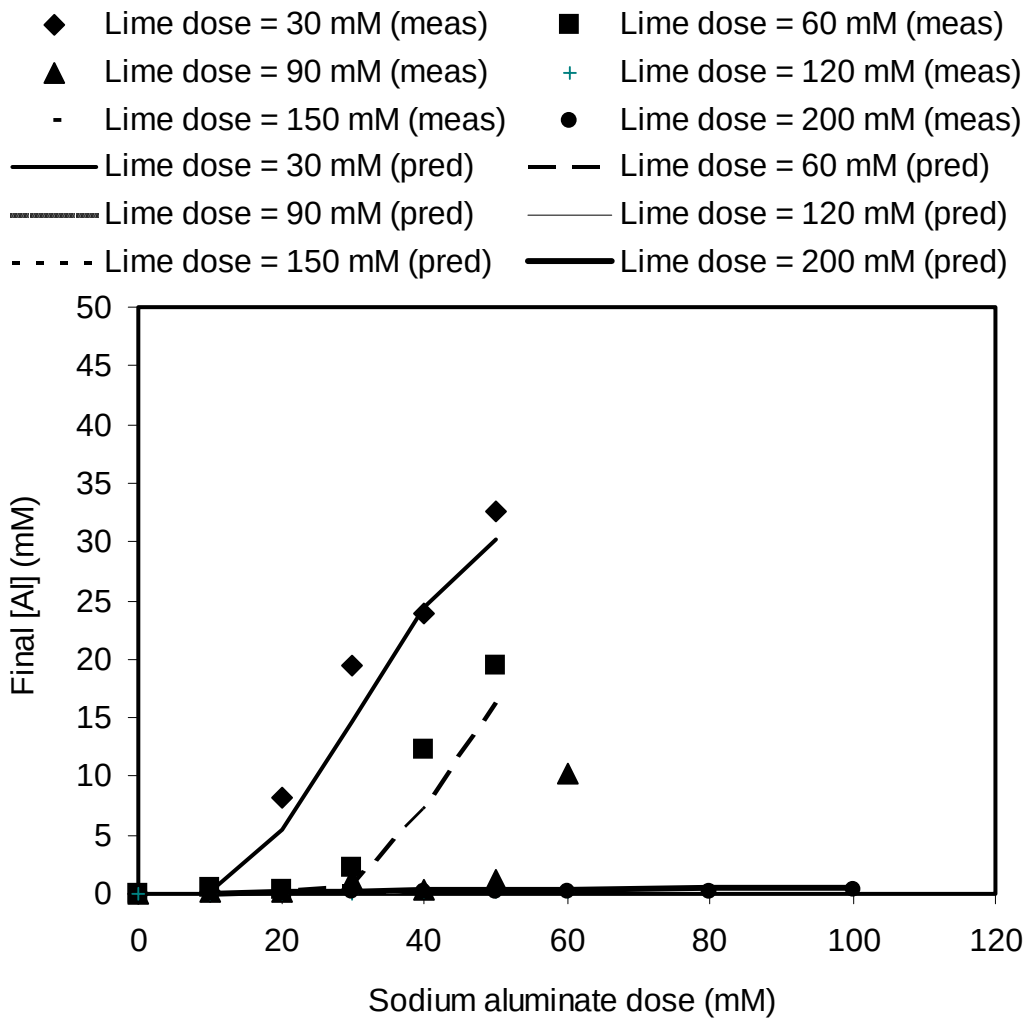

Figure 4.13 Predicted aluminum concentrations after corrections of $Al(OH)_3$ solubility product.

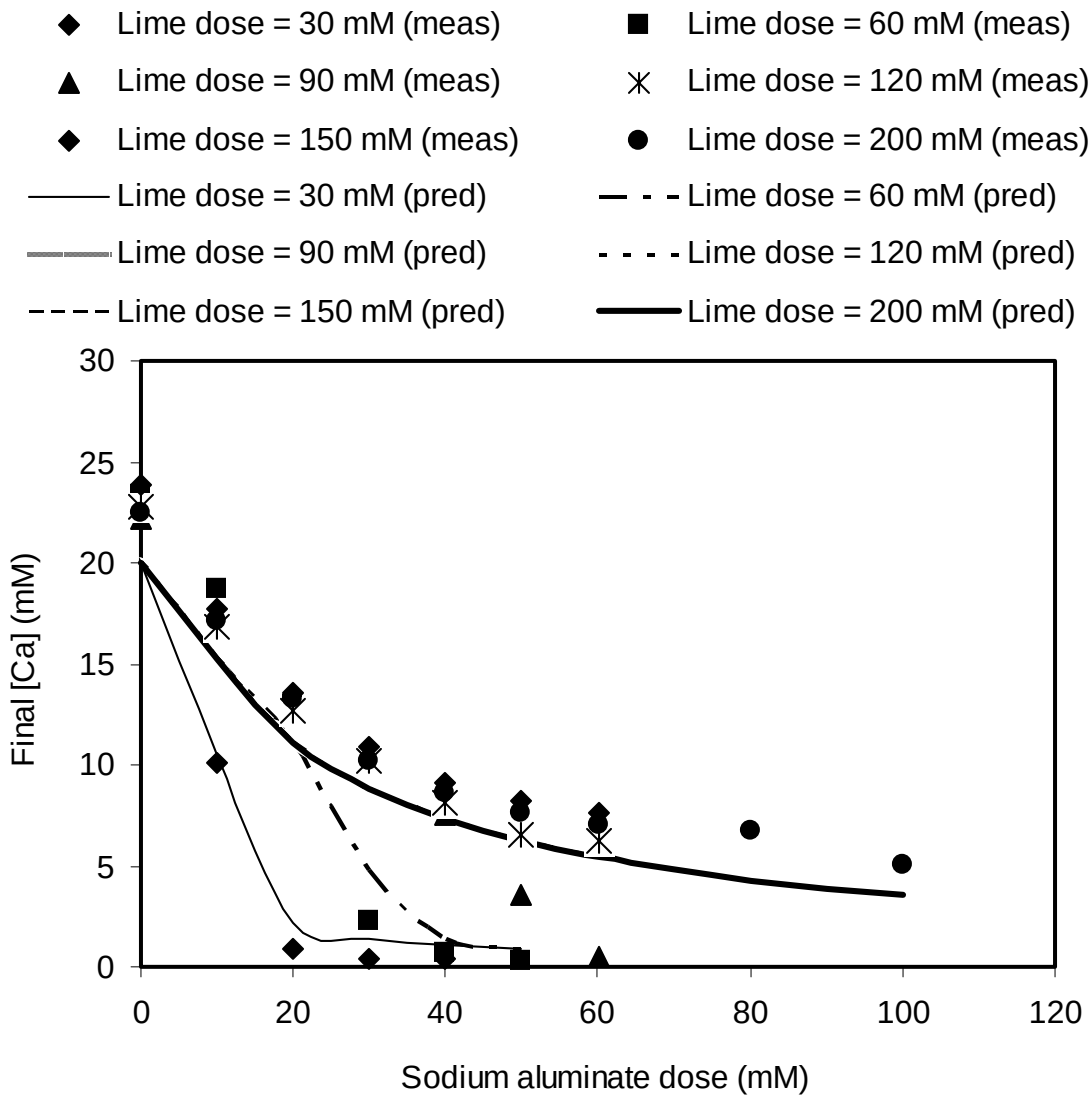

Figure 4.14 Comparison between predicted and measured calcium concentration.

experimental results and model predictions showed that calcium concentration was controlled by lime solubility when the ratio of lime dose to aluminum dose was greater than the stoichiometric ratio (2.0) for the solid solution formation. However, when calcium concentrations were controlled by lime solubility, the model slightly underestimated the experimental data. This could be due to some uncertainty in the solubility product of $Ca(OH)_2$ ($10^{-5.19}$) that was reported by Stumm and Morgan (1996) and was used in this study. pH values were also predicted accurately as shown in Figure 4.15.

4.3.2 Interactions Among Solids in the Solid Solution

Model predictions showed that chloride precipitation was controlled by a solid solution formed from a mixture of $Ca_4Al_2Cl_2(OH)_{12}$, $Ca_4Al_2(OH)_{14}$, and $Ca_3Al_2(OH)_{12}$. Understanding relationships and interactions among these solids is critical in selecting sources of reagents and their optimal doses for effective chloride removal. In order to further understand the relationships among solids in the solid solution, fractions of chloroaluminate and hydroxyaluminate solids in the solid solution were calculated for each data point using PHREEQC. Total initial concentrations of chloride, aluminum, calcium, and pH values were used as input data to PHREEQC and the model was allowed to predict the final total concentrations of the solid solution and fractions of solids in the solid solution (Appendix C-3). Figures 4.16 shows the effect of $NaAlO_2$ dose on the fractions of chloroaluminate and hydroxyaluminate solids in the solid solution. Fractions of hydroxyaluminate solids (tricalcium hydroxyaluminate + tetracalcium hydroxyaluminate) increased with increasing $NaAlO_2$ dose while the

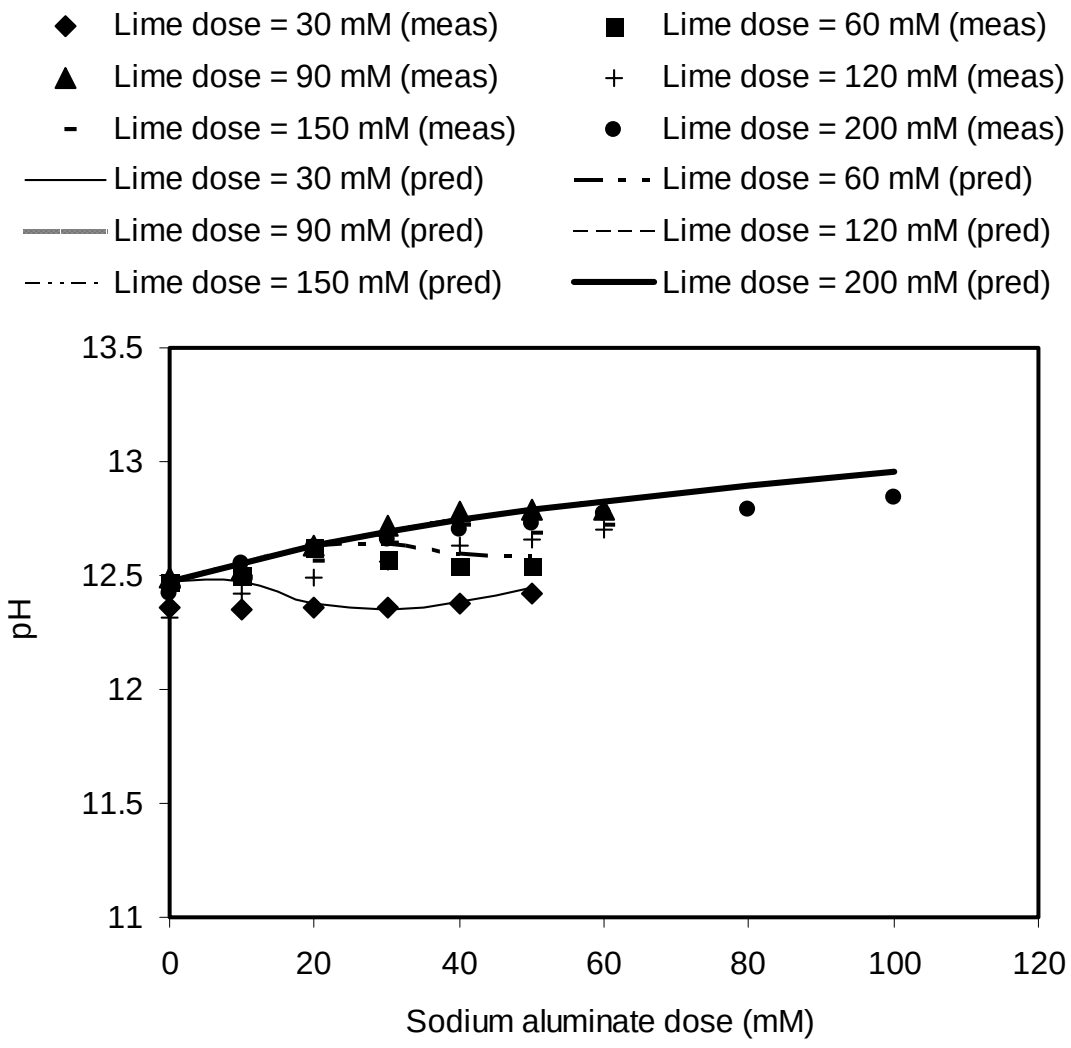

Figure 4.15 Comparison between predicted and measured pH.

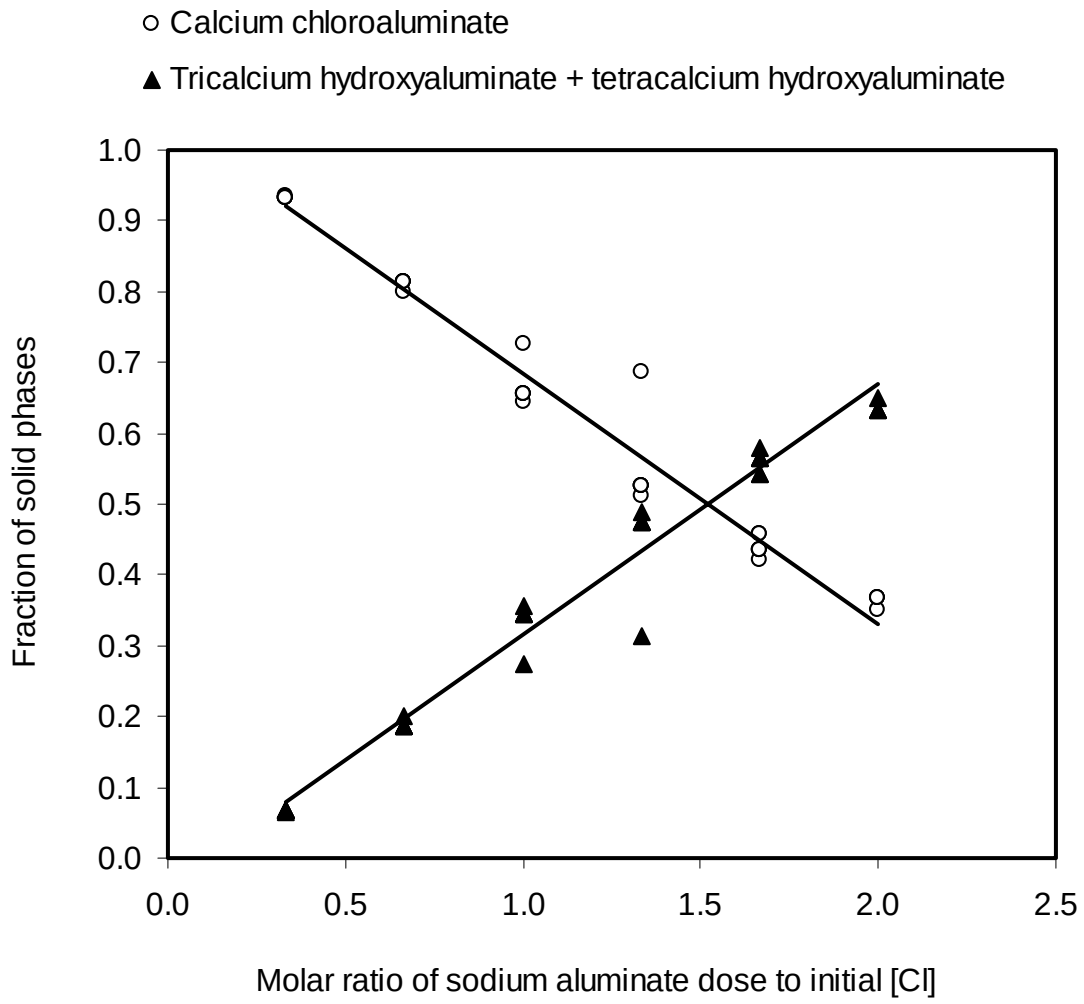

Figure 4.16 Effect of sodium aluminate dose on the fraction of precipitated solids in the solid solution.

fraction of calcium chloroaluminate solid decreased. Additions of $NaAlO_2$ results in increasing $Al(OH)_4^-$ and OH^- ions in the solution. This favors precipitation of $Ca_3Al_2(OH)_{12}$ and $Ca_4Al_2(OH)_{14}$ over $Ca_4Al_2Cl_2(OH)_{12}$. Increasing hydroxide ion concentration results in substitution of Cl^- by OH^- in the solid solution, which increases the fraction of tetracalcium hydroxyaluminate solid and decreases the fraction of chloroaluminate solid. Similarly, increasing the concentration of $Al(OH)_4^-$ will favor formation of $Ca_3Al_2(OH)_{12}$ over $Ca_4Al_2Cl_2(OH)_{12}$ and will increase the total fraction of hydroxyaluminate solids. Model predictions indicated that the increase in chloride concentration that was observed when the ratio of $NaAlO_2$ dose to lime dose was greater than the stoichiometric value of 0.5 (Figure 4.7) was associated with changes in the composition of the solid solution. Figure 4.17 shows that the ratio of $Ca_3Al_2(OH)_{12}$ to $Ca_4Al_2(OH)_{14}$ in the solid solution begins to increase at a ratio of $NaAlO_2$ dose to lime dose equal to 0.5, which is the same value that resulted in an increase in chloride concentration (Figure 4.7).

Additions of lime had a negligible effect on the distribution of solids in the solid solution (Figure 4.18). Although addition of lime could result in increased concentration of hydroxide ion, which could exchange with chloride ion, this apparently did not occur. This could be due to the failure of the lime to dissolve, particularly at doses beyond the amount required to form chloroaluminate or hydroxyaluminate solid phases.

The following stoichiometric reactions were derived from Equations 4-1, 4-2, and 4-3. They are based on the model predictions for the composition of the solid phase and the composition changes when different reagent doses were applied. These

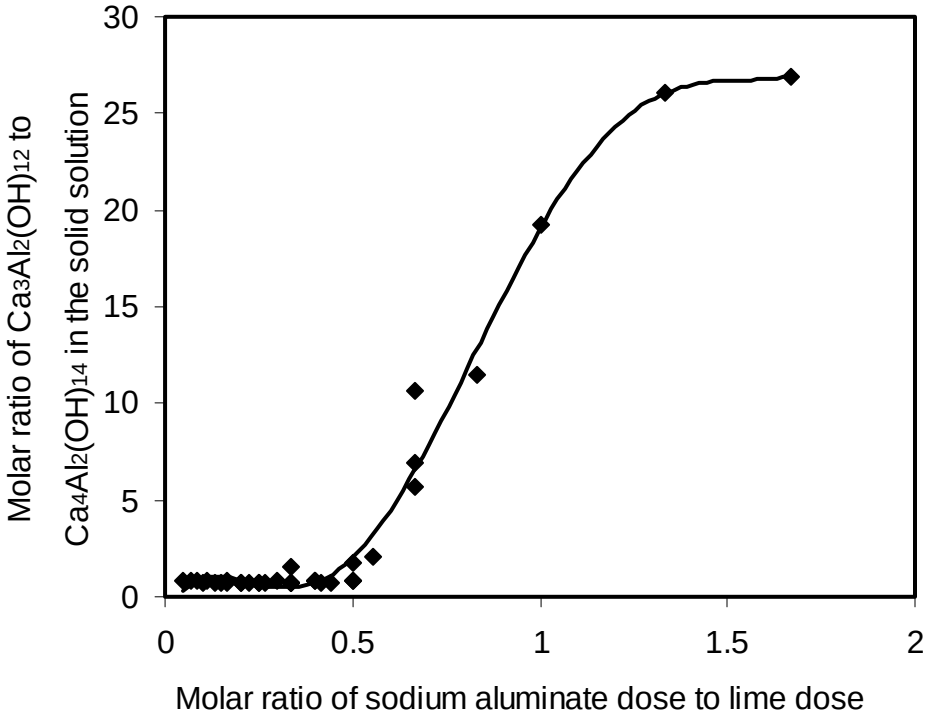

Figure 4.17 Effect of sodium aluminate dose on the ratio of $Ca_3Al_2(OH)_{12}$ to $Ca_4Al_2(OH)_{14}$ in the solid solution.

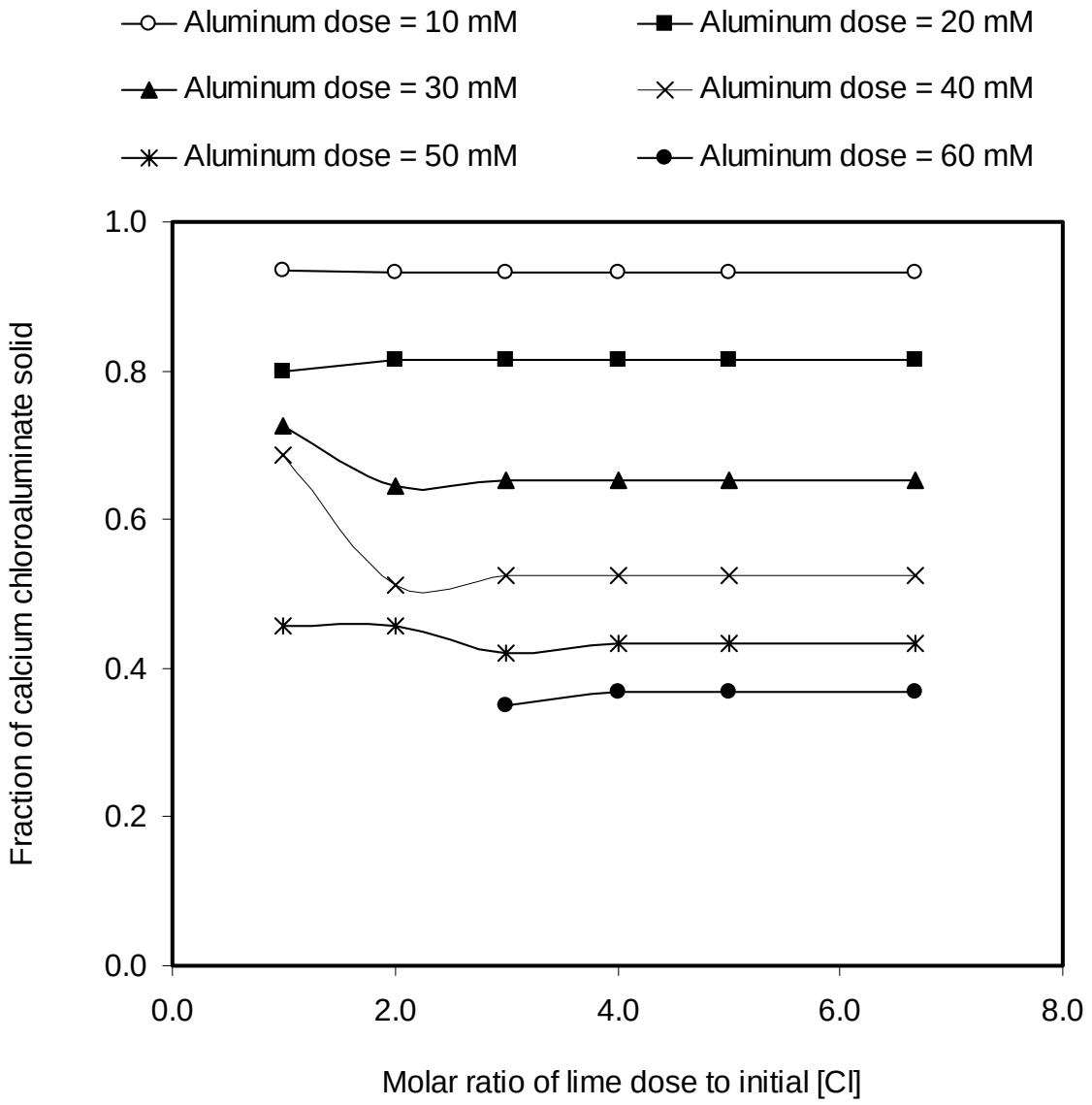

Figure 4.18 Effect of lime additions on the fraction of calcium chloroaluminate in the solid solution.

reactions can describe the interactions among the solids during formation of the solid solution.

$$Ca_4Al_2Cl_2(OH)_{12} + 2\ OH^- = Ca_4Al_2(OH)_{14} + 2\ Cl^- \quad (4\text{-}4)$$

$$3\ Ca_4Al_2Cl_2(OH)_{12} + 2\ Al(OH)_4^- + 4\ OH^- = 4\ Ca_3Al_2(OH)_{12} + 6\ Cl^- \quad (4\text{-}5)$$

$$3\ Ca_4Al_2(OH)_{14} + 2\ Al(OH)_4^- = 4\ Ca_3Al_2(OH)_{12} + 2\ OH^- \quad (4\text{-}6)$$

By assuming that the solid solution is ideal, i.e., the activity of each solid is equal to its mole fraction in the solid solution, the following equations can be derived from the definitions of the solubility products.

$$\frac{\{Cl^-\}^2 X_{tet}}{\{OH^-\}^2 X_{chl}} = \frac{K_{sp,chl}}{K_{sp,tet}} \quad (4\text{-}7)$$

$$\frac{\{Cl^-\}^6 (X_{tri})^4}{\{OH^-\}^4 \{Al(OH)_4^-\}^2 (X_{chl})^3} = \frac{(K_{sp,chl})^3}{(K_{sp,tri})^4} \quad (4\text{-}8)$$

$$\frac{\{OH^-\}^2 (X_{tri})^4}{\{Al(OH)_4^-\}^2 (X_{tet})^3} = \frac{(K_{sp,tet})^3}{(K_{sp,tri})^4} \quad (4\text{-}9)$$

where,

$\{Cl^-\}$, $\{OH^-\}$, $\{Al(OH)_4^-\}$ = the activities of Cl^-, OH^-, and $Al(OH)_4^-$ respectively in the solution,

X_{tet} = the molar fraction of $Ca_4Al_2(OH)_{14}$ in the solid solution , i.e. the number of moles of $Ca_4Al_2(OH)_{14}$ divided by the total number of moles in the solid solution,

X_{chl} = the molar fraction of $Ca_4Al_2Cl_2(OH)_{12}$ in the solid solution, i.e. the number of moles of $Ca_4Al_2Cl_2(OH)_{12}$ divided by the total number of moles in the solid solution,

X_{tri} = the molar fraction of $Ca_3Al_2OH_{12}$ in the solid solution, i.e. the number of moles of $Ca_3Al_2OH_{12}$ divided by the total number of moles in the solid solution, (note that $X_{tet} + X_{chl} + X_{tri} = 1.0$)

$K_{sp,tet}$, $K_{sp,chl}$, and $K_{sp,tri}$ are the solubility products of $Ca_4Al_2(OH)_{14}$, $Ca_4Al_2Cl_2(OH)_{12}$, and $Ca_3Al_2(OH)_{12}$ ($10^{-25.02}$, $10^{-27.10}$, and $10^{-19.72}$ respectively)

The following equation can be derived by algebraically manipulating Equations 4-7, 4-8 and 4-9, and substituting with values for the solubility products.

$$\mathbf{2\log\{Cl^-\} - \log\{OH^-\} - \log\{Al(OH)_4^-\} = -0.17 + \log(X_{chl}) + 0.5\log(X_{tet}) - 2\log(X_{tri})} \quad (4\text{-}10)$$

The activities of Cl^-, OH^-, and $Al(OH)_4^-$ were calculated from the measured concentrations using activity coefficients calculated by PHREEQC, which used the Davies Equation (Stumm and Morgan, 1996). The observed values of [2 log $\{Cl^-\}$ - log $\{OH^-\}$ - log $\{Al(OH)_4^-\}$] are shown in Figure 4.19 versus the predicted values, which were calculated using the right-hand side of Equation 4-10 and model predictions for the composition of the solid solution. The data are scattered about a 45-degree line indicating that the chemical equilibrium model that assumes a solid solution is reasonable. The predicted values at lime dose above 100 mM are a small amount below the 45-degree line. This could be due to some error in $\{Al(OH)_4^-\}$ calculated at these points, because aluminum concentrations at these points were very low. At these points

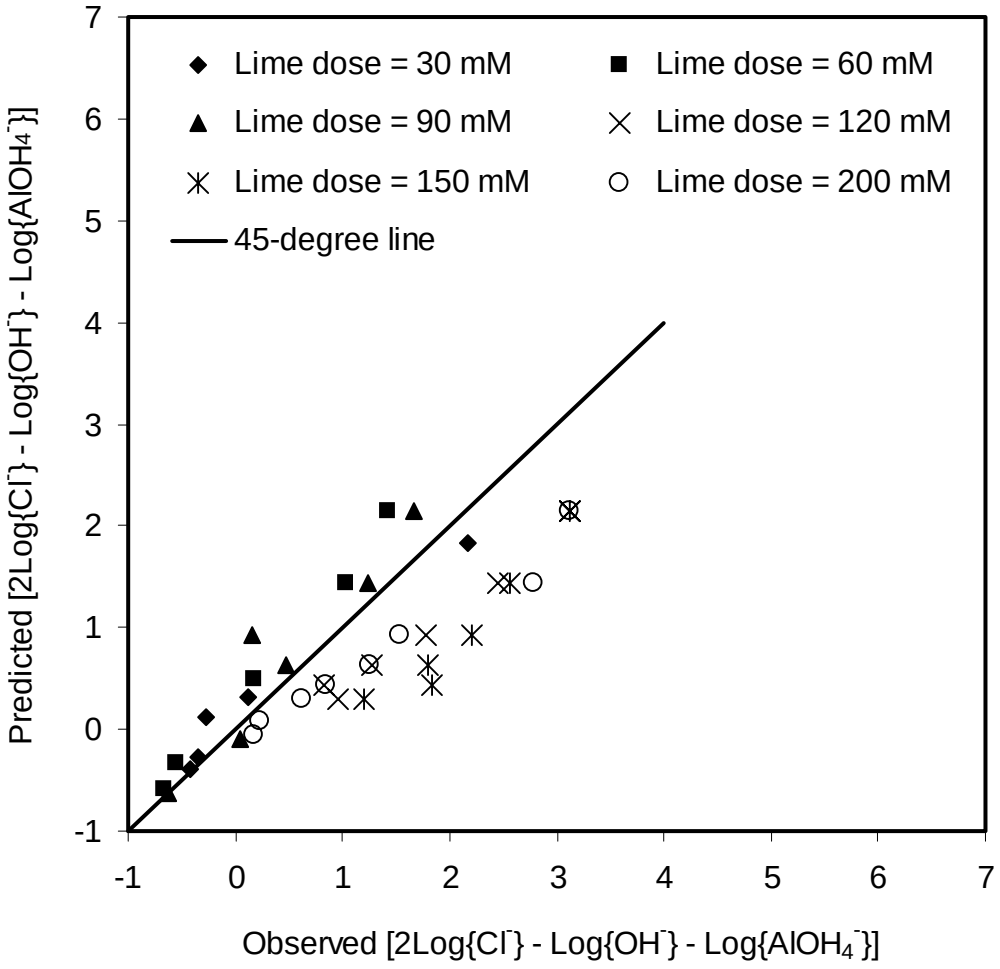

Figure 4.19 Observed versus predicted [2Log{Cl^-} - Log{OH^-} - Log{$Al(OH)_4^-$}].

the model overestimated $\{Al(OH)_4^-\}$ values and this resulted in lower calculated values of $(2\log\{Cl^-\} - \log\{OH^-\} - \log\{Al(OH)_4^-\})$ when the right-hand side of Equation 4-10 was used than the calculated values when experimental data were used.

In order to achieve high chloride removal efficiency, the fraction of calcium chloroaluminate in the solid solution must be maximized and the fractions of hydroxyaluminate solids must be minimized. This can be achieved by minimizing ratios of soluble concentrations of $Al(OH)_4^-$ and OH^- relative to Cl^- concentration. Soluble $Al(OH)_4^-$ concentrations can be reduced and the fraction of $Ca_3Al_2(OH)_{12}$ can be minimized by adding lime at doses above the stoichiometric ratio to aluminum (2.0). The fraction of $Ca_4Al_2(OH)_{14}$ can be minimized by using aluminum sources that do not cause an increase in the concentration of OH^-. One such aluminum source would be amorphous $Al(OH)_3(s)$. An attractive alternative source of aluminum could be waste alum sludge produced from water treatment plants. This sludge was reported to contain approximately 39% aluminum by weight (Chu, 1999).

Equations 4-4, 4-5, and 4-6 show that the fraction of calcium hydroxyaluminate solids in the solid solution can be limited by lowering pH. This will increase the fraction of calcium chloroaluminate and result in high chloride removal efficiency. However, high pH is required in order to form calcium chloroaluminate. Therefore, the fractions of calcium hydroxyaluminate solids cannot be eliminated, but they can be minimized by adjusting pH to the value that gives maximum chloride removal. The effect of pH on chloride removal will be discussed in a subsequent section.

4.4 Effect of Initial Chloride Concentration on Chloride Removal with UHLA

4.4.1 Experimental Results

Three different initial concentrations of chloride (10, 50, 100 mM) were investigated. The ratios of the doses of lime and aluminum to the initial chloride concentration were kept constant at 400% and 160%, respectively. Experimental results showed that chloride removal efficiency at initial chloride concentration of 10 mM is significantly lower than that at initial concentrations of 50 and 100 mM (Table 4.3). This could be because when the concentration of chloride is low with respect to the concentration of hydroxide ion, the precipitation of calcium hydroxyaluminate becomes favorable relative to precipitation of calcium chloroaluminate. Although the ratio of chemical doses to initial chloride concentrations was constant for all of these experiments, the final solution pH increased with increasing initial chloride concentration due to the higher lime and sodium aluminate doses. However, the composition of the solid solution depends on the activity ratio of aqueous chloride to hydroxide, which was constant for all initial chloride concentrations (Table 4.3).

Table 4.3 Effect of initial chloride concentration on the removal efficiency of chloride.

Initial [Cl] (mM)	10	50	100
Removal efficiency (%)	50.3 ± 0.2	68.7 ± 0.9	69.6 ± 0.4
Final solution pH	12.63 ± 0.01	13.13 ± 0.03	13.36 ± 0.01
Ratio of ($\{Cl^-\}/\{OH^-\}$)	0.10	0.11	0.10

4.4.2 Equilibrium Modeling

The equilibrium model was tested for this set of experiments. Figure 4.20 shows comparison among experimental results and model predictions for final concentrations of chloride, calcium, and aluminum. The pH was fixed at the measured values shown in Table 4.2 during calculations of the predicted concentrations of Cl, Al, and Ca using the equilibrium model solved by PHREEQC. Very good agreement between measured and predicted chloride concentrations was observed. Predicted calcium concentrations at initial chloride concentrations of 50 and 100 mM are lower than the measured calcium concentrations. This could be due to the uncertainty in the solubility product of calcium hydroxide solid. The model predicted that calcium hydroxide would precipitate at the pH observed for initial chloride concentrations of 50 and 100 mM, but that it would not precipitate at conditions observed for the experiments with 10 mM initial chloride. Good agreement between measured and predicted aluminum concentrations was observed. Results of the model indicate that the model succeeded in predicting chemical behavior accurately at different initial chloride concentrations.

4.5 Effect of pH on Chloride Removal with UHLA

4.5.1 Experimental Results

A range of pH values (10.80 – 13.05) was investigated with three different initial concentrations of chloride (10, 50, 100 mM) in order to study the effect of pH on chloride removal with UHLA. Stoichiometric ratios of doses of lime and aluminum to initial chloride concentration were kept constant at 200% and 100%, respectively. Lime

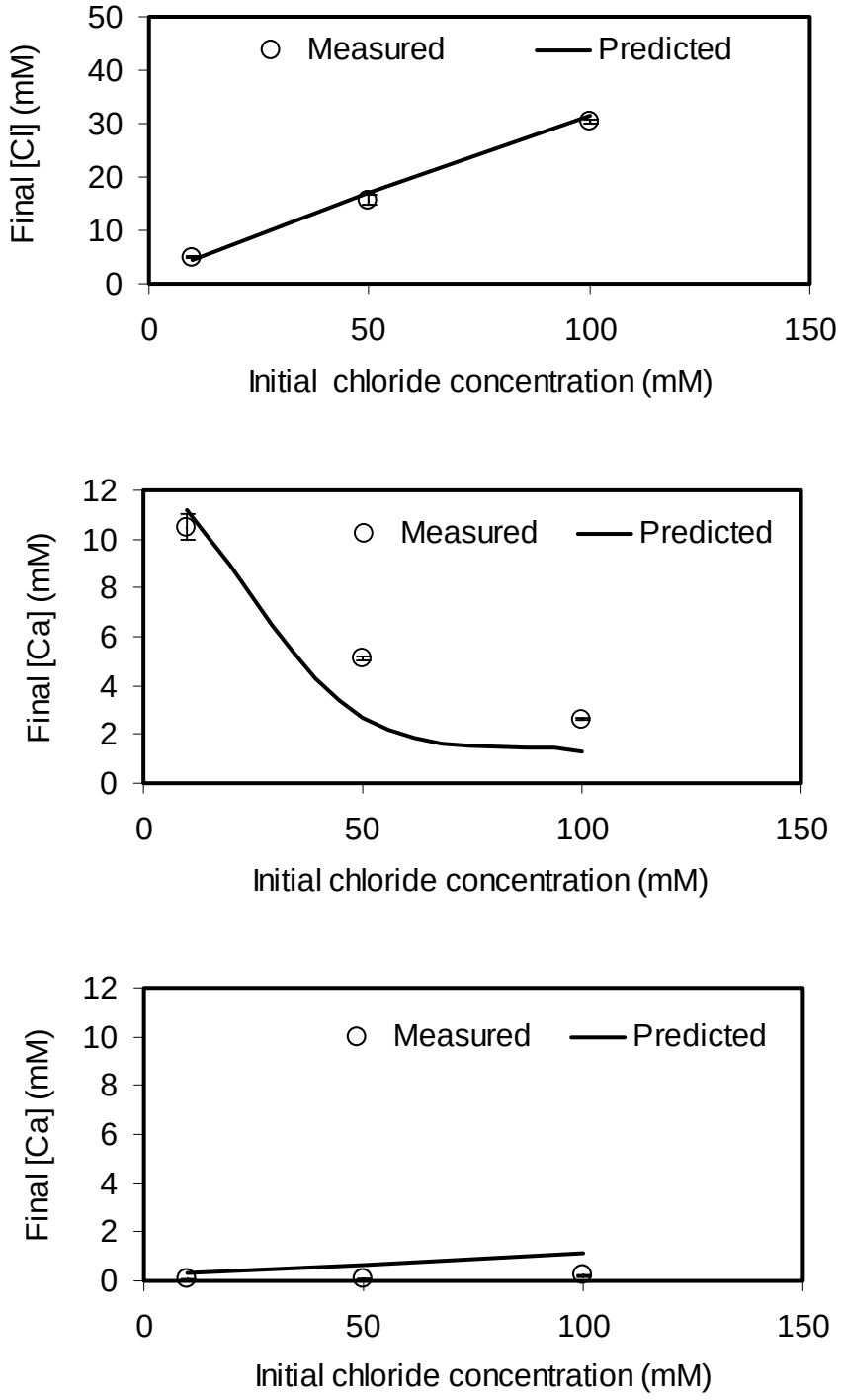

Figure 4.20 Comparison between predicted and measured concentrations for chloride, calcium, and aluminum at various initial chloride concentrations.

and sodium aluminate were used as sources of calcium and aluminum, respectively.

In the preliminary experiments $Ca(NO_3)_2$ and $Al(NO_3)_3$ were used as calcium and aluminum sources, respectively, and pH was adjusted to the desired values using NaOH. However, when these chemicals were used, negligible chloride removal was observed at lime dose of 40 mM, aluminum dose of 16 mM, initial nitrate concentration of 128 mM, and initial chloride concentration of 10 mM (Figure 4.21). Concentrations of nitrate were measured and indicated that the reason for negligible chloride removal was that a Ca-Al-NO_3 precipitate formed and consumed all of the calcium and aluminum in the solution, thereby precluding formation of a Ca-Al-Cl precipitate. Figure 4.21 shows a comparison between chloride removed and nitrate removed and indicates that chloride removal was negligible compared to nitrate removal.

Nitrate removal increased with increasing pH until it reached a maximum at pH 12.60 and then it decreased as the pH increased. The initial increase of nitrate removal with pH was probably caused by the formation of a nitrated AFm phase ($Ca_4\ Al_2\ (OH)_{12}\ (NO_3)_2$) (Renaudin et al., 2000, and Renaudin and Francois, 1999). However, at higher pH values, precipitation of calcium hydroxyaluminate becomes more favorable than precipitation of the nitrated AFm phase due to the higher concentrations of OH^- relative to NO_3^-.

Using any other salts of calcium or aluminum could cause the same problem. Furthermore, using $CaCl_2$ and $AlCl_3$ would result in very high initial chloride concentrations with respect to calcium and aluminum doses. The final choice was to use

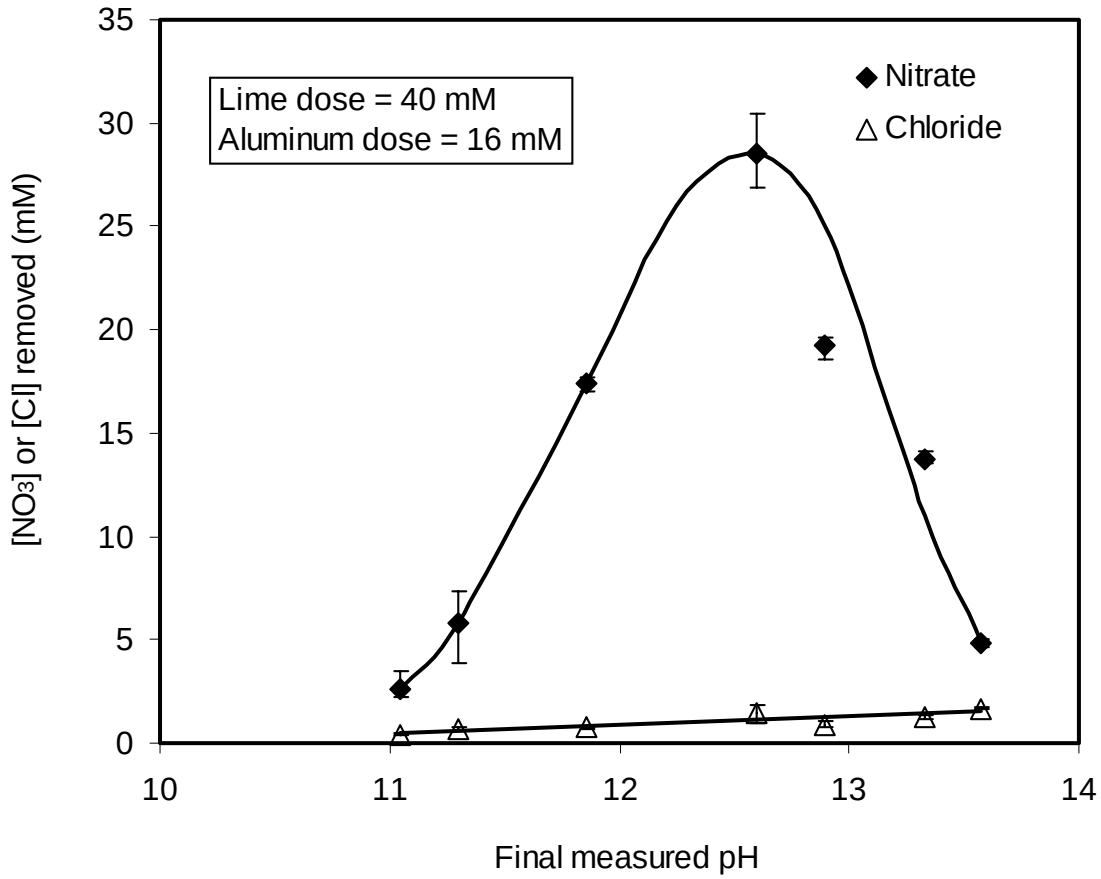

Figure 4-21 Comparison between nitrate and chloride removal.

the same calcium and aluminum sources that were used in other experiments, which were lime and sodium aluminate, respectively. This required addition of acid to lower pH for some experiments. Using nitric acid or sulfuric acid would cause the same problem associated with nitrate and sulfate. The final decision was to use acetic acid, because acetate anions are much larger than chloride and might not compete with chloride. Additionally, the amount of acid required to lower pH to the desired minimum value (pH 10.80) was determined and that amount of acetic acid was added to all the experiments along with an amount of NaOH necessary to obtain the desired pH. For each set of experiments, one experiment was conducted without additions of acid or base in order to study if acetate had an effect on chemical behavior in the system.

Figure 4.22 shows the effect of pH on final chloride concentrations. For all initial chloride concentrations, chloride concentration decreased with increasing pH until it reached a minimum and then it increased as the pH was increased further. This behavior can be explained by how pH affects formation of different solids phases. At low pH values, formation of AFm-type LDHs (e.g. calcium chloroaluminate, calcium hydroxyaluminate) is not favored, so chloride concentration is high. As pH is increased, the formation of AFm phases becomes favorable and both calcium chloroaluminate and calcium hydroxyaluminate are formed and chloride removal increases. This trend continues until pH reaches the optimum value for calcium chloroaluminate precipitation (pH12 ± 0.2)). At pH values above this optimum, precipitation of calcium hydroxyaluminate becomes more favorable than precipitation of calcium chloroaluminate, so that chloride concentration increases.

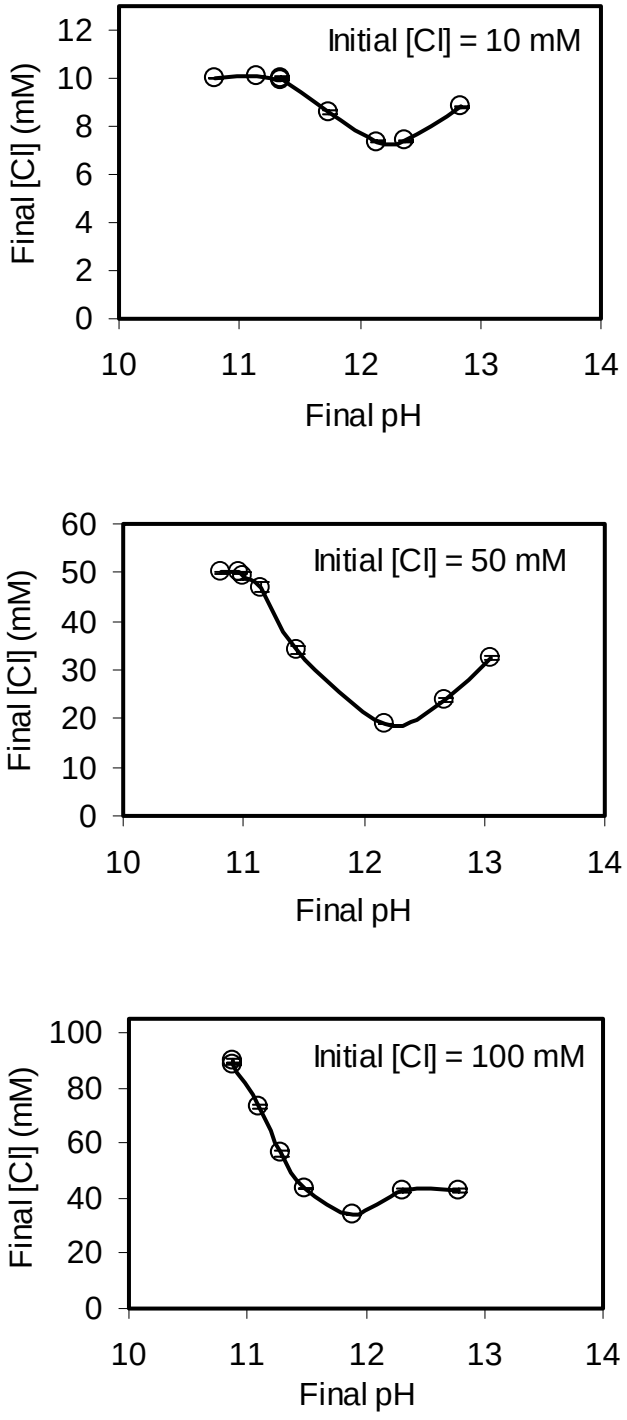

Figure 4.22 Effect of pH on final chloride concentration.

Removal efficiency of chloride increased with increasing initial chloride concentration at the same pH value (Figure 4.23). This occurs because increasing the initial chloride concentration at constant pH increases the ratio of chloride to hydroxide in the solution. This thermodynamically favors the precipitation of calcium chloroaluminate over calcium hydroxyaluminate and results greater chloride removal. Experimental results indicated that the optimum pH for maximum chloride removal with UHLA is pH 12 ± 0.2.

Figure 4.24 shows the effect of pH on final calcium concentrations and indicates that final calcium concentrations follow the same trend that was observed for final chloride concentrations at low pH values. However, at high pH values, calcium concentrations continue to decrease with increasing pH values, which is unlike the behavior of chloride. The behavior of calcium can be explained by the fact that the increase in hydroxyaluminate relative to chloroaluminate at higher pH does not affect calcium concentrations in solution, because both of these solid phases contain about the same amount of calcium.

The effect of pH on soluble aluminum concentrations is shown in Figure 4.25. Aluminum concentrations increased with increasing pH values until a maximum and then decreased with increasing pH. This was because at low pH values, aluminum concentrations are controlled by aluminum hydroxide precipitation and the solubility of aluminum hydroxide solid increases with increasing pH (see Figure 4-12). At a pH value that depends on the composition of the solution, control of the aluminum concentration shifts from aluminum hydroxide to the solid solution and this results in decreasing

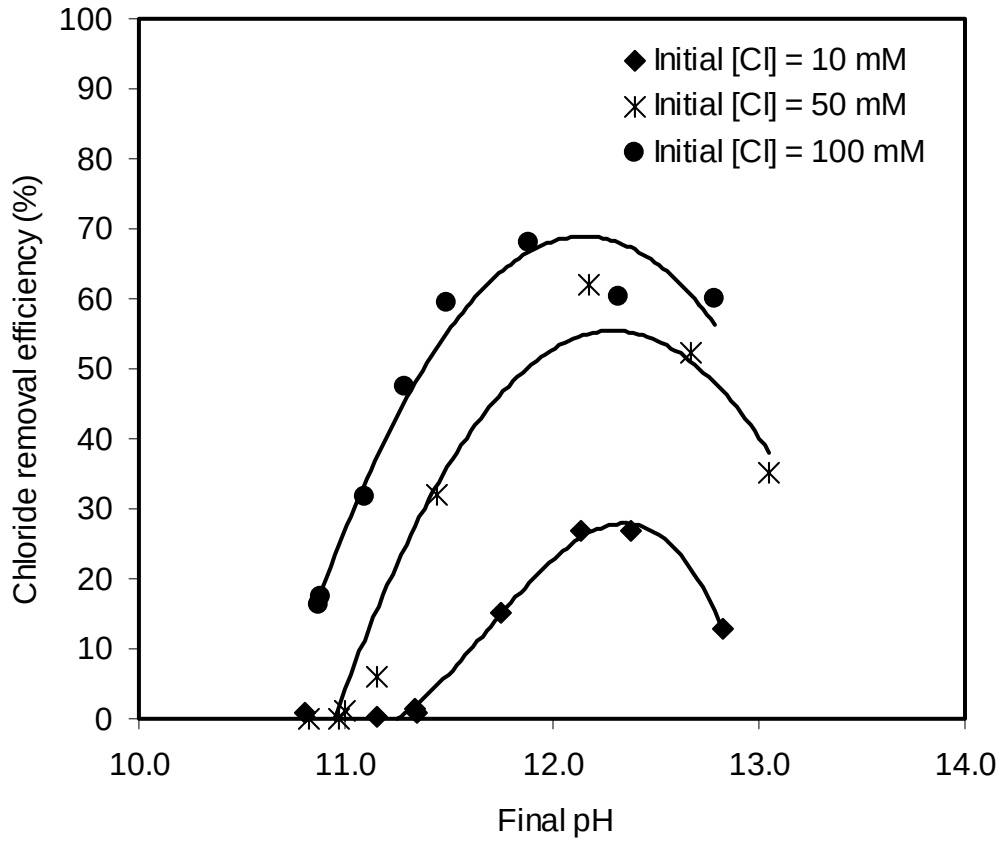

Figure 4.23 Effect of pH on chloride removal efficiency.

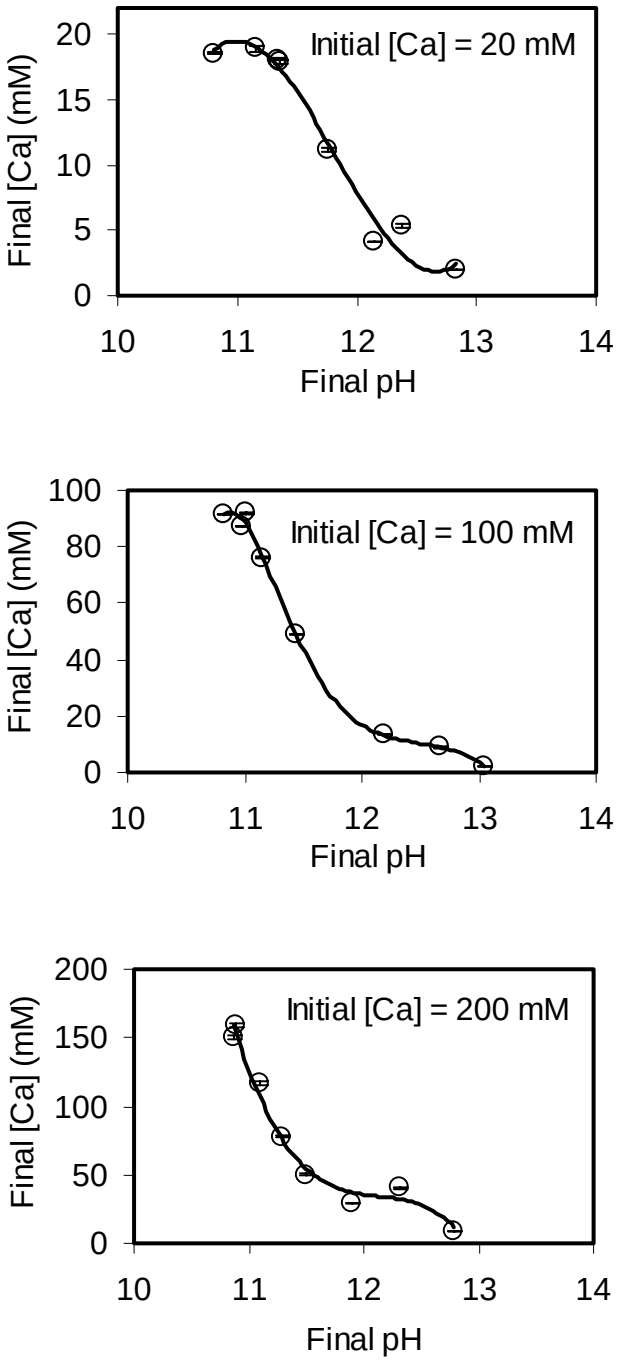

Figure 4.24 Effect of pH on final calcium concentration.

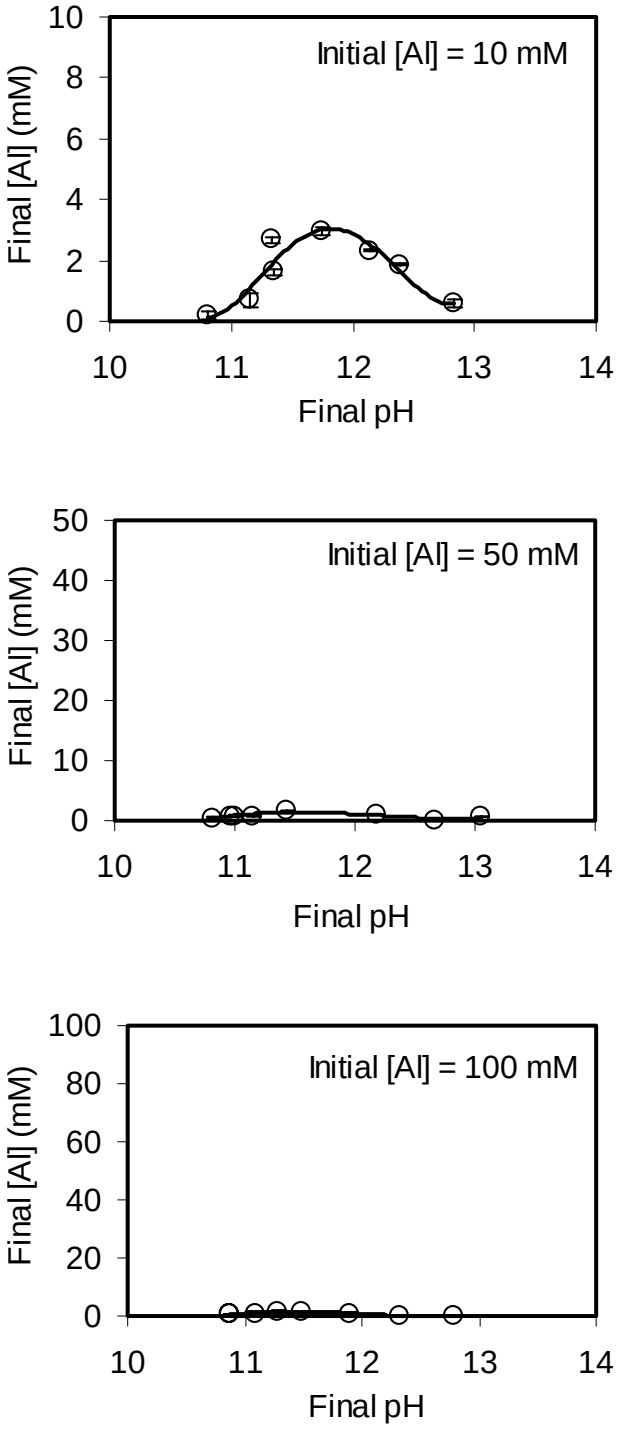

Figure 4.25 Effect of pH on final aluminum concentration.

aluminum concentrations with increasing pH.

4.5.2 Model Predictions

In order to test the validity of the equilibrium model and its ability to predict chemical behavior in the UHLA process over a range of pH values, the equilibrium model was used to predict experimental results. The model was modified to include reactions of acetate and other compounds present in the solutions by modifying the database file of PHREEQC using data associated with the MINTEQ equilibrium model (Allison et al., 1991). These reactions and their equilibrium constants are listed in Table 4.4. Total initial concentrations of chloride, calcium, and aluminum were used as input data to PHREEQC, while pH was fixed at the measured value for each data point (Appendix B-3). Then the final total concentrations of chloride, calcium, and aluminum were calculated from the model using PHREEQC.

Figure 4.26 show comparison between measured and model-predicted concentrations of chloride over the investigated range of pH. This figure shows that the model succeeded in predicting measured chloride concentrations reasonably well. However, at high pH values the model underestimated measured chloride concentrations. This could be due to the effect of the high ionic strength that was caused by the need to add high concentrations of NaOH in order to achieve high values of pH. Chloride concentrations that were measured in experiments that did not require addition of acid or base to achieve the desired pH agreed well with the model-predicted concentrations.

Table 4.4 Acetate reactions added to the database of the equilibrium model (Allison et al., 1991).

$Acetate^- = Acetate^-$	Log K = 0.0
$Acetate^- + H^+ = HAcetate$	Log K = 4.76
$Na^+ + Acetate^- = NaAcetate$	Log K = -0.18
$Ca^{2+} + Acetate^- = CaAcetate^+$	Log K = 1.18
$2.0\ HAcetate + 1.0\ Ca^{2+} = Ca(Acetate)_2 + 2.0\ H^+$	Log K = -7.38
$1.0\ Ca^{2+} + 1.0\ HAcetate = CaAcetate^+ + 1.0\ H^+$	Log K = -3.83
$2.0\ HAcetate + 1.0\ Al^{3+} = Al(Acetate)_2^+ + 2.0\ H^+$	Log K = -5.60
$1.0\ Al^{3+} + 1.0\ HAcetate = AlAcetate^{2+} + 1.0\ H^+$	Log K = -2.69

A comparison between measured and model-predicted calcium concentrations is shown in Figure 4-27 and indicates that the model accurately predicted measured calcium concentrations over a range of pH values. Similarly, Figure 4-28 shows that the model succeeded in reasonably predicting the final aluminum concentrations at different pH values.

4.6 Effect of Temperature on Chloride Removal with UHLA

Figure 4.29 shows the effect of temperature on final chloride concentrations. Final chloride concentrations slightly increased when water temperature increased at

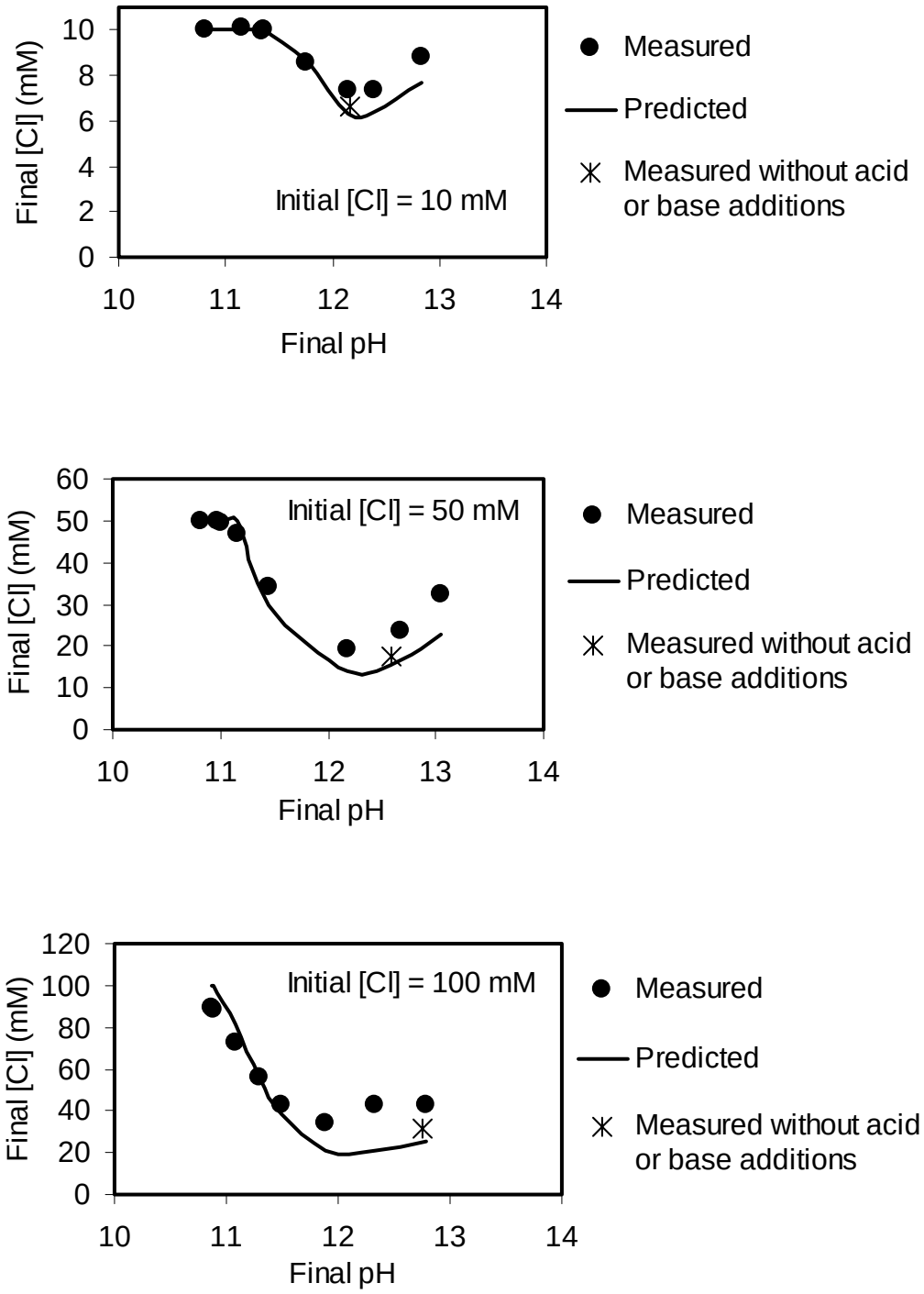

Figure 4.26 Effect of pH on model-predicted concentrations of chloride.

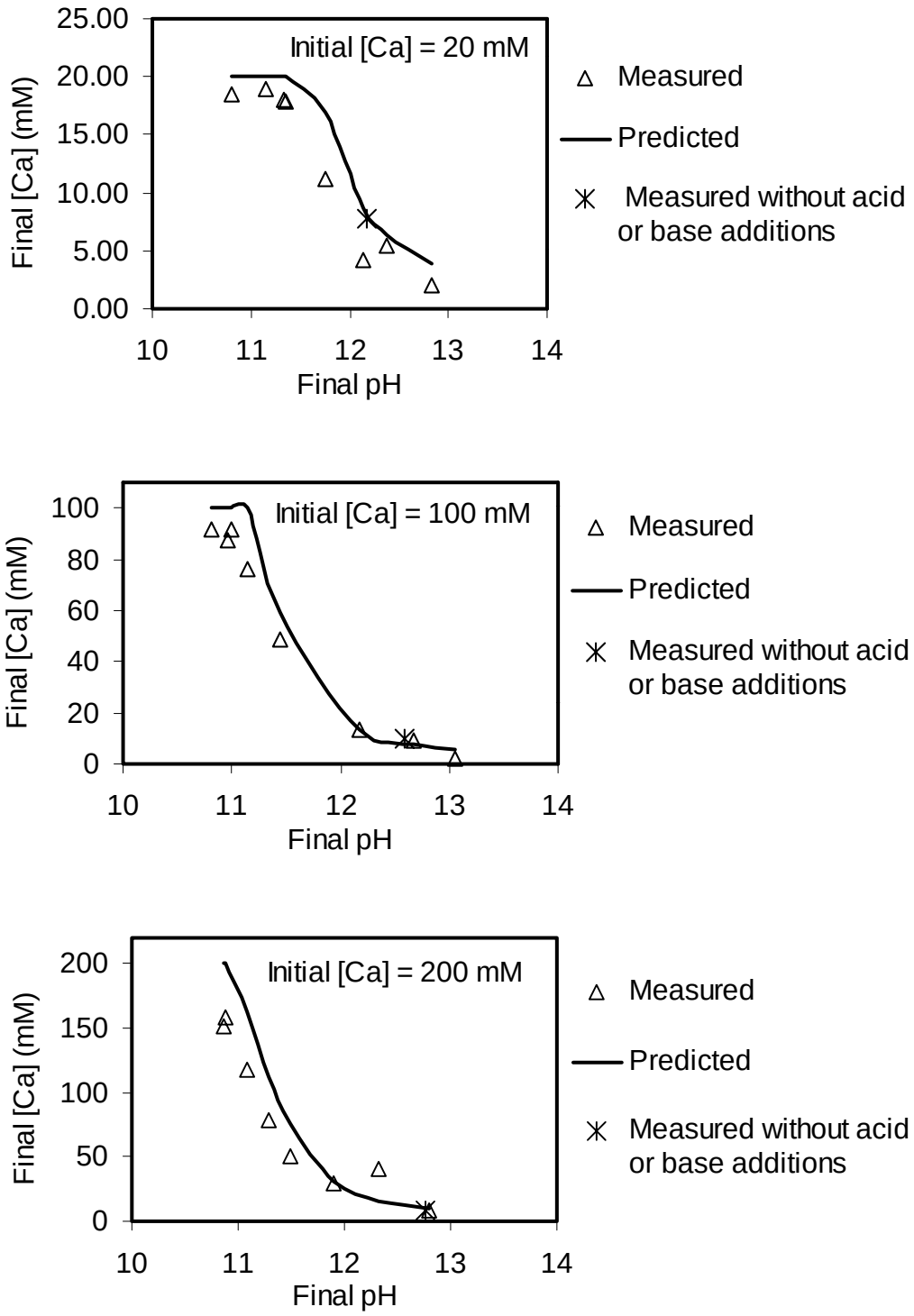

Figure 4.27 Effect of pH on model-predicted concentrations of calcium.

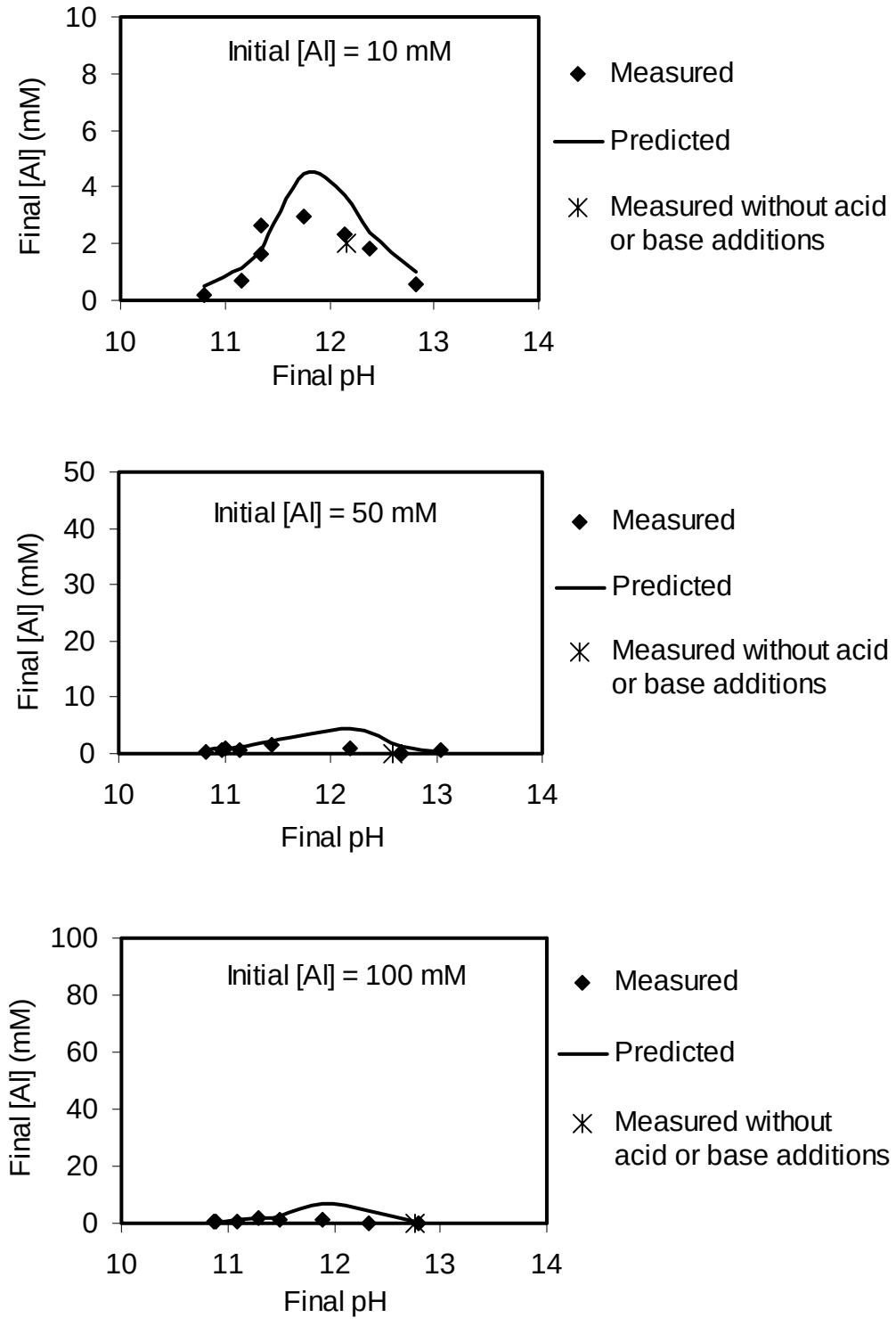

Figure 4.28 Effect of pH on model-predicted concentrations of aluminum.

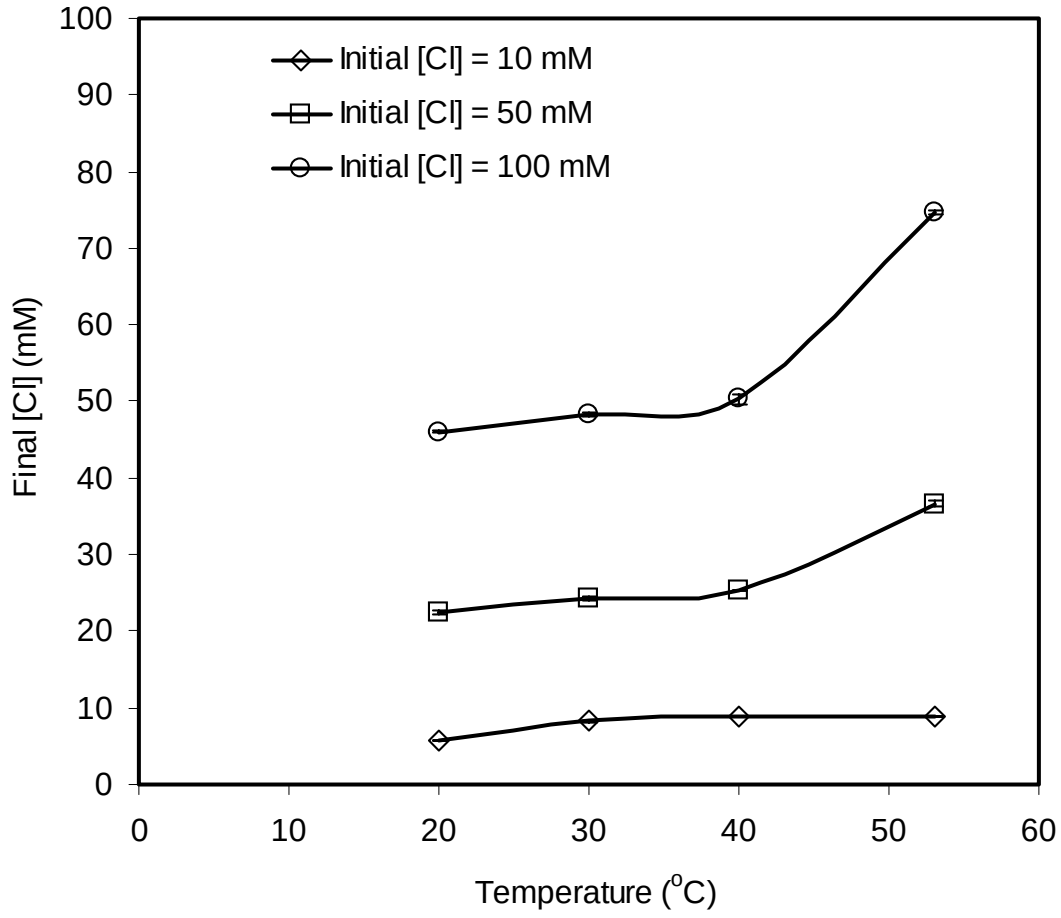

Figure 4.29 Effect of temperature on final chloride concentration.

temperatures below 40^{o}C. However, at temperatures above 40^{o}C, chloride concentration substantially increased with increasing water temperature. This could be because calcium chloroaluminate is unstable with respect to calcium hydroxyaluminate at temperatures above 40^{o}C. This agrees with the findings of Glasser et al. (1999) who reported that anion substitution may partially stabilize calcium aluminate (CAH_x) phases over AFm phases at temperatures above 40^{o}C.

4.7 X Ray Diffraction Results for Solids Formed in Cl – OH System

XRD analysis was conducted to identify the precipitated solids formed in UHLA process. Figure 4.30 shows diffractograms of solids that precipitated under different experimental conditions as described in Chapter III. The solids were identified at each experimental condition by comparing the peaks and the corresponding interplanar spacings (d values, in Å) with standard data in the Joint Committee on Powder Diffraction Standards (JCPDS) cards (JCPDS, 1990). The XRD patterns at all investigated experimental conditions show the presence of Friedel salt (calcium chloroaluminate) (at d = 7.85, 3.93, 3.81, 2.87, 2.32, 2.29, and 1.66 Å), tricalcium hydroxyaluminate (at d = 2.80, 2.70, and 2.43 Å), and tetracalcium hydroxyaluminate (at d = 7.85, 2.87, 2.70, 2.51, 2.43, and 2.32 Å). XRD patterns at initial chloride concentrations 30, 50, and 100 mM (XRD30, XRD50, and XRD100 respectively) have similar peaks. However, at the initial chloride concentration of 10 mM (XRD10), small peaks associated with gibbsite were observed (at d = 5.10, 4.42, and 2.04 Å). The pH value of this experiment was low (pH = 12.32) compared to experiments at higher initial

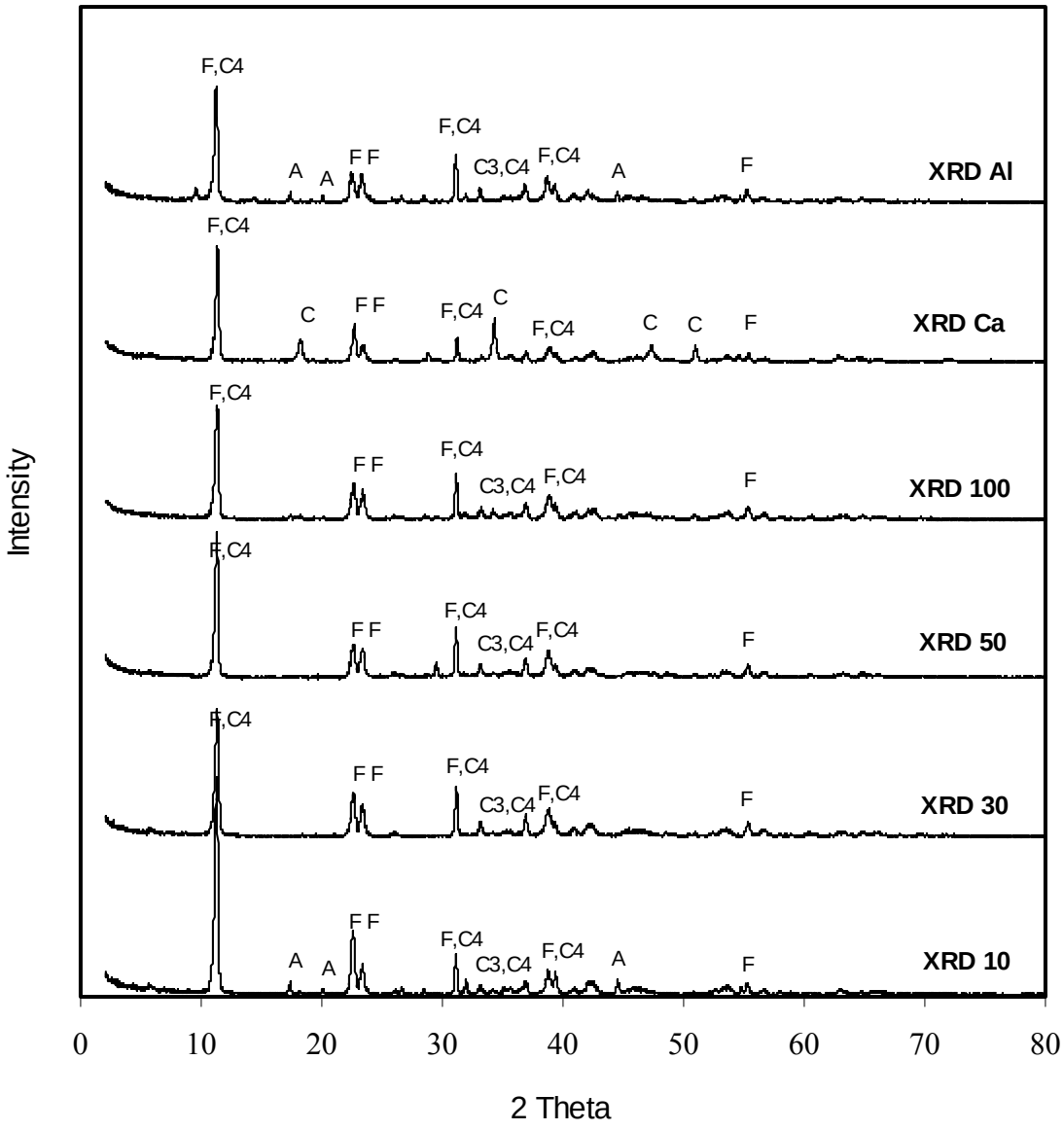

Figure 4.30 Diffraction patterns for detected solids in Cl – OH system. A = aluminum hydroxide (gibbsite), C = calcium hydroxide (portlandite), C3 = tricalcium hydroxyaluminate, C4 = tetracalcium hydroxyaluminate, and F = Friedel salt (calcium chloroaluminate).

chloride concentrations (pH = 12.85 at 50 mM initial [Cl] and pH = 13.04 at 100 mM initial [Cl]) and it was suitable for precipitation of aluminum hydroxide solids such as gibbsite. XRD patterns show the presence of calcium hydroxide solid (portlandite; d = 4.87, 2.61, 1.92, and 1.79 Å) when excess lime dose was added with respect to aluminum dose (XRDCa) (stoichiometric ratio of calcium dose to aluminum dose = 4.0). Similarly, when excess sodium aluminate was added relative to calcium (XRDAl; stoichiometric ratio of aluminum dose to lime dose = 1.0), XRD patterns show the presence of aluminum hydroxide (gibbsite) at the same d values that were observed in XRD10. These results agree with the results of the equilibrium model, which predicted the formation of calcium hydroxide or aluminum hydroxide solids when calcium or aluminum concentrations are above the stoichiometric amount needed to form the solid solution. Table 4.5 shows the XRD peaks of the identified solids. The raw data for XRD results are shown in Appendix E.

XRD analysis showed the presence of the same solid phases that were assumed present by the equilibrium model, which supports the validity of that model in describing mechanisms of chloride removal by the UHLA process.

4.8 Interactions between Chloride and Sulfate in UHLA

4.8.1 Effect of Chemical Doses on Sulfate Removal with UHLA

Three initial concentrations of sulfate (10, 50, and 100 mM) were investigated at each of three ratios of chemical doses to initial sulfate concentrations. Ratios of lime dose to initial sulfate concentrations were 100%, 200%, and 300%, while the aluminum

Table 4.5 XRD data for identified solids in UHLA process.

Solid phase	**2θ**	**d values (Å)**		**Relative intensity**
		This work	JCPDS cards	
Calcium chloroaluminate			JCPDS Card No. 35-105	
	11.26	7.85	7.87	100
	22.6	3.93	3.94	90
	23.34	3.81	3.81	5
	31.12	2.87	2.87	60
	38.78	2.32	2.32	70
	39.38	2.29	2.28	40
	55.28	1.66	1.66	50
Tricalcium hydroxyaluminate			JCPDS Card No.38-1429	
	31.92	2.80	2.79	8
	33.18	2.70	2.699	100
	36.90	2.43	2.41	5
Tetracalcium hydroxyaluminate			JCPDS Card No.33-255	
	11.26	7.85	7.85	100
	31.12	2.87	2.87	100
	33.18	2.70	2.70	50
	35.66	2.51	2.48	50
	36.90	2.43	2.43	50
	38.78	2.32	2.31	50
Calcium hydroxide (portlandite)			JCPDS Card No.4-733	
	18.20	4.87	4.90	74
	34.28	2.614	2.628	100
	47.32	1.92	1.927	42
	50.98	1.79	1.796	36
	54.54	1.681	1.687	21
Aluminum hydroxide (gibbsite)			JCPDS Card No.33-18	
	17.36	5.10	4.85	100
	20.08	4.42	4.37	70
	44.48	2.04	2.05	40

dose were chosen to be equal to 50% of the lime dose for all experiments. Figure 4.30 shows the effect of chemical doses on final sulfate concentrations and shows that sulfate concentrations decreased with increasing lime and aluminum doses. The hypothesis was made that sulfate removal is controlled by the precipitation of a calcium sulfoaluminate called ettringite ($Ca_6Al_2(SO_4)_3(OH)_{12}$) according to the following reaction.

$$6\ Ca^{2+} + 2\ Al(OH)_4^- + 3\ SO_4^{2-} + 4\ OH^- = Ca_6Al_2(SO_4)_3(OH)_{12}\ (s) \qquad (4\text{-}10)$$

If calcium sulfoaluminate is the only important solid that is precipitated, the ratio of calcium removed to sulfate removed should equal 2.0, i.e., at lime dose equal to 200% of initial sulfate concentration, the theoretical final sulfate concentration should be zero, as shown by the doted line in Figure 4.31. The ratios of calcium removed to sulfate removed and the ratios of aluminum removed to sulfate removed are shown in Figures 4.32 and 4.33, respectively. This figure indicates that these ratios agreed with the stoichiometric ratios of ettringite precipitation at low chemical doses of lime and sodium aluminate. However, at higher lime and aluminum doses, the ratios deviated from theoretical stoichiometry (Figures 4.31, 4.32, and 4.33). Figures 4.32 and 4.33 show that ratios of calcium removed to sulfate removed and ratios of aluminum removed to sulfate removed increased with increasing lime dose and aluminum dose. This indicates that other solids that are rich in calcium and aluminum with respect to sulfate were formed. One such solid is calcium monosulfoaluminate, which is called monosulfate ($Ca_4Al_2(SO_4)(OH)_{12}$) and has the following formation reaction.

$$4\ Ca^{2+} + 2\ Al(OH)_4^- + SO_4^{2-} + 4\ OH^- = Ca_4Al_2(SO_4)(OH)_{12}\ (s) \qquad (4\text{-}11)$$

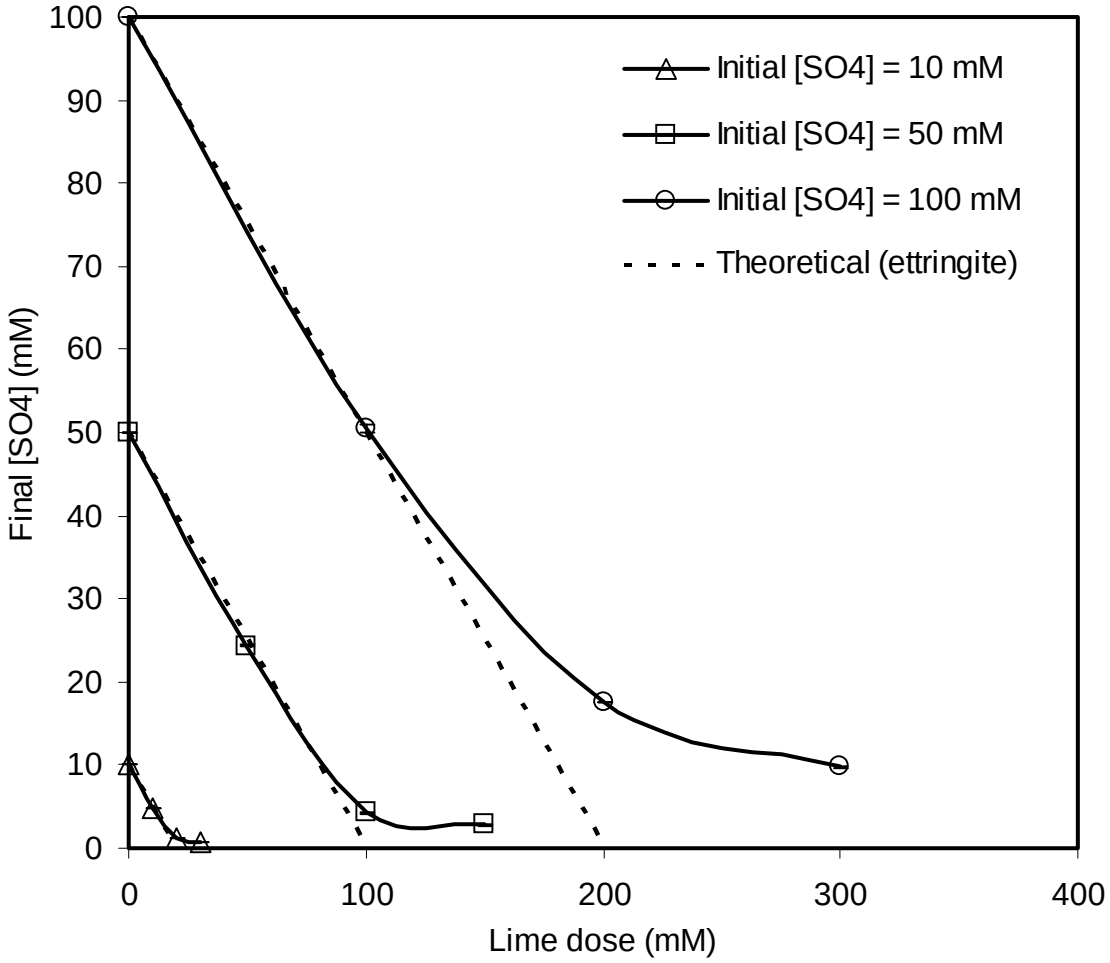

Figure 4.31 Effect of chemical doses on sulfate removal with UHLA.

Note: Aluminum dose = 50% of lime dose for all data points.

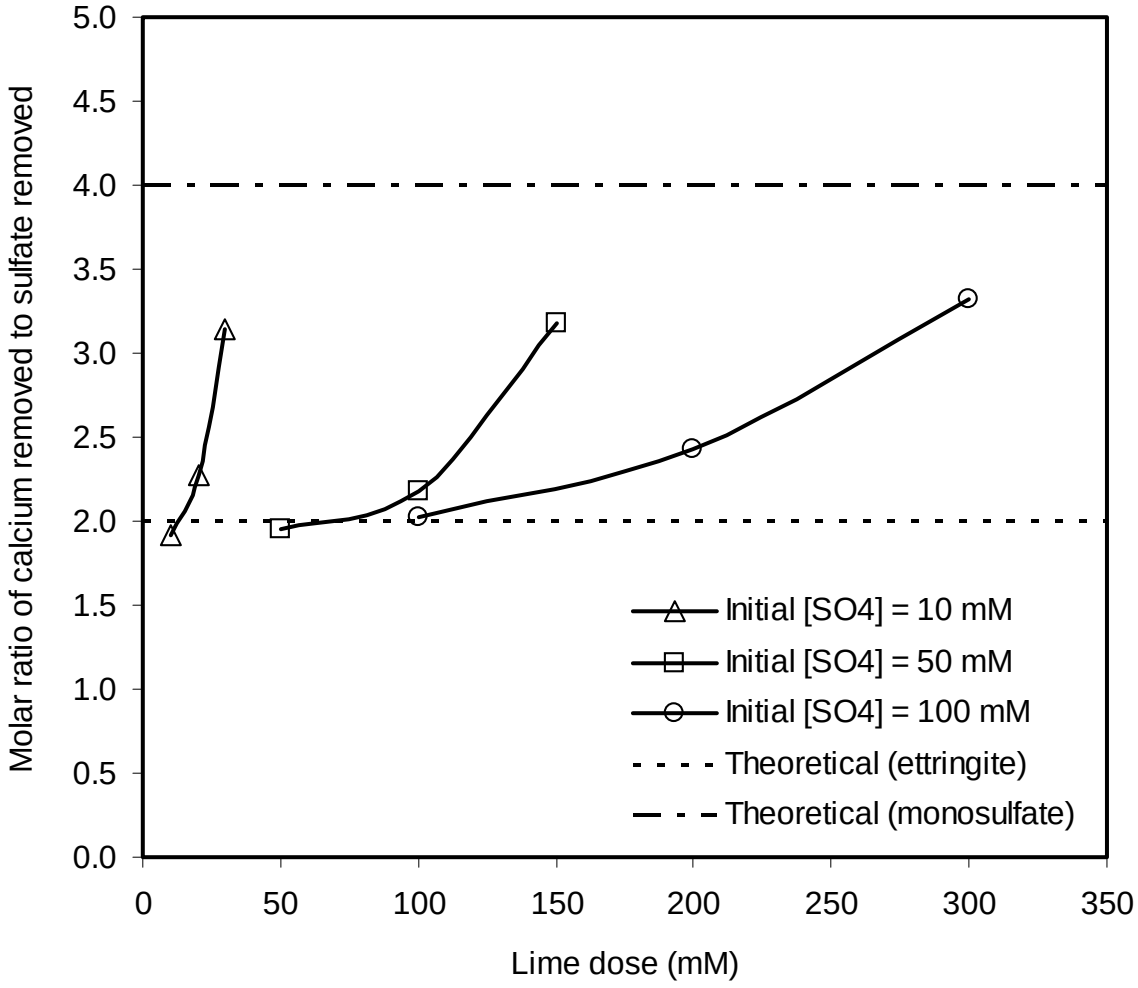

Figure 4.32 Effect of lime dose on the ratio of calcium removed to sulfate removed with UHLA.

Note: Aluminum dose = 50% of lime dose for all data points.

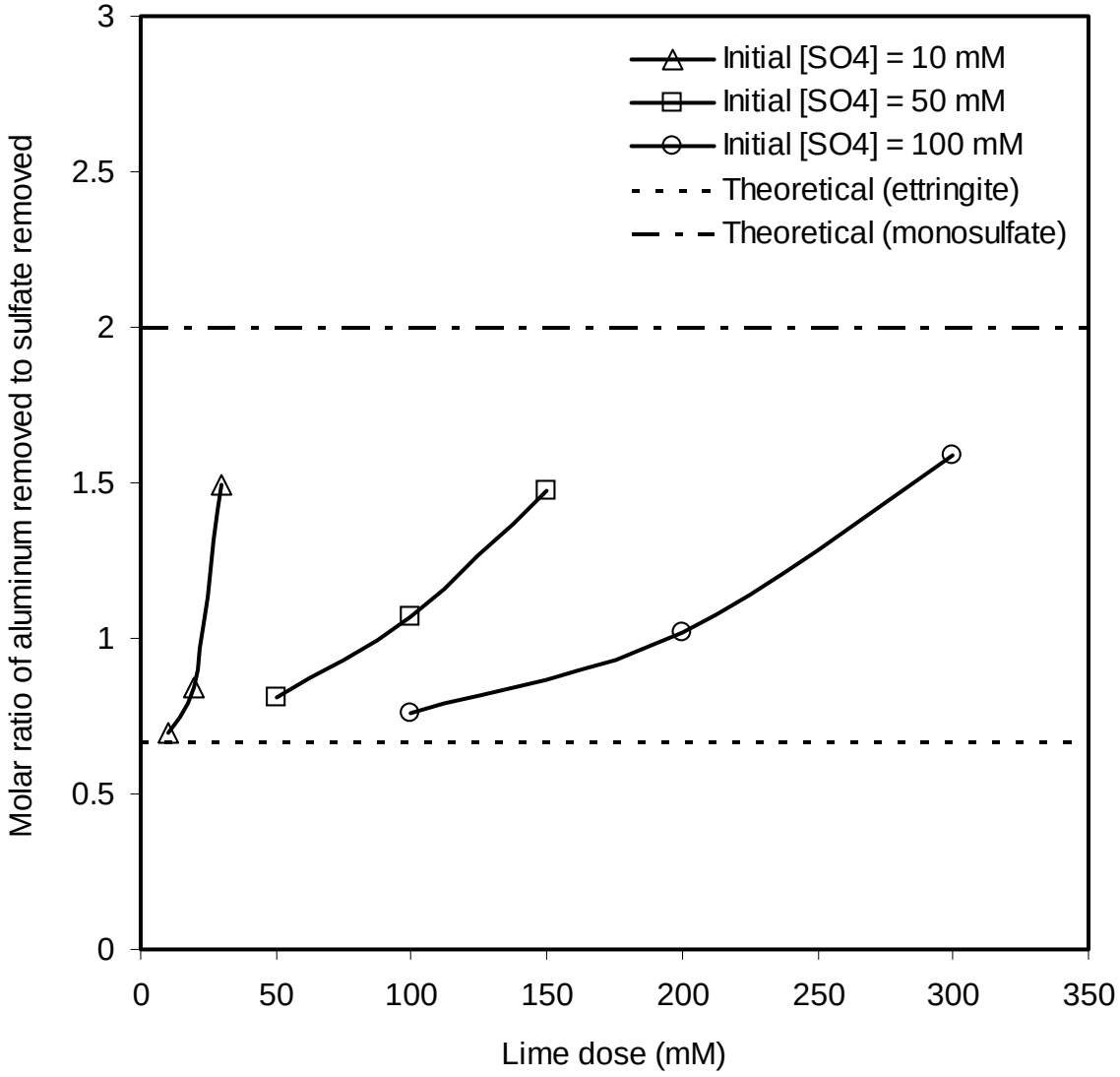

Figure 4.33 Effect of lime dose on the ratio of aluminum removed to sulfate removed with UHLA.

Note: Aluminum dose = 50% of lime dose for all data points.

The changes in stoichiometric ratios could also be explained by formation of other solids such as tricalcium hydroxyaluminate, tetracalcium hydroxyaluminate, calcium hydroxide, aluminum hydroxide, and calcium sulfate.

4.8.2 Equilibrium Modeling for SO_4 – OH System

An equilibrium model was developed and tested in order to develop a tool to describe the chemical behavior of sulfate removal with UHLA. The hypothesis was made that sulfate removal was controlled by the formation of a solid solution containing ettringite, monosulfate, tricalcium hydroxyaluminate, and tetracalcium hydroxyaluminate. The database of PHREEQC was modified to include new solids (ettringite, monosulfate) and their solubility products. The solubility products of ettringite and monosulfate were chosen to be $10^{-44.55}$ and $10^{-29.43}$ respectively (Damidot and Glasser 1993). The solubility products for tricalcium hydroxyaluminate, tetracalcium hydroxyaluminate, and aluminum hydroxide that were obtained by regression from Cl – OH data were also used. Table 4.6 shows a summary of the solubility products of possible solids that were allowed to precipitate by PHREEQC in SO_4 – OH system. In order to evaluate the equilibrium model, the model was used to predict final concentrations with PHREEQC using initial solution compositions and equilibrium constants listed in Table 4.6. Total initial concentrations of sulfate, calcium, aluminum, and hydroxide were used as input data to PHREEQC and the model was used to predict final concentrations of all species. Assumptions that pure solids were formed and that solid solutions were formed were tested. Error analysis indicated that the results can be best described by assuming a solid solution of ettringite, monosulfate, tricalcium

hydroxyaluminate, and tetracalcium hydroxyaluminate. The solution was found to be undersaturated with respect to calcium sulfate for all data points. A comparison between measured and model-predicted sulfate concentrations is shown in Figure 4.34 and indicates that the model succeeded in adequately predicting final sulfate concentrations.

Table 4.6 Solid phases used in SO_4 – OH data modeling.

Solid name	Log (Ksp)	Source
Ettringite	-44.55	Damidot and Glasser (1993)
Monosulfate	-29.43	Damidot and Glasser (1993)
Tricalcium hydroxyaluminate	-19.72	This work (Cl-OH data)
Tetracalcium hydroxyaluminate	-25.02	This work (Cl-OH data)
Calcium sulfate	-4.58	Stumm and Morgan (1996)
Calcium hydroxide	-5.19	Stumm and Morgan (1996)
Aluminum hydroxide	-33.33	This work (Cl-OH data)

4.8.3 Interactions Among Solids in the Solid Solution Formed in The SO4 – OH System

Fractions of each solid in the solid solution were calculated for each data point using PHREEQC and are shown in Figure 4.35 as functions of lime and sodium aluminate doses. The fraction of monosulfate in the solid solution increased with increasing lime and sodium aluminate doses while the fraction of ettringite decreased. Additions of lime and sodium aluminate resulted in increasing Ca, Al, and OH

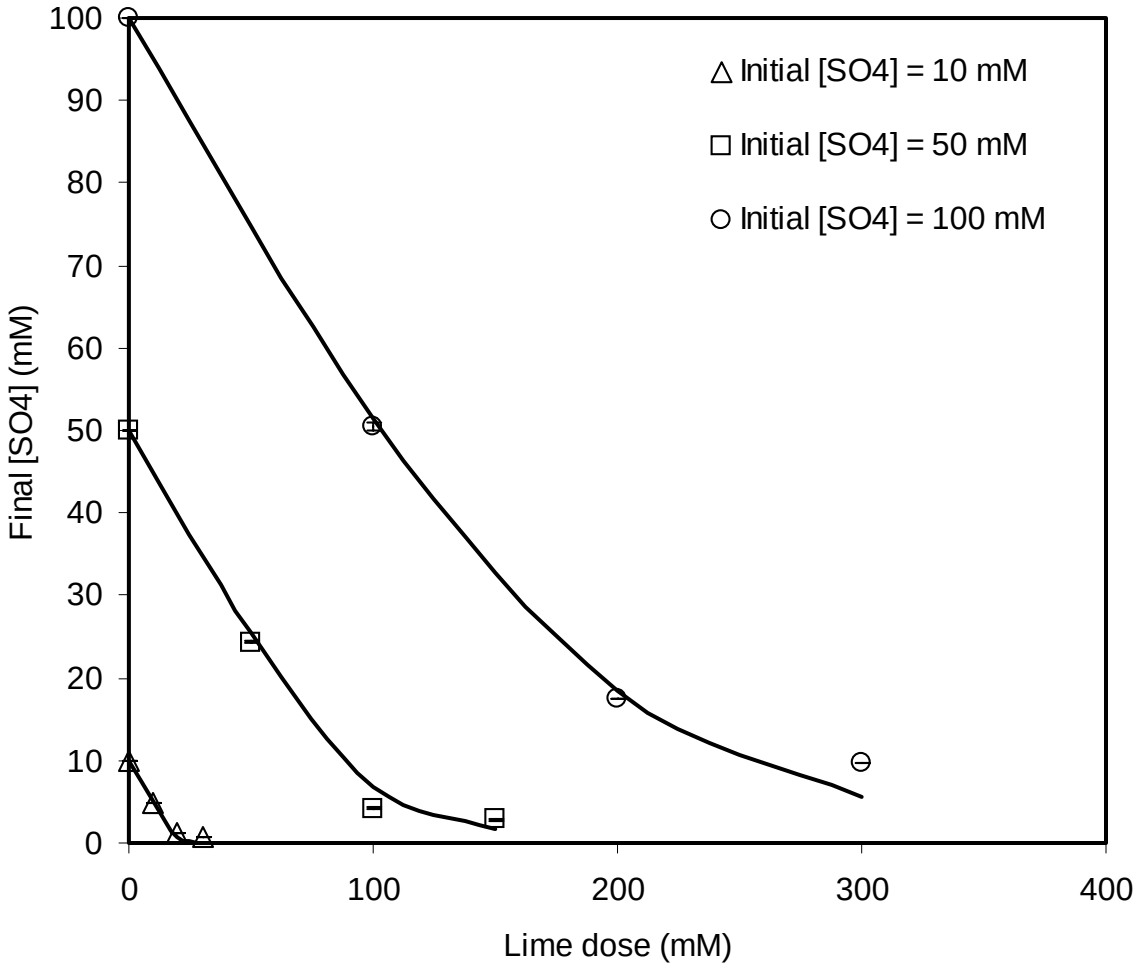

Figure 4.34 Comparison between measured and model-predicted concentrations in SO_4 – OH system. Symbols represent measured concentrations and lines represent predicted concentrations.

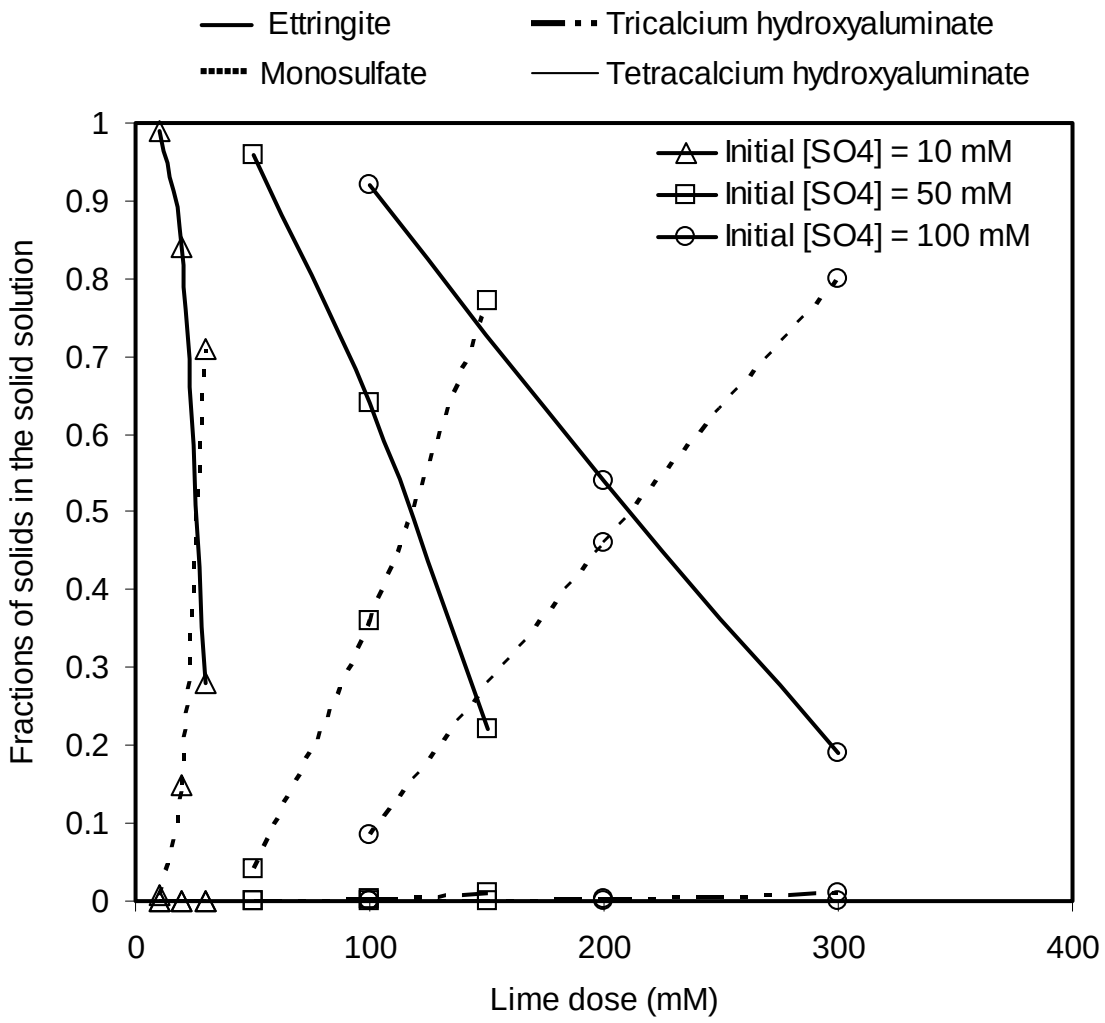

Figure 4.35 Fractions of solids in the solid solution in SO_4 – OH system.

concentrations in the solution with respect to sulfate. This makes favors precipitation of $Ca_4Al_2(SO_4)(OH)_{12}$ over $Ca_6Al_2(SO_4)_3(OH)_{12}$. Figure 4.35 shows that the fractions of tricalcium hydroxyaluminate and tetracalcium hydroxyaluminate are negligible for all data points. This indicates that precipitation of solids containing sulfate in the UHLA process is more favorable than that of solids containing hydroxide. These results agree with previous research on layered double hydroxides (LDHs), which indicated that divalent anions in general have greater affinities to bind in the interlayer space of the LDHs than monovalent anions (Rives, 2001, and De Roy et al., 2001).

The ratio of lime dose to aluminum dose is also important in controlling the fractions of solids in the solid solution and in the removal efficiency of sulfate. Ettringite contains high ratio of calcium to aluminum. Therefore, if the ratio of lime dose to aluminum dose increased above the stoichiometric ratio of 2, this would thermodynamically favor the precipitation of ettringite over monosulfate and would result in increasing the fraction of ettringite in the solid solution and thus increasing sulfate removal efficiency. The equilibrium model was used to simulate the effect of the ratio of lime dose to aluminum dose on sulfate removal. PHREEQC was used with aluminum doses that varied and with lime doses that were maintained at a fixed ratio to the initial sulfate concentration. This ratio was set at the stoichiometric value for ettringite precipitation (2). Figure 4.36 shows effect of the ratio of lime dose to aluminum dose on the fractions of solids in the solid solution. The fraction of ettringite increased and the fraction of monosulfate decreased with increasing ratio of lime dose to aluminum dose. The fraction of monosulfate becomes negligible with respect to the

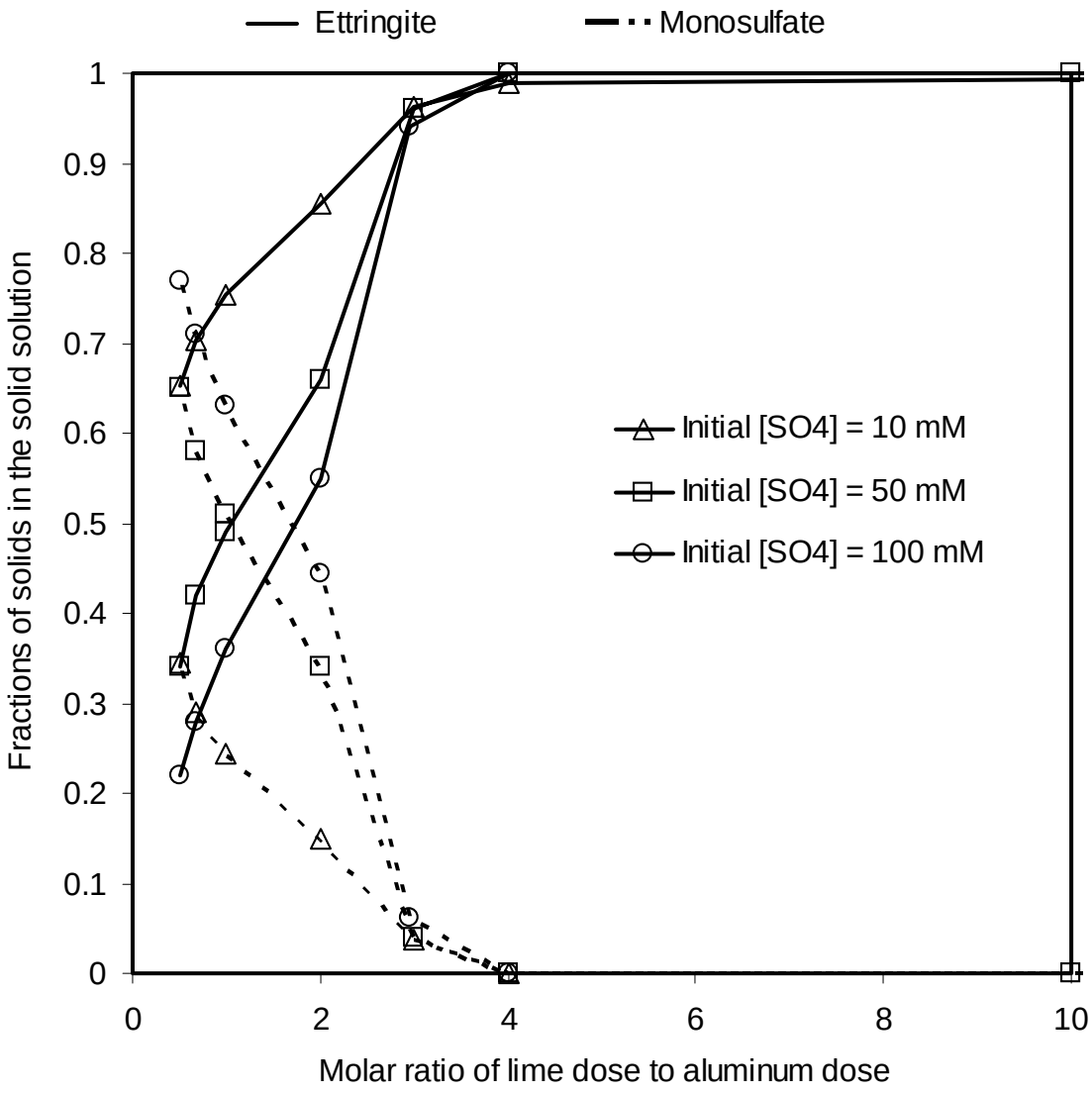

Figure 4.36 Effect of ratio of lime dose to aluminum dose on the fraction of solids in SO_4 – OH system.

fraction of ettringite, when the stoichiometric ratio of lime dose to aluminum dose approached the stoichiometric ratio of ettringite precipitation (3.0). Therefore, in order to maximize the fraction of ettringite and maximize sulfate removal efficiency, the ratio of lime dose to aluminum dose should be at least 3.0.

4.8.4 Effect of Chloride Concentration on Sulfate Removal with UHLA

Three initial concentrations of sulfate (10, 50, and 100 mM) were investigated at three initial concentrations of chloride (10, 50, and 100 mM). Each Cl-SO_4 combination was investigated at three molar ratios (100%, 200%, and 300%) of lime dose to the sum of the initial concentrations of chloride and sulfate (Cl + SO_4). Aluminum doses were chosen to be 50% of lime dose for all experiments. Final sulfate concentrations versus lime dose at different initial chloride and sulfate concentrations are shown in Figure 4.37. Chloride was found to have negligible effect on final sulfate concentrations. The differences among final sulfate concentrations are negligible over a range of 0 to 100 mM initial chloride concentrations at the same lime dose. This indicates that removal of sulfate does not depend on chloride concentration.

4.8.5 Effect of Sulfate Concentration on Chloride Removal with UHLA

Figure 4.38 shows a comparison between the removal efficiency of chloride and the removal efficiency of sulfate. Removal efficiencies for both chloride and sulfate increase with increasing lime and aluminum doses. However, sulfate removal efficiency is much higher than chloride removal efficiency at the same chemical doses and at the same initial concentrations of sulfate and chloride. This indicates that sulfate

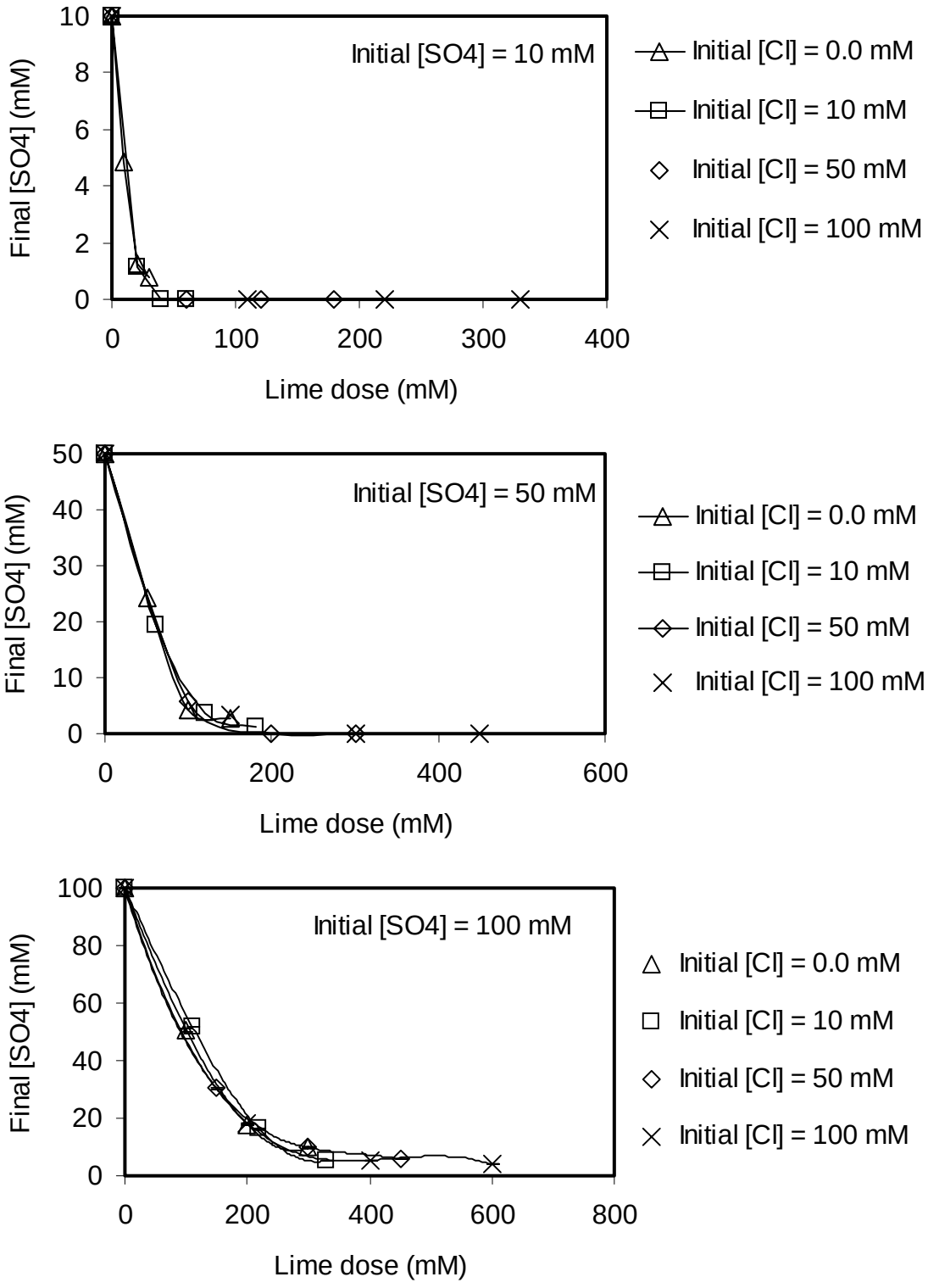

Figure 4.37 Effect of chloride concentration on sulfate removal with UHLA.

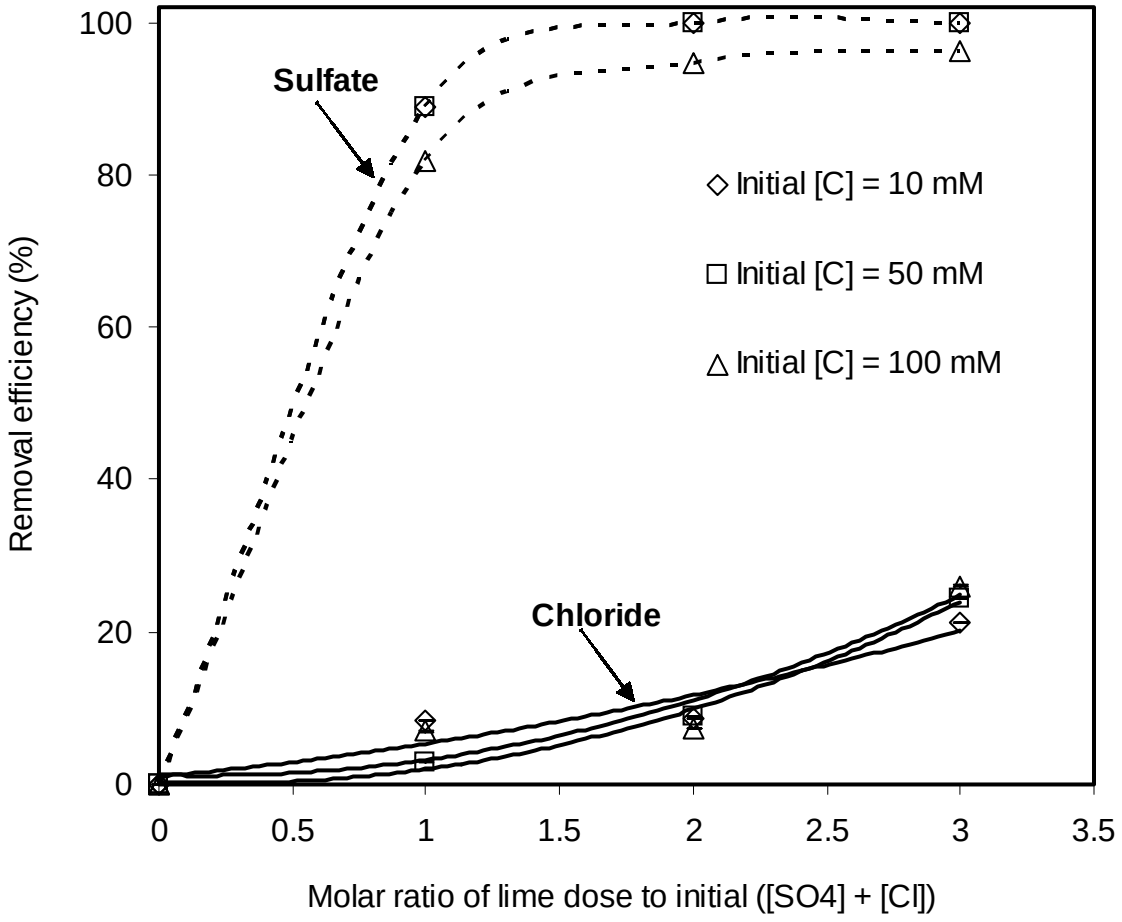

Figure 4.38 Comparison between sulfate and chloride removal efficiencies. [C] refers to the initial concentrations of both sulfate and chloride.

precipitation with Ca, Al, and OH is more favorable than chloride precipitation. These results agree with the results of Ulibarri and Hermosin (2001), Rives (2001), and De Roy et al. (2001), who all concluded that sulfate anions have a higher affinity for the interlayer space of the LDHs than chloride anions.

Figure 4.39 shows final chloride concentrations affected by initial sulfate concentrations at initial chloride concentrations 10, 50, and 100 mM. Final chloride concentrations increased with increasing initial sulfate concentrations at all investigated ratios of chemical doses to initial ($[SO_4]$ + [Cl]). If the chemical doses required to precipitate both sulfate and chloride are additives (i.e. the chemical doses required to precipitate (sulfate + chloride) = chemical doses required to precipitate sulfate + chemical doses required to precipitate chloride) and if the increase of chloride concentrations with increasing sulfate concentrations is due to the consumption of chemical doses to precipitate sulfate before chloride, then sulfate should not have had an effect on chloride concentrations when there is enough stoichiometric chemical doses to precipitate both sulfate and chloride (e.g., at ratio of lime dose to initial ($[SO_4]$ + [Cl]) equal 3 (R = 3 in Figure 4.39)). However, chloride concentrations increased with increasing sulfate concentrations at all chemical doses. This indicates that presence of sulfate resulted in increasing calcium chloroaluminate solubility and thus lowering chloride removal efficiency. This could be due to an increase in the activity of calcium chloroaluminate solid in the presence of sulfate and resulted in increasing the observed solubility product of the solid. Stumm and Morgan (1996) reported that the solubility of a constituent in the solid solution formation is greatly reduced and its activity increased

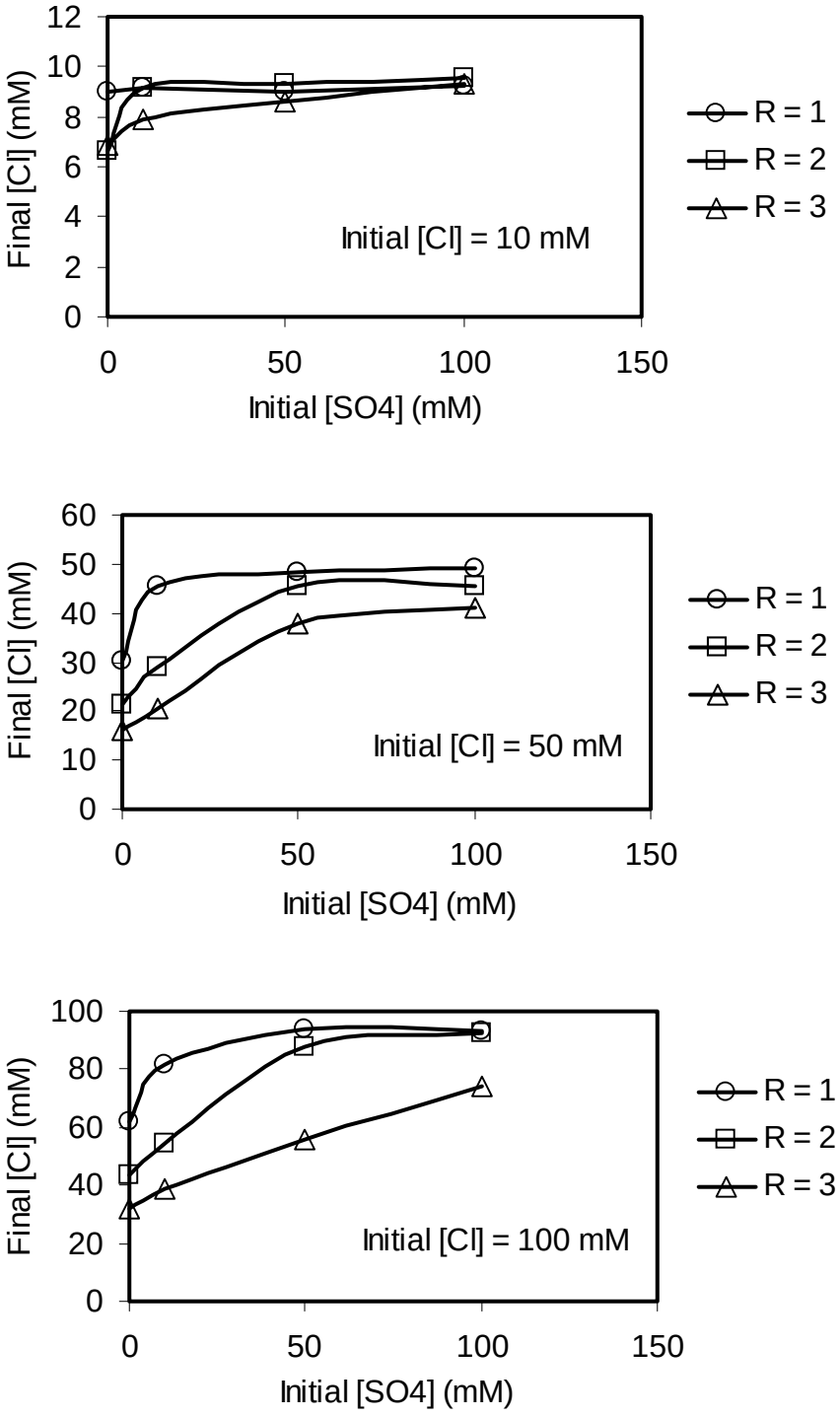

Figure 4.39 Effect of sulfate on final chloride concentrations. "R" represents the ratio of lime dose to initial ($[SO_4] + [Cl]$).

when it becomes a minor constituent of a solid solution phase. Therefore, and due to the higher affinity of sulfate to form solids with calcium and aluminum in UHLA with respect to chloride and due to the low solubility of these solids with respect to calcium chloroaluminate solid, the fraction of calcium chloroaluminate solid is small comparing to fraction of sulfoaluminate solids especially at high initial sulfate concentrations with respect to chloride concentrations. This can describe the increase of final chloride concentrations in the presence of sulfate. It could be also due to an effect of sulfate on the solid solution structure that weakens the ability of chloride to be held in the interlayer space of the solid solution formation.

4.8.6 Equilibrium Modeling of Cl – SO_4 – OH System

The same database file that was used to model the Cl – OH system and was modified to model the SO_4 – OH system was used to model the Cl – SO_4 – OH system. Total initial constituent concentrations were used as input data to PHREEQC (Appendix B-4). The assumptions that pure solids precipitated and that solid solutions precipitated were tested. Error analysis indicated that the results could be best described by assuming the formation of a solid solution containing calcium chloroaluminate, ettringite, monosulfate, tricalcium hydroxyaluminate, and tetracalcium hydroxyaluminate.

Measured concentrations and model-predicted concentrations of sulfate, chloride, calcium, and aluminum as well as final pH are shown in Figures 4.40, 4.41, 4.42, 4.43, and 4.44 respectively. Figures 4.40 to 4.44 indicated that the model succeeded in

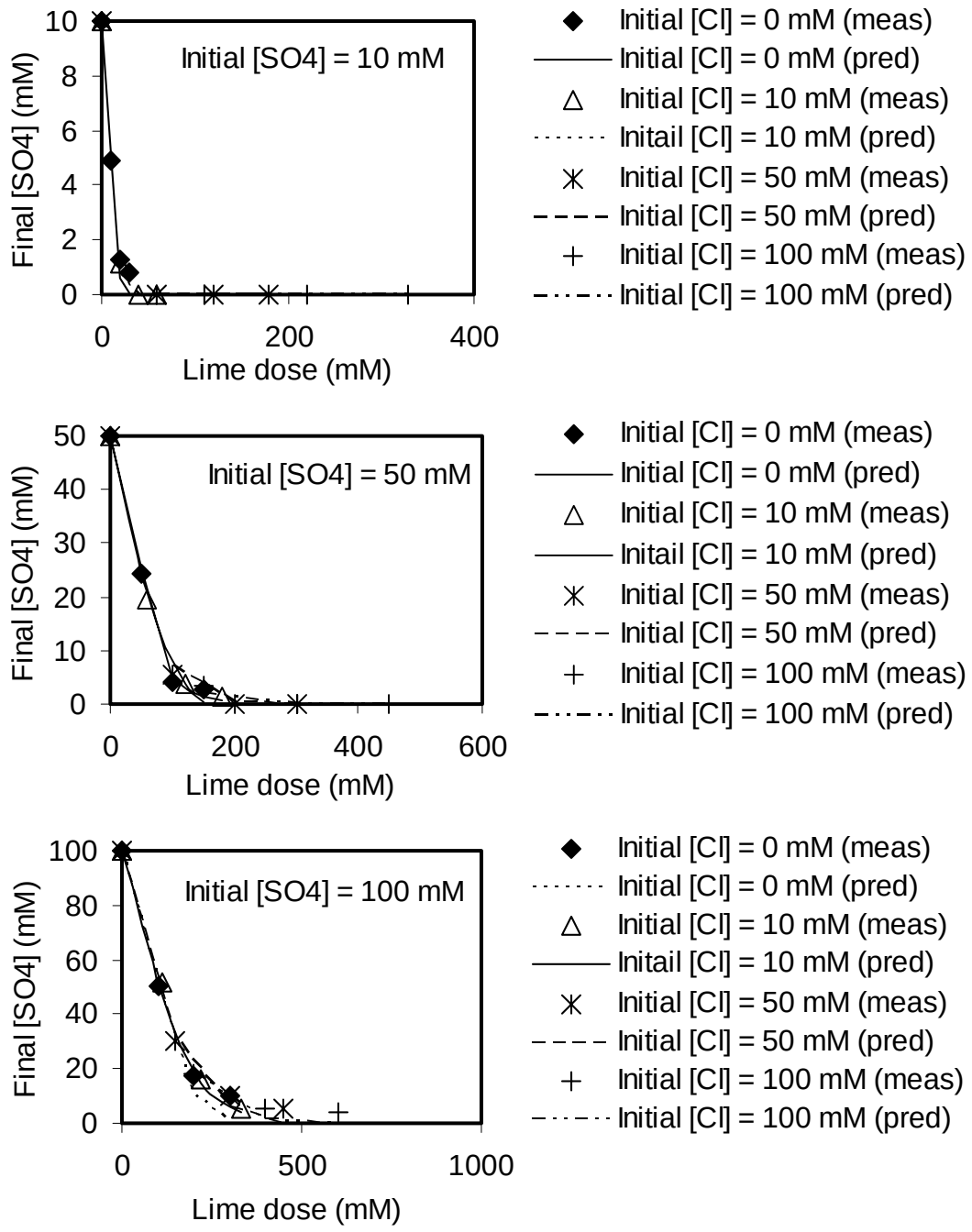

Figure 4.40 Comparison between measured and predicted sulfate concentrations in SO_4 – Cl – OH system. (Meas) refers to measured concentrations and (pred) refers to predicted concentrations.

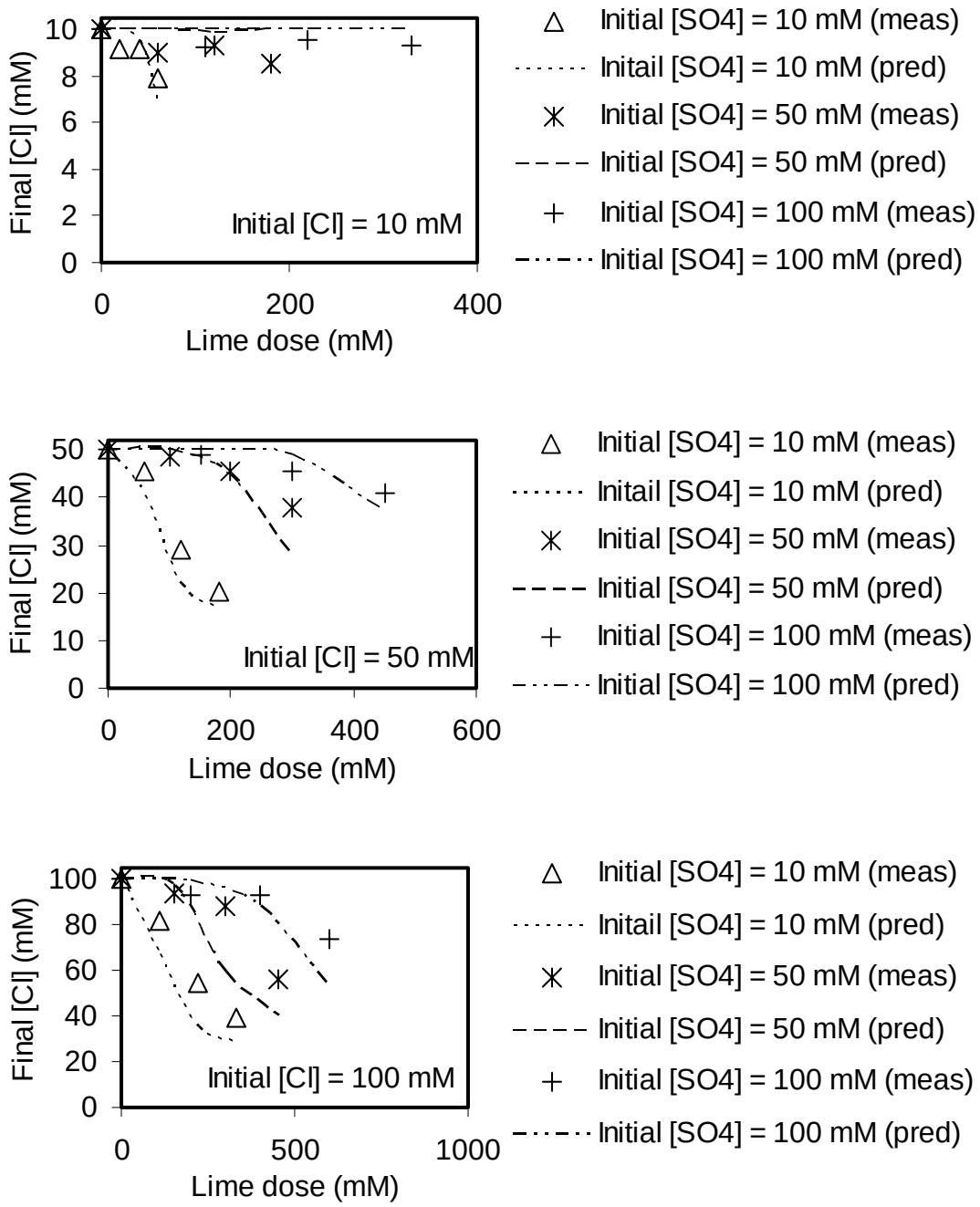

Figure 4.41 Comparison between measured and predicted chloride concentrations in SO_4 – Cl – OH system. (Meas) refers to measured concentrations and (pred) refers to predicted concentrations.

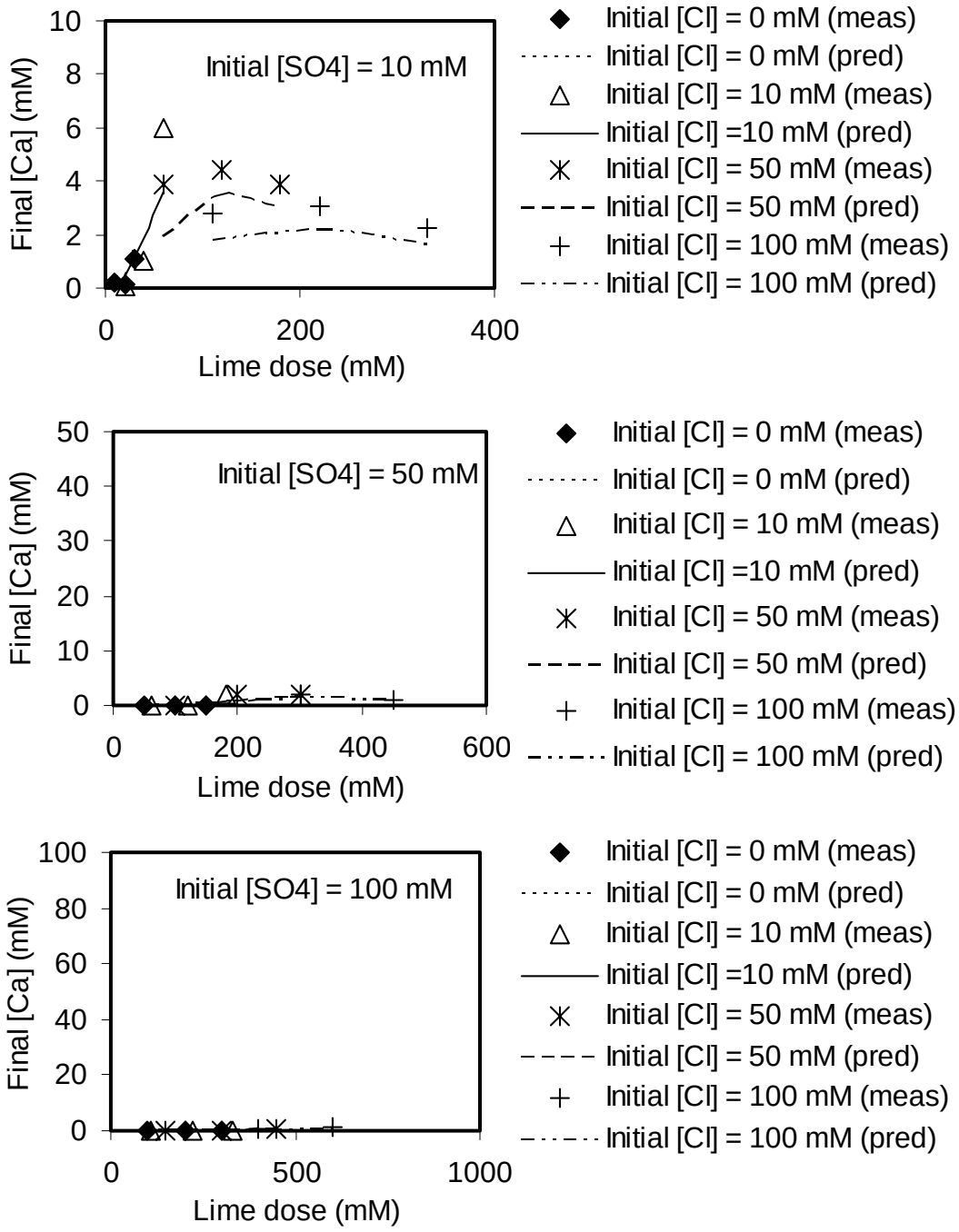

Figure 4.42 Comparison between measured and predicted calcium concentrations in SO_4 – Cl – OH system. (Meas) refers to measured concentrations and (pred) refers to predicted concentrations.

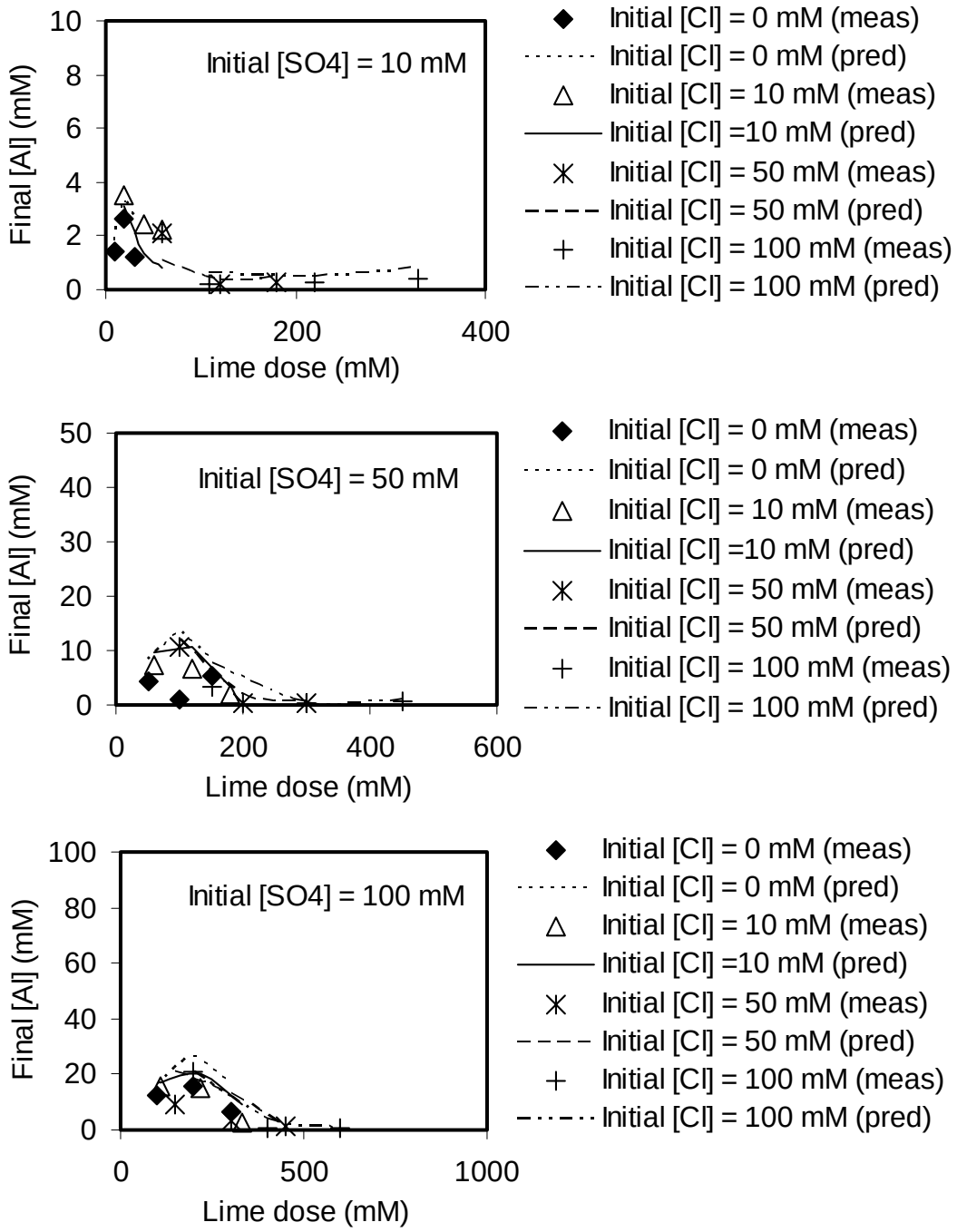

Figure 4.43 Comparison between measured and predicted aluminum concentrations in SO_4 – Cl – OH system. (Meas) refers to measured concentrations and (pred) refers to predicted concentrations.

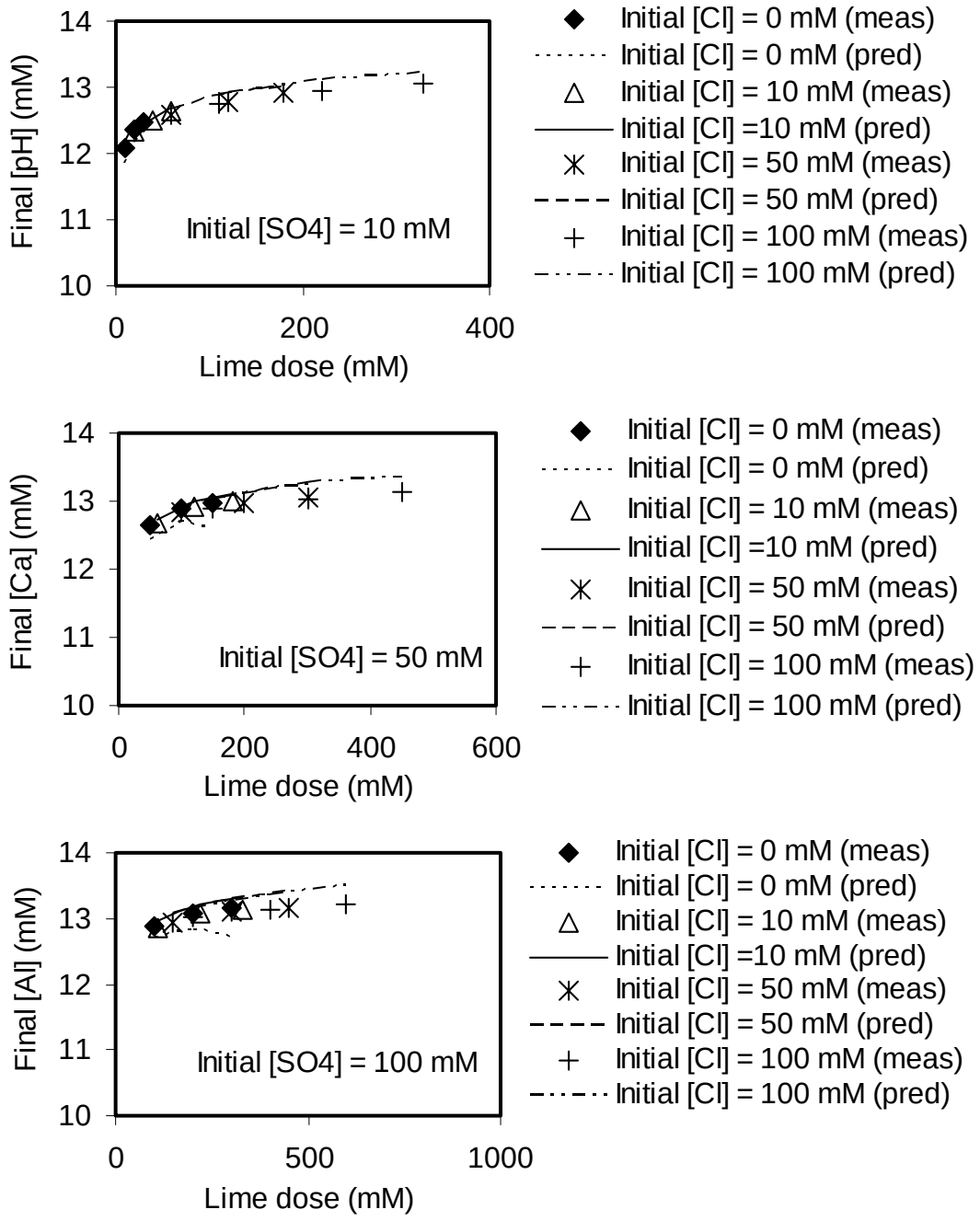

Figure 4.44 Comparison between measured and predicted pH values in SO_4 – Cl – OH system. (Meas) refers to measured concentrations and (pred) refers to predicted concentrations.

adequately predicting chemical behavior during the simultaneous removal of chloride and sulfate in UHLA. However, the model moderately underestimated final chloride concentrations. The hypothesis was made that the increase of final chloride concentrations is due to the increase of the activity of calcium chloroaluminate solid in the solid solution formation in the presence of sulfate-containing solids. The observed solubility product of calcium chloroaluminate solid was calculated by non-linear regression routine using INVRSK and PHREEQC. Measured final chloride concentrations in Cl - SO_4 - OH system were used as dependent variables. The observed solubility product of calcium chloroaluminate was obtained to be $10^{-26.42}$ compared to the value of $10^{-27.10}$ that was reported by Bin-Yauri and Glasser (1998) and was used in the original model. The new value of the solubility product of calcium chloroaluminate was used in the model to more accurately predict final chloride concentrations (Figure 4.45).

4.8.7 X Ray Diffraction Results for Solids Formed in Cl - SO_4 - OH system

Figure 4.46 shows diffractograms of solids precipitated in Cl - SO_4 – OH system (XRDSO4). XRD patterns show the presence of ettringite (at d = 9.84, 4.95, 3.90, and 3.018 Å), monosulfate (at d = 8.77, 4.43, 3.97, 2.86, 2.44, and 2.4 Å), and another solid called Kuzel salt ($Ca_4Al_2Cl(SO_4)_{0.5}(OH)_{12}$) (Glasser et al., 1999) (at d = 8.39, 4.22, 2.86, 2.72, and 2.23 Å). These are in addition to the same solids that were found in Cl- OH system, i.e. Friedel salt, tricalcium hydroxyaluminate, and tetracalcium hydroxyaluminate. The XRD data for new solids obtained in Cl - SO_4 - OH system are

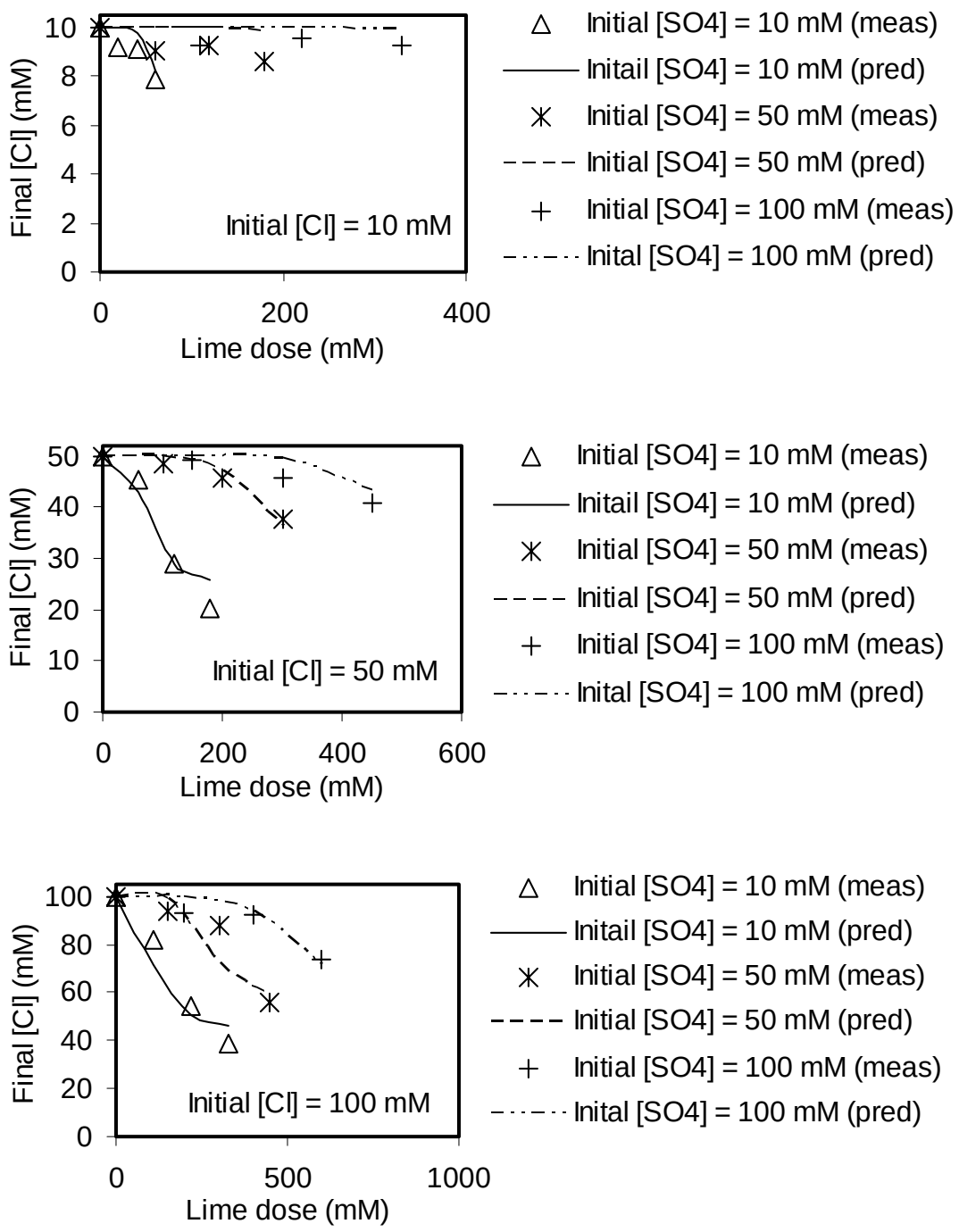

Figure 4.45 Comparison between measured and model-predicted concentrations of chloride using the new model. (Meas) refers to measured concentrations and (pred) refers to predicted concentrations.

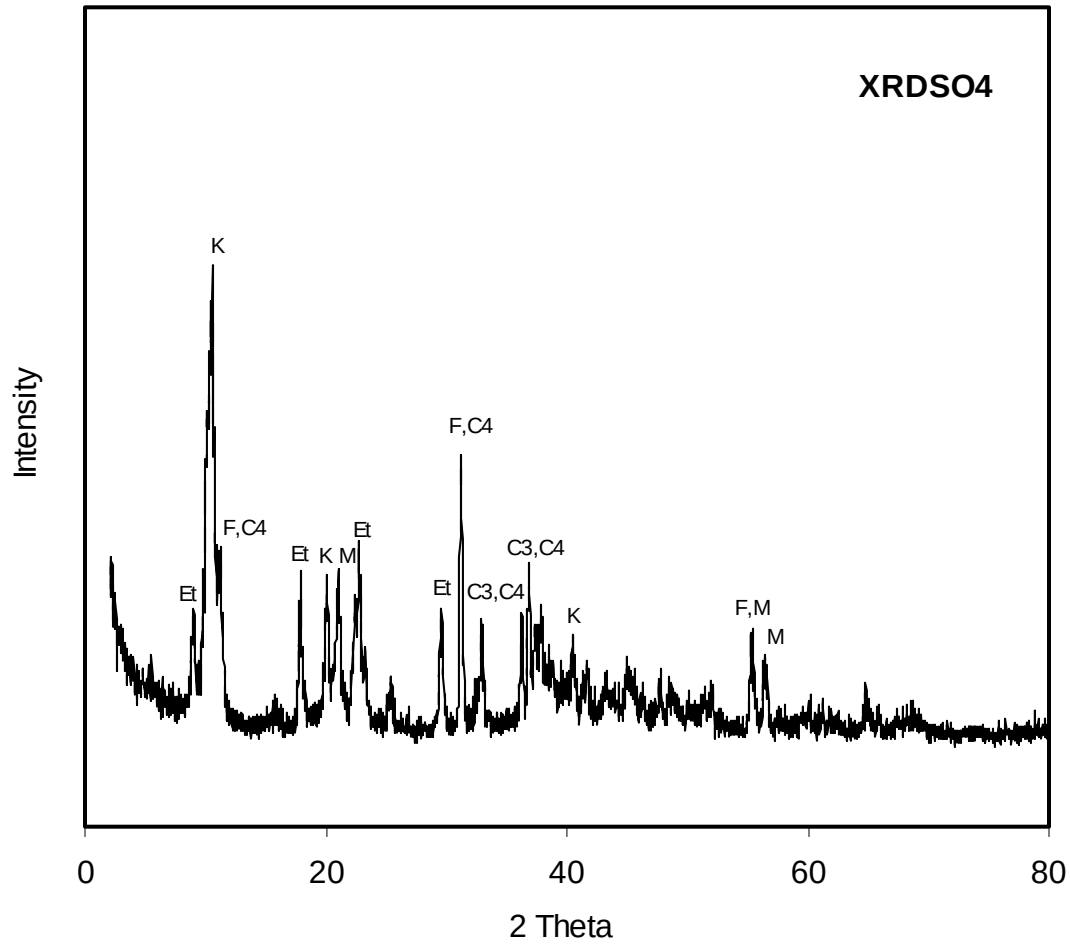

Figure 4.46 Diffraction patterns for precipitated solids in Cl - SO_4 - OH system. C3 = tricalcium hydroxyaluminate, C4 = tetracalcium hydroxyaluminate, Et = ettringite (calcium sulfoaluminate), F = Friedel salt (calcium chloroaluminate), K = Kuzel salt, and M = monosulfate (calcium monosulfoaluminate).

compared to JCPDS cards data are in Table 4.7. Results of XRD analysis for precipitated solids in systems containing both Cl and SO_4 agree with the hypothesis that ettringite and monosulfate are formed. However, the XRD patterns also showed the presence of Kuzel salt, which was not included in the equilibrium model.

Table 4.7 XRD data for new solids found in Cl – SO_4 – OH system.

Solid phase	**2θ**	**d values (Å)**		**Relative intensity**
		This work	JCPDS cards	
Calcium sulfoaluminate (ettringite)			JCPDS Card No. 37-1476	
	8.98	9.84	9.72	92
	17.90	4.95	4.98	30
	22.78	3.90	3.88	100
	29.58	3.018	3.018	15
Calcium monosulfoaluminate (monosulfate)			JCPDS Card No.11-179	
	10.08	8.77	8.92	100
	20.04	4.43	4.46	60
	22.4	3.97	3.99	60
	31.2	2.86	2.87	70
	36.84	2.44	2.45	60
	37.38	2.40	2.41	50
Kuzel salt			JCPDS Card No.19-203	
	10.54	8.39	8.32	100
	21.06	4.22	4.18	100
	31.2	2.86	2.87	50
	32.92	2.72	2.72	10
	40.44	2.23	2.24	20

The solubility product of Kuzel salt was calculated to be $10^{-27.20}$ using data from Glasser et al. (1999) and the following reaction.

$$Ca_4Al_2Cl(SO_4)_{0.5}(OH)_{12} = 4Ca^{2+} + 2Al(OH)_4^- + Cl^- + 0.5\ SO_4^{2-} + 4\ OH^- \qquad (4\text{-}12)$$

Kuzel salt was included in the equilibrium model but no significant changes were observed in the predicted final concentrations, even though the modified model predictions showed that Kuzel salt was formed as part of the solid solution. This was because the formula for Kuzel salt is just another expression of a solid solution formed by the combination of calcium chloroaluminate and monosulfate.

$$Ca_4Al_2Cl_2(OH)_{12} + Ca_4Al_2(SO_4)(OH)_{12} \quad = \quad 2\ Ca_4Al_2Cl(SO_4)_{0.5}(OH)_{12} \qquad (4\text{-}13)$$

The negligible changes in final predicted concentrations were the result of using a value for the solubility product of Kuzel salt ($10^{-27.20}$) that was similar to the value that can be derived from the solubility products of calcium chloroaluminate and calcium monosulfate. The following Equations can be derived using Equations 4-1, 4-11, and 4-12 and the definition of the solubility products,

$$K_{sp,\,chl} = \{Ca^{2+}\}^4\ \{Al(OH)_4^-\}^2\ \{Cl^-\}^2\ \{OH^-\}^4 \qquad (4\text{-}14)$$

$$K_{sp,\,mos} = \{Ca^{2+}\}^4\ \{Al(OH)_4^-\}^2\ \{SO_4^{2-}\}\ \{OH^-\}^4 \qquad (4\text{-}15)$$

$$K_{sp,\,kuzel} = \{Ca^{2+}\}^4\ \{Al(OH)_4^-\}^2\ \{Cl^-\}\ \{SO_4^{2-}\}^{0.5}\ \{OH^-\}^4 \qquad (4\text{-}16)$$

Where $K_{sp,\,mos}$, $K_{sp,\,kuzel}$ are the solubility products of calcium monosulfate and Kuzel salt respectively. The following two equations can be derived by algebraically manipulating Equation 4-16 with Equations 4-14 and 4-15.

$$K_{sp,\,kuzel} = K_{sp,\,chl} * \{Cl^-\}/\{SO_4^{2-}\}^{0.5} \quad (4\text{-}17)$$

$$K_{sp,\,kuzel} = K_{sp,\,mos} * \{SO_4^{2-}\}^{0.5}/\{Cl^-\} \quad (4\text{-}18)$$

By algebraically manipulating Equations 4-17 and 4-18, the solubility product of Kuzel salt can be calculated from the solubility products of calcium chloroaluminate and calcium monosulfate as follows,

$$K_{sp,\,kuzel} = (K_{sp,chl} * K_{sp,mos})^{0.5} = (10^{-26.42} * 10^{-29.43})^{0.5} = 10^{-27.93} \quad (4\text{-}19)$$

The difference between the two values of the solubility product of kuzel salt could be due to the effect of the solid solution mechanism on the solubility of the solid. However, Kuzel salt was not included in the final model because its addition would not improve the accuracy of predictions but would increase complexity.

4.8 Interactions between Chloride and Silica in UHLA Process

4.8.1 Effect of Chemical Doses on Silica Removal with UHLA Process

Three initial concentrations of silica (1.5 and 3.0 mM) were investigated at each of three ratios of chemical doses to initial silica concentrations. Ratios of lime dose to initial silica concentrations were 100%, 200%, and 300%, while ratios of aluminum doses were chosen at 50% of lime doses for all experiments. Figure 4.47 shows the effect of chemical doses on final silica concentrations and indicates that silica concentrations decreased with increasing lime and sodium aluminate doses. However, removal efficiency of silica is higher at initial silica concentration of 3.0 mM than at 1.5 mM (Figure 4.48). This is because pH values were lower in experiments with initial

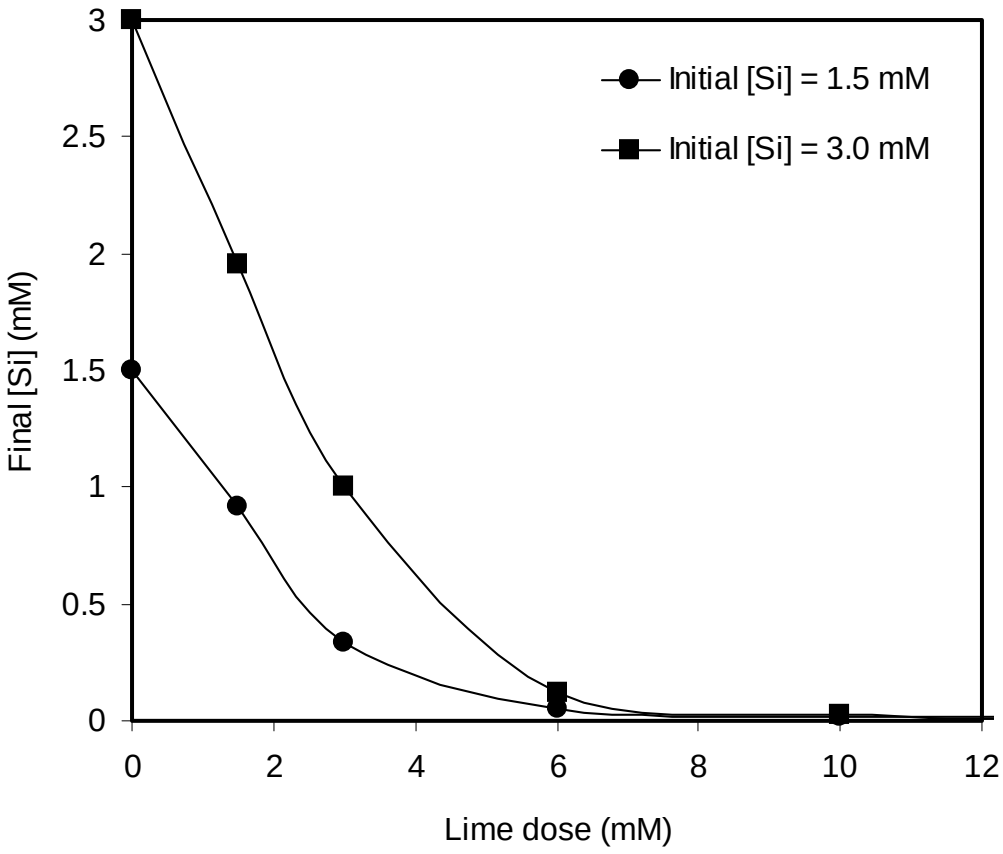

Figure 4.47 Effect of lime dose on silica removal with UHLA.

Note: Aluminum dose = 50% of lime dose for all data points

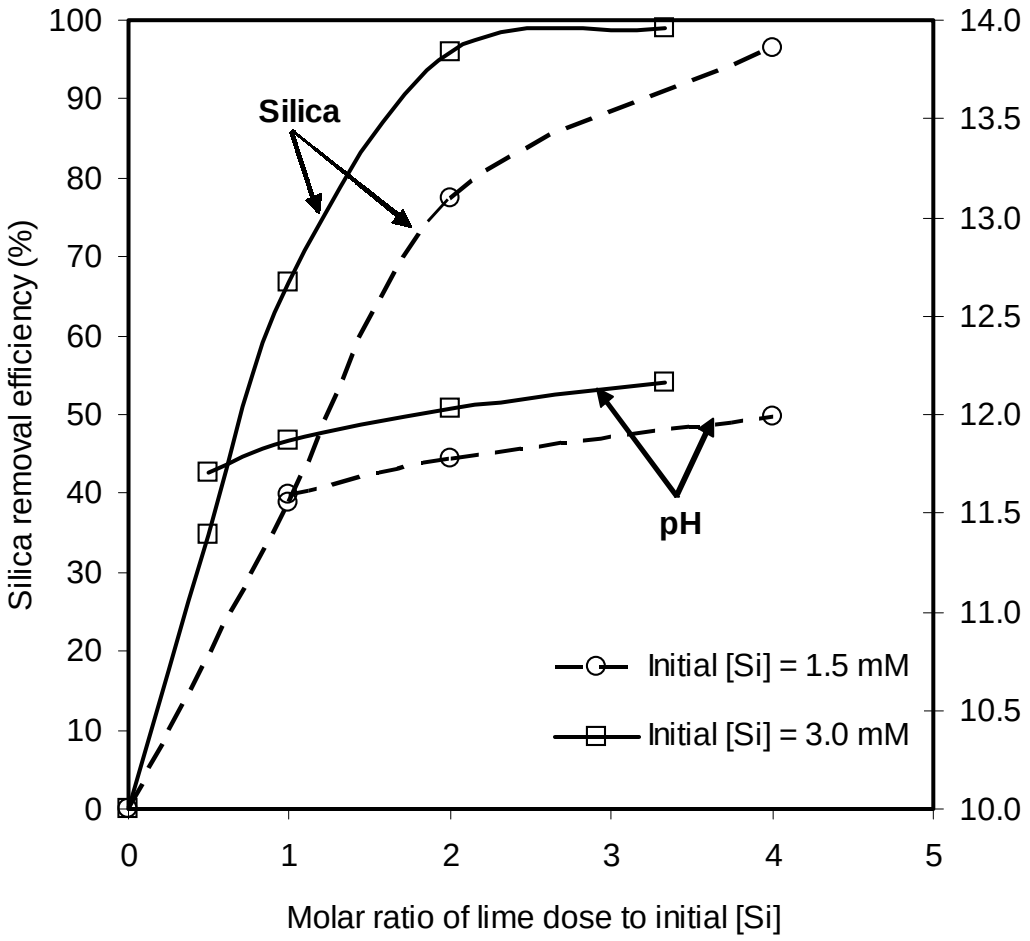

Figure 4.48 Comparison of removal efficiencies and final pH for silica removal with UHLA.

silica concentration of 1.5 mM compared to experiments with initial silica concentration of 3.0 mM (Figure 4.48). The hypothesis was made that silica removal could be described as the precipitation of calcium silicate (CaH_2SiO_4) (Batchelor et al., 1991, Batchelor and McDevitt, 1984) and/or calcium aluminosilicate ($Ca_2Al_2Si(OH)_{14}$) (Glasser et al., 1999). If calcium silicate is the only important precipitated solid, the ratio of calcium removed to silica removed should equal 1.0. Similarly, if calcium aluminosilicate is the only important precipitated solid, the ratio of calcium removed to silica removed should equal 2. Figure 4.49 shows that when the ratio of lime dose to initial silica concentration is less than 1.0, the ratio of calcium removed to silica removed is approximately equal to the theoretical ratio of 1.0. However, this ratio increased as the lime dose increased and approached the theoretical stoichiometric ratio of calcium aluminosilicate precipitation (2.0). This behavior indicates that both calcium silicate and calcium aluminosilicate precipitated. Note that the pH values in these experiments were in the range of pH 11.59 to 12.16, which are below the pH at which calcium hydroxide would precipitate. Therefore, the only important calcium-containing solids in the system are believed to be calcium silicate and calcium aluminosilicate.

4.8.2 Equilibrium Modeling of Silica Removal with UHLA

The ion activity product of calcium silicate and calcium aluminosilicate were calculated from the following reactions, which are based on the assumption that CaH_2SiO_4 and $Ca_2Al_2Si(OH)_{14}$ are the proper formulas for calcium silicate and calcium aluminosilicate solids, respectively.

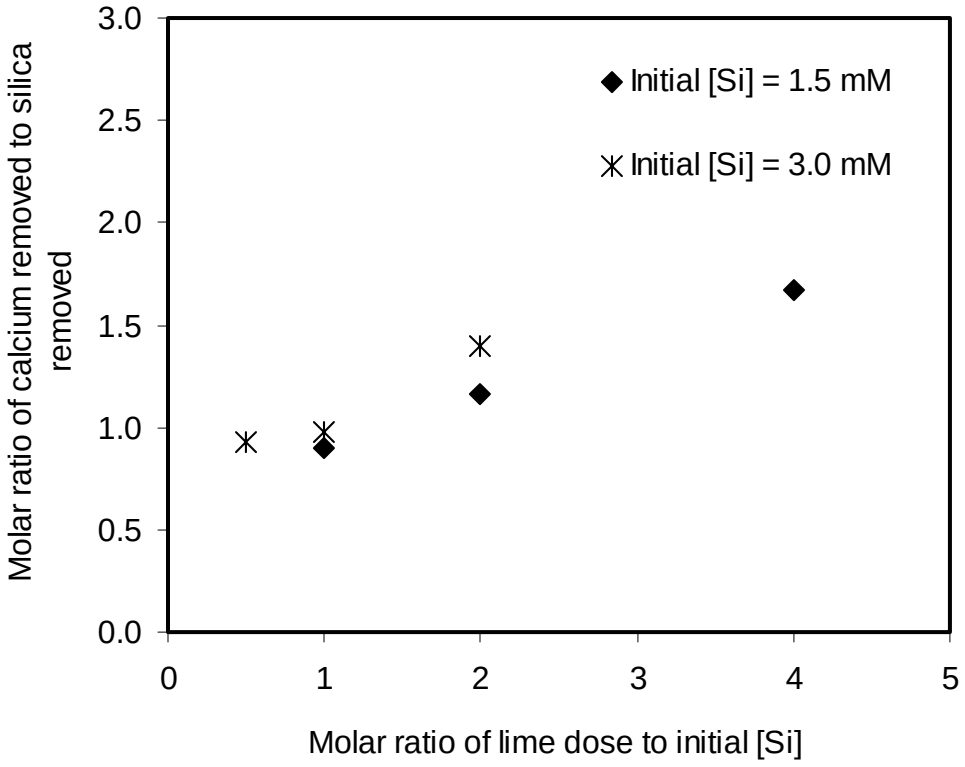

Figure 4.49 Effect of chemical doses on the ratio of calcium removed to silica removed.

$$CaH_2SiO_4 = Ca^{2+} + H_2SiO_4^{2-} \quad (4\text{-}20)$$

$$Ca_2Al_2Si(OH)_{14} = 2Ca^{2+} + 2Al(OH)_4^- + H_4SiO_4 + 2OH^- \quad (4\text{-}21)$$

The activities of species were calculated from the measured total concentrations of Ca, Al, Si, and pH by PHREEQC using the Davies Equation. The measured concentrations were used as input values to PHREEQC and no precipitates were allowed to form. An average value of the IAP of $10^{-8.02 \pm 0.5}$ for calcium silicate and $10^{-23.09 \pm 0.8}$ for calcium aluminosilicate were obtained. The average value of IAP of calcium silicate is consistent with the value of $10^{-7.8}$ obtained by Batchelor at al. (1984). In order to test the hypothesis that silica removal can be described as the precipitation of both calcium silicate and calcium aluminosilicate and in order to model silica removal with UHLA, a new chemical equilibrium model was developed. This model used a modified PHREEQC database that contained the average values of the IAPs of calcium silicate and calcium aluminosilicate as their solubility products. The model was used to predict final total silica concentrations using the total initial concentrations of Ca, Al, Si, Cl, OH, and Na as input. Figure 4.50 compares the measured and model-predicted final silica concentrations over a range of chemical doses and initial chloride concentrations. These results indicate that the model succeeded in adequately predicting measured silica concentrations, which supports the hypothesis that silica removal with UHLA can be described as precipitation of calcium silicate and calcium aluminosilicate.

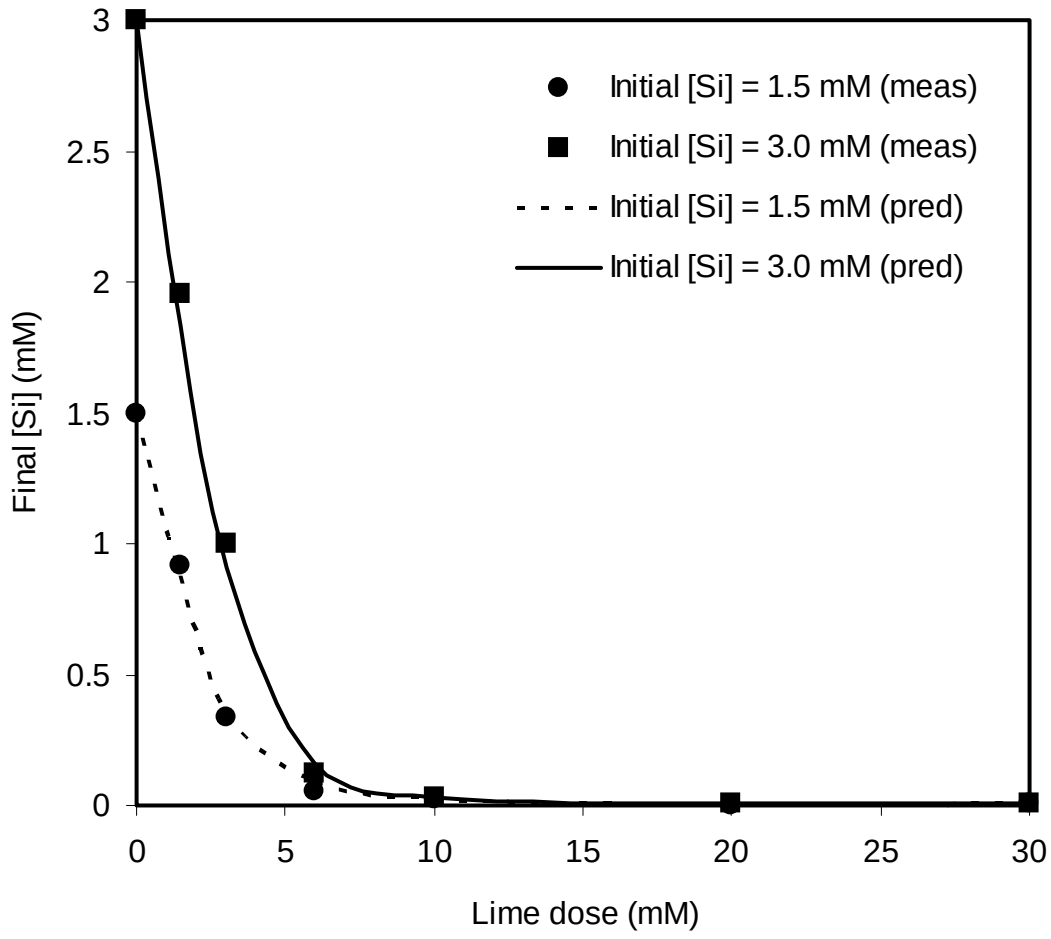

Figure 4.50 Comparison between measured and predicted silica concentrations. (Meas) refers to measured concentrations and (pred) refers to predicted concentrations.

4.8.3 Effect of Chloride on Silica Removal with UHLA

Figure 4.51 shows final silica concentrations at different initial chloride concentrations and indicates that chloride has a negligible effect on silica removal. Final silica concentrations approached zero at high lime and aluminum doses and increased chloride concentrations did not affect silica removal.

4.8.4 Effect of Silica on Chloride Removal with UHLA

Figure 4.52 shows effect of silica on chloride removal with UHLA at different initial chloride concentrations and different chemical doses. Silica has a negligible effect on chloride removal with UHLA. This could be because the investigated initial silica concentrations (1.5 and 3.0 mM) are low compared to chloride concentrations, although they are typical of concentrations usually found in recycled cooling water. Therefore, the chemical doses that were consumed in precipitating silica were negligible compared to total chemical doses in the system and resulted in small effect on final chloride concentrations.

4.8.5 X Ray Diffraction Results for Solids Formed in Cl - Si - OH system

Figure 4.53 shows diffractograms of solids precipitated in Cl - Si - OH system (XRDSi). XRD patterns show at least two peaks of calcium aluminosilicate (at d = 12.34 and 4.16 Å) in addition to solids that were identified previously in the Cl-OH system. The XRD data for calcium aluminosilicate compared to JCPDS cards data are shown in Table 4.8. Detection of aluminosilicate solid agrees with the hypothesis that calcium aluminosilicate is formed during UHLA. However, the presence of calcium silicate

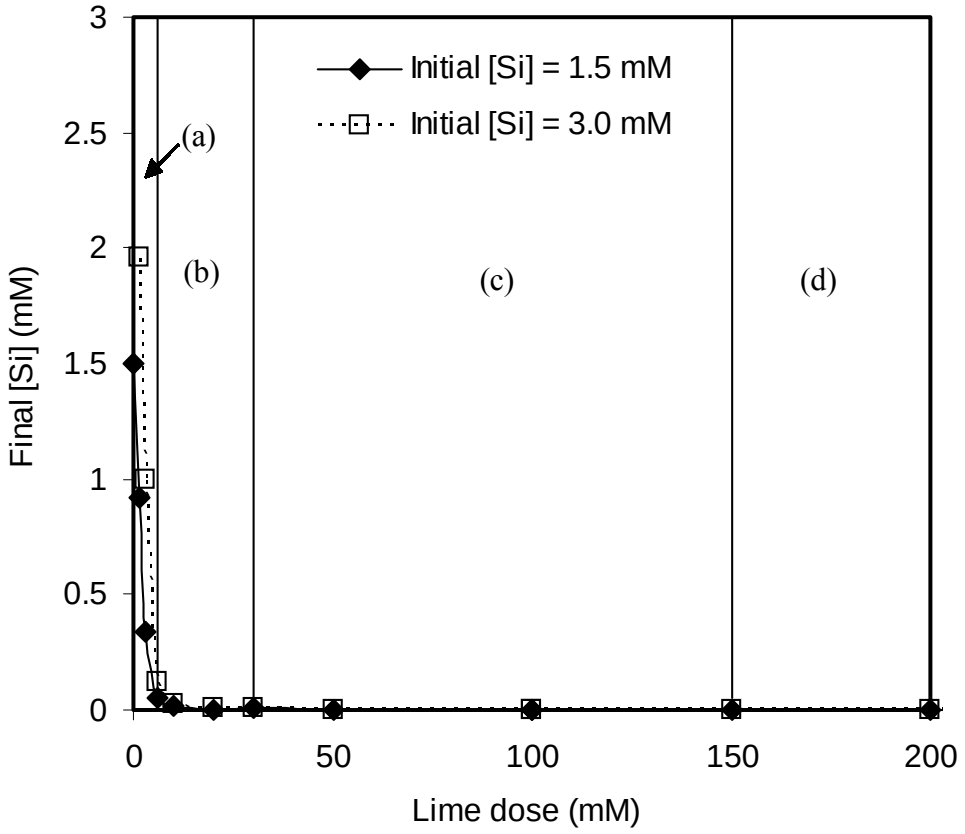

Figure 4.51 Effect of initial chloride concentration on silica removal with UHLA. (a) at initial [Cl] = 0.0 mM, (b) at initial [Cl] = 10 mM, (c) at initial [Cl] = 50 mM, (d) at initial [Cl] = 100 mM.

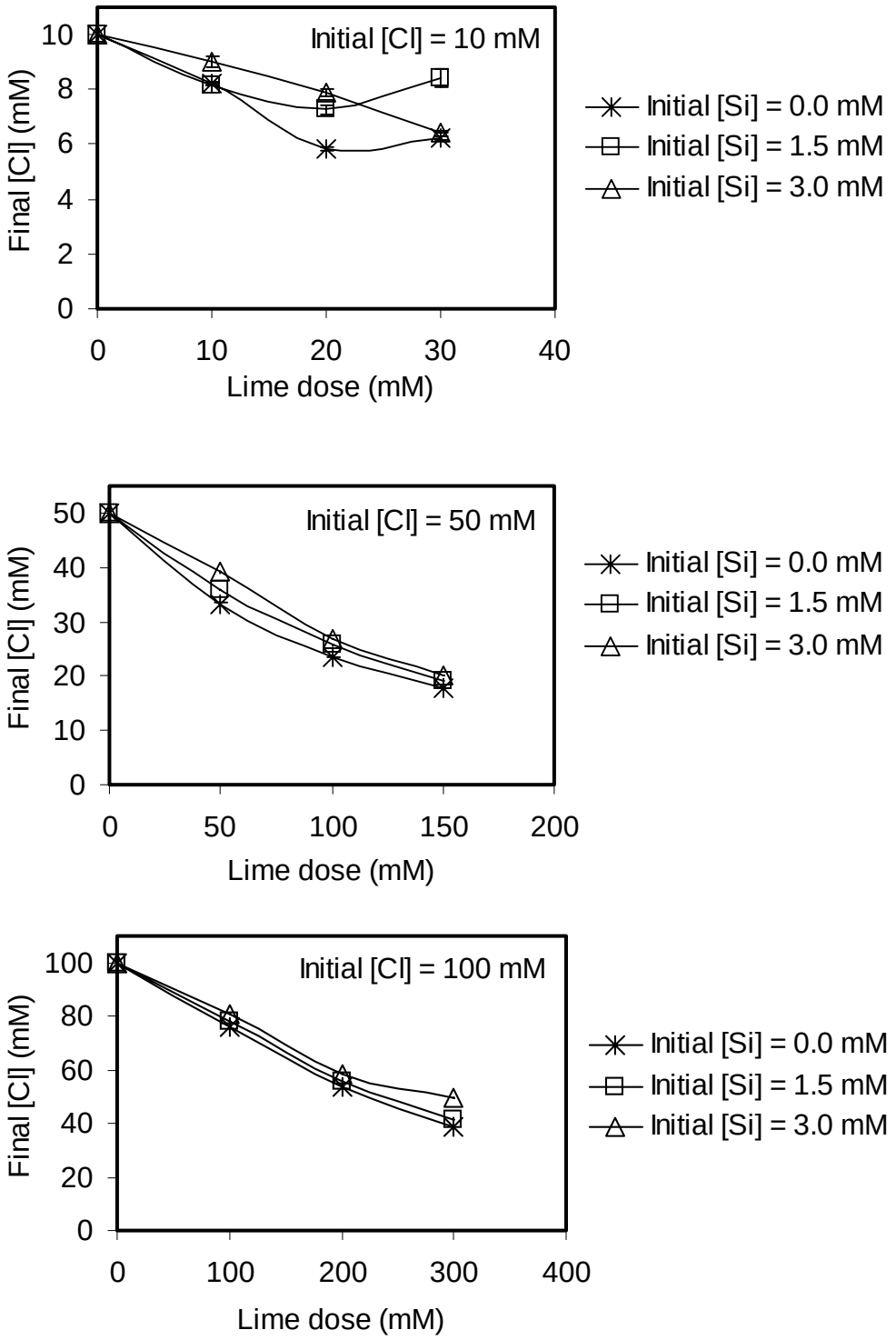

Figure 4.52 Effect of initial silica concentration on chloride removal with UHLA.

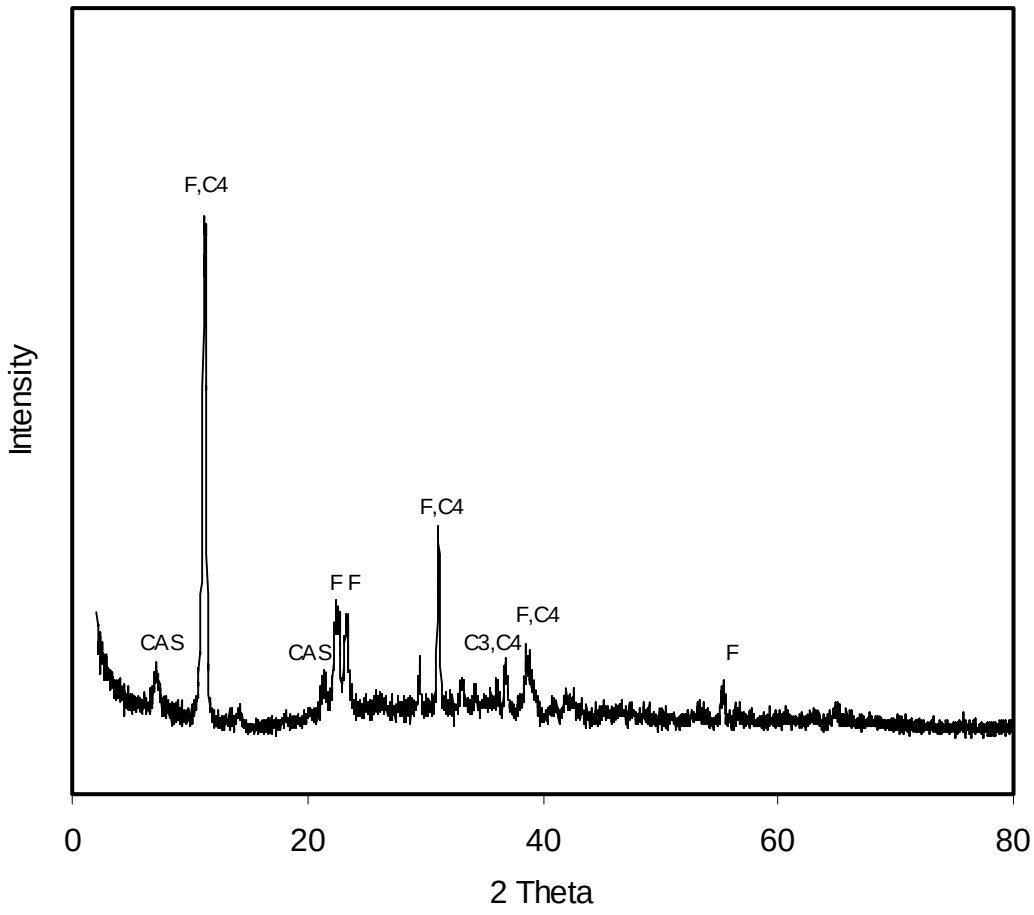

Figure 4.53 Diffraction patterns for precipitated solids in Cl - Si - OH system. C3 = tricalcium hydroxyaluminate, C4 = tetracalcium hydroxyaluminate, CAS = calcium aluminosilicate, F = Friedel salt (calcium chloroaluminate).

could not be confirmed. There were no peaks that matched the JCPDS cards for calcium silicate solids. This could be because at such high chemical doses (60 mM lime and 30 mM sodium aluminate), the concentration of calcium silicate is negligible and the dominant silica-containing solid phase is calcium aluminosilicate.

Table 4.8 XRD data for new solids found in Cl – Si – OH system.

Solid phase	2θ	d values (Å)		Relative intensity
		This work	JCPDS cards	
Calcium aluminosilicate			JCPDS Card No. 29-285	
	7.16	12.34	12.50	100
	21.32	4.16	4.18	70

CHAPTER V

SUMMARY AND CONCLUSIONS

Environmental impacts resulting from discharge of industrial wastewaters make zero discharge and closed water systems a real need and potentially a legal requirement. Chloride and sulfate are compounds that make zero discharge difficult to obtain in many cases. The ultra-high lime with aluminum (UHLA) process has demonstrated the ability to achieve high sulfate removal at low cost. Expanding the capabilities of the process to include removal of chloride and developing a model for removal of multiple components will facilitate practical applications of the UHLA process so that it will meet its potential as a low-cost tool for improved industrial water management. Despite the attractiveness of UHLA technology, there was limited data to support its use for chloride removal. Furthermore, there is limited data to evaluate and model multicomponent removal. Therefore, experimental studies were conducted to characterize the equilibrium conditions and kinetics of chloride removal with UHLA and to develop a model for multicomponent removal by UHLA. Effects of chemical doses, initial chloride concentration, pH, and temperature on chloride removal with UHLA were evaluated. Also interactions between chloride and either sulfate or silica were investigated and an equilibrium model was developed that can be used to predict chemical behavior in UHLA process.

Kinetic and equilibrium characteristics of chloride precipitation using UHLA process have been evaluated. First, a kinetic experiment to study the kinetics of calcium

chloroaluminate precipitation and to obtain the reaction time for equilibrium experiments was conducted. Results of the kinetic experiment showed that chloride removal is fast, being essentially complete at the first sampling time of one hour. This indicates that kinetics should not be a limitation to applying the UHLA process.

Forty-eight batch equilibrium experiments were conducted to study the effects of lime dose and aluminum dose on chloride removal. These experiments used an initial solution of 30 mM NaCl and applied doses of lime (0 – 200 mM) and sodium aluminate (0 – 100 mM). Good chloride removal was observed at reasonable ranges of lime dose and aluminum dose. The hypothesis was made that chloride removal was primarily controlled by calcium chloroaluminate ($Ca_4Al_2Cl_2(OH)_{12}$) precipitation. However, deviations from the stoichiometry of calcium chloroaluminate precipitation occurred in the equilibrium experiments. The observed stoichiometry showed that the ratio of aluminum removed to chloride removed and the ratio of calcium removed to chloride removed were usually higher than the theoretical stoichiometry. This indicated that other solid phases were being formed in addition to calcium chloroaluminate. Results of these experiments also showed that a ratio of aluminum dose to lime dose greater than the stoichiometric value of 0.5 adversely affected chloride removal. This behavior was first hypothesized to be the result of the formation of soluble aluminum-chloride-hydroxide complexes. However, equilibrium experiments that were conducted to test this hypothesis showed that there were no chloride complexes being formed in the system.

In an effort to further understand the behavior of chloride in the UHLA process and the mechanisms of chloride removal, a fundamental chemical equilibrium model was developed. Experimental data obtained from studying the effects of lime dose and aluminum dose on chloride removal were used in the model development. The model was based on the geochemical modeling software, PHREEQC, and its development used a new program called INVRS K. This new program was integrated with PHREEQC to calculate values of unknown or poorly defined chemical equilibrium constants using a Gauss-Newton nonlinear regression routine. Error analysis indicated that formation of a solid solution of calcium chloroaluminate ($Ca_4Al_2Cl_2(OH)_{12}$), tricalcium hydroxyaluminate ($Ca_3Al_2(OH)_{12}$), and tetracalcium hydroxyaluminate ($Ca_4Al_2(OH)_{14}$) was found to be the best mechanism to describe the chemical behavior of chloride removal with UHLA. The solubility products of tricalcium hydroxyaluminate and tetracalcium hydroxyaluminate were determined with INVRS K and were found to be $10^{-19.72}$ and $10^{-25.02}$ respectively, while the solubility product of calcium chloroaluminate ($Ca_4Al_2Cl_2(OH)_{12}$) was fixed at the value that was reported in the literature ($10^{-27.10}$).

When calcium or aluminum concentrations are above the stoichiometric amount needed to form the solid solution, the model allows formation of calcium hydroxide or aluminum hydroxide solids. Comparison between experimental data and model predictions at different lime and aluminum doses indicated that the model adequately predicted the measured concentrations of chloride, calcium, aluminum, and measured pH values. Both experimental results and model predictions showed that the aluminum hydroxide solid produced during experiments at low lime doses had a higher solubility

product than gibbsite (Ksp = $10^{-33.33}$). The predicted and measured concentrations of chloride followed the same trend of decreasing to a minimum and then increasing as the aluminum dose increased. The increase of chloride concentration at higher sodium aluminate doses was explained by the effect of higher aluminum concentrations favoring the formation of tricalcium hydroxyaluminate over both calcium chloroaluminate and tetracalcium hydroxyaluminate.

Fractions of the solids in the solid solution were found to be controlled by the ratios of Cl^-, OH^-, and $Al(OH)_4^-$ in the solution as well as the stoichiometric coefficients and the equilibrium constants of the solids. Fractions of calcium hydroxyaluminate solids increased and fractions of calcium chloroaluminate solid decreased with increasing sodium aluminate dose. However, lime dose had a negligible effect on the composition of the solid solution. The fraction of tricalcium hydroxyaluminate in the solid solution can be minimized by adding lime at doses above the stoichiometric ratio to aluminum (> 2.0). The ratio of the fraction of calcium chloroaluminate to the fraction of tetracalcium hydroxyaluminate was controlled by the ratio of chloride to hydroxide ions in the solution. Therefore, the fraction of tetracalcium hydroxyaluminate can be minimized by using aluminum sources that do not cause an increase in the concentration of OH^-. One such aluminum source would be freshly precipitated amorphous $Al(OH)_3(s)$. Also, waste alum sludge produced from water treatment plants could be an attractive alternative source of aluminum. A set of chemical equilibrium reactions was developed and can be used to describe interactions among the solids in the solid solution.

Equilibrium experiments to study the effect of initial chloride concentration on chloride removal were conducted. Experimental results showed that chloride removal efficiency at initial chloride concentration of 10 mM is significantly lower than that at initial concentrations of 50 and 100 mM. This was because when the concentration of chloride is low with respect to the concentration hydroxide, precipitation of calcium hydroxyaluminate becomes favorable relative to precipitation of calcium chloroaluminate. The equilibrium model was tested for this set of experiments and it succeeded in predicting chemical behavior accurately at different chloride concentrations.

The effect of pH on chloride precipitation was studied for a range of pH values (10.80 – 13.05). Lime and sodium aluminate were used as calcium and aluminum sources, respectively. The pH was adjusted to the desired values using acetic acid and NaOH. Results of these experiments indicated that the optimum pH for maximum chloride removal was pH 12 ± 0.2. Removal efficiency of chloride increased with increasing initial chloride concentration at the same pH value, because the fraction of chloroaluminate solid in the solid solution increased by increasing the ratio of chloride to hydroxide in the solution. The model was tested for this set of experiments and succeeded in accurately predicting experimental data at different pH values.

A set of experiments was conducted to evaluate the effect of temperature on chloride precipitation. Final chloride concentrations slightly increased when water temperature increased at temperatures below 40^{o}C. However, at temperatures above 40^{o}C, chloride concentrations substantially increased with increasing water temperature.

This was explained as being caused by lower stability of calcium chloroaluminate solid with respect to calcium hydroxyaluminate solids at temperatures above 40^{o}C.

Interactions between chloride and sulfate have been investigated. Results of these experiments indicated that formation of calcium sulfoaluminate and calcium monosulfate is more favorable than formation of calcium chloroaluminate. Therefore, chloride concentration was found to have negligible effect on sulfate removal with UHLA. On the other hand, increased sulfate concentrations resulted in decreasing the removal efficiency of chloride, even at high stoichiometric doses with respect to (initial [Cl] + initial [SO_4]) in the solution. This was explained by an increase of the activity of calcium chloroaluminate solid in the solid solution in the presence of sulfate. Equilibrium modeling indicated that the chemical behavior of simultaneous removal of both chloride and sulfate with UHLA can be best described as the formation of a solid solution containing calcium chloroaluminate, calcium sulfoaluminate, calcium monosulfate, tricalcium hydroxyaluminate, and tetracalcium hydroxyaluminate in addition to calcium hydroxide or aluminum hydroxide when calcium or aluminum doses are above the stoichiometry of the solid solution formation.

Silica was found to have a small effect on chloride removal with UHLA. Similarly, chloride was found to have a negligible effect on silica removal with UHLA. The equilibrium model was modified to include silica removal with UHLA and it succeeded in predicting the simultaneous removal of chloride, sulfate, and silica with UHLA.

XRD analysis for precipitated solids in UHLA process have been conducted and showed that the presence of the same solids that were assumed by the equilibrium model.

One of the initial focuses of future research should be to study the effectiveness and cost of alternative aluminum sources in the UHLA process. The potential for using aluminum in waste alum sludge from water treatment plants as an inexpensive source of aluminum should be investigated. This will make UHLA technology capable not only of improving industrial water use management, but also of contributing to maintaining a sustainable environment through resource conservation by waste reuse. A large amount (10,000 ton/day) of this sludge is being produced and most of it is being disposed as waste material (Dharmappa et al, 1997). Unlike sodium aluminate, use of alum sludge as an aluminum source will not produce hydroxide ion that can compete with chloride in the forming the solid solution. Therefore, the removal efficiency of chloride is expected to be higher when using alum sludge than when using sodium aluminate, if the same equivalent concentration of aluminum is used.

The potential of using UHLA in other applications, such as treatment of brines prior to evaporation/crystallization, and pretreatment before desalination in order to improve water recoveries and membrane life should be evaluated. Silica and sulfate have been described as the major cause of membrane fouling and the major unresolved problem in desalination. Despite the attractiveness of UHLA as a powerful method for removing all the scale forming materials, there is limited data to support its use to remove silica and sulfate from brine concentrates. The high ionic strength in these

concentrates is a much different chemical environment than that found in conventional water or wastewaters. Therefore, research is needed to evaluate the feasibility of applying the UHLA process to concentrates rejected from desalination plants.

Other primary focus of future research should be to evaluate the feasibility and costs of recycling and/or reusing the solids formed in the UHLA process in order to minimize the sludge that needs to be disposed. The solids that are formed are layer double hydroxides (LDHs) and have many physical and chemical properties that make them useful in many industrial and environmental applications (Rives, 2001). LDHs are receiving considerable attention, because they are used as anion-exchange and adsorption materials, carriers for drugs, antacids in medicine, electrode modifiers, catalysts, precursors and supports of catalysts, decolorizing agents, polymer stabilizers, optical hosts and ceramic precursors. Many of their most important applications are due to their permanent anion-exchange and adsorption capacity, the mobility of their interlayer anions and water molecules, their large surface areas and their stability (Yong and Rodrigues, 2002). Such properties make them very good adsorbents for variety of contaminants. Furthermore, LDHs were proven to remove contaminants similar to the corrosion and scale inhibitors that are added in cooling water systems (e.g. phosphonates) (Ulibarri and Hermosin, 2001). Therefore, research is needed to evaluate the use of these solids in the treatment of effluent blowdown from cooling water systems before discharge. Also, research is needed to evaluate the cost and effectiveness of different configurations of the UHLA process in cooling water treatment systems such as sidestream treatment, makeup treatment, or a combination of both. Research is also

needed to evaluate the performance of UHLA in saving and/or loss of inhibitors, water conservation, pollution prevention, and to determine process costs for each of the configurations.

The substantial increase of chloride concentration at temperatures above 40^{o}C indicates that chloride is expected to be totally released from the solid at moderate temperatures and mixed hydroxides of divalent and trivalent cations would be formed. The effect of temperature on sulfate removal has not been evaluated, but it is expected to be similar to that for chloride. This indicates that the produced solids in UHLA process can be recycled easily at low temperatures.

REFERENCES

Abate, C.; Scheetz, B E.; (1993) Aqueous Phase Equilibria in the System CaO-Al_2O_3-$CaCl_2$-H_2O: the Significance and Stability of Friedel's Salt. *J Am. Ceram. Soc.*, **78**, 4, 939.

Allison, J.D; Brown, D.S.; Novo-Gradac, K.J. (1991) *MINTEQA2/PRODEFA2, A Geochemical Assessment Model for Environmental Systems,* EPA/600/3-91/021, US Environmental Protection Agency, Environmental Research Laboratory: Athens, Georgia..

American Public Health Association (APHA); American Water Works Association (AWWA); Water Environment Federation (WEF) (1995) *Standard Methods for the Examination of Water and Wastewater*. American Public Health Association, 19th Ed, Washington, DC.

Aronson, J.T.; Galyon, G.D.; Nelson, D.F.; Martin, H.J.; Printz, J.; Micheletti, W.C.; Noblett, Jr. J.G.; Wilde, K.A. (1982) Design and Operating Guidelines Manual for Cooling-Water Treatment: Treatment of Recirculated Cooling Water, *Electric Power Research Institute (EPRI),* CS-2276, 1st Ed., Project 1261-1, Final Report, Palo Alto, California.

Balaban, M. (1991) Desalination and Water Re-Use, *Proceedings of the Twelfth International Symposium, Institution of Chemical Engineers*, **4**, 125, Hemisphere Pub., New York.

Batchelor, B.; Lasala, M. B.; McDevitt, M; Peacock, E. (1991) Technical and Economical Feasibility of Ultra-High Lime Treatment of Recycled Cooling Water, *J. Water Pollut. Control Fed.*, **63**, 7, 982.

Batchelor, B.; McDevitt, M. (1984) An Innovative Process for Treating Recycled Cooling Water, *J. Water Pollut. Control Fed.*, **56,** 10, 1110.

Batchelor, B.; McDevitt, M.; Chan, D. (1985) Removal of Sulfate from Recycled Cooling Water by the Ultra-High Lime Process, *Proceedings Water Reuse Symposium III, AWWA Research Foundation*, Denver, **2**, 798.

Bell, G. R.; Leineweber, J. P.; Yang, J. C. (1968) Characterization and Removal of Silica from Webster, South Dakota Well Water, Progress Rep. 286, U.S., Dep. of Interior, Office of Saline Water Res. and Dev., Washington, D.C.

Ben-Yair, M. (1974) the Effect of Chloride on Concrete in Hot and Arid Regions, *Cem. Concr. Res.*, **4**, 405.

Birnin-Yauri, U. A. (1993) *Chloride in Cement: Study of the System CaO-Al_2O_3-$CaCl_2$-H_2O*, Ph.D. Thesis, University of Aberdeen, Scotland, UK.

Birnin-Yauri, U. A.; Glasser, F. P. (1998) Friedel's Salt, $Ca_2Al(OH)_6(Cl,OH)2H_2O$: Its Solid Solutions and Their Role in Chloride Binding, *Cem. Concr. Res.*, **28**, 1713.

Boffardi, B. P. (1984) Corrosion Control of Industrial Cooling Water Systems, *Mater. Perform.*, **23**, 11.

Bohnsack, G.; Lee, K.H.; Johnson, D. A.; Buss, E. (1986) Mechanisms of Organic Inhibitors Used in Cooling Water Corrosion Control, *Mater. Perform.*, **25**, 5, 32.

Bos, M.; Meershoek, H.Q.J. (1972) A Computer Program for the Calculation of Equilibrium Concentrations in Complex Systems, *Anal. Chim. Acta*, **61**, 185-194.

Breske, T. C. (1976) Testing and Field Experience with Nonheavy Metal Corrosion Inhibitors, Paper presented at National Association of Corrosion Engineers Conference, Houston, Texas.

Chapra, S.C.; Canale R.P. (1998) *Numerical Methods for Engineers*; 3rd Ed., McGraw Hill: Boston, Massachusetts.

Charentanyarak, L. (1999) Heavy Metals Removal by Chemical Coagulation and Precipitation, *Water. Sci. Technol.*, **39**, 10-11,135.

Chu, W. (1999) Lead Metal Removal by Recycled Alum Sludge, *Wat. Res.*, **33**, 13, 3019.

Clark, B.A.; Brown, P.W. (2000) the Formation of Calcium Sulfoaluminate Hydrate Compounds Part II, *Cem. Concr. Res.*, **30**, 233.

Clark, J. W.; Viesman, W.; Hammer, M., J. (1977) *Water Supply and Pollution Control*; Harper and Row: New York.

Crepaldi, E.L; Paven, P.C., Valim, J.B. (2000) Anion Exchange in Layered Double Hydroxides by Surfactant Salt Formation. *J. Mater. Chem.*, **10**, 1337.

Damidot, D.; Glasser F. P. (1993) Thermodynamic Investigation of the CaO-Al_2O_3-$CaSO_4$-H_2O at 25°C and the Influence of Na_2O, *Cem. Concr. Res.*, **23**, 221.

Dean, A.J. (1985) *Lang's Handbook of Chemistry*; 13th Ed., McGraw-Hill: NewYork.

De Roy, A.; Forano, C; El Malki, K.; Besse, J.P. (1992) Anionic Clays: Trends in Pillaring Chemistry. In *Expanded Clay and Other Microporous Solids*; Edited by Occelli, M.L.; Robson, H.E. Vol II, pp108-169, Van Nostrand Reinhold: New York.

Dharmappa, H. B.; Hasia, A.; Hagare, P. (1997) Water Treatment Plant Residuals Management, *Water. Sci. Technol.*, **35**, 8, 45.

Drits, V.A.; Bookin, A.S. (2001) Crystal Structure and X-Ray Identification of Layered Double Hydroxides. In *Layered Double Hydroxides: Present and Future*. Edited by Vicente Rives, pp39-92, Nova Science Publishers, Inc.: New York.

Ericsson, B.; Hallmans, B.; (1996) Treatment of Saline Wastewater for Zero Discharge at the Debiensko Coal Mines in Poland, *Desalination*, **105**, 115.

Fair, G. M.; Geyer, J. C.; Okun, D. A. (1968) *Water and Wastewater Engineering, Vol. 2, Water Purification and Wastewater Treatment and Disposal,* Wiley: New York.

Fisher, D. J.; Burton, D. T.; Yonkos, L. T.; Turley, S. D.; Ziegler, G. P. (1999) the Relative Acute Toxicity of Continuous and Intermitted Exposures of Chlorine and Bromine to Aquatic Organisms in the Presence and Absence of Ammonia, *Wat. Res.*, **33**, 3, 760.

Foley, R.T. (1970) Role of the Chloride Ion in Iron Corrosion, *Corrosion*, (Houston, Texas, U.S.), **26**, 2, 58.

Francois, M.; Renaudin, G.; Evrard, O. (1998) A Cementitious Compound with Composition 3CaO Al_2 O_3 $CaCO_3$ $11H_2O$. *Acta Crystallogr*., **C54,** 1214.

Frazer, H.W. (1975) *Sidestream Treatment of Recirculating Cooling Water*. In: Cooling Towers (vol. 2), A Chemical Engineering Progress Technical Manual, American Institute of Chemical Engineers, NY, USA, 77-81.

Friedel, P. M. (1897) Sur Un Chloro-Aluminate de Calcium Hydrate Se maclant par Compression, *Bull Soc Franc Minera,l* **19**, 122.

Fu, Y.; Ding, J.; Beaudoin, J.J. (1996) Corrosion Protection of Reinforcement in Modified High-Alimina Cement Concrete. *ACI Mater. J.*, **93**, 6, 609.

Garrels, R.M.; Thompson M.E. (1962) A Chemical Model for Seawater at 25 ^{0}C and One Atmosphere Total Pressure. *Amr. J. Sci*., **260**, 57-66.

Geiger, G. E. (1996). Improve Corrosion and Deposition Control in Alkaline Cooling Water Systems, *Hydrocarbon Process.*, **75**, 1, 93.

Glasser, F.P.; Kindness, A.; Stronach, S.A. (1999) Stability and Solubility Relationships in AFm Phases Part I. Chloride, Sulfate, and Hydroxide, *Cem. Concr. Res.,* **29**, 861.

Goldstein, P.; Griffin, R.W. (1975) *Cooling Tower Water Management to Eliminate Pollution.* In: Cooling Towers (vol. 2), A Chemical Engineering Progress Technical Manual, American Institute of Chemical Engineers, NY, USA, 71-76.

Goswamee, R.L.; Sengupta, P; Bhattacharyya, K.G.; Dutta, D.K. (1998) Adsorption of Cr(VI) in Layered Double Hydroxides. *Appl. Clay Sci.*, **13**, 21.

Grutzeck, M. W.; Roy D. M. (1998) *Experimental Characterization and Stability of Salt- and Nonsalt-Containing Grouts and Mortars,* UC-70, Office of Nuclear Waste Isolation, Battelle Memorial Institute: Columbus, OH.

Gunasekaran, G.; Natarajan, R.; Muralidharan, V. S.; Palaniswamy, N.; Appa Rao, B. V. (1997) Inhibition by Phosphonic Acids – An Overview, *Anti-Corrosion Meth. and Mater.*, **44**, 4, 248.

Helgeson, H.C.; Brown, T.H; Nigrini A.; Jones, T.A. (1970) Calculation of Mass Transfer in Geochemical Processes Involving Aqueous Solutions, *Geochim. Cosmochim. Acta*, **34**, 569-592.

Hoek, J. P.; Hofamn, J A. M. H.; Bonne, P. A. C.; Nederlof, M. M.; Vrouwenvelder H. S. (2000), RO Treatment: Selection of Pretreatment Scheme Based on Fouling Characteristics and Operating Conditions Based on Environmental Impact, *Desalination,* **127**, 89.

Hussain, S. E.; Rasheeduzzafar; Al-Musallam, A.; Al-Gahtani, A. S. (1995) Factors Affecting Threshold Chloride For Reinforcement Corrosion in Concrete. *Cem. Concr. Res.,* **25,** 1543.

Janotka, I.; Krajci, L.; Komlos, K; Frt'alova, M.D.; Haias, P. (1992) Investigation on the Relationship between Phase Composition and Chloride Corrosion of Steel Fiber Reinforcement in Cement Mortar. *ACI Mater. J.*, **89**, 3, 223.

JCPDS (1990) *Powder Diffraction File, Inorganic Volume*, JCPDS: Swarthmore, Philadelphia.

Jones, F. E. (1944) the Quaternary System CaO-Al_2O_3-$CaSO_4$-H_2O at 25°C: Equilibria with Crystalline $Al_2O_3.3H_2O$ Alumina Gel, and Solid Solution, *J. Phys. Chem.*, **48**, 311.

Jones, R.L. (1991) *A Water Chemistry Model for Open recirculating Cooling Water Systems*, Ph.D. Dissertation, University of Houston: Houston, Texas.

Kharaka, Y.K., Barnes, I. (1973) SOLMNEQ: Solution-Mineral Equilibrium Computations, U.S. Department of Commerce, National Technical Information Service Technical Report PB215-899.

Kolk, B. J.W.; Ropert, J. S. (1996) Design Alternatives for the Use of Cooling Water in the Process Industry: Minimization of the Environmental Impact from Cooling systems, *J. Cleaner Prod.,* **4**, 1, 21.

Kumar, J.; Fairfax, J. P. (1976), Rating Alternatives to Chromates in Cooling water Treatment, *Chem. Eng.,* **83**, 111.

Kunz, R. G.; Yen, A. F.; Hess, T.C. (1977) Cooling Water Calculations, *Chem. Eng.,* **84,** 16, 61.

Lambert, P.; Page, C. L.; Short, N. R. (1985) Pore Solution Chemistry of the Hydrated System C_3S-NaCl-H_2O. *Cem. Concr. Res.,* **15**, 675.

Lancaster, R. L.; Sanderson W. G. (1993) the Staged High Recycle Cooling Process – An Overview, Eau Tech Partners: Redmond, Washington. Presented at *the Integrated Energy & environmental Management International Symposium*, New Orleans, LA. March 10-12.

Larson, T E.; Sullo, F. W. (1967) Loss in Water Main Carrying Capacity, J. AWWA, **59**, 1564.

Lea, F. M. (1956) *the Chemistry of Cement and Concrete*, ST. Martin's Press Inc.: New York.

Lide, D. (1991-1992) *CRC Handbook of Chemistry and Physics*, 72nd Edition, CRC Press, Inc: Boston, USA, pp8-36.

Lidsay, F. F.; Ryznar, J. W. (1939) Removal of Silica from Water by Sodium Aluminate, *Ind. Eng. Chem.*, **31**, 859.

Masson, M.; Deans, G. (1996) Membrane Filtration and Reverse Osmosis Purification of Sewage: Secondary Effluent For Reuse at Eraring Power Station, *Desalination*, **106**, 11.

Mathie, A. J. (1998) *Chemical Treatment for Cooling Water*, the Fairmont Press, Inc.: Lilburn, Georgia.

Matson, J. V.; Harris, T. G. (1979) Zero Discharge of Cooling Water by Sidestream Softening, *J. water Pollut. Control Fed.,* **51**, 11, 2602.

Mehta, P.K. (1991) *Concrete in the Marine Environment*. Elsevier Science Publishing Co. Inc.: New York.

Micheletti, W.C.; Owen, M.L (1979) Summary of Equilibrium and Process Model Data Acquisition: Treatment of Recirculating Cooling Water, Resource Document 1 Electric Power Research Institute Report No. EPRI FP – 1251, Palo Alto, California.

Moccari, A. A. (1999), Corrosion Inhibitors Evaluation for Materials Used in Closed Cooling Water Systems, *Mater. Perform.*, **38**, 11, 54.

Morel, F. M. M.; Hering, J. G.; (1993). *Principles and Applications of Aquatic Chemistry.* John Wiley & Sons, Inc.: New York.

Mujeriego, R. (1976) *Silica Removal from Industrial Water*, Ph.D. Dissertation, University of California: Berkeley, California.

Mustafa, C. M.; Shahinoor, S. M. (1996) Molybdate and Nitrite as Corrosion Inhibitors for Copper-Coupled Steel in Simulated Cooling Water, *Corrosion Sci.*, NACE, **52**, 1, 16.

Myneni, S.C.B.; Traina, S.J.; Logan, T.J. (1998) Ettringite Solubility and Geochemistry of the $Ca(OH)_2$-$Al_2(SO_4)_3$ –H_2O System at 1 atm Pressure and 298 K, *Chemical Geology*, **148**, 1.

Nacken, R.; Mosebach, R. (1936) Untersuchungen an den Vierstoffsystemen CaO-Al_2O_3-$CaCl_2$-H_2O und CaO-SiO_2-$CaCl_2$-H_2O. Zeitschr. *Anorg. Alleg. Chem.*, **228**, 19.

National Association of Corrosion Engineers (1976) *Cooling Water Treatment Manual*, TPC Publication No. 1: Houston, Texas.

Nebgen, J. W.; Shea, E. P.; Chin, S.T. (1973) the Alumina-Lime-Soda Water Treatment Process: Midwest Research Institute, Office of Saline Water Research and Development, Kansas City, Missouri, Report. 820,.

Nurdogan, Y.; Goldman, E.; Dawes, S. (1998) Optimizing Chemical Treatment of a Power Plant Water Softener, *Water Sci. Technol.*, **38**, 4-5, 347.

Olanrewaju, J.; Newalkar, B.L.; Mancino, C.; Komarneni, S. (2000) Simplified Synthesis of Nitrate Form of Layered Double Hydroxide, *Mater. Letters*, **45**, 307.

Orion (2001) *Chloride/Chloride Combination Electrode Instruction Manual*, Orion Research, Inc.: Beverly, Massachusetts.

Page, C.L.; Short, N.R.; Holden, W.R. (1986) the Influence of Different Cements on Chloride-Induced Corrosion of Reinforcing Steel. *Cem. Concr. Res.,* **16**, 79.

Parkhurst, D.L. (1995) *User's Guide to PHREEQC – A Computer Program for Speciation, Reaction-Path, Advictive-Transport, and Inverse Geochemical Calculations:* U.S. Geological Survey Water-Resources Investigations Report 95-4227, Denver, Colorado.

Parkhurst, D.L.; Appelo, C.A.J. (1999) *User's Guide to PHREEQC (Version 2) – A Computer Program for Speciation, Batch-Reaction, One-Dimensional Trasport, and Inverse Geochemical Calculations.* U.S. Geological Survey Water-Resources Investigation Report 99-4259, Denver, Colorado.

Parkhurst, D.L.; Thorstenson, D.C.; Plummer, N.L. (1980) *PHREEQE – A Computer Program for Geochemical Calculations.* U.S. Geological Survey, USGS-WRI-80-96, Denver, Colorado.

Patel, S.; Nicol, A. J. (1996) Developing a Cooling Water Inhibitor with Multifunctional Deposit Control Properties, *Mater. Perform.*, **35**, 6, 41.

Perkins, R.B.; Palmer C.D. (1999) Solubility of Ettringite ($Ca_6[Al(OH)_6]_2(SO_4)_3$. 26 H_2O at 5-75 ^oC, *Geochim. Cosmochim. Acta*, **63**, 13-14, 1969.

Pitzer, K. S. (1991) *Activity Coefficients in Electrolyte Solutions*; 2nd Ed., CRC Press: Boca Rato, Florida.

Plummer, L.N.; Jones, B.F.; Truesdell, A.H. (1976) WATEQF – A Fortran IV Version of WATEQ. A Computer Program for Calculating Chemical Equilibia of Natural Waters, *U.S. Geological Survey Water-Resources Investigations*, 76-13.

Pöllmann, H. (1986) Solid Solution of Complex Calcium Aluminate Hydrates Containing Cl^-, OH^- and CO_3^{2-} Anions, In *Proceedings. 8th Intl Symp. Chemistry of Cements*, Vol. III, Rio de Janeiro, Brazil, 300.

Rapin, J.-P.; Noor, M.N.; Francois, M. (1999a) Double Layered Hydroxide 3CaO Al_2 O_3 $CaBr_2$ 10H_2 O. *Acta Crystallogr.*, **C55**, http://www.iucr.ac.uk.

Rapin, J.P.; Renaudin, G.; Elkaim, E.; Francois, M. (2002) Structural Transition of Friedel's Salt 3Ca).Al_2O_3.$CaCl_2$.10H_2O Studied by Synchrotron Powder Diffraction, *Cem. Concr. Res.*, **32**, 513.

Rapin, J.-P.; Walcarius, A.; Lefevre, G.; Francois, M. (1999b) Double Layered Hydroxide 3CaO Al_2 O_3 CaI_2 10H_2O. *Acta Crystallogr.*, **C55**, 1957.

Rapp, H. J.; Pfromm, P. H. (1998) Electrodialysis Field Test for Selective Chloride Removal from the Chemical Recovery Cycle of Kraft Pulp Mill, *Ind. Eng. Chem. Res.,* **37**, 4761.

Rasheeduzzafar; Hussain, S. E.; Al-Saadoun, S. S. (1992) Effect of Tricalcium Aluminate Content of Cement on Chloride Binding and Corrosion of Reinforcing Steel in Concrete. *ACI Mater. J.,* **89**, 1, 3.

Reed, D.T. (1977) *Side Stream Softening as a Means to Achieving Zero Blowdown from Evaporative Cooling Systems*, Cooling Tower Institute, Houston, Texas.

Renaudin, G.; Francois, M. (1999a) the Lamellar Double Hydroxide (LDH) Compound with Composition 3CaO Al_2 O_3 $Ca(NO_3)$ 10H_2O. *Acta Crystallogr.,* **C55**, 838.

Renaudin, G.; Kubel, F.; Rivera, J. P.; Francois M. (1999b) Structural Phase Transition and High Temperature Phase Structure of Friedel's Salt, 3CaO.Al_2O_3.$CaCl_2$.10H_2O, *Cem. Concr. Res.,* **29**, 1937.

Renaudin, G.; Rapin, J.P.; Humbert, B.; Francois, M. (2000) Thermal Behavior of the Nitrated AFm Phase Ca_4 Al_2 $(OH)_{12}$ $(NO_3)_2$. 4H_2O and Structure Determination of the Intermediate Hydrate Ca_4 Al_2 $(OH)_{12}$ $(NO_3)_2$. 2H_2O. *Cem. Concr. Res.*, **30**, 307.

Renaudin, M.; Francois, G.; Evrard, O. (1999c) Order and Disorder in the Lamellar Hydrated Tetracalcium Monocarboaluminate Compound. *Cem. Concr. Res.,* **29**,63.

Rives, V. (2001) *Layered Double Hydroxides: Present and Future*, Nova Science Publisher, Inc.: Huntington, New York.

Ruisinger, T. (1996) Ozonation in Cooling Water Systems, *Plant Engineering*, **50**, 9, 98.

Schaezler, D. J. (1978) Precipitation of Calcium Aluminates and Sulfoaluminates from Water, *J. Water Pollut. Control Fed.*, **50**, 7, 1821.

Schroeder, C.D. (1986) *Solutions to Boiler and Cooling Water Problems*, the Fairmont Press, Inc.: Lilburn, Georgia.

Schwantes, J.M. (2002) *Equilibrium, Kinetic, and Reactive Transport Models for Plutonium*, Ph.D. Dissertation, Texas A&M University, College Station, Texas.

Sekine, I.; Sanbongi, M., Hagiuda, H.; Oshibe, T.; Yuasa M. (1992) Corrosion Inhibition of Mild Steel by Cationic and Anionic Polymers in Cooling Water System", *J. Electrochem. Soc.*, **139,** 11, 3167.

Singh, I. B.; Venkatachari, G.; Balakrishnan, K. (1994) Inhibition Effect of Sodium Boro-Gluconate on Mild Steel with and without Nitrite Ions in Low Chloride Containing Water, *J. Appl. Electrochemistry*, **24**, 179.

Singley, J. E.; Beaudet, B. A.; Markey, P. H. (1985) *Corrosion Prevention and Control in Water Treatment and Supply Systems*, NOYES Publications: Park Ridge, New Jersey, USA.

Stronach, S.A. (1996) *Thermodynamic Modeling and Phase Relations of Cementitious Systems*, Ph.D. Thesis, University of Aberdeen, Aberdeen, UK.

Stumm, W.; Morgan, J. J. (1996) *Aquatic Chemistry: An Introduction Emphasizing Chemical Equilibria in Natural Waters,* 3rd Ed.; John Wiley & Sons, Inc.: New York.

Suryavanshi, A. K.; Scantlebury, J. D.; Lyon S. B. (1996) Mechanism of Friedel's Salt Formation in Cements Rich in Tri-Calcium Aluminate. *Cem. Concr. Res.*, **26**, 717.

Sussman, S (1975) Facts on Water Use in Cooling Towers, *Hydrocarbon Process.,* **54**, 7, 147.

Truesdell, A.H., Jones, B.J. (1974) WATEQ, A Computer Program for Calculating Chemical Equilibria of Natural Waters, *J. Res. U.S. Geol. Survey*, **2**, 233-274.

Turriziani, R. (1960) *the Calcium Aluminate Hydrates and Related Compounds, the Chemistry of Cements,* Vol. 2, H.F.W. Taylor; Academic Press: London.

U.S. Department of the Interior (1996) *Water Use in the United States*, U.S. Geological Survey.

Ulibarri, M.A.; Hermosin, M.D. (2001) Layered Double Hydroxides in Water Decontamination. In: *Layered Double Hydroxides: Present and Future;* Vicente Rives; Chapter 9, PP251-284, Nova Science Publishers, Inc.: New York.

Wells, L.S. (1928) Reaction of Water on Calcium Aluminates, Bureau of Standards, *J. Res.*, **1**, 951.

Westall, J.C.; Zachary, J.L.; Morel, F.F.M. (1976) *MINEQL, A Computer Program for the Calculation of Chemical Equilibrium Composition of Aqueous Systems.* Technical

Note 18, R.M. Parsons Labotarory, Department of Civil and Environmental Engineering, Massachusetts Institute of Technology, Cambridge, Massachusetts.

Westbrook, G. T. (1977) *Cooling Tower Salinity Optimization Via Sidestream Desalination*, Cooling Tower Inst., Houston, Texas.

Wohlberg, C.; Bucholz, J.R. (1974) *Silica in Water in Relation to Cooling Tower Operation*, Los Alamos Scientific Laboratories, LA-UR-74-1895.

Wolery, T.J. (1992) *EQ3/EQ6, A Software Package for Geochemical Modeling of Aqueous Systems: Package Overview and Installation Guide (Version 7.0)*. Lawrence Livermore National Laboratory Report UCRL-MA-110662 (1).

Worthington, J.C.; Bonner, D.G.; Nowell, D.V. (1988) Influence of Cement Chemistry on Chloride Attack of Concrete. *Mater. Sci. Technol.*, **4**, 305.

Yonezawa, T.; Ashworth, V.; Procter R. (1988) Pore Solution Composition and Chloride Effects on the Corrosion of Steel in Concrete. *Corrosion Engineering*, **44**, 7, 489.

Yong, Z.; Rodrigues, A.E. (2002) Hydrotalcite-Like Compounds as Adsorbents for Carbon Dioxide, *Energy Conservation and Management*, **43**, 1865.

Yong, Z.; Mata, V.; Rodrigues, A.E. (2002) Adsorption of Carbon Dioxide at High Temperature – A Review, *Separation Purification Technology*, **26**, 195.

You, S. H.; Tseng, D. H.; Guo, G. L.; Yang, J. J. (1999), the Potential for the Recovery and Reuse of Cooling Water in Taiwan, Resources, *Conservation and Recycling*, **26**, 53.

You, Y.; Zhao, H.; Vance, G.F. (2002) Surfactant-Enhanced Adsorption of Organic Compounds by Layered Double Hydroxides. Colloids and Surfaces A: *Physicochemical and Engineering Aspects*, **205**, 161.

APPENDIX A

NOMENCLATURE

[]	Concentration
$[C_i]$	Concentration of the i^{th} ion
{}	Activity
AAS	Atomic absorption spectroscopy
AFm	Aluminoferrite mono
AFt	Aluminoferrite tri
ALK	Alkalinity
AMP	Amino-trimethylene-phosphonate
A^{n-}	Interlayer anion with charge (n-)
B_{ij}	The second virial coefficient
C3	Tri-calcium hydroxyaluminate
C_3A	Tricalcium aluminate
C4	Tetra-calcium hydroxyaluminate
$Ca_3Al_2(OH)_{12}$	Tri-calcium hydroxyaluminate
$Ca_4Al_2(NO_3)_2(OH)_{12}$	Nitrated AFm phase
$Ca_4Al_2(OH)_{14}$	Tetra-calcium hydroxyaluminate
$Ca_4Al_2(SO_4)(OH)_{12}$	Calcium monosulfoaluminate
$Ca_4Al_2Cl_2(OH)_{12}$	Calcium chloroaluminate (Friedel salt)
$Ca_6(SO_4)_3Fe_2(OH)_{12}$	Calcium sulfoferrate
$Ca_6Al_2(SO_4)_3(OH)_{12}$	Calcium sulfoaluminate (ettringite)
CAP	Complex amino-phosphonates

CAS	Calcium aluminosilicate
C_B	Dissolved ion concentration in blowdown
C_D	Dissolved ion concentration in drift
C_E	Dissolved ion concentration in water vapor plume
C_I	Dissolved ion concentration from the treatment system to the cooling tower
C_{ijk}	The third virial coefficients
C_M	Dissolved ion concentration in makeup
COC	Cycles of concentration
C_P	Heat capacity of water
C_S	Ion concentration from the first stage of the UHLA process
C_{Si}	Residual concentration of the adsorbed species of silica
C_T	Dissolved ion concentration in the cooling tower
ΔAl	Concentration of aluminum removed from the solution
ΔCa	Concentration of calcium removed from the solution
ΔCl	Concentration of chloride removed from the solution
D_F	Drift factor
ΔH	Latent heat of evaporation of water
ΔT	Temperature differential between the hot cooling water return and the cold cooling water supply
EDTA	Ethylenediamine-tetraacetic acid
Et	Ettringite
F	Friedel salt
γ	Activity coefficient
γ_H	Debye-Hückel activity coefficient

HEPT	Hydroxy-ethylene-diphosphonic acid
HPA	Hydroxy-phospho-acetic acid
I	Ionic strength
IAP	Ion activity product
IC	Ion chromatography
K	Kuzel salt
K_{sp}	Solubility product
LDH(s)	Layered double hydroxide(s)
LIC	Larson index of corrosion
M	Monosulfate (calcium monosulfoaluminate)
M^{2+} (M(II))	Divalent cation
M^{3+} (M(III))	Trivalent cation
PBTC	Phosphono-butane-tricarboxylic acid
POCA	Phosphono-carboxylic acid
q	Silica removed (mg/l) per mg magnesium in the precipitated or solid form
Q_B	Cooling tower blowdown water flow rate
Q_D	Cooling tower drift water flow rate
Q_E	Cooling tower evaporation water flow rate
Q_M	Cooling tower makeup water flow rate
Q_S	Sidestream softener flow rate
SSE	Sum of square error
TDS	Total dissolved solids
TOT(Al)	Total aluminum concentration
TOT(Ca)	Total calcium concentration

TOT(Cl)	Total chloride concentration
TOT(Si)	Total silicon concentration
TOT(SO_4)	Total sulfate concentration
UHL	Ultra-high lime softening
UHLA	Ultra-high lime with aluminum process
X_{chl}	Fraction of calcium chloroaluminate in the solid solution
XRD	X-ray diffraction
X_{tet}	Fraction of tetra-calcium hydroxyaluminte in the solid solution
X_{tri}	Fraction of tri-calcium hydroxyaluminate in the solid solution
Z_i	charge (valence) of the i^{th} ion

APPENDIX B

INPUT FILES FOR PHREEQC/INVRS K

Table B-1 PHREEQC/INVRS K input file for calculating unknown equilibrium constants in Cl-OH system.

TITLE Evaluation of chloride removal with Ultra-high lime with aluminum process.

SOLUTION_S

Number	pH charge	Ca	Al	Cl	Na	Description
1	12.60	30	10	30	40	lime dose = 30mM, Al dose = 10mM
2	12.60	30	20	30	50	lime dose = 30mM, Al dose = 20mM
3	12.60	30	30	30	60	lime dose = 30mM, Al dose = 30mM
4	12.60	30	40	30	70	lime dose = 30mM, Al dose = 40mM
5	12.59	30	50	30	80	lime dose = 30mM, Al dose = 50mM
6	12.86	60	10	30	40	lime dose = 60mM, Al dose = 10mM
7	12.85	60	20	30	50	lime dose = 60mM, Al dose = 20mM
8	12.85	60	30	30	60	lime dose = 60mM, Al dose = 30mM
9	12.85	60	40	30	70	lime dose = 60mM, Al dose = 40mM
10	12.85	60	50	30	80	lime dose = 60mM, Al dose = 50mM
11	13.01	90	10	30	40	lime dose = 90mM, Al dose = 10mM
12	13.00	90	20	30	50	lime dose = 90mM, Al dose = 20mM
13	13.00	90	30	30	60	lime dose = 90mM, Al dose = 30mM
14	13.00	90	40	30	70	lime dose = 90mM, Al dose = 40mM
15	13.00	90	50	30	80	lime dose = 90mM, Al dose = 50mM
16	13.00	90	60	30	90	lime dose = 90mM, Al dose = 60mM
17	13.11	120	10	30	40	lime dose = 120mM, Al dose = 10mM
18	13.11	120	20	30	50	lime dose = 120mM, Al dose = 20mM
19	13.11	120	30	30	60	lime dose = 120mM, Al dose = 30mM
20	13.11	120	40	30	70	lime dose = 120mM, Al dose = 40mM
21	13.11	120	50	30	80	lime dose = 120mM, Al dose = 50mM
22	13.11	120	60	30	90	lime dose = 120mM, Al dose = 60mM
23	13.19	150	10	30	40	lime dose = 150mM, Al dose = 10mM
24	13.19	150	20	30	50	lime dose = 150mM, Al dose = 20mM
25	13.19	150	30	30	60	lime dose = 150mM, Al dose = 30mM
26	13.19	150	40	30	70	lime dose = 150mM, Al dose = 40mM
27	13.19	150	50	30	80	lime dose = 150mM, Al dose = 50mM
28	13.19	150	60	30	90	lime dose = 150mM, Al dose = 60mM
29	13.30	200	10	30	40	lime dose = 200mM, Al dose = 10mM
30	13.30	200	20	30	50	lime dose = 200mM, Al dose = 20mM
31	13.30	200	30	30	60	lime dose = 200mM, Al dose = 30mM
32	13.30	200	40	30	70	lime dose = 200mM, Al dose = 40mM
33	13.30	200	50	30	80	lime dose = 200mM, Al dose = 50mM

```
    34      13.30      200      60      30      90    lime dose = 200mM, Al dose = 60mM
    35      13.30      200      80      30      110   lime dose = 200mM, Al dose = 80mM
    36      13.30      200      100     30      130   lime dose = 200mM, Al dose = 100mM

SAVE SOLUTION 1-36

#Regress On

PHASES
        calcium-chloroaluminate
                Ca4Al2Cl2(OH)12 = 4Ca+2 + 2Al(OH)4- + 2Cl- + 4OH-
                log_k           -27.10

#Unknown
        tricalcium-hydroxyaluminate
                Ca3Al2(OH)12  = 3Ca+2 + 2Al(OH)4- + 4OH-
                log_K           -21.22

#Unknown
        tetracalcium-hydroxyaluminate
                Ca4Al2(OH)14 = 4Ca+2 + 2Al(OH)4- + 6OH-
                Log_K           -23.82

SOLID_SOLUTIONS 1
        chlorohydroxy
-comp   calcium-chloroaluminate         0.0
-comp   tricalcium-hydroxyaluminate     0.0
-comp   tetracalcium-hydroxyaluminate   0.0

#Regress Off

EQUILIBRIUM_PHASES 1
        calcium-chloroaluminate         0.0     0.0
        tricalcium-hydroxyaluminate     0.0     0.0
        tetracalcium-hydroxyaluminate   0.0     0.0
        Ca(OH)2                         0.0     0.0
        Gibbsite                        0.0     0.0

SAVE EQUILIBRIUM_PHASES 1
USE SOLUTION none
END

TITLE  Start Dataset 1
USE SOLUTION 1
USE EQUILIBRIUM_PHASES 1
USE SOLID_SOLUTIONS 1
END #End Dataset

TITLE  Start Dataset 2
USE SOLUTION 2
USE EQUILIBRIUM_PHASES 1
USE SOLID_SOLUTIONS 1
END #End Dataset

TITLE  Start Dataset 3
USE SOLUTION 3
USE EQUILIBRIUM_PHASES 1
USE SOLID_SOLUTIONS 1
END #End Dataset

TITLE  Start Dataset 4
USE SOLUTION 4
USE EQUILIBRIUM_PHASES 1
USE SOLID_SOLUTIONS 1
END #End Dataset
```

```
TITLE  Start Dataset 5
USE SOLUTION 5
USE EQUILIBRIUM_PHASES 1
USE SOLID_SOLUTIONS 1
END #End Dataset

TITLE  Start Dataset 7
USE SOLUTION 7
USE EQUILIBRIUM_PHASES 1
USE SOLID_SOLUTIONS 1
END #End Dataset

TITLE  Start Dataset 9
USE SOLUTION 9
USE EQUILIBRIUM_PHASES 1
USE SOLID_SOLUTIONS 1
END #End Dataset

TITLE  Start Dataset 11
USE SOLUTION 11
USE EQUILIBRIUM_PHASES 1
USE SOLID_SOLUTIONS 1
END #End Dataset

TITLE  Start Dataset 13
USE SOLUTION 13
USE EQUILIBRIUM_PHASES 1
USE SOLID_SOLUTIONS 1
END #End Dataset

TITLE  Start Dataset 15
USE SOLUTION 15
USE EQUILIBRIUM_PHASES 1
USE SOLID_SOLUTIONS 1
END #End Dataset

TITLE  Start Dataset 17
USE SOLUTION 17
USE EQUILIBRIUM_PHASES 1
USE SOLID_SOLUTIONS 1
END #End Dataset

TITLE  Start Dataset 19
USE SOLUTION 19
USE EQUILIBRIUM_PHASES 1
USE SOLID_SOLUTIONS 1
END #End Dataset

TITLE  Start Dataset 21
USE SOLUTION 21
USE EQUILIBRIUM_PHASES 1
USE SOLID_SOLUTIONS 1
```

```
TITLE  Start Dataset 6
USE SOLUTION 6
USE EQUILIBRIUM_PHASES 1
USE SOLID_SOLUTIONS 1
END #End Dataset

TITLE  Start Dataset 8
USE SOLUTION 8
USE EQUILIBRIUM_PHASES 1
USE SOLID_SOLUTIONS 1
END #End Dataset

TITLE  Start Dataset 10
USE SOLUTION 10
USE EQUILIBRIUM_PHASES 1
USE SOLID_SOLUTIONS 1
END #End Dataset

TITLE  Start Dataset 12
USE SOLUTION 12
USE EQUILIBRIUM_PHASES 1
USE SOLID_SOLUTIONS 1
END #End Dataset

TITLE  Start Dataset 14
USE SOLUTION 14
USE EQUILIBRIUM_PHASES 1
USE SOLID_SOLUTIONS 1
END #End Dataset

TITLE  Start Dataset 16
USE SOLUTION 16
USE EQUILIBRIUM_PHASES 1
USE SOLID_SOLUTIONS 1
END #End Dataset

TITLE  Start Dataset 18
USE SOLUTION 18
USE EQUILIBRIUM_PHASES 1
USE SOLID_SOLUTIONS 1
END #End Dataset

TITLE  Start Dataset 20
USE SOLUTION 20
USE EQUILIBRIUM_PHASES 1
USE SOLID_SOLUTIONS 1
END #End Dataset

TITLE  Start Dataset 22
USE SOLUTION 22
USE EQUILIBRIUM_PHASES 1
USE SOLID_SOLUTIONS 1
```

```
END #End Dataset

TITLE  Start Dataset 23
USE SOLUTION 23
USE EQUILIBRIUM_PHASES 1
USE SOLID_SOLUTIONS 1
END #End Dataset

TITLE  Start Dataset 25
USE SOLUTION 25
USE EQUILIBRIUM_PHASES 1
USE SOLID_SOLUTIONS 1
END #End Dataset

TITLE  Start Dataset 27
USE SOLUTION 27
USE EQUILIBRIUM_PHASES 1
USE SOLID_SOLUTIONS 1
END #End Dataset

TITLE  Start Dataset 29
USE SOLUTION 29
USE EQUILIBRIUM_PHASES 1
USE SOLID_SOLUTIONS 1
END #End Dataset

TITLE  Start Dataset 31
USE SOLUTION 31
USE EQUILIBRIUM_PHASES 1
USE SOLID_SOLUTIONS 1
END #End Dataset

TITLE  Start Dataset 33
USE SOLUTION 33
USE EQUILIBRIUM_PHASES 1
USE SOLID_SOLUTIONS 1
END #End Dataset

TITLE  Start Dataset 35
USE SOLUTION 35
USE EQUILIBRIUM_PHASES 1
USE SOLID_SOLUTIONS 1
END #End Dataset
```

```
END #End Dataset

TITLE  Start Dataset 24
USE SOLUTION 24
USE EQUILIBRIUM_PHASES 1
USE SOLID_SOLUTIONS 1
END #End Dataset

TITLE  Start Dataset 26
USE SOLUTION 26
USE EQUILIBRIUM_PHASES 1
USE SOLID_SOLUTIONS 1
END #End Dataset

TITLE  Start Dataset 28
USE SOLUTION 28
USE EQUILIBRIUM_PHASES 1
USE SOLID_SOLUTIONS 1
END #End Dataset

TITLE  Start Dataset 30
USE SOLUTION 30
USE EQUILIBRIUM_PHASES 1
USE SOLID_SOLUTIONS 1
END #End Dataset

TITLE  Start Dataset 32
USE SOLUTION 32
USE EQUILIBRIUM_PHASES 1
USE SOLID_SOLUTIONS 1
END #End Dataset

TITLE  Start Dataset 34
USE SOLUTION 34
USE EQUILIBRIUM_PHASES 1
USE SOLID_SOLUTIONS 1
END #End Dataset

TITLE  Start Dataset 36
USE SOLUTION 36
USE EQUILIBRIUM_PHASES 1
USE SOLID_SOLUTIONS 1
END #End Dataset
```

Table B-2 PHREEQC input data for modeling effect of initial chloride concentration on chloride removal.

```
TITLE Effect of Initial Chloride Concentration

SOLUTION_S

  Number     pH       Ca       Al       Cl       Na
           charge
    1      12.63     40       16       10       26
    2      13.13    200       80       50      130
    3      13.36    400      160      100      260

SAVE SOLUTION 1-3

EQUILIBRIUM_PHASES 1
calcium-chloroaluminate              0.0     0.0
tricalcium-hydroxyaluminate          0.0     0.0
tetracalcium-hydroxyaluminate        0.0     0.0
Ca(OH)2                              0.0     0.0
Al(OH)3                              0.0     0.0
pH_Fix       -12.63       NaOH   10.0

EQUILIBRIUM_PHASES 2
calcium-chloroaluminate              0.0     0.0
tricalcium-hydroxyaluminate          0.0     0.0
tetracalcium-hydroxyaluminate        0.0     0.0
Ca(OH)2                              0.0     0.0
Al(OH)3                              0.0     0.0
pH_Fix       -12.63       NaOH   10.0

EQUILIBRIUM_PHASES 3
calcium-chloroaluminate              0.0     0.0
tricalcium-hydroxyaluminate          0.0     0.0
tetracalcium-hydroxyaluminate        0.0     0.0
Ca(OH)2                              0.0     0.0
Al(OH)3                              0.0     0.0
pH_Fix       -13.13       NaOH   10.0


SAVE EQUILIBRIUM_PHASES 1-3
USE SOLUTION none
END

SOLID_SOLUTIONS 1
        chlorohydroxy
-comp   calcium-chloroaluminate          0.0
-comp   tricalcium-hydroxyaluminate      0.0
-comp   tetracalcium-hydroxyaluminate    0.0

TITLE  Start Dataset x*
USE SOLUTION x*
USE EQUILIBRIUM_PHASES 1
USE SOLID_SOLUTIONS 1
END #End Dataset
```

* x is the solution number (1, 2, and 3)

Table B-3 PHREEQC input data for modeling effect of pH on chloride removal.

```
TITLE Effect of pH on chloride removal

SOLUTION_S
```

Number	pH charge	Ca	Al	Cl	Na	Acetate
1	10.80	20	10	10	10	43
2	11.15	20	10	10	10	43
3	11.35	20	10	10	10	43
4	11.34	20	10	10	10	43
5	11.75	20	10	10	10	43
6	12.38	20	10	10	10	43
7	11.83	20	10	10	10	43
8	12.14	20	10	10	10	43
9	12.17	20	10	10	10	0
10	10.82	100	50	50	50	183
11	11.00	100	50	50	50	183
12	10.97	100	50	50	50	183
13	11.15	100	50	50	50	183
14	12.18	100	50	50	50	183
15	11.44	100	50	50	50	183
16	12.67	100	50	50	50	183
17	13.05	100	50	50	50	183
18	12.59	100	50	50	50	0
19	10.88	200	100	100	100	330
20	10.87	200	100	100	100	333
21	11.09	200	100	100	100	330
22	11.29	200	100	100	100	330
23	11.49	200	100	100	100	330
24	12.32	200	100	100	100	330
25	11.89	200	100	100	100	330
26	12.79	200	100	100	100	330
27	12.76	200	100	100	100	330

```
SAVE SOLUTION 1-27

EQUILIBRIUM_PHASES 1
calcium-chloroaluminate                0.0    0.0
tricalcium-hydroxyaluminate            0.0    0.0
tetracalcium-hydroxyaluminate          0.0    0.0
Ca(OH)2                                0.0    0.0
Al(OH)3                                0.0    0.0
pH_Fix        -10.80        NaOH       10

EQUILIBRIUM_PHASES 2
calcium-chloroaluminate                0.0    0.0
tricalcium-hydroxyaluminate            0.0    0.0
tetracalcium-hydroxyaluminate          0.0    0.0
Ca(OH)2                                0.0    0.0
Al(OH)3                                0.0    0.0
pH_Fix        -11.15        NaOH       10

EQUILIBRIUM_PHASES 3
calcium-chloroaluminate                0.0    0.0
tricalcium-hydroxyaluminate            0.0    0.0

EQUILIBRIUM_PHASES 4
calcium-chloroaluminate                0.0    0.0
tricalcium-hydroxyaluminate            0.0    0.0
```

```
tetracalcium-hydroxyaluminate  0.0   0.0
Ca(OH)2                        0.0   0.0
Al(OH)3                        0.0   0.0

pH_Fix       -11.34            NaOH  10.0
EQUILIBRIUM_PHASES 5
calcium-chloroaluminate        0.0   0.0
tricalcium-hydroxyaluminate    0.0   0.0
tetracalcium-hydroxyaluminate  0.0   0.0
Ca(OH)2                        0.0   0.0
Al(OH)3                        0.0   0.0
pH_Fix       -11.75            NaOH  10

EQUILIBRIUM_PHASES 7
calcium-chloroaluminate        0.0   0.0
tricalcium-hydroxyaluminate    0.0   0.0
tetracalcium-hydroxyaluminate  0.0   0.0
Ca(OH)2                        0.0   0.0
Al(OH)3                        0.0   0.0
pH_Fix       -12.38            NaOH  10

EQUILIBRIUM_PHASES 9
calcium-chloroaluminate        0.0   0.0
tricalcium-hydroxyaluminate    0.0   0.0
tetracalcium-hydroxyaluminate  0.0   0.0
Ca(OH)2                        0.0   0.0
Al(OH)3                        0.0   0.0
pH_Fix       -12.17            NaOH  10

EQUILIBRIUM_PHASES 11
calcium-chloroaluminate        0.0   0.0
tricalcium-hydroxyaluminate    0.0   0.0
tetracalcium-hydroxyaluminate  0.0   0.0
Ca(OH)2                        0.0   0.0
Al(OH)3                        0.0   0.0
pH_Fix       -10.97            NaOH  10

EQUILIBRIUM_PHASES 13
calcium-chloroaluminate        0.0   0.0
tricalcium-hydroxyaluminate    0.0   0.0
tetracalcium-hydroxyaluminate  0.0   0.0
Ca(OH)2                        0.0   0.0
Al(OH)3                        0.0   0.0
pH_Fix       -11.15            NaOH  10

EQUILIBRIUM_PHASES 15
calcium-chloroaluminate        0.0   0.0
tricalcium-hydroxyaluminate    0.0   0.0
tetracalcium-hydroxyaluminate  0.0   0.0
Ca(OH)2                        0.0   0.0
Al(OH)3                        0.0   0.0
pH_Fix       -12.18            NaOH  10
```

```
tetracalcium-hydroxyaluminate  0.0   0.0
Ca(OH)2                        0.0   0.0
Al(OH)3                        0.0   0.0

pH_Fix       -11.35            NaOH  10.0
EQUILIBRIUM_PHASES 6
calcium-chloroaluminate        0.0   0.0
tricalcium-hydroxyaluminate    0.0   0.0
tetracalcium-hydroxyaluminate  0.0   0.0
Ca(OH)2                        0.0   0.0
Al(OH)3                        0.0   0.0
pH_Fix       -12.14            NaOH  10

EQUILIBRIUM_PHASES 8
calcium-chloroaluminate        0.0   0.0
tricalcium-hydroxyaluminate    0.0   0.0
tetracalcium-hydroxyaluminate  0.0   0.0
Ca(OH)2                        0.0   0.0
Al(OH)3                        0.0   0.0
pH_Fix       -12.83            NaOH  10

EQUILIBRIUM_PHASES 10
calcium-chloroaluminate        0.0   0.0
tricalcium-hydroxyaluminate    0.0   0.0
tetracalcium-hydroxyaluminate  0.0   0.0
Ca(OH)2                        0.0   0.0
Al(OH)3                        0.0   0.0
pH_Fix       -10.82            NaOH  10

EQUILIBRIUM_PHASES 12
calcium-chloroaluminate        0.0   0.0
tricalcium-hydroxyaluminate    0.0   0.0
tetracalcium-hydroxyaluminate  0.0   0.0
Ca(OH)2                        0.0   0.0
Al(OH)3                        0.0   0.0
pH_Fix       -11.00            NaOH  10

EQUILIBRIUM_PHASES 14
calcium-chloroaluminate        0.0   0.0
tricalcium-hydroxyaluminate    0.0   0.0
tetracalcium-hydroxyaluminate  0.0   0.0
Ca(OH)2                        0.0   0.0
Al(OH)3                        0.0   0.0
pH_Fix       -11.44            NaOH  10

EQUILIBRIUM_PHASES 16
calcium-chloroaluminate        0.0   0.0
tricalcium-hydroxyaluminate    0.0   0.0
tetracalcium-hydroxyaluminate  0.0   0.0
Ca(OH)2                        0.0   0.0
Al(OH)3                        0.0   0.0
pH_Fix       -12.67            NaOH  10
```

```
EQUILIBRIUM_PHASES 17
calcium-chloroaluminate          0.0     0.0
tricalcium-hydroxyaluminate      0.0     0.0
tetracalcium-hydroxyaluminate    0.0     0.0
Ca(OH)2                          0.0     0.0
Al(OH)3                          0.0     0.0
pH_Fix          -13.05           NaOH    10

EQUILIBRIUM_PHASES 18
calcium-chloroaluminate          0.0     0.0
tricalcium-hydroxyaluminate      0.0     0.0
tetracalcium-hydroxyaluminate    0.0     0.0
Ca(OH)2                          0.0     0.0
Al(OH)3                          0.0     0.0
pH_Fix          -12.59           NaOH    10

EQUILIBRIUM_PHASES 19
calcium-chloroaluminate          0.0     0.0
tricalcium-hydroxyaluminate      0.0     0.0
tetracalcium-hydroxyaluminate    0.0     0.0
Ca(OH)2                          0.0     0.0
Al(OH)3                          0.0     0.0
pH_Fix          -10.87           NaOH    10

EQUILIBRIUM_PHASES 20
calcium-chloroaluminate          0.0     0.0
tricalcium-hydroxyaluminate      0.0     0.0
tetracalcium-hydroxyaluminate    0.0     0.0
Ca(OH)2                          0.0     0.0
Al(OH)3                          0.0     0.0
pH_Fix          -10.88           NaOH    10

EQUILIBRIUM_PHASES 21
calcium-chloroaluminate          0.0     0.0
tricalcium-hydroxyaluminate      0.0     0.0
tetracalcium-hydroxyaluminate    0.0     0.0
Ca(OH)2                          0.0     0.0
Al(OH)3                          0.0     0.0
pH_Fix          -11.09           NaOH    10

EQUILIBRIUM_PHASES 22
calcium-chloroaluminate          0.0     0.0
tricalcium-hydroxyaluminate      0.0     0.0
tetracalcium-hydroxyaluminate    0.0     0.0
Ca(OH)2                          0.0     0.0
Al(OH)3                          0.0     0.0
pH_Fix          -11.29           NaOH    10

EQUILIBRIUM_PHASES 23
calcium-chloroaluminate          0.0     0.0
tricalcium-hydroxyaluminate      0.0     0.0
tetracalcium-hydroxyaluminate    0.0     0.0
Ca(OH)2                          0.0     0.0
Al(OH)3                          0.0     0.0
pH_Fix          -11.49           NaOH    10

EQUILIBRIUM_PHASES 24
calcium-chloroaluminate          0.0     0.0
tricalcium-hydroxyaluminate      0.0     0.0
tetracalcium-hydroxyaluminate    0.0     0.0
Ca(OH)2                          0.0     0.0
Al(OH)3                          0.0     0.0
pH_Fix          -11.89           NaOH    10

EQUILIBRIUM_PHASES 25
calcium-chloroaluminate          0.0     0.0
tricalcium-hydroxyaluminate      0.0     0.0
tetracalcium-hydroxyaluminate    0.0     0.0
Ca(OH)2                          0.0     0.0
Al(OH)3                          0.0     0.0
pH_Fix          -12.32           NaOH    10

EQUILIBRIUM_PHASES 26
calcium-chloroaluminate          0.0     0.0
tricalcium-hydroxyaluminate      0.0     0.0
tetracalcium-hydroxyaluminate    0.0     0.0
Ca(OH)2                          0.0     0.0
Al(OH)3                          0.0     0.0
pH_Fix          -12.79           NaOH    10

EQUILIBRIUM_PHASES 27
calcium-chloroaluminate          0.0     0.0
tricalcium-hydroxyaluminate      0.0     0.0
tetracalcium-hydroxyaluminate    0.0     0.0
Ca(OH)2                          0.0     0.0
Al(OH)3                          0.0     0.0
pH_Fix          -12.76           NaOH    10

SAVE EQUILIBRIUM_PHASES 1-27
USE SOLUTION none
END

SOLID_SOLUTIONS 1
```

```
          chlorohydroxy
-comp     calcium-chloroaluminate          0.0
-comp     tricalcium-hydroxyaluminate      0.0
-comp     tetracalcium-hydroxyaluminate    0.0
```

```
TITLE  Start Dataset x*
USE SOLUTION x*
USE EQUILIBRIUM_PHASES x*
USE SOLID_SOLUTIONS 1
END #End Dataset
```

* x is the solution number (1, 2, 3, 4, ... and 27)

Table B-4 PHREEQC input data for modeling Cl-OH-SO_4 system.

```
TITLE Interaction between chloride and sulfate

SOLUTION_S
```

Number	pH charge	Ca	Al	Cl	SO_4	Na
1	12.07	10	5	0	10	25
2	12.35	20	10	0	10	30
3	12.48	30	15	0	10	35
4	12.64	50	25	0	50	125
5	12.89	100	50	0	50	150
6	12.97	150	75	0	50	175
7	12.89	100	50	0	100	250
8	13.07	200	100	0	100	300
9	13.15	300	150	0	100	350
10	12.33	20	10	10	10	40
11	12.51	40	20	10	10	50
12	12.64	60	30	10	10	60
13	12.68	60	30	10	50	140
14	12.91	120	60	10	50	170
15	12.99	180	90	10	50	200
16	12.85	110	55	10	100	265
17	13.08	220	110	10	100	320
18	13.14	330	165	10	100	375
19	12.58	60	30	50	10	100
20	12.79	120	60	50	10	130
21	12.91	180	90	50	10	160
22	12.84	100	50	50	50	200
23	12.98	200	100	50	50	250
24	13.05	300	150	50	50	300
25	12.94	150	75	50	100	325
26	13.10	300	150	50	100	400
27	13.17	450	225	50	100	475
28	12.75	110	55	100	10	175
29	12.94	220	110	100	10	230
30	13.05	330	165	100	10	285
31	12.90	150	75	100	50	275
32	13.03	300	150	100	50	350
33	13.13	450	225	100	50	425
34	13.01	200	100	100	100	400
35	13.14	400	200	100	100	500
36	13.21	600	300	100	100	600

```
SAVE SOLUTION 1-36
```

```
EQUILIBRIUM_PHASES 1
calcium sulfoaluminate          0.0     0.0
calcium monosulfate             0.0     0.0
tricalcium-hydroxyaluminate     0.0     0.0
tetracalcium-hydroxyaluminate   0.0     0.0
Ca(OH)2                         0.0     0.0
Al(OH)3                         0.0     0.0

EQUILIBRIUM_PHASES 2
calcium-chloroaluminate         0.0     0.0
tricalcium-hydroxyaluminate     0.0     0.0
tetracalcium-hydroxyaluminate   0.0     0.0
calcium monosulfate             0.0     0.0
calcium sulfoaluminate          0.0     0.0
kuzel salt                      0.0     0.0
Ca(OH)2                         0.0     0.0
Al(OH)3                         0.0     0.0

SAVE EQUILIBRIUM_PHASES 1-2
USE SOLUTION none
END

SOLID_SOLUTIONS 2
        sulfohydroxy
-comp   calcium-sulfoaluminate          0.0
-comp   calcium-monosulfate             0.0
-comp   tricalcium-hydroxyaluminate     0.0
-comp   tetracalcium-hydroxyaluminate   0.0

SOLID_SOLUTIONS 3
        chlorosulfohydroxy
-comp   calcium-chloroaluminate         0.0
-comp   calcium-sulfoaluminate          0.0
-comp   calcium-monosulfate             0.0
-comp   tricalcium-hydroxyaluminate     0.0
-comp   tetracalcium-hydroxyaluminate   0.0


TITLE  Start Dataset x
USE SOLUTION x
USE EQUILIBRIUM_PHASES 1*
USE SOLID_SOLUTIONS 2
END #End Dataset
```

* x is the solution number (1, 2, 3, 4, ... and 9)

```
TITLE  Start Dataset y**
USE SOLUTION y**
USE EQUILIBRIUM_PHASES 2
USE SOLID_SOLUTIONS 3
END #End Dataset
```

** y is the solution number (10, 11, 12, 13, 14, ... and 36)

APPENDIX C

RESULTS OF NON-LINEAR REGRESSION USING INVRS K

Table C-1 Calculated values of solubility products of tricalcium hydroxyaluminate ($K_{sp,tri}$) and tetracalcium hydroxyaluminate ($K_{sp,tet}$).

Iteration	$K_{sp,tri}$	$K_{sp,tet}$	Standard error
1	-21.22	-23.82	0.336904
2	-21.12	-23.92	0.316058
3	-21.02	-24.02	0.294384
4	-20.92	-24.12	0.272037
5	-20.82	-24.22	0.249226
6	-20.72	-24.32	0.226296
7	-20.62	-24.42	0.203648
8	-20.52	-24.52	0.181752
9	-20.42	-24.62	0.161302
10	-20.32	-24.72	0.143129
11	-20.22	-24.82	0.128073
12	-20.12	-24.92	0.116755
13	-20.02	-25.02	0.109372
14	-19.92	-25.12	0.105781
15	-19.82	-25.07	0.096832
16	-19.72	-25.04	0.094022
17	-19.72	-25.02	0.093961
18	-19.72	-25.02	0.093959
19	-19.72	-25.02	0.093958
20	-19.72	-25.02	0.093958
21	-19.72	-25.02	0.093958
22	-19.72	-25.02	0.093958
23	-19.72	-25.02	0.093958
24	-19.72	-25.02	0.093958
25	-19.72	-25.02	0.093958

Table C-2 Comparison between measured and model predicted final concentrations in Cl-OH system.

Solution No.	Chemical doses		TOT(Cl)		TOT(Al)		TOT(Ca)		pH	
	$Ca(OH)_2$	$NaAlO_2$	Measured	Predicted	Measured	Predicted	Measured	Predicted	Measured	Predicted
1	30	10	20.90	20.79	0.12	0.17	10.08	10.52	12.35	12.47
2	30	20	17.84	18.33	8.13	5.39	0.87	2.13	12.36	12.38
3	30	30	17.62	18.87	19.37	14.69	0.43	1.36	12.36	12.35
4	30	40	18.47	19.39	23.97	20.73	0.43	1.08	12.38	12.39
5	30	50	20.50	19.96	32.52	24.22	0.43	0.89	12.42	12.45
6	60	10	21.77	20.73	0.43	0.06	18.70	15.28	12.5	12.55
7	60	20	15.25	13.83	0.41	0.13	12.97	11.13	12.62	12.63
8	60	30	12.37	11.14	2.24	0.72	2.30	4.74	12.57	12.64
9	60	40	12.30	13.22	12.37	7.20	0.66	1.40	12.54	12.60
10	60	50	13.71	14.54	19.48	16.26	0.34	0.92	12.54	12.58
11	90	10	20.63	20.73	0.21	0.06	17.66	15.28	12.53	12.55
12	90	20	15.14	13.83	0.24	0.13	13.37	11.13	12.63	12.63
13	90	30	10.56	10.51	0.30	0.20	10.47	8.78	12.72	12.69
14	90	40	8.64	9.10	0.33	0.27	7.57	7.30	12.78	12.74
15	90	50	10.46	9.67	1.22	1.61	3.56	2.71	12.79	12.74
16	90	60	14.06	11.94	10.32	8.40	0.45	1.07	12.79	12.73
17	120	10	21.17	20.73	0.01	0.06	16.85	15.28	12.42	12.55
18	120	20	16.49	13.83	0.02	0.13	12.69	11.13	12.49	12.63
19	120	30	12.21	10.51	0.06	0.20	10.16	8.78	12.56	12.69
20	120	40	9.63	9.10	0.09	0.27	8.14	7.30	12.63	12.74
21	120	50	7.45	8.43	0.15	0.32	6.58	6.24	12.66	12.79
22	120	60	10.07	8.10	0.17	0.38	6.20	5.44	12.7	12.83
23	150	10	22.83	20.73	0.01	0.06	17.74	15.28	12.49	12.55
24	150	20	16.67	13.83	0.02	0.13	13.57	11.13	12.56	12.63
25	150	30	12.55	10.51	0.02	0.20	10.90	8.78	12.64	12.69
26	150	40	9.67	9.10	0.02	0.27	9.15	7.30	12.72	12.74
27	150	50	7.93	8.43	0.03	0.32	8.23	6.24	12.68	12.79
28	150	60	6.83	8.10	0.04	0.38	7.59	5.44	12.72	12.83
29	200	10	24.25	20.73	0.00	0.06	17.14	15.28	12.55	12.55
30	200	20	17.96	13.83	0.00	0.13	13.30	11.13	12.62	12.63
31	200	30	13.32	10.51	0.09	0.20	10.21	8.78	12.66	12.69
32	200	40	10.46	9.10	0.09	0.27	8.58	7.30	12.7	12.74
33	200	50	7.92	8.43	0.13	0.32	7.66	6.24	12.73	12.79
34	200	60	6.47	8.10	0.13	0.38	7.00	5.44	12.77	12.83
35	200	80	5.05	7.86	0.19	0.48	6.74	4.29	12.79	12.90
36	200	100	6.10	7.88	0.28	0.58	5.08	3.52	12.84	12.96

Table C-3 Predicted final concentrations of precipitated solids in Cl-OH system.

Solution No.	Chemical doses		Concentrations of precipitated solids					
	$Ca(OH)_2$	$NaAlO_2$	Solid Solution				$Ca(OH)_2$ (mM)	$Al(OH)_3$ (mM)
			Total (mM)	Fraction of chloro*	Fraction of tri**	Fraction of tetra***		
1	30	10	4.91	0.94	0.04	0.03	0.00	0.00
2	30	20	7.31	0.80	0.18	0.02	0.00	0.00
3	30	30	9.75	0.73	0.26	0.01	0.00	0.00
4	30	40	7.82	0.69	0.30	0.01	0.00	3.60
5	30	50	7.95	0.64	0.34	0.01	0.00	9.81
6	60	10	4.96	0.93	0.03	0.04	24.99	0.00
7	60	20	9.94	0.81	0.08	0.11	9.94	0.00
8	60	30	14.64	0.64	0.23	0.13	0.00	0.00
9	60	40	16.40	0.51	0.43	0.06	0.00	0.00
10	60	50	16.87	0.46	0.50	0.04	0.00	0.00
11	90	10	4.96	0.93	0.03	0.04	54.99	0.00
12	90	20	9.94	0.81	0.08	0.11	39.94	0.00
13	90	30	14.90	0.65	0.15	0.20	23.87	0.00
14	90	40	19.91	0.53	0.21	0.27	7.35	0.00
15	90	50	24.23	0.42	0.39	0.19	0.00	0.00
16	90	60	25.83	0.35	0.55	0.10	0.00	0.00
17	120	10	4.96	0.93	0.03	0.04	84.99	0.00
18	120	20	9.94	0.81	0.08	0.11	69.94	0.00
19	120	30	14.90	0.65	0.15	0.20	53.87	0.00
20	120	40	19.91	0.53	0.21	0.27	37.35	0.00
21	120	50	24.85	0.43	0.25	0.32	20.55	0.00
22	120	60	29.84	0.37	0.28	0.36	3.56	0.00
23	150	10	4.96	0.93	0.03	0.04	115.00	0.00
24	150	20	9.94	0.81	0.08	0.11	99.94	0.00
25	150	30	14.90	0.65	0.15	0.20	83.87	0.00
26	150	40	19.91	0.53	0.21	0.27	67.35	0.00
27	150	50	24.85	0.43	0.25	0.32	50.55	0.00
28	150	60	29.84	0.37	0.28	0.36	33.56	0.00
29	200	10	4.96	0.93	0.03	0.04	165.00	0.00
30	200	20	9.94	0.81	0.08	0.11	149.90	0.00
31	200	30	14.90	0.65	0.15	0.20	133.90	0.00
32	200	40	19.91	0.53	0.21	0.27	117.30	0.00
33	200	50	24.85	0.43	0.25	0.32	100.50	0.00
34	200	60	29.84	0.37	0.28	0.36	83.56	0.00
35	200	80	39.80	0.28	0.32	0.41	49.21	0.00
36	200	100	49.80	0.22	0.34	0.44	14.52	0.00

(*) “chloro” refers to calcium chloroaluminate
(**) “tri” refers to tricalcium hydroxyaluminate
(***) “tetra” refers to tetracalcium hydroxyaluminate

APPENDIX D

TABULATED DATA

Table D-1 Measured final concentrations in Cl-OH system.

Initial conditions			Final concentrations			
$Ca(OH)_2$ (mM)	$NaAlO_2$ (mM)	NaCl (mM)	Final [Cl] (mM)	Final [Al] (mM)	Final [Ca] (mM)	Final pH
10	0	30	28.82	0.00	9.68	11.99
10	10	30	25.35	6.76	1.29	11.87
10	20	30	25.66	14.63	0.36	11.87
10	30	30	26.09	21.30	0.29	11.90
10	40	30	26.08	33.48	0.18	11.94
10	50	30	26.48	38.79	0.12	11.96
30	0	30	29.31	0.00	23.02	12.36
30	10	30	20.90	0.11	10.08	12.35
30	20	30	17.84	8.13	0.87	12.36
30	30	30	17.62	19.37	0.43	12.36
30	40	30	18.47	23.97	0.43	12.38
30	50	30	20.50	32.52	0.43	12.42
60	0	30	26.02	0.00	23.40	12.47
60	10	30	21.77	0.43	18.70	12.5
60	20	30	15.25	0.41	12.97	12.62
60	30	30	12.37	2.24	2.30	12.57
60	40	30	12.30	12.37	0.66	12.54
60	50	30	13.71	19.48	0.34	12.54
90	0	30	27.93	0.00	22.21	12.49
90	10	30	20.63	0.21	17.66	12.53
90	20	30	15.14	0.24	13.37	12.63
90	30	30	10.56	1.16	10.47	12.72
90	40	30	8.64	0.33	7.57	12.78
90	50	30	10.46	1.22	3.56	12.79
90	60	30	14.06	10.32	0.45	12.79
120	0	30	27.34	0.00	22.75	12.32
120	10	30	21.17	0.01	16.85	12.42
120	20	30	16.49	0.02	12.69	12.49
120	30	30	12.21	0.06	10.16	12.56
120	40	30	9.63	0.09	8.14	12.63

120	50	30	7.45	0.15	6.58	12.66
120	60	30	10.07	0.17	6.20	12.70
150	0	30	27.26	0.00	23.86	12.45
150	10	30	22.83	0.01	17.74	12.49
150	20	30	16.67	0.02	13.57	12.56
150	30	30	12.55	0.02	10.90	12.64
150	40	30	9.67	0.02	9.15	12.72
150	50	30	7.93	0.03	8.23	12.68
150	60	30	6.83	0.04	7.59	12.72
200	0	30	26.89	0.00	22.46	12.42
200	10	30	24.25	0.00	17.14	12.55
200	20	30	17.96	0.00	13.30	12.62
200	30	30	13.31	0.09	10.21	12.66
200	40	30	10.45	0.09	8.58	12.7
200	50	30	7.92	0.13	7.66	12.73
200	60	30	6.47	0.13	7.00	12.77
200	80	30	5.05	0.19	6.74	12.79
200	100	30	6.10	0.28	5.08	12.84

Table D-2 Effect of initial chloride concentrations on chloride removal with UHLA

Initial conditions			Final concentrations			
$Ca(OH)_2$ (mM)	$NaAlO_2$ (mM)	NaCl (mM)	Final [Cl] (mM)	Final [Al] (mM)	Final [Ca] (mM)	Final pH
			Measured concentrations			
40	16	10	4.97	0.06	10.49	12.63
200	80	50	15.67	0.07	5.14	13.13
400	160	100	30.42	0.20	2.63	13.36
			Predicted concentrations			
40	16	10	4.29	0.31	11.15	N/A*
200	80	50	16.98	0.66	2.69	N/A
400	160	100	31.52	1.11	1.30	N/A

* N/A means not applicable because pH was fixed at the measured values

Table D-3 Effect of pH on chloride removal with UHLA

Initial conditions			Final concentrations			
$Ca(OH)_2$ (mM)	$NaAlO_2$ (mM)	$CaCl_2$ (mM)	Final [Cl] (mM)	Final [Al] (mM)	Final [Ca] (mM)	Final pH
			Measured concentrations			
15	10	5	10.00	0.22	18.56	10.8
15	10	5	10.08	0.69	18.91	11.15
15	10	5	9.96	1.62	18.08	11.34
15	10	5	10.03	2.67	17.84	11.35
15	10	5	8.58	2.97	11.13	11.75
15	10	5	7.37	1.85	4.13	12.14
15	10	5	7.39	0.59	5.39	12.38
15	10	5	8.80	2.33	1.95	12.83
15	10	5	6.63	2.02	7.78	12.17*
75	50	25	50.00	0.47	91.46	10.82
75	50	25	49.98	0.67	87.15	10.97
75	50	25	49.36	0.81	91.94	11
75	50	25	46.99	0.79	76.14	11.15
75	50	25	34.05	1.66	48.84	11.44
75	50	25	19.07	1.04	13.17	12.18
75	50	25	23.86	0.15	8.98	12.67
75	50	25	32.46	0.56	2.39	13.05
75	50	25	17.41	0.07	9.70	12.59*
150	100	50	95.65	0.59	150.84	10.87
150	100	50	94.56	0.59	158.50	10.88
150	100	50	78.18	0.82	117.32	11.09
150	100	50	60.08	1.67	78.05	11.29
150	100	50	46.30	1.49	50.28	11.49
150	100	50	36.55	0.95	29.45	11.89
150	100	50	45.59	0.13	40.22	12.32
150	100	50	45.84	0.14	9.10	12.79
150	100	50	33.58	0.04	8.02	12.76*
			Predicted concentrations			
15	10	5	10.00	0.5	20	N/A
15	10	5	10.00	1.12	20	N/A
15	10	5	10.00	1.73	20	N/A
15	10	5	10.00	1.77	20	N/A
15	10	5	8.67	4.47	17	N/A
15	10	5	6.30	3.74	8.63	N/A

15	10	5	6.40	2.39	6.42	N/A
15	10	5	7.65	1.03	3.91	N/A
15	10	5	5.65	2.60	6.54	N/A*
75	50	25	50	0.56	100	N/A
75	50	25	50	0.8	100	N/A
75	50	25	50	0.85	100	N/A
75	50	25	50	1.21	100	N/A
75	50	25	29.73	2.34	59.16	N/A
75	50	25	13.85	4.42	13.18	N/A
75	50	25	16.71	1.28	7.93	N/A
75	50	25	22.56	0.47	5.46	N/A
75	50	25	13.64	0.69	5.63	N/A
150	100	50	100	0.64	200	N/A*
150	100	50	100	0.65	200	N/A
150	100	50	81.54	1.06	163.1	N/A
150	100	50	56.05	1.68	111.9	N/A
150	100	50	38.55	2.65	76.34	N/A
150	100	50	20.84	6.67	31.28	N/A
150	100	50	20.68	4.17	15.83	N/A
150	100	50	25.65	0.4	10.18	N/A
150	100	50	24.83	1.08	5.57	N/A*

* without pH adjustments (i.e., without additions of acid or base)

Table D-4 Effect of temperature on chloride removal with UHLA

Initial conditions				Final concentrations			
$Ca(OH)_2$ (mM)	$NaAlO_2$ (mM)	NaCl (mM)	Temperature (^oC)	Final [Cl] (mM)	Final [Al] (mM)	Final [Ca] (mM)	Final pH
20	10	10	20	5.84	1.94	4.73	12.36
20	10	10	30	8.28	0.99	6.08	12.05
20	10	10	40	8.95	0.68	6.08	11.80
20	10	10	53	8.92	0.53	5.79	11.52
100	50	50	20	22.49	0.11	6.03	12.97
100	50	50	30	24.33	0.04	5.85	12.63
100	50	50	40	25.33	0.04	5.91	12.34
100	50	50	53	36.65	0.04	4.14	11.81
200	100	100	20	46.06	0.09	3.49	13.22
200	100	100	30	48.22	0.07	3.37	12.85
200	100	100	40	50.32	0.09	2.60	12.56
200	100	100	53	74.67	0.20	1.95	12.01

Table D-5 Interaction between chloride and sulfate in UHLA process

Initial conditions				Final concentrations				
$Ca(OH)_2$ (mM)	$NaAlO_2$ (mM)	NaCl (mM)	Na_2SO_4 (mM)	Final [Cl] (mM)	Final [SO_4] (mM)	Final [Al] (mM)	Final [Ca] (mM)	Final pH
				Measured concentrations				
10	5	0	10	0.00	4.88	1.42	0.21	12.07
20	10	0	10	0.00	1.26	2.64	0.16	12.35
30	15	0	10	0.00	0.80	1.23	1.06	12.48
50	25	0	50	0.00	24.38	4.32	0.06	12.64
100	50	0	50	0.00	4.21	1.16	0.06	12.89
150	75	0	50	0.00	2.80	5.36	0.07	12.97
100	50	0	100	0.00	50.53	12.37	0.04	12.89
200	100	0	100	0.00	17.56	15.91	0.04	13.07
300	150	0	100	0.00	9.74	6.35	0.11	13.15
20	10	10	10	9.16	1.11	3.48	0.06	12.33
40	20	10	10	9.13	0.40	2.46	1.02	12.51
60	30	10	10	7.88	0.40	2.21	6.02	12.64
60	30	10	50	9.01	19.52	7.24	0.04	12.68
120	60	10	50	9.29	3.73	6.52	0.08	12.91
180	90	10	50	8.57	1.35	2.00	1.84	12.99
110	55	10	100	9.23	51.82	15.81	0.05	12.85
220	110	10	100	9.53	16.19	14.76	0.05	13.08
330	165	10	100	9.29	5.40	2.47	0.10	13.14
60	30	50	10	45.53	0.40	2.07	3.88	12.58
120	60	50	10	29.03	0.40	0.19	4.41	12.79
180	90	50	10	20.39	0.40	0.29	3.88	12.91
100	50	50	50	48.51	5.61	10.52	0.04	12.84
200	100	50	50	45.55	0.40	0.20	1.95	12.98
300	150	50	50	37.84	0.40	0.29	1.88	13.05
150	75	50	100	49.08	30.35	9.21	0.11	12.94
300	150	50	100	45.60	9.77	3.54	0.13	13.10
450	225	50	100	40.96	5.70	1.16	0.91	13.17
110	55	100	10	81.57	0.40	0.22	2.76	12.75
220	110	100	10	54.45	0.40	0.27	3.05	12.94
330	165	100	10	39.03	0.40	0.38	2.24	13.05
150	75	100	50	93.96	3.35	3.23	0.02	12.90
300	150	100	50	87.77	0.40	0.25	1.95	13.03
450	225	100	50	56.07	0.40	0.59	0.98	13.13
200	100	100	100	93.05	18.18	20.81	0.02	13.01
400	200	100	100	92.66	5.40	0.38	0.81	13.14
600	300	100	100	73.94	3.87	0.42	0.99	13.21

				Predicted Concentrations				
10	5	0	10	0	5.20	1.80	0.40	11.87
20	10	0	10	0	0.63	3.24	0.50	12.18
30	15	0	10	0	0.05	2.61	1.46	12.22
50	25	0	50	0	25.20	8.27	0.12	12.44
100	50	0	50	0	4.80	13.60	0.11	12.7
150	75	0	50	0	0.36	8.33	0.33	12.6
100	50	0	100	0	50.73	16.23	0.07	12.7
200	100	0	100	0	10.90	26.10	0.07	12.83
300	150	0	100	0	0.70	16.30	0.20	12.7
20	10	10	10	10.00	0.78	3.12	0.46	12.33
40	20	10	10	9.90	0.03	1.36	1.83	12.52
60	30	10	10	8.57	0.00	0.80	3.60	12.7
60	30	10	50	10.00	20.77	9.54	0.09	12.74
120	60	10	50	10.00	3.92	10.80	0.12	13.10
180	90	10	50	9.97	0.60	3.40	0.35	13.10
110	55	10	100	10.00	47.09	17.00	0.05	12.96
220	110	10	100	10.00	14.90	20.10	0.06	13.21
330	165	10	100	10.00	3.72	9.38	0.12	13.33
60	30	50	10	43.05	0.03	1.05	1.90	12.66
120	60	50	10	29.52	0.00	0.36	3.50	12.91
180	90	50	10	26.25	0.00	0.50	3.00	13.01
100	50	50	50	50.00	7.06	12.10	0.10	12.92
200	100	50	50	48.03	0.34	2.09	0.50	13.12
300	150	50	50	37.92	0.04	0.60	1.50	13.24
150	75	50	100	50.00	31.70	20.60	0.05	13.07
300	150	50	100	49.90	6.03	12.90	0.09	13.29
450	225	50	100	45.28	0.23	0.60	0.90	13.41
110	55	100	10	71.54	0.03	0.64	1.80	12.88
220	110	100	10	51.32	0.00	0.50	2.20	13.11
330	165	100	10	46.79	0.00	0.80	1.60	13.22
150	75	100	50	99.45	2.12	7.83	0.19	13.02
300	150	100	50	73.50	0.09	0.38	1.42	13.26
450	225	100	50	61.03	0.03	0.92	1.01	13.36
200	100	100	100	99.00	18.73	21.00	0.06	13.16
400	200	100	100	95.30	1.30	3.64	0.24	13.37
600	300	100	100	74.30	0.14	0.96	0.70	13.49

Table D-6 Interaction between chloride and silica in UHLA process

Initial conditions				Final concentrations				
$Ca(OH)_2$ (mM)	$NaAlO_2$ (mM)	NaCl (mM)	Na_2SiO_3 (mM)	Final [Cl] (mM)	Final [Si] (mM)	Final [Al] (mM)	Final [Ca] (mM)	Final pH
1.5	0.75	0	0	0.00	0.00	0.62	1.19	11.35
3	1.5	0	0	0.00	0.00	1.25	2.15	11.67
6	3	0	0	0.00	0.00	1.70	4.13	11.99
1.5	0.75	0	1.5	0.00	0.92	0.18	0.98	11.65
3	1.5	0	1.5	0.00	0.34	0.45	1.65	11.84
6	3	0	1.5	0.00	0.05	1.68	3.58	12.05
1.5	0.75	0	3	0.00	1.96	0.10	0.53	11.77
3	1.5	0	3	0.00	1.00	0.14	1.05	11.93
6	3	0	3	0.00	0.12	1.10	1.99	12.09
10	5	10	0	8.97	0.00	1.86	4.93	12.15
20	10	10	0	6.60	0.00	1.52	4.69	12.32
30	15	10	0	6.99	0.00	0.56	5.56	12.43
10	5	10	1.5	8.94	0.02	0.69	3.58	12.20
20	10	10	1.5	8.02	0.00	0.54	5.48	12.40
30	15	10	1.5	9.17	0.01	0.01	7.07	12.49
10	5	10	3	9.78	0.03	0.81	2.70	12.22
20	10	10	3	8.65	0.01	0.29	5.33	12.44
30	15	10	3	7.19	0.01	0.04	6.76	12.55
50	25	50	0	33.18	0.00	0.14	4.37	12.65
100	50	50	0	23.38	0.00	0.05	5.09	12.85
150	75	50	0	17.68	0.00	0.06	4.05	12.96
50	25	50	1.5	35.87	0.00	0.12	4.05	12.67
100	50	50	1.5	25.68	0.00	0.02	4.53	12.87
150	75	50	1.5	19.28	0.00	0.01	3.10	12.97
50	25	50	3	39.14	0.00	0.12	3.89	12.67
100	50	50	3	26.80	0.00	0.20	4.21	12.87
150	75	50	3	20.05	0.00	0.30	3.02	12.97
100	50	100	0	75.72	0.00	0.08	4.93	12.84
200	100	100	0	53.49	0.00	0.07	2.31	13.04
300	150	100	0	38.73	0.00	0.16	2.05	13.15
100	50	100	1.5	78.36	0.00	0.10	4.45	12.85
200	100	100	1.5	55.46	0.00	0.07	2.27	13.04
300	150	100	1.5	41.50	0.00	0.31	1.86	13.14
100	50	100	3	80.72	0.00	0.11	3.89	12.85
200	100	100	3	58.64	0.00	0.06	1.59	13.01
300	150	100	3	49.82	0.00	0.33	1.57	13.15

APPENDIX E

XRD DATA FOR PRECIPITATED SOLIDS

Table E-1 XRD10

D/MAX-B PEAK FINDING PROGRAM V1.8

DATA FILE: C:\DATA\Z00806.RAW
COLLECTED ON 28-OCT-82 AT 12:52:47
SAMPLE IDENTIFICATION: WAHAB--10
DATE OF PEAK SEARCH: 10-30-82 AT 12:46:59

START 2THETA: 2.100 STOP 2THETA: 80.000
STEP SIZE: 0.020 SCAN SPEED: 2.000
KV: 40, MA: 20

PEAK FINDING PARAMETERS

THRESHOLD VALUES : 0.1, 0.2
RELATIVE CUTOFF INTENSITY : 2.5
TYPICAL FULL WIDTH-HALF MAXIMUM : 0.20
MINIMUM FULL WIDTH-HALF MAXIMUM : 0.10
PEAK SPAN : 15

BACKGROUND-SUBTRACTED DATA WILL BE IN FILE C:\DATA\Z00806.BSD
PEAKS DATA WILL BE IN THE NEW FILE C:\DATA\Z00806.PKS
THRESHOLD DATA WILL BE IN FILE C:\DATA\Z00806.THD

PEAK	2-THETA	D-SPACE	I(REL)	I(CPS)	FWHM
1	10.660	8.2924	4.08	108.5	0.280
2	11.260	7.8519	100.00	2661.1	0.318
3	17.380	5.0983	6.63	176.3	0.218
4	20.080	4.4185	2.75	73.0	0.235
5	22.600	3.9312	28.27	752.2	0.418
6	23.340	3.8082	14.67	390.3	0.398
7	26.640	3.3435	4.07	108.4	0.276
8	28.540	3.1251	3.19	85.0	0.256
9	31.120	2.8716	18.17	483.5	0.253
10	31.980	2.7963	6.53	173.7	0.254
11	33.180	2.6979	3.71	98.7	0.318
12	35.660	2.5157	2.83	75.2	0.759
13	36.580	2.4545	3.67	97.5	0.258
14	36.900	2.4340	5.64	150.1	0.537
15	38.520	2.3353	4.98	132.5	0.158
16	38.780	2.3202	10.89	289.8	0.559
17	39.380	2.2862	9.52	253.2	0.397
18	40.780	2.2109	2.58	68.5	0.319
19	40.980	2.2006	3.29	87.5	0.497
20	42.040	2.1475	4.90	130.5	0.338
21	42.480	2.1263	5.60	149.1	0.639
22	42.700	2.1158	4.30	114.4	0.320
23	42.960	2.1036	3.00	79.8	0.279
24	44.580	2.0309	5.52	147.0	0.316
25	45.800	1.9796	4.27	113.7	1.119
26	46.040	1.9698	2.59	69.0	0.120
27	46.300	1.9594	2.76	73.4	1.120
28	46.500	1.9514	2.69	71.6	0.859
29	46.680	1.9443	3.15	83.9	0.860
30	52.580	1.7392	2.66	70.8	0.579
31	53.220	1.7197	4.01	106.8	0.639
32	53.700	1.7055	5.02	133.7	1.018
33	53.980	1.6973	3.60	95.7	0.299
34	54.780	1.6744	2.88	76.6	0.498
35	55.280	1.6604	5.88	156.5	0.377
36	56.720	1.6216	2.95	78.4	0.477
37	63.060	1.4730	3.00	79.9	0.714

Table E-2 XRD30

D/MAX-B PEAK FINDING PROGRAM V1.8

DATA FILE: C:\DATA\Z00801.RAW
COLLECTED ON 28-OCT-82 AT 12:52:40
SAMPLE IDENTIFICATION: WAHAB--30
DATE OF PEAK SEARCH: 10-30-82 AT 12:24:49

START 2THETA: 2.100 STOP 2THETA: 80.000
STEP SIZE: 0.020 SCAN SPEED: 2.000
KV: 40, MA: 20

PEAK FINDING PARAMETERS

THRESHOLD VALUES : 0.1, 0.2
RELATIVE CUTOFF INTENSITY : 2.5
TYPICAL FULL WIDTH-HALF MAXIMUM : 0.20
MINIMUM FULL WIDTH-HALF MAXIMUM : 0.10
PEAK SPAN : 15

BACKGROUND-SUBTRACTED DATA WILL BE IN FILE C:\DATA\Z00801.BSD
PEAKS DATA WILL BE IN THE NEW FILE C:\DATA\Z00801.PKS
THRESHOLD DATA WILL BE IN FILE C:\DATA\Z00801.THD

PEAK	2-THETA	D-SPACE	I(REL)	I(CPS)	FWHM
1	10.760	8.2156	8.61	124.2	0.119
2	11.320	7.8104	100.00	1441.9	0.377
3	22.580	3.9346	30.72	443.0	0.479
4	23.400	3.7986	25.82	372.3	0.438
5	23.880	3.7233	3.52	50.8	0.199
6	31.160	2.8680	43.07	621.0	0.256
7	33.200	2.6963	10.76	155.2	0.398
8	34.140	2.6242	3.54	51.0	0.497
9	34.300	2.6123	2.77	39.9	0.260
10	35.020	2.5602	3.60	51.9	0.419
11	35.400	2.5336	4.26	61.5	0.640
12	35.620	2.5185	4.14	59.7	1.240
13	35.960	2.4954	3.26	47.0	0.960
14	36.220	2.4781	2.58	37.3	0.320
15	36.940	2.4314	16.15	232.8	0.358
16	37.280	2.4100	2.85	41.0	0.139
17	38.040	2.3636	3.15	45.4	0.275
18	38.740	2.3225	21.96	316.6	0.679
19	39.120	2.3008	12.53	180.7	0.439
20	39.320	2.2896	9.62	138.7	0.319
21	39.480	2.2807	8.79	126.7	0.200
22	39.700	2.2685	2.89	41.7	0.240
23	40.540	2.2234	2.66	38.4	0.139
24	40.740	2.2130	5.29	76.3	0.177
25	41.000	2.1986	7.85	113.2	0.439
26	41.220	2.1883	3.89	56.0	0.440
27	41.420	2.1782	2.77	39.9	0.380
28	41.880	2.1553	7.28	104.9	0.180
29	42.040	2.1475	7.63	110.1	0.339
30	42.400	2.1301	9.46	136.4	0.499
31	45.060	2.0103	3.67	52.9	0.339
32	45.320	1.9994	3.76	54.2	0.180
33	45.480	1.9928	5.50	79.3	0.979
34	45.820	1.9788	5.18	74.7	0.940
35	46.040	1.9698	6.58	94.9	2.539
36	46.340	1.9578	4.80	69.1	1.180
37	46.620	1.9466	5.23	75.4	2.518
38	46.840	1.9380	5.24	75.6	2.319
39	47.020	1.9310	3.52	50.8	0.300

40	47.280	1.9210	2.99	43.0	0.360
41	47.600	1.9088	2.52	36.3	0.917
42	48.540	1.8740	3.28	47.2	1.011
43	48.860	1.8625	3.64	52.5	0.637
44	49.040	1.8561	2.62	37.7	0.970
45	50.980	1.7899	2.74	39.6	0.417
46	52.440	1.7435	2.58	37.3	0.640
47	52.880	1.7300	2.94	42.3	0.440
48	53.080	1.7239	4.88	70.3	0.340
49	53.360	1.7156	6.06	87.4	0.599
50	53.600	1.7084	6.41	92.4	0.638
51	54.000	1.6967	4.47	64.4	0.299
52	55.360	1.6582	9.75	140.6	0.477
53	56.560	1.6259	5.04	72.7	0.379
54	56.820	1.6190	5.60	80.7	0.279
55	60.380	1.5318	3.89	56.1	0.617
56	60.580	1.5272	3.13	45.1	0.618
57	62.700	1.4806	3.71	53.5	0.337
58	62.960	1.4751	5.31	76.6	0.977
59	63.180	1.4705	4.28	61.7	0.360
60	63.380	1.4663	4.97	71.7	0.979
* 61	63.560	1.4662	2.55	36.8	0.772
62	63.920	1.4552	2.56	36.9	0.692
63	64.580	1.4420	3.19	46.0	0.154
64	64.660	1.4404	3.61	52.0	0.214
65	64.800	1.4376	3.89	56.1	0.373
66	65.000	1.4336	4.93	71.1	0.637
67	65.500	1.4239	2.58	37.3	0.420
68	65.880	1.4166	4.26	61.4	1.498
69	66.060	1.4132	4.12	59.4	1.498
70	66.180	1.4109	2.87	41.4	0.280
71	66.420	1.4064	2.53	36.5	0.375
72	67.960	1.3782	2.77	39.9	0.236
73	69.600	1.3497	2.80	40.3	0.930

73 PEAKS WERE FOUND AND WRITTEN TO THE PEAKS FILE

* - possible alpha-2 peak(s)

Table E-3 XRD 50

D/MAX-B PEAK FINDING PROGRAM V1.8

DATA FILE: C:\DATA\Z00807.RAW
COLLECTED ON 28-OCT-82 AT 12:52:48
SAMPLE IDENTIFICATION: WAHAB--50
DATE OF PEAK SEARCH: 10-30-82 AT 12:50:29

START 2THETA: 2.100 STOP 2THETA: 80.000
STEP SIZE: 0.020 SCAN SPEED: 2.000
KV: 40, MA: 20

PEAK FINDING PARAMETERS

THRESHOLD VALUES : 0.1, 0.2
RELATIVE CUTOFF INTENSITY : 2.5
TYPICAL FULL WIDTH-HALF MAXIMUM : 0.20
MINIMUM FULL WIDTH-HALF MAXIMUM : 0.10
PEAK SPAN : 15

BACKGROUND-SUBTRACTED DATA WILL BE IN FILE C:\DATA\Z00807.BSD
PEAKS DATA WILL BE IN THE NEW FILE C:\DATA\Z00807.PKS
THRESHOLD DATA WILL BE IN FILE C:\DATA\Z00807.THD

PEAK	2-THETA	D-SPACE	I(REL)	I(CPS)	FWHM
1	10.660	8.2924	3.53	65.1	0.132
2	11.300	7.8242	100.00	1843.4	0.297
3	11.780	7.5064	3.01	55.5	0.360
4	22.600	3.9312	22.58	416.2	0.478
5	23.140	3.8406	11.09	204.4	0.179
6	23.400	3.7986	19.03	350.7	0.496
7	23.860	3.7264	3.25	59.9	0.158
8	25.860	3.4425	2.68	49.3	0.297
9	25.980	3.4269	2.72	50.1	0.615
10	26.200	3.3986	2.52	46.4	0.279
11	29.500	3.0255	8.67	159.8	0.254
12	31.140	2.8698	32.74	603.6	0.255
13	33.180	2.6979	7.14	131.6	0.357
14	35.080	2.5560	2.92	53.8	0.477
15	35.460	2.5295	4.49	82.9	0.756
16	35.640	2.5171	4.80	88.5	0.537
17	35.960	2.4954	3.25	59.8	0.699
18	36.920	2.4327	10.62	195.7	0.356
19	38.540	2.3341	9.08	167.4	0.159
20	38.800	2.3191	16.55	305.0	0.598
21	39.400	2.2851	7.59	139.9	0.479
22	39.580	2.2751	4.43	81.7	0.118
23	41.020	2.1985	4.40	81.1	0.618
24	42.000	2.1495	6.10	112.5	0.679
25	42.260	2.1368	6.60	121.7	0.700
26	42.540	2.1234	6.67	123.0	0.959
27	42.720	2.1149	4.89	90.2	0.239
28	43.300	2.0879	2.75	50.7	0.239
29	45.340	1.9986	3.83	70.6	0.436
30	45.520	1.9911	3.95	72.8	2.536
31	46.060	1.9690	3.43	63.3	1.240
32	46.340	1.9578	2.91	53.6	0.320
33	46.620	1.9466	3.84	70.8	1.340
34	46.860	1.9372	3.91	72.1	2.357
35	47.160	1.9256	2.84	52.3	0.460
36	47.620	1.9081	3.68	67.8	1.018
37	48.620	1.8711	2.75	50.7	0.798

	38	53.080	1.7239	3.01	55.6	0.199
	39	53.300	1.7174	3.29	60.6	0.120
	40	53.520	1.7108	5.08	93.6	0.974
	41	53.680	1.7061	3.88	71.6	0.579
	42	53.900	1.6996	3.07	56.6	0.399
	43	55.100	1.6654	5.35	98.5	0.178
	44	55.360	1.6582	8.71	160.5	0.418
	45	55.700	1.6489	2.80	51.5	0.238
	46	56.520	1.6269	2.63	48.5	0.274
	47	56.700	1.6222	4.64	85.5	0.517
	48	56.880	1.6175	3.45	63.5	0.159
	49	60.600	1.5268	2.90	53.5	0.516
	50	63.220	1.4697	3.36	61.9	0.977
	51	63.440	1.4651	3.47	64.0	0.777
	52	63.640	1.4610	3.37	62.1	0.957
	53	64.720	1.4392	4.14	76.4	0.438
*	54	64.880	1.4396	2.85	52.5	0.400

54 PEAKS WERE FOUND AND WRITTEN TO THE PEAKS FILE

* - possible alpha-2 peak(s)

Table E-4 XRD100

D/MAX-B PEAK FINDING PROGRAM V1.8

DATA FILE: C:\DATA\Z00804.RAW
COLLECTED ON 28-OCT-82 AT 12:52:44
SAMPLE IDENTIFICATION: WAHAB--100
DATE OF PEAK SEARCH: 10-30-82 AT 12:36:19

START 2THETA: 2.100 STOP 2THETA: 80.000
STEP SIZE: 0.020 SCAN SPEED: 2.000
KV: 40, MA: 20

PEAK FINDING PARAMETERS

THRESHOLD VALUES : 0.1, 0.2
RELATIVE CUTOFF INTENSITY : 2.5
TYPICAL FULL WIDTH-HALF MAXIMUM : 0.20
MINIMUM FULL WIDTH-HALF MAXIMUM : 0.10
PEAK SPAN : 15

BACKGROUND-SUBTRACTED DATA WILL BE IN FILE C:\DATA\Z00804.BSD
PEAKS DATA WILL BE IN THE NEW FILE C:\DATA\Z00804.PKS
THRESHOLD DATA WILL BE IN FILE C:\DATA\Z00804.THD

PEAK	2-THETA	D-SPACE	I(REL)	I(CPS)	FWHM
1	11.300	7.8242	100.00	1363.0	0.358
2	17.440	5.0809	4.69	63.9	0.198
3	18.200	4.8704	3.93	53.6	0.439
4	22.360	3.9728	16.35	222.9	0.159
5	22.500	3.9484	23.29	317.4	0.219
6	22.720	3.9107	27.27	371.7	0.559
7	23.220	3.8276	18.27	249.0	0.238
8	23.440	3.7922	25.62	349.1	0.458
9	26.060	3.4165	2.86	39.0	0.375
10	28.580	3.1208	4.60	62.8	0.236
* 11	28.680	3.1178	3.02	41.2	0.399
12	31.160	2.8680	39.71	541.3	0.275
13	31.840	2.8083	6.14	83.6	0.414
14	32.040	2.7912	5.14	70.0	0.260
15	33.060	2.7074	5.48	74.7	0.155
16	33.240	2.6931	10.06	137.1	0.357
17	34.240	2.6167	9.06	123.5	0.236
18	35.480	2.5281	2.73	37.2	0.220
19	35.740	2.5103	5.10	69.6	0.513
20	36.920	2.4327	13.96	190.3	0.360
21	38.580	2.3318	10.60	144.5	0.219
22	38.860	2.3156	19.40	264.4	0.978
23	39.420	2.2840	11.47	156.4	0.477
24	40.840	2.2078	6.27	85.4	0.451
25	41.040	2.1975	6.60	90.0	0.451
26	41.840	2.1573	4.58	62.4	0.198
27	42.040	2.1475	6.81	92.9	0.640
28	42.560	2.1225	8.89	121.1	0.996
29	42.720	2.1149	7.67	104.5	0.258
30	44.680	2.0266	2.66	36.2	0.439
31	45.060	2.0103	3.61	49.2	0.358
32	45.460	1.9936	5.00	68.1	0.420
33	45.700	1.9837	5.19	70.7	1.798
34	46.060	1.9690	5.69	77.6	1.699
35	46.320	1.9586	5.30	72.2	1.699
36	46.540	1.9498	3.57	48.7	0.240
37	46.760	1.9411	5.01	68.3	1.440
38	46.900	1.9357	3.79	51.6	0.120

	39	47.220	1.9233	6.78	92.4	0.299
	40	47.820	1.9006	2.70	36.8	0.657
	41	49.120	1.8533	3.08	41.9	0.937
	42	50.900	1.7925	5.74	78.2	0.438
	43	51.140	1.7847	2.85	38.8	0.340
	44	52.060	1.7553	3.37	45.9	0.395
	45	52.620	1.7379	4.45	60.7	0.739
	46	52.940	1.7282	4.37	59.6	0.919
	47	53.180	1.7209	4.07	55.5	0.180
	48	53.420	1.7138	6.63	90.4	0.719
	49	53.680	1.7061	6.40	87.3	0.578
	50	53.940	1.6985	6.03	82.2	0.338
*	51	54.080	1.6986	3.83	52.1	0.520
	52	54.260	1.6892	2.50	34.1	0.580
	53	54.880	1.6716	3.22	43.9	0.378
	54	55.320	1.6593	12.96	176.7	0.417
	55	55.580	1.6522	5.99	81.6	0.159
	56	55.980	1.6413	2.90	39.5	0.540
	57	56.160	1.6365	3.04	41.4	0.539
	58	56.420	1.6296	3.25	44.3	0.658
	59	56.760	1.6206	5.08	69.2	0.459
	60	57.960	1.5899	2.62	35.8	0.795
	61	60.440	1.5304	2.56	34.9	0.320
	62	60.640	1.5259	4.75	64.8	0.399
	63	62.760	1.4793	3.84	52.3	0.376
	64	62.940	1.4755	3.83	52.3	0.280
	65	63.100	1.4722	5.08	69.2	0.952
	66	63.340	1.4672	5.30	72.2	0.952
	67	63.740	1.4589	3.39	46.2	0.358
	68	64.740	1.4388	3.01	41.0	0.317
	69	64.900	1.4356	5.65	77.0	0.378
	70	65.800	1.4181	3.37	45.9	0.977
	71	66.000	1.4143	3.07	41.9	0.659
	72	66.240	1.4098	2.70	36.8	0.160
	73	66.700	1.4012	2.99	40.8	0.619
	74	69.540	1.3507	2.67	36.4	0.396

74 PEAKS WERE FOUND AND WRITTEN TO THE PEAKS FILE

* - possible alpha-2 peak(s)

Table E-5 XRDCa

D/MAX-B PEAK FINDING PROGRAM V1.B

DATA FILE: C:\DATA\Z00803.RAW
COLLECTED ON 28-OCT-82 AT 12:52:43
SAMPLE IDENTIFICATION: WAHAB--CA
DATE OF PEAK SEARCH: 10-30-82 AT 12:32:41

START 2THETA: 2.100 STOP 2THETA: 80.000
STEP SIZE: 0.020 SCAN SPEED: 2.000
KV: 40, MA: 20

PEAK FINDING PARAMETERS

THRESHOLD VALUES : 0.1, 0.2
RELATIVE CUTOFF INTENSITY : 2.5
TYPICAL FULL WIDTH-HALF MAXIMUM : 0.20
MINIMUM FULL WIDTH-HALF MAXIMUM : 0.10
PEAK SPAN : 15

BACKGROUND-SUBTRACTED DATA WILL BE IN FILE C:\DATA\Z00803.BSD
PEAKS DATA WILL BE IN THE NEW FILE C:\DATA\Z00803.PKS
THRESHOLD DATA WILL BE IN FILE C:\DATA\Z00803.THD

PEAK	2-THETA	D-SPACE	I(REL)	I(CPS)	FWHM
1	11.360	7.7830	100.00	1445.2	0.317
2	18.200	4.8704	17.98	259.9	0.396
3	22.380	3.9693	7.63	110.3	0.158
4	22.720	3.9107	33.41	482.8	0.317
5	23.360	3.8050	11.37	164.3	0.559
6	23.820	3.7325	4.06	58.7	0.240
7	28.860	3.0911	7.55	109.0	0.299
8	31.200	2.8644	18.68	269.9	0.257
9	33.280	2.6900	4.60	66.5	0.478
10	34.280	2.6138	33.76	487.8	0.338
11	35.180	2.5489	2.94	42.4	0.240
12	35.500	2.5267	5.35	77.2	0.359
13	35.680	2.5144	6.53	94.4	0.578
14	35.840	2.5035	5.36	77.5	0.298
15	36.940	2.4314	6.07	87.8	0.475
16	38.740	2.3225	9.75	140.9	0.319
17	38.960	2.3099	12.50	180.7	0.539
18	39.440	2.2829	6.65	96.2	0.500
19	41.120	2.1934	3.58	51.8	0.279
20	42.280	2.1359	7.13	103.0	0.600
21	42.500	2.1253	8.86	128.0	0.799
22	42.700	2.1158	5.32	76.9	0.299
23	45.980	1.9722	3.62	52.4	0.237
24	46.180	1.9642	4.80	69.3	1.115
25	46.440	1.9538	3.89	56.3	0.540
26	46.780	1.9404	3.54	51.2	0.360
27	46.980	1.9326	6.65	96.2	0.379
28	47.320	1.9195	13.29	192.1	0.460
29	50.980	1.7899	14.98	216.4	0.240
30	53.520	1.7108	4.83	69.9	0.598
31	53.760	1.7037	4.64	67.1	0.640
32	54.000	1.6967	3.14	45.3	0.359
33	54.540	1.6812	5.94	85.8	0.379
34	54.780	1.6744	3.19	46.0	0.199
35	55.400	1.6571	5.79	83.6	0.399
36	56.740	1.6211	3.17	45.9	0.319
37	62.820	1.4781	5.19	75.0	0.896
38	63.180	1.4705	3.81	55.1	0.514

39	63.320	1.4676	3.33	48.1	0.335
40	64.340	1.4468	3.01	43.5	0.140
41	64.560	1.4424	3.57	51.5	0.340
42	64.860	1.4364	4.06	58.6	0.798
43	66.100	1.4124	3.25	47.0	0.783
44	72.180	1.3077	2.93	42.4	0.179

44 PEAKS WERE FOUND AND WRITTEN TO THE PEAKS FILE

Table E-6 XRDAl

D/MAX-B PEAK FINDING PROGRAM V1.8

DATA FILE: C:\DATA\Z00802.RAW
COLLECTED ON 28-OCT-82 AT 12:52:41
SAMPLE IDENTIFICATION: WAHAB--AL
DATE OF PEAK SEARCH: 10-30-82 AT 12:28:41

START 2THETA: 2.100 STOP 2THETA: 80.000
STEP SIZE: 0.020 SCAN SPEED: 2.000
KV: 40, MA: 20

PEAK FINDING PARAMETERS

THRESHOLD VALUES : 0.1, 0.2
RELATIVE CUTOFF INTENSITY : 2.5
TYPICAL FULL WIDTH-HALF MAXIMUM : 0.20
MINIMUM FULL WIDTH-HALF MAXIMUM : 0.10
PEAK SPAN : 15

BACKGROUND-SUBTRACTED DATA WILL BE IN FILE C:\DATA\Z00802.BSD
PEAKS DATA WILL BE IN THE NEW FILE C:\DATA\Z00802.PKS
THRESHOLD DATA WILL BE IN FILE C:\DATA\Z00802.THD

PEAK	2-THETA	D-SPACE	I(REL)	I(CPS)	FWHM
1	9.580	9.2247	11.11	161.2	0.235
2	11.240	7.8658	100.00	1451.2	0.318
3	14.340	6.1716	3.81	55.2	0.337
4	17.360	5.1042	8.32	120.7	0.255
5	20.080	4.4185	4.32	62.7	0.156
6	22.520	3.9450	21.33	309.5	0.597
7	23.320	3.8114	24.99	362.6	0.439
8	23.840	3.7294	6.96	100.9	0.420
9	24.000	3.7049	4.02	58.4	0.399
10	25.860	3.4425	2.97	43.2	0.359
11	26.620	3.3459	4.93	71.6	0.218
12	28.480	3.1315	5.41	78.6	0.192
13	31.120	2.8716	38.64	560.7	0.274
14	31.920	2.8014	7.96	115.5	0.216
15	33.120	2.7026	11.27	163.5	0.315
16	33.540	2.6697	2.65	38.4	0.519
17	35.040	2.5588	3.64	52.9	0.280
18	35.180	2.5489	2.88	41.8	0.120
19	35.340	2.5378	4.26	61.8	0.717
20	35.620	2.5185	4.67	67.8	0.899
21	36.440	2.4636	3.45	50.1	0.240
22	36.880	2.4353	14.30	207.6	0.356
23	38.080	2.3612	3.63	52.6	0.277
24	38.620	2.3294	20.67	299.9	0.519
25	38.860	2.3156	16.85	244.5	0.260
26	39.320	2.2896	11.97	173.8	0.559
27	40.560	2.2224	3.90	56.6	0.195
28	40.740	2.2130	4.78	69.3	0.300
29	40.980	2.2006	6.26	90.9	0.479
30	41.900	2.1544	7.36	106.8	0.239
31	42.060	2.1465	8.69	126.1	0.539
32	42.560	2.1225	5.32	77.2	0.639
33	44.480	2.0352	7.52	109.1	0.256
34	44.860	2.0188	2.61	37.9	0.360
35	45.140	2.0070	2.99	43.5	0.560
36	45.340	1.9986	5.57	80.9	0.917
37	45.660	1.9853	4.79	69.5	1.420
38	45.920	1.9747	3.45	50.0	0.560

39	46.120	1.9666	3.82	55.5	0.620
40	46.360	1.9570	2.96	42.9	0.300
41	46.560	1.9490	4.37	63.4	1.120
42	46.760	1.9411	4.74	68.8	0.519
43	47.020	1.9310	3.19	46.3	1.059
44	47.620	1.9081	2.65	38.5	0.799
45	48.920	1.8604	3.18	46.2	0.538
46	50.820	1.7952	3.11	45.1	0.472
47	51.900	1.7603	2.99	43.5	0.576
48	52.140	1.7528	3.82	55.5	0.538
49	52.540	1.7404	5.20	75.5	0.638
50	52.920	1.7288	4.72	68.6	0.440
51	53.140	1.7221	5.07	73.6	0.660
52	53.640	1.7073	4.18	60.6	0.759
53	53.960	1.6979	3.35	48.6	0.280
54	54.700	1.6767	4.25	61.7	0.498
55	55.260	1.6610	10.60	153.8	0.438
56	55.980	1.6413	3.02	43.8	0.220
57	56.140	1.6370	3.71	53.8	0.360
58	56.340	1.6317	4.61	66.9	0.360
59	56.540	1.6264	5.78	83.9	0.597
60	56.820	1.6190	4.75	68.9	0.339
* 61	57.000	1.6183	2.82	40.9	0.259
62	62.720	1.4802	3.93	57.0	0.419
63	62.980	1.4747	4.35	63.1	0.978
64	63.400	1.4659	2.57	37.4	0.460
65	64.660	1.4404	4.00	58.0	0.256
66	64.840	1.4368	3.52	51.1	1.600
67	65.320	1.4274	2.65	38.4	0.700
68	65.740	1.4193	3.08	44.6	1.898
69	66.020	1.4139	3.09	44.8	1.899
70	66.800	1.3993	2.56	37.2	0.719

70 PEAKS WERE FOUND AND WRITTEN TO THE PEAKS FILE

* - possible alpha-2 peak(s)

Table E-7 $XRDSO_4$

D/MAX-B PEAK FINDING PROGRAM V1.8

DATA FILE: C:\DATA\Z00805.RAW
COLLECTED ON 28-OCT-82 AT 12:52:46
SAMPLE IDENTIFICATION: WAHAB--SO4
DATE OF PEAK SEARCH: 10-30-82 AT 12:40:13

START 2THETA: 2.100 STOP 2THETA: 80.000
STEP SIZE: 0.020 SCAN SPEED: 2.000
KV: 40, MA: 20

PEAK FINDING PARAMETERS

THRESHOLD VALUES : 0.1, 0.2
RELATIVE CUTOFF INTENSITY : 2.5
TYPICAL FULL WIDTH-HALF MAXIMUM : 0.20
MINIMUM FULL WIDTH-HALF MAXIMUM : 0.10
PEAK SPAN : 15

BACKGROUND-SUBTRACTED DATA WILL BE IN FILE C:\DATA\Z00805.BSD
PEAKS DATA WILL BE IN THE NEW FILE C:\DATA\Z00805.PKS
THRESHOLD DATA WILL BE IN FILE C:\DATA\Z00805.THD

PEAK	2-THETA	D-SPACE	I(REL)	I(CPS)	FWHM
1	5.540	15.9394	9.58	58.4	0.480
2	8.980	9.8397	18.50	112.8	0.818
3	9.420	9.3810	10.94	66.7	0.380
4	9.700	9.1109	16.38	99.9	0.220
5	10.080	8.7682	58.30	355.5	0.340
6	10.540	8.3866	100.00	609.8	0.799
7	11.040	8.0078	37.52	228.8	1.080
8	11.260	7.8519	31.47	191.9	0.360
9	17.900	4.9514	35.38	215.7	0.279
10	20.040	4.4272	30.37	185.2	0.436
11	20.540	4.3206	13.53	82.5	0.340
12	21.060	4.2150	36.40	222.0	0.440
13	21.400	4.1488	11.05	67.4	0.318
14	22.400	3.9658	26.42	161.1	0.477
15	22.780	3.9005	41.80	254.9	0.679
16	23.240	3.8243	16.53	100.8	0.399
17	25.380	3.5065	14.42	87.9	0.399
18	29.580	3.0175	25.59	156.0	0.357
19	31.200	2.8644	55.32	337.4	0.297
20	32.620	2.7429	9.62	58.7	0.220
21	32.920	2.7186	18.31	111.7	0.476
22	33.160	2.6995	9.34	56.9	0.119
23	36.280	2.4741	19.81	120.8	0.235
24	36.840	2.4378	23.73	144.7	0.275
25	37.380	2.4038	13.76	83.9	0.355
26	37.860	2.3744	14.59	89.0	0.395
27	39.940	2.2554	10.32	62.9	0.452
28	40.440	2.2287	17.34	105.8	0.514
29	40.640	2.2182	10.41	63.4	0.319
30	41.340	2.1822	9.88	60.3	0.297
31	41.700	2.1642	13.25	80.8	0.637
32	43.280	2.0888	6.67	40.7	0.240
33	43.940	2.0590	8.60	52.4	0.420
34	44.820	2.0206	11.22	68.4	0.177
35	45.020	2.0120	11.25	68.6	0.857
36	45.280	2.0011	11.14	67.9	0.480
37	45.620	1.9870	13.66	83.3	1.054
38	47.720	1.9043	7.65	46.6	0.577

39	48.440	1.8777	7.29	44.4	0.160
40	48.700	1.8683	10.94	66.7	0.837
41	49.040	1.8561	7.40	45.1	0.477
42	51.440	1.7750	10.79	65.8	0.460
43	52.100	1.7540	10.40	63.4	0.199
44	55.300	1.6598	17.67	107.7	0.514
45	55.520	1.6538	14.41	87.9	0.238
46	56.400	1.6301	17.96	109.5	0.419
47	56.660	1.6232	8.81	53.7	0.198
48	64.800	1.4376	12.90	78.7	0.372

48 PEAKS WERE FOUND AND WRITTEN TO THE PEAKS FILE

Table E-8 XRDSi

D/MAX-B PEAK FINDING PROGRAM V1.8

DATA FILE: C:\DATA\Z00800.RAW
COLLECTED ON 28-OCT-82 AT 12:52:38
SAMPLE IDENTIFICATION: WAHAB--SI
DATE OF PEAK SEARCH: 10-30-82 AT 12:21:07

START 2THETA: 2.100 STOP 2THETA: 80.000
STEP SIZE: 0.020 SCAN SPEED: 2.000
KV: 40, MA: 20

PEAK FINDING PARAMETERS

THRESHOLD VALUES : 0.1, 0.2
RELATIVE CUTOFF INTENSITY : 2.5
TYPICAL FULL WIDTH-HALF MAXIMUM : 0.20
MINIMUM FULL WIDTH-HALF MAXIMUM : 0.10
PEAK SPAN : 15

BACKGROUND-SUBTRACTED DATA WILL BE IN FILE C:\DATA\Z00800.BSD
PEAKS DATA WILL BE IN THE NEW FILE C:\DATA\Z00800.PKS
THRESHOLD DATA WILL BE IN FILE C:\DATA\Z00800.THD

PEAK	2-THETA	D-SPACE	I(REL)	I(CPS)	FWHM
1	6.940	12.7268	7.89	85.0	0.256
2	7.160	12.3362	11.39	122.6	0.579
3	7.400	11.9366	7.11	76.5	0.259
4	11.260	7.8519	100.00	1076.8	0.396
5	21.320	4.1642	7.35	79.1	0.453
6	22.340	3.9763	15.66	168.7	0.239
7	22.660	3.9209	21.16	227.8	0.559
8	23.220	3.8276	16.37	176.3	0.259
9	23.400	3.7986	20.00	215.4	0.438
10	29.380	3.0376	5.60	60.3	0.118
11	29.520	3.0235	11.81	127.1	0.235
12	31.120	2.8716	36.57	393.8	0.238
13	33.020	2.7106	7.12	76.6	0.238
14	33.160	2.6995	7.65	82.4	0.435
15	36.900	2.4340	6.95	74.8	0.473
16	38.460	2.3388	9.36	100.8	0.177
17	38.600	2.3306	15.71	169.2	0.659
18	38.840	2.3168	8.72	93.9	0.140
19	39.040	2.3053	10.63	114.5	0.579
20	39.200	2.2963	8.35	90.0	0.518
21	39.380	2.2862	6.36	68.5	0.414
22	42.400	2.1301	5.43	58.5	0.400
23	42.600	2.1206	7.60	81.8	0.396
24	55.320	1.6593	8.97	96.6	0.478
* 25	55.500	1.6585	5.25	56.5	0.179

25 PEAKS WERE FOUND AND WRITTEN TO THE PEAKS FILE

* - possible alpha-2 peak(s)

VITA

Ahmed Abdel-Wahab was born in Al-Minia, Egypt. He completed his Bachelor of Science degree in Civil Engineering at Al-Minia University in 1990. In 1995, he received his Master of Science degree in Civil Engineering from Al-Minia University. His research activities at Texas A&M University have been focused on recycled industrial wastewater treatment. His research interests include chemical and physical treatment of water, wastewater, hazardous wastes, contaminated soils, and sludges.

Permanent address:

Department of Civil Engineering, Al-Minia University, Al-Minia 61111, Egypt.